CHARACTERISATION OF DISSIMILAR FRICTION STIR WELDED 7075 AND 6101 ALUMINUM ALLOYS

BY

OLATUNJI PETER ABOLUSORO

A THESIS SUBMITTED TO THE UNIVERSITY OF JOHANNESBURG

IN FULFILMENT OF THE DEGREE OF

DOCTOR OF PHILOSOPHY IN MECHANICAL ENGINEERING

FACULTY OF ENGINEERING AND THE BUILT ENVIRONMENT

SUPERVISOR: PROF. ESTHER T. AKINLABI

CO - SUPERVISOR: PROF. SATISH V. KAILAS

APRIL 2020

DEDICATION

This project work is dedicated to God Almighty who strengthened me through the thick and thin of the PhD programme.

ACKNOWLEDGEMENTS

My gratitude goes first and foremost to the Almighty God who singled me out for favour by providing a wonderful opportunity to undertake and successfully finish this PhD programme at the University of Johannesburg, South Africa.

My profound gratitude goes to my benefactor, mentor and supervisor, Professor Esther Titilayo Akinlabi for being instrumental in my enrolling at the university of Johannesburg for a PhD programme. Her guidance, moral and financial support have made this work a success. Thank you and may God bless you.

I equally appreciate my co-supervisor, Professor Satish Kailas in whose laboratory in the Indian Institute of Science (IISC), Bangalore, India, part of this work was carried out. His guidance and support have contributed immensely to the success of this work. My appreciation also goes to all the PhD scholars and staff members at the surface interaction and manufacturing laboratory of the IISC for their assistance throughout the experiments.

I sincerely acknowledge and thank Professor Surya Pal who is head of the friction stir laboratory of the Indian Institute of Technology (IIT), Kharagpur, India where the main experiment was carried out. I am equally grateful to all the PhD scholars in this laboratory - especially Omkar Mypati, Suryakanta Sahu, Rajan Viswakhama and Raju Prasad for their assistance in carrying out the FSW experiments.

I would also like to express my sincere appreciation to my loving and caring wife, Mary Olatunji, for her support, understanding and encouragement from the beginning to the end of this programme while she had to be a mother and father to our children because of my absence. I love you my darling wife.

To my lovely God-given children, Ayotomiwa Caleb, Olasunkanmi Cornelius and Jesutomi Victory, I thank you for your cooperation, understanding and prayers. I am blessed indeed to have you as children.

My special appreciation goes to Dr. Stephen Akinlabi for his care and support throughout this work. I also wish to thank all my colleagues in the Modern and Advanced Manufacturing System (MAMS) research group, especially Ikumapayi Omolayo, Olayinka Abegunde, Paul Adedeji, Dr Samuel Fatoba, Babarinde Taiwo, Opeoluwa Dada, Simeon Ogbonna and Kayode Damola for their advice and assistance.

I am also grateful to my father, Chief Simon Abolusoro of blessed memory for inspiring me to go further in my academic career. I equally appreciate my mother Mrs Rebecca Abolusoro and all my siblings for their support and prayers.

Also worthy of appreciation are my spiritual father and mother, family and friends, Pastor and Professor (Mrs) Rotimi Adejumo, Hon Vatsa Tsado, Dr Gbenga Olorunfemi, Chief Taiwo Ejibunu, Barr George Olorunmotito, Clement Ojo, Dr Joseph Iseolorunkanmi, Dr Mathew Rotimi and others too numerous to mention - for all their support.

DECLARATION

I, Abolusoro Olatunji Peter hereby declares that this work submitted to the University of Johannesburg, South Africa, for a doctoral degree in Mechanical Engineering Science in the Faculty of Engineering and the Built Environment (FEBE) was completely carried out by me and has not been presented anywhere for academic purposes by me or anyone else. I equally affirm that there is no plagiarism in the work. All sources referred to have been duly acknowledged.

Signed: Olatunji Peter Abolusoro

ABSTRACT

Friction Stir Welding (FSW), a technique invented in 1991, has become a successful welding technology for joining ferrous and non-ferrous materials. It is used to join varieties of aluminium alloys in automotive, marine, aerospace and other industrial applications. However, in order to broaden the scope and further establish the viability of FSW technology, more studies to characterise and institute the process outputs are imperative.

The object of this research work was to characterise the friction stir welded joints of 6101-T6 and 7075-T651 aluminium alloys. After the preliminary investigations, a final matrix design of the weld using Taguchi minitab software was produced. Sixteen processing parameters of different combinations of rotational speed between 950 and 1850 rpm and travel speed between 20 and 110 mm/min, were investigated. Tapered threaded and tapered unthreaded tool pin profiles were designed and used for the welding, and the weld characteristics of both tools were compared in order to obtain the best tool suited for joining the two alloys. The welds were optimised using mechanical properties, i.e. tensile behaviour and microhardness profiling as outputs. In-situ temperature measurement was also carried out and other characterisations such as mechanical properties, material flow and mixing, microstructures and wear behaviours were evaluated.

An analysis of the microstructures, material flow characteristics, and mechanical properties of some selected welds with the same process parameters from both threaded and unthreaded tool pins revealed that better material flow and mixing was achieved in welds produced with threaded tool pin compared to welds produced with unthreaded tool pin. The compared mechanical properties of both tools also showed that both the ultimate tensile strength and average hardness values at the nugget zone of welds produced with threaded pin, were higher compared to welds

produced with an unthreaded pin. The optimisation carried out on welds from the better performing tapered threaded tool pins in the Taguchi experimental design and analysis, gave combinations of 950 rpm rotational speed and 50 mm/min travel speed as the optimum parameter combinations for achieving maximum Ultimate Tensile Strength (UTS). Similarly, 1550 rpm and 20 mm/min rotational speed and travel speed respectively was obtained to give maximum hardness at the nugget zone (NZ) of the welds. The rotational and travel speeds were found to contribute 63% and 37% respectively towards achieving the optimum UTS, whereas the travel speed was the predominant factor in attaining optimum hardness.

All the prepared and tested tensile samples fractured at the heat affected zone (HAZ) of the 6101-T6 alloy that was on the advancing side of the butt-welding configuration. The scanning electron microscope (SEM) analysis of the fractured surfaces revealed fibrous structures and dimples; an indication of the ductility of the joined alloys.

The in-situ temperature measurement carried out on some selected parameters based on their UTS performance, shows that the highest temperature of 560^{o}C was obtained and occurred at the highest rotational speed of 1850rpm. The temperature profile indicated that the temperature increases with time up to the middle of the weld, and further demonstrated that the processing parameter, especially the rotational speed, influences the temperature variations in the welds. The temperature was found to increase as the tool rotational speed increases.

The microstructural analysis of the NZ of the welds revealed three distinct regions, namely unmixed, mixed and mechanically mixed regions. Onion ring structures and alternate layers in lamellae flow pattern characterised the microstructure of the NZ.

The findings on the influence of the process parameters show that tool features, rotation, and travel speed affect the mechanical properties of the welds. The UTS decreases with an increase in rotational speed but increases with an increase in travel speed. The volume and penetration of materials into each other and the mixing at the NZ were found to be influenced by the processing parameters. The average hardness values obtained at the NZ also varied with different parameters. The wear rate evaluated at different welding process parameters shows that it decreases with an increase in the travel speed but increases as the rotational speed increases. The highest resistance to wear was found to have occurred at medium travel speed.

Keywords: Aluminium alloys, friction stir welding, mechanical properties, microstructures, process parameters, temperature, wear.

TABLE OF CONTENTS

LIST OF FIGURES

ABBREVIATIONS

AA:	Aluminium alloy
Al:	Aluminium
AS:	Advancing side
ASTM:	American society for testing and materials
EDS:	Energy dispersion spectroscopy
FSW:	Friction stir welding
HAZ:	Heat affected zone
HV:	Vickers hardness
IGC:	Intergranular corrosion
MPa:	Mega pascal
MIG:	Metal inert gas
mm/min:	millimeter per minute
NA:	Natural aging
NZ:	Nugget zone
PWAA:	Post weld artificial aging
RS:	Retreating side
RW:	Resistance welding
RRA:	Retrogression reaging
rpm:	revolution per minute
SEM:	Scanning electron microscope
SAW:	Submerged arc welding

SiC:	Silicon carbide
SCC:	Stress corrosion cracking
TIG:	Tungsten inert gas
TMAZ:	Thermomechanically affected zone
UTS:	Ultimate tensile strength
WJE:	Weld joint efficiency
XRD:	X-ray diffraction

GLOSSARY OF TERMS

A

Aging- This refers to the heating of metal to certain temperatures and then quenching it in water to improve its mechanical properties

Alloy- Elements added to change the properties of materials.

Advancing side- The side of the workpiece facing in the same direction as the direction of the rotating tool.

B

Backing plate- The material upon which the metal to be welded is placed to resist the downward force of the machine during welding.

Bending stress- Combination of tensile and compressive forces on a material which extends its grain fibre at the outer part and compresses the fibre at the inner side.

C

Clamping system- Mechanical devices employed to firmly grip a workpiece during welding.

D

Defects- Failure in weld or part of welds that fall short of the required standard.

Deformation- Changes in a body as a result of applied force.

Degree of freedom- Available numbers of autonomous comparison used to evaluate a parameter.

E

Elongation-Difference between the initial gauge length and final gauge length of a material when subjected to tensile force. Usually expressed as a percentage of the initial gauge length.

Engineering Strain- Expressed as ratio of extension of the original length of a material.

Etchant- Chemical solution used on already grinded and polished metal surface to expose details of its microstructure.

F

Filler metal- A metal introduced to welding, brazing or soldering to form a bond.

Fusion- Melting of metals together.

Friction- The force acting between two surfaces in close contact which tends to oppose their movement.

Fractograph- Surface of a broken tensile tested sample.

Flash- Excess materials removed by the tool during friction stir welding.

G

Grain- A particular crystal in metal.

Grain growth- Increase in the original size of grains due to an increase in temperature**.**

Grain size- The volume or area occupied by the grain.

Grain boundary- The interface between two grains where the lattice of one grain differs from that of the other.

Grinding- The removal of materials off the surface of a metal by the use of grinding papers or a wheel.

H

Hardness- The ability of a material to resist deformation.

Heat affected zone- The region of the parent metal that is not melted during welding, but experiences change in mechanical properties owing to heat generated during welding or cutting.

Homogenous- A state of chemical composition and physical properties of one portion being uniform to any other portion.

I

Indentation Hardness- The hardness obtained by pressing an indenter into the surface of a material.

Intermetallic compound- A combination of two or more metallic atoms in a definite proportion, producing a metallic structure different from the original metal constituents.

J

Joint integrity or efficiency- A measure of the ratio of joint strength to the strength of the parent metal usually expressed as a percentage.

K

Key-hole- The hole left behind after the retraction of the friction stir welding tool.

L

Length of weld- Distance between the start of the weld and the finish of the weld.

M

Macrograph- Magnification of graphic reproduction of specimen surface of not more than 25x.

Magnification- The ratio of the length of line in the image plane to the length of line on the material.

Mechanical properties- The elastic and inelastic behaviour of materials indicating its suitability for mechanical application.

O

Oxidation- When a substance absorbs oxygen.

P

Probe- The part of the welding tool that is plunged into the workpiece**.**

Parameters-Values or arguments that define a variable.

Parent materials- The sheet metal as produced by the manufacturers.

Plastic deformation- Permanent alteration of materials caused by stress.

Polished surface- Surface that reflects a large proportion of incident light.

Plunge depth- The maximum distance into the weld that the tool shoulder penetrates.

R

Residual stress- The stress inherent in a material when no external force is applied to it.

Retreating side- The side of the weld opposite to the direction of rotation of the tool.

Rolling direction- The direction in which the extruded billet was rolled during sheet production.

S

Scanning electron microscope- Electron microscope that scans the image of an object using electron beams.

Spindle speed- The speed at which the tool rotates. Also known as rotational speed.

Stress- A material upon which load is acting tends to oppose the load by its internal forces. These forces are known as stress and is expressed as the ratio of the load to the cross-sectional area.

T

Tensile test- The test applied to measure elasticity, strength and ductility.

Tool displacement- The distance of the tool from the weld center line.

Tool shoulder- Part of the rotating tool at the base of the pin.

Tool pin- Part of the rotating tool which penetrates into the workpiece.

Tilt angle- The position angle of the welding tool.

V

Vickers hardness number- The number associated with applied load and the permanent impression created by the diamond indenter.

W

Welding- The joining process by which materials are metallurgically bonded through pressure or heat applications.

Weld nugget Zone- The region at the joint interface of the workpiece that has been plastically deformed by the stirring tool action.

Welding speed- The speed at which the tool moves along the joint interface.

LIST OF PUBLICATIONS

This thesis is presented in publication format in accordance with the guidelines of the Faculty of Engineering and the Built Environment, University of Johannesburg.

Excerpt from the guideline reads:

4.3.1 Only ISI, IBSS, Scopus and Norwegian listed journal articles will be recognised. Articles in specialised international conferences will be recognised only as additional items if the minimum journal publication requirements are not met. Book chapters and essays are not acceptable for this purpose. Author(s) of articles must carry the UJ affiliation.

4.3.2 For a thesis to be accepted for submission and examination, a minimum of three (3) ISI/IBSS/Scopus/Norwegian-listed journal articles must be accepted or published.

4.3.3 A minimum of three (3) accepted or published journal articles is required for a thesis. In exceptional cases, an international peer-reviewed specialised conference article can be considered with motivation from the supervisor.

Journal articles (SCOPUS- Indexed)

1. **0latunji P Abolusoro** and Esther T. Akinlabi, Wear and Corrosion Behaviour of Friction Stir Welded Aluminium Alloys- An Overview**. Published** in *International Journal of Mechanical and Production Engineering Research and Development* (IJMPERD). Vol. 9, Issue 3, Jun 2019, 967-982. IJMPERDJUN2019105

2. **0latunji P Abolusoro** and Esther T. Akinlabi, In- Process Cooling in Friction Stir Welding of Aluminium Alloys-An Overview**. Published** in *Lecture Note in Mechanical Engineering.* 435-444. 2019. https://doi.org/10.1007/978-981-13-8297-0_45.
3. **0latunji P Abolusoro** and Esther T. Akinlabi**,** Optimization of Process Parameters Using Taguchi for Friction Stir Welding of Dissimilar Aluminium Alloys. **Accepted for publication** in *Lecture Note in Mechanical Engineering* 2019.
4. **0latunji P Abolusoro** and Esther T. Akinlabi, Effects of processing parameters on mechanical, material flow and wear behaviour of friction stir welded 6101-T6 and 7075-T651 aluminium alloys. **Published** in *Manufacturing Review,* vol 7, 1-14, 2020. https://doi.org/10.1051/mfreview/2019026.
5. **0latunji P Abolusoro** and Esther T. Akinlabi, Effects of Processing Parameters on Temperature Distributions, Tensile Behaviour, and Microstructure of Friction Stir Welding of Dissimilar Aluminium Alloys. **Accepted for publication** in *Lecture Note in Mechanical Engineering* 2019.

Journal articles (ISI- Indexed)

1. **0latunji P Abolusoro** and Esther T. Akinlabi, Satish V. Kailas. Tool Rotational speed Impact on Temperature variations, Mechanical Properties and Microstructures of Friction Stir welding of Dissimilar high Strength Aluminium Alloys. **Published** in *The Brazilian Society of Mechanical Science and Engineering* 2020. DOI: 10.1007/s40430-020-2259-9.
2. **0latunji P Abolusoro** and Esther T. Akinlabi, Satish V. Kailas. Impact of Tool Profile on Mechanical Behaviour and Material Flow in Friction Stir Welding of Dissimilar Aluminium Alloys. **Published** in *Material Science and Engineering Technology.* 2020. DOI 10.1002/mawe.202000002

Peer Reviewed SCOPUS- indexed International Conference Articles

1. **0latunji P Abolusoro** and Esther T. Akinlabi, Experimental Investigations of Tool Pin Geometry and Process Parameter Influence on Mechanical Property of Friction Stir Welded 6101-T6 and 7075-T651 Aluminium Alloys**. Published** *in Journal of Physics Conference Series, IOP Publishing* 1378 (2019) 032077 doi:10.1088/1742-6596/1378/3/032077.
2. **0latunji P Abolusoro** and Esther T. Akinlabi, Review and Analysis of Mechanical Properties of Friction Stir Welds of High Strength Aluminium Alloys. **Published** *in Journal of Physics Conference Series, IOP Publishing* 1378 (2019) 042045 doi:10.1088/1742-6596/1378/4/042045

CHAPTER ONE

INTRODUCTION

1.1 OVERVIEW

This research work emanates from previously conducted research in the field of welding. This chapter explains the background of welding techniques, aluminium alloys, the use of friction stir welding methods to join aluminium alloys, the statement of the problem and the solution. This section also covers the aims and objectives of the study, the methodologies adopted and the thesis organisation.

1.2 BACKGROUND OF STUDY

Welding is a process of fabrication that joins or melts two or more pieces of materials, especially metals and thermoplastics, together. Pressure alone or heat or the combination of the two generates the bond with or without the addition of metals during welding**.** Welding processes are employed to join complex shapes and geometries impossible to achieve with other methods like machining, forming etc. They are used to construct structures at a reduced rate of material consumption than other processes like working, machining, or forging - thereby reducing costs.

Welding began a long time ago in human history when man started using metal. This time is known as the iron age. People like the ancient Egyptians and other societies developed tools for welding during this era. However, welding was limited by the tools employed. By the 19^{th} century, advances were made in welding and its capacity enabled wider applications. In 1800, Sir Humphry Davy developed the arc to welding within double carbon electrodes with the use of a battery.

Further to this Edmund Davy in 1836 invented acetylene gas which produces the hottest flame. By 1850 this development had gained popularity. The next major development occurred in the 20th century. [1], [2]. There was a bigger advancement in welding during this time due to electrical power distribution which enabled scientists to develop another welding method using electrical power. In 1920 automatic welding using wire electrodes was developed by General Electric Nobel. Research following this development culminated in different electrodes and other forms of welding such as gas and resistance welding. Research into welding continued into the 1950s and 1960s [3]. Dualshield welding with shielding gas externally supplied was invented in 1954 [4], [5] Although it was a more efficient welding process, it was soon replaced by innershield welding as a result of the cumbersomeness of the equipments. This improvement permitted outdoor welding without the fear of weld contamination and the shielding gas being blown away by wind. Further advancements in technology over time have led to the development of other welding processes such as friction stir welding, laser beam welding, electron beam welding, TIG etc.

1.3 WELDING CLASSIFICATIONS

Different welding techniques are classified based on the way in which pressure and temperature relate during the welding process. These techniques can be classed into two types, namely fusion welding and solid state welding [6], [7].

1.3.1 Fusion Welding

In fusion or non-pressure welding the materials to be joined are heated to melting state and left to cool and solidify. The solidification of the molten materials causes it to coalesce. Fusion welding processes usually employ the use of filler material to fill up the joint. Other requirements are heat, shielding, and proper preparation of the material surfaces. Examples include manual metal arc

welding, metal inert gas welding, gas tungsten arc welding, submerged arc welding, laser welding, and electron beam welding.

1.3.2 Solid State Welding

Solid state or pressure welding are techniques which produce bonding at temperatures significantly lower than the melting point of the parent materials to be joined. The welding process under this category does not require the use of filler metals. Examples include cold pressure welding, diffusion welding, resistance welding, explosive welding, magnetically impelled arc butt welding, and friction stir welding.

1.4 FRICTION STIR WELDING

Friction stir welding came into existence in 1991. It was developed at the welding institute (TWI) in Cambridge UK. It has since become a widely used method of joining metals especially low temperature alloys. The first commercially constituted FSW equipment were used by ESAB in their factory at laxa in Sweden [8].

FSW equipment consists of a non-consumable tool made of a probe and a shoulder. The probe/pin is an elongation whose length is designed from the shoulder to fit the thickness of the workpiece. During welding the workpiece to be joined is usually configured in a butt or lap setting. Welding starts when the rotating probe is plunged into the workpiece, and the shoulder part of the tool rests on the surface of the component. With force applied by the machine, heat is produced as the shoulder rotates and rubs the top surface of the workpiece. As enough heat is produced and transferred via conduction into the workpiece from the shoulder, the rotating tool is moved forward. The heated workpiece becomes softened and a joint is facilitated [9] [10]. When the rotating probe moves in the same direction as the traverse direction, that side of the weld is called

the ‘advancing side’. The other side where the probe rotation direction counters the traverse direction, is called ‘retreating side’ Figure 1.1 shows a schematic diagram of friction stir welding.

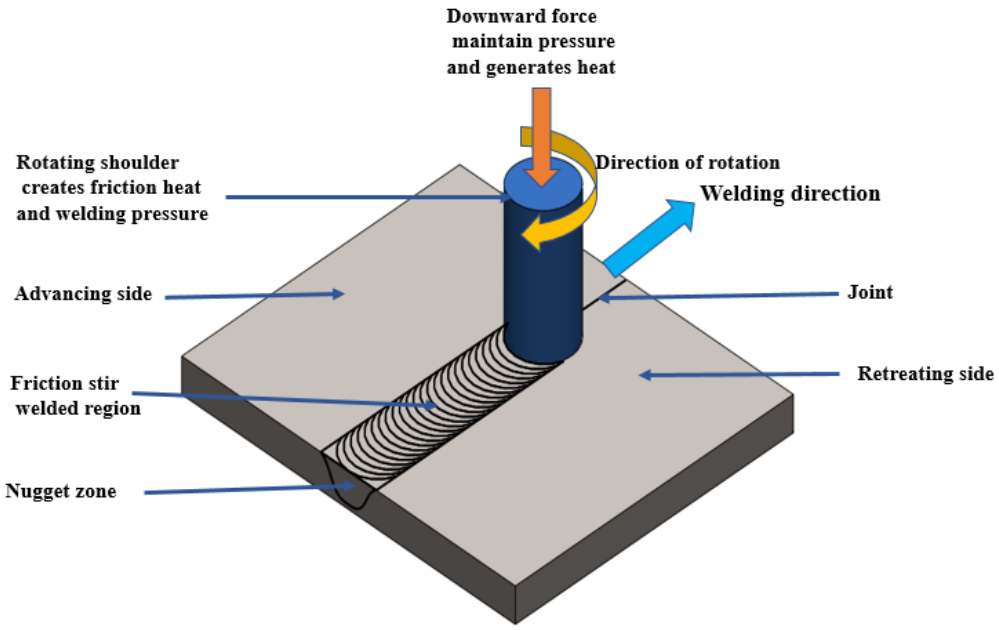

Figure 1.1. Schematic diagram of friction stir butt welding

1.4.1 Advantages of Friction Stir Welding

One of the advantages of friction stir welding is that it can be used to weld low temperature alloys such as aluminium, copper, and magnesium. FSW is applicable to all aluminium alloys. Problems like hot cracking and porosity usually associated with aluminium fusion welding are eliminated in FSW. Although FSW is not totally distortion free, the solidification and cooling involved reduces distortion significantly. Another advantage is that filler metal or shielding gas is not required, and the process considerably tolerates low quality edge preparations. FSW can be completed in a single pass unlike other welding processes. This translates into a greater rate of weld completion speed. Another significant metallurgical merit is that FSW enables the welding of long lengths of

aluminium alloys while the base material remains unmelted and the alloying elements are retained. FSW also eliminates grinding waste and solvents. It allows welding of different thicknesses of material and very significantly reduces fuel consumption in low weight applications in automobiles, marine and aerospace industries.

1.4.2 Applications of Friction Stir Welding

FSW has been successfully employed in many industries in the construction of mechanical parts that are not weldable or difficult to weld with fusion welding. Aerospace is one area where FSW is significantly used. Aircrafts structures like fuselage, fuel tanks, wings, and fins have been welded over time with FSW. A reduction of aircraft weight of up to 25% has been achieved in some situations with the use of FSW compared to other coupling methods like riveting and fusion welding. Other significant areas of use of FSW in aerospace include fuel tank construction and outer disposable tanks for fighter jets. Applications in space vehicles are the joining of aircraft stringers and spars to aluminium cabin panels, cryogenic fuel tanks, and rockets (Figure1.2). FSW has also been used in marine industries in the construction of ship floors, deck fuels, hulls, aircraft landing platform, mast, and sailing boats (Figure 1.3). Automobile applications include wheel rim fabrication, suspension struts, tail lifts for lorries, mobile cranes, fuel tankers, and tailored blanking. In rail transportation FSW is used to produce rolling stock, railway tankers, wagons, and panels. This welding technique is also widely applied in aircraft construction (Figure 1.4). Other applications include pipe construction (Figure 1.5), gas cylinders, bicycle and motorcycle frames, construction of refrigeration panels, and many household items.

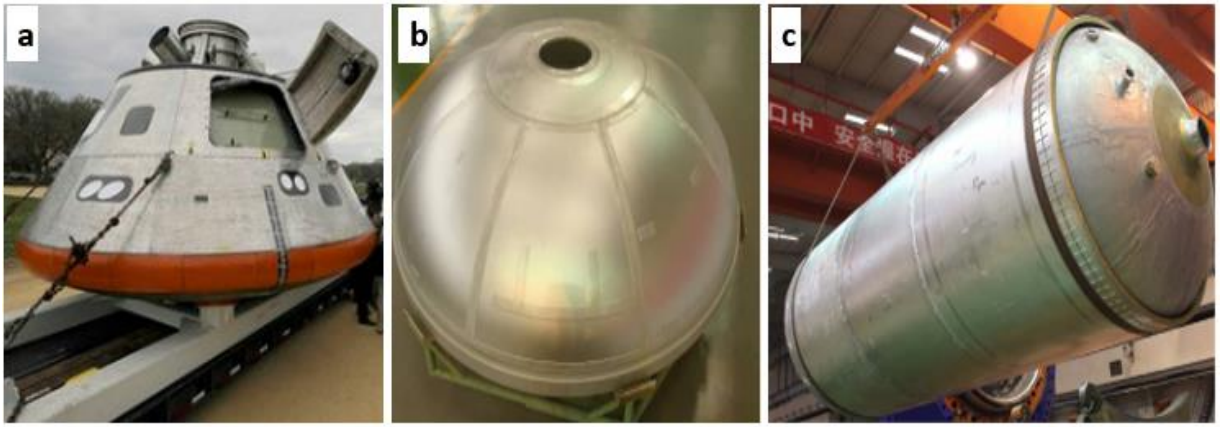

Figure 1.2. Application of friction stir welding in space crafts (a) NASA's Orion Spacecraft joined together with FSW of 425 inch (obtained from https://www.holroyd.com/blog/friction-stir-welding-applications) [11] (b) Dome constructed with FSW [12] (C) Space craft fuel tank fabricated with FSW [12]

Figure 1.3 Application of friction stir welding in marine vessels (a) A cruise ship "THE WORLD" with friction stir welded deck (obtained from https://www.twi-global.com/technical-knowledge/published-papers/nz-fabricators-begin-to-use-friction-stir-welding-to-produce aluminium-components-and-panels-august 2006) [13] (b) Friction stir welded bow section of the ocean viewer vessel at RFI in Cairns (obtained from https://www.twi-global.com/technical-knowledge/published-papers/application-of-friction-stir-welding-in-the-shipbuilding-industry-

february-2000) [14] (c) Prefabricated friction stir welded panel for catamaran side-wall folded to be transported on the road (Hydro Marine) [15]

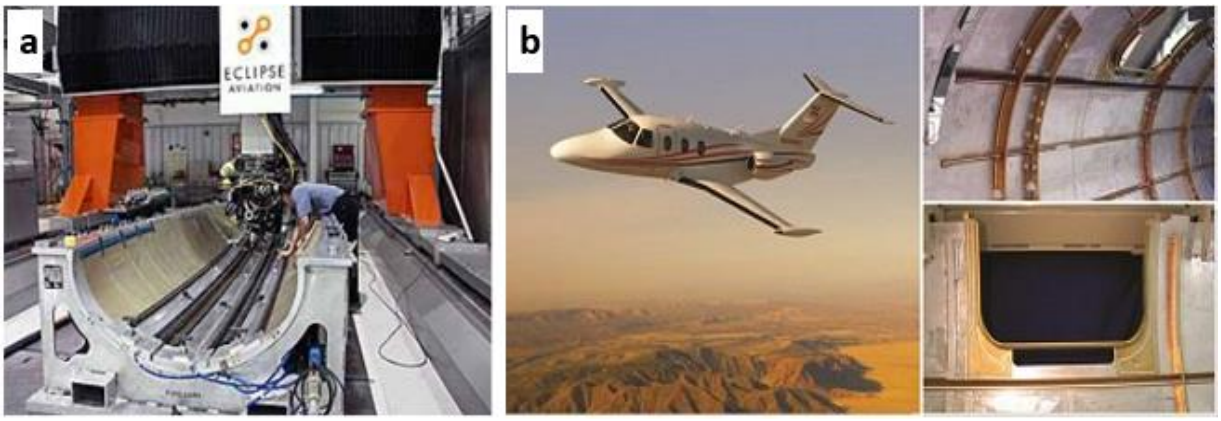

Figure 1.4 Application of friction stir welding in Aircrafts. (a) FSW gantry at Eclipse Aviation for welding aircraft stringers and spars to aluminium cabin panels [24]. (b) Eclipse jet with circumferential aluminum fuselage stiffeners and door doublers joined using FSW (obtained from https://insights.globalspec.com/article/12966/applications-of-friction-stir-welding) [16]

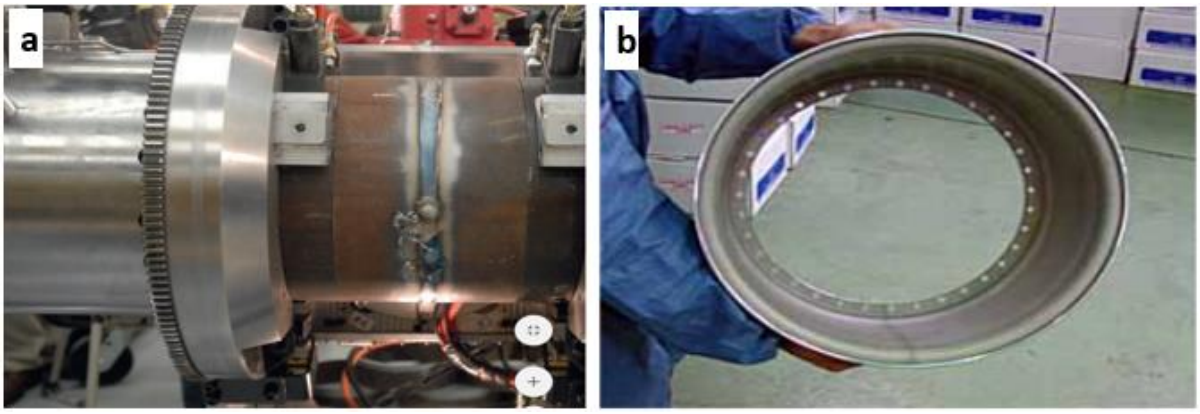

Figure 1.5 Miscellaneous application of friction stir welding (a) Orbital friction stir welded steel pipe (obtained from http://assets.esab.com/asset-bank/assetfile/12296.pdf) [28] (b) Aftermarket three-piece wheel constructed from friction stir welded and spinformed aluminium cylinders [29]

1.5 ALUMINIUM AND ITS ALLOYS

Aluminium is one of the most versatile metals in the world today. It constitutes about 8% of the earth's crust and is the most common metal after silicon and oxygen. Aluminium appears in silvery to dull gray colours depending on the roughness of the surface.

The use of aluminium dates back to about 170 years ago, and the global demand for aluminium has grown to about 29 million tonnes per year. Of this total, 22 million is new aluminium while the remaining 7 million comes from aluminium scrap. Recycled aluminium usage has become economically profitable and contributes to environmental metal pollution control. About 14,000kwh is required to produce one tonne of new aluminium while only 5% of this is needed to recycle one tonne of aluminium. Both recycled and new aluminium are widely used as the quality remains the same [17]. Aluminium in its pure form is soft, ductile, and highly resistant to corrosion. It has a high strength to weight ratio and high electrical conductivity that makes it suitable for use as foil, electrical cables, and aircraft constructions. Its properties have been further enhanced through the addition of other elements to make it suitable for a range of engineering applications [18], [19], [20].

Aluminium alloys can be grouped into two: cast alloy and wrought alloys. These alloys are classified into eight different series generally written as 1xxx, 2xxx, 3xxx, 4xxx. 5xxx, 6xxx, 7xxx and 8xxx, where x is an integer from 0 to 9 based on the alloying elements. Alloying materials are added to improve certain properties of aluminium to suit specific applications [18], [19].

1.5.1 Applications of Aluminium Alloys

The advantageous properties of aluminium alloys have made it suitable for use in industries such as transportation, packaging, power generation and transmission, architecture, aerospace, marine,

and domestic use. Aluminium can serve as alternative material to concrete composites, stainless steel, paper, copper, tin, and titanium [21], [22]. Some of the areas of application for aluminium alloys are given in Figure 1.6.

1.6 6XXX ALUMINIUM ALLOY SERIES

This aluminium series contains magnesium and silicon as the principal alloys. These alloys combine to form magnesium silicide; a compound which improves the alloy strength and permits solution heat treatment. Other characteristics of this group of aluminium alloys include formability, weldability, and good resistance to corrosion. One of the prominent members of this series is the 6101. The 6101 aluminium alloys possesses good corrosion resistance properties, it's highly conductive in terms of electricity, and has good mechanical strength, machinability, and forming behavior. It is very weldable using inert gas arc welding and friction stir welding without filler metals although filler metals may be required in some other welding techniques [23]. Welding the alloy in tempered conditions may lead to low strength in the affected part due to heat input. The strength of these alloys reduces when heated to high temperatures but can be increased at sub-zero. The alloy generally exhibits good cold working behaviour in aged and annealed conditions and does not require hot working. It is similar to 6063 but differs a little in composition [24]. Various temper conditions are available for the 6101, however the T6 condition of the 6101 alloy was used in this work. The T6 temper is a heat treated and artificially aged alloy.

The 6101 alloy is highly suitable for applications involving high strength and high electrical conductivity [25]. These applications include aircraft structures, boat and ship building, construction of pipes and tubes, fabrication of architectural designs and power stations, construction of power transmission accessories such as electrical bus conductors, beams, tubes and custom shapes [23].

1.7 7XXX ALUMINIUM ALLOY SERIES

The 7xxx aluminium alloys series contains Al-Zn-Mg as alloying elements, with Zn being the principal element of the series. They generally exhibit strength higher than the other series of aluminium alloys, with the AL-Zn-Mg-Cu brands having the highest strength but being more susceptible to corrosion. These alloys obtain their strength from the precipitation of Mg_2Zn and Al_2CuMg. The 7xxx series aluminium alloys are employed in the constructions of aircraft stringers, upper wings, stabilizers (both horizontal and vertical), the aircraft tail, elevators and rudders. [21]. The high strength to weight ratio of this series offers a tremendous advantage for applications in aerospace. Other advantages which contribute to their use in the aerospace industry are machinability, weldability, heat treatability, weldability and low cost. [27]. The 7075 alloy is the most prominent of this series. It exists in different temper conditions such as T6, T7, and T651. The choice of these temper conditions depends on the area of application [22]. The 7075-T651 alloy which started being used in 1943 and got designated in 1954 by the American Association, was chosen for this research work. It is highly suitable for applications involving high strength. These applications include aircraft structures, cars, boat and ship building, the construction of pipes and tubes, and the fabrication of architectural designs, engines, and construction accessories (Figure 1.6).

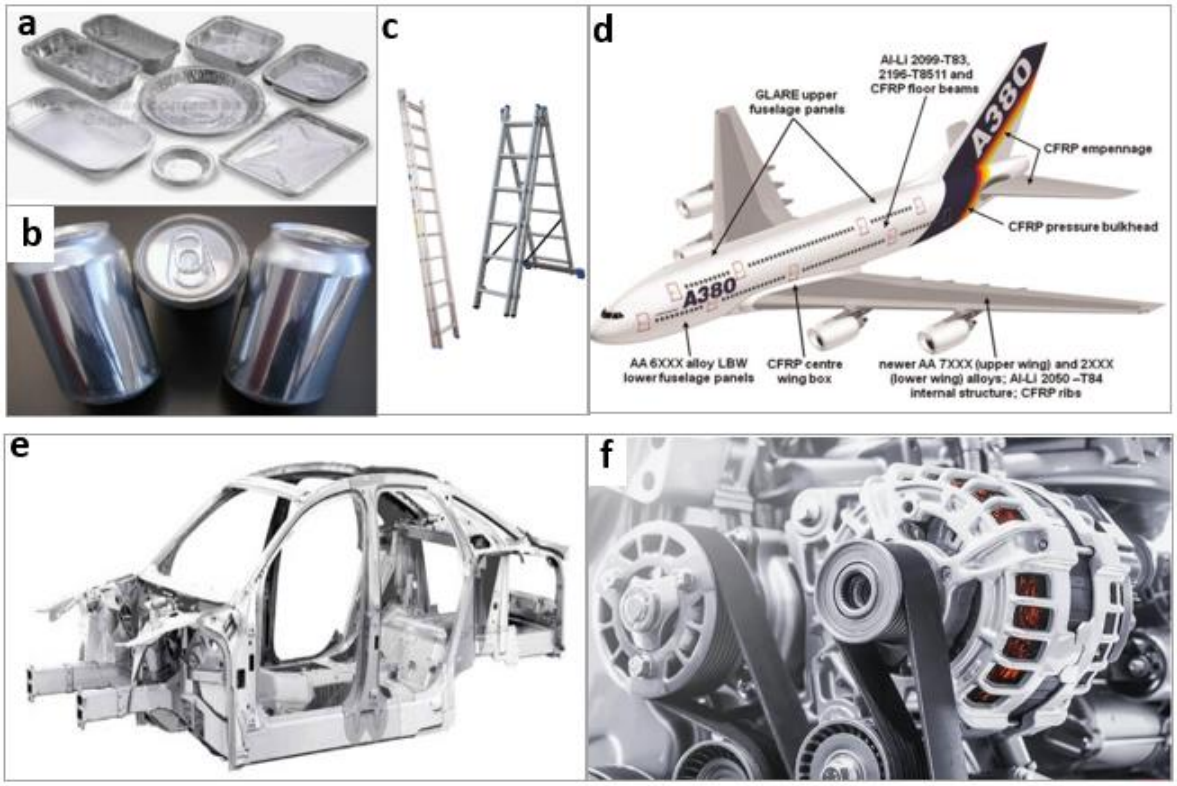

Figure 1. **6** Miscellaneous applications of aluminium alloys. (a) Food packs made from aluminium foil [26] (b) Drink cans made from aluminium [27] (c) Aluminium ladder [28] (d) Aircrafts with different components made from 6xxx and 7xxx aluminium alloys series [29] (e) Car frame constructed with high strength aluminium alloys [30]. (f) Generators and car engine made from aluminium alloys [31].

1.8 FRICTION STIR WELDING OF ALUMINIUM AND ITS ALLOYS

The demand for aluminium alloys is increasing by the day and its applications are expanding. The welding of these alloys often takes place in industries and by friction stir welding which remains one of the best techniques. And although FSW is predominantly used for joining aluminium alloys, copper, magnesium, steel and other materials are also welded with FSW [32]. Since the introduction of FSW, there has been considerable research culminating in many publications about

its use in aluminium alloys. Similar and dissimilar FSW of aluminium alloys have been investigated [9], [33], and aluminium alloys of different grades, temper conditions, and thickness have also received researcher's attention. Various factors such as tool geometry, axial force, tilt angle, welding speed, and tool rotational speed which influence welding processes and their mechanism have been examined by researchers [34],[35],[36]. Attempts have also been made to investigate factors such as mechanical properties, microstructural evolutions, and the corrosion and wear performance of friction stir welded aluminium alloys. This is because the quality or integrity of any weld is determined by the performance of these factors and have been great areas of interest to researchers from the onset. The mechanical properties of welds are the measure of its hardness and strength when subjected to tensile forces, and is widely reported in the literature on friction stir welds of aluminium alloys [37], [35]. It is a major factor that determines weld performance. Microstructural evolutions and reorientation occur during FSW and it is the basis which other factors such as mechanical properties, corrosion and wear behavior of the weld depend upon. Several findings on microstructural changes during FSW of some aluminium alloys have also been researched [38], [39]. Although aluminium alloys are generally resistant to corrosion, the 2xxx and 7xxx series are known to be susceptible to corrosion. Much research on corrosion has also been carried out on various friction stir welded series of aluminium alloys [40].

The tribological behavior of FSW of aluminium has received the attention of researchers, but the literature in this area is poor [40]. Reports available on both wear and corrosion were reviewed in the published article attached to this work and summarised in section 2.2.

In conclusion, dissimilar FSW of some 6xxx and 7xxx series of aluminium alloys has not been reported or fully investigated. These grades of aluminium possess high strength to weight ratio which makes it suitable to many structural applications such as ship buildings, automobile frames,

and aircrafts components such as the lower fuselage panels and the upper wings (Figure 1.6 d and e). This research therefore focuses on bridging the existing gaps, particularly through the FSW of high strength aluminium alloys 6101-T6 and 7075-T65. The study investigates the relationship between process parameters, temperature distributions, tool geometry and the evolving microstructures, mechanical properties, and wear behaviour in the FSW of both aluminium alloys.

1.9 PROBLEM STATEMENT

Several techniques have been employed in joining engineering materials together. These include the use of bolts, rivets and welding, and each method has limitations regarding strength of the joint and durability. The joining of low temperature alloys particularly Aluminium is difficult with non-solid-state welding technology. Aluminium alloys used for the construction in aerospace application has in the past mostly been joined with bolts and rivets. This method involves the use of so many rivets and bolts which add to the weight of the aircrafts and that they sometimes initiate crack propagations in the structures due to stress concentrations. The need for an efficient joining method to join aerospace aluminium alloys which is practically difficult to join with non-solid-state and other conventional welding techniques and to overcome the problems associated with these joining methods, gave birth to the use of friction stir welding technology in the aerospace industries. The technique is relatively new and has successfully overcome many of the setbacks such as hot cracking, porosity, distortions and environmental pollutions associated with conventional welding methods. However, during FSW of aluminium alloys, plasticization occurs which changes the welded joint microstructure and hence alters most of the material properties at the joint interface. These alterations affect the mechanical properties and mechano-electrochemical degradation processes of the welded joint. [41]. Research has shown that the processing variables employed for FSW affects the joint microstructures which determine the mechanical properties,

corrosion, and wear behaviour of the joints. The relationship between the process parameters, tool pin profile, mechanical properties, wear, material flow and microstructure of the friction stir welded joints in most of the high strength series (aerospace alloys) of the aluminium alloys is yet to be properly established. This work is a research effort into FSW of two dissimilar aerospace alloys namely 6101-T6 and 7075-T651 to further establish the relationship between the process variables and resulting behaviours of the friction stir welded joints of these typically high strength aluminium alloys. The findings of this research are aimed at expanding the scope and uses of this important FSW technology in various industries especially aerospace [42].

1.10 MOTIVATION

Because aluminium alloys are widely used in various manufacturing and construction industries today, and the demand for the alloy is increasing day by day as a result of expansions in its applications, two aluminium alloys (6101-T6 and 7075-T651) have been selected for this research work because of their unique properties which include high resistance to corrosion, high thermal and electrical conductivity, and high strength to weight ratio which make them strategic and significant materials in aerospace, automobile and marine industries for building aircrafts components such as the lower fuselage panels and the upper wings, automobile frames and ship structures. However, the challenge of weldability in these alloys has caused them to be joined using rivets and other mechanical fasteners. This has led to increases in material cost, installation labour, and additional weight in the aircraft – all disadvantages which can be overcome using FSW. The use of FSW to join aerospace aluminium alloys has been actively researched in recent years to investigate the joint properties of the weld and to incorporate FSW technology into the

design and fabrication of aircraft components and structures. The characterisation of welded joint properties is therefore a necessity.

FSW still remains one of the best methods for joining aluminium alloys. However, the microstructural reorientation of the alloy during welding affects its mechanical and electrochemical properties. Wear and corrosion and evidence of their interaction has been reported in the literature on aluminum alloys. The complex and rigorous conditions of use of aluminium alloys calls for improvement in the manufacturing and welding of aluminium alloys that are resistant to mechanical degradation and corrosion. Considerable research efforts have been made on FSW of aluminium alloys, but little data relating to the contribution of various alloys and the systematic correlation between temperature, wear, mechanical properties, microstructures and material flow behaviour of FSW of these chosen aluminium alloys, is available. Tool geometry is a key factor that determines the mixing and material movement at the joint interface of FSW. Several tools of different pin profiles have been designed and their effectiveness investigated in FSW of different materials. The tapered threaded and tapered unthreaded tool pins were found to perform optimally out of the numerous tool pin profiles investigated. However, the performance of the two pin profiles have not been studied for joining dissimilar 6101-T6 and 7075-T651 aluminium alloys. This informed their choice for this research work. Other important factors governing the characteristics of friction stir welded aluminium alloys are the rotational and travel speed of the tool. The optimisation of these parameters in achieving the best weld in terms of mechanical properties and resistance to mechanical degradation processes in the FSW of these two alloys, is yet to be reported. The combined effects of welding speed and rotational speed on microstructural evolution, wear behaviour, and material flow pattern in the NZ have also not been investigated on the two aluminium alloys selected for this research.

Temperature measurement and control are important in reducing the degradation of microstructures during FSW and for the effective design of a feedback control system for application in industries. In-situ temperature measurements in FSW of 6101-T6 and 7075-T651 alloys have not been carried out to ascertain the relationship between heat input and process parameters during welding. Also, the correlation between weld temperatures and their reliability in terms of output such as mechanical properties and resistance to mechanical degradation processes is also yet to be established. All these identified gaps in the literature have been the motivating factors for this research effort.

1.11 HYPOTHESIS STATEMENT

The integrity of friction stir welds can only be improved if there is better understanding and control of the governing variables through appropriate characterisation of the welds. This research work encompasses the characterisation of friction stir welded 7075-T651 and 6101-T6 aluminium alloys with the objective of understanding the behaviour of the welds. It is expected that proper control of variable parameters through optimisation techniques will produce better quality welds. It is also envisaged that a correlation between temperature, process parameters, microstructures, material flow and wear behaviour will be established to provide a comprehensive understanding of the aluminium alloys friction stir weld mechanism and control for various applications.

1.12 SIGNIFICANCE OF THE RESEARCH

Aluminium being a highly useful materials in many industries demands that an efficient and reliable joining technique which produces joints with high integrity, be used for joining. Friction stir welding is a favourite option to meet this demand. Optimisation of the process parameters and establishment of a better welding tool pin geometry in this research will no doubt assist in obtaining welds with sound mechanical and electrochemical properties. This work is also a significant

approach to provide more information and understanding of the mechanism of interactions of process parameters, mechanical properties, temperatures, microstructures, and material movements that are found in FSW of aluminium alloys to promote high quality and durable welded joints. The findings from this work is expected to expand the scope and use of FSW in joining aerospace alloys and also to assist in developing a robust approach to predict the performance and lifetime extension of aluminium alloys dissimilar welds for better industrial applications in aerospace, marine and other industries where 6101-T6 and 7075-T651 under research in this work have been found to have tremendous applications.

1.13 AIM

The aim of this research work was to characterise FSW of 7075-T651 and 6101-T6 aluminum alloys. This is meant to provide useful information on the mechanical behaviour, microstructures, material flow, wear, and temperature distributions in relation to the processing parameters for welding the alloys to engineers and manufactures especially in aerospace and marine industrial sectors as a guide in designing, manufacturing and welding fabrications of components including selection of optimum welding techniques and parameters that could result in long weldlife, promote durability, and reduce maintenance costs.

1.14 OBJECTIVES

i. To carry out an extensive literature survey on FSW of aluminium alloys especially on the mechanical properties of high strength aluminium alloys, the effects of in-process cooling, and mechano-electrochemical degradation processes such as wear and corrosion.

ii. To investigate the chemical compositions of the two aluminium alloys: 7075-T651 and 6101-T6.

iii. To determine the mechanical properties (tensile behaviour and hardness) of the two dissimilar aluminium alloys, 7075-T651 and 6101-T6.

iv. To design and fabricate two different tools namely a tapered threaded pin and a tapered unthreaded pin.

v. To conduct a trial welding based on the literature to ascertain workable process parameter ranges and to design a welding matrix for the experiment using Taguchi mini-tab software.

vi. To carry out friction stir welding with the experimental design matrix for each tool.

vii. To investigate the integrity of the welded samples from both tools through physical observation and mechanical testing (microhardness and tensile strength) and to then determine the better tool and optimise the parameters from the tool.

viii. To carry out in-situ temperature measurements on selected parameters of the welds.

ix. To make metallographic preparations of the welded samples for further characterisation which will be done using a mounting press, and grinding and polishing machines.

x. To perform wear tests using a tribometer on selected welds based on their tensile performance.

xi. To make microstructural observations of the metallographically prepared and etched samples using an optical microscope, (OM) and a scanning electron microscope (SEM).

xii. To establish the correlation between welding parameters (tool rotational speed and welding speed) and outputs such as mechanical properties, temperature, wear, microstructures and material flow behaviour of the welds.

1.15 THESIS OVERVIEW

The research content is schematically represented in Figure 1.7. The thesis presentation comprises four chapters and is presented in **article format** in accordance with the approved guidelines of the Faculty of Engineering and the Built Environment, University of Johannesburg. Presentations in each chapter are elaborate and logically related to one another to give a clear understanding of the work.

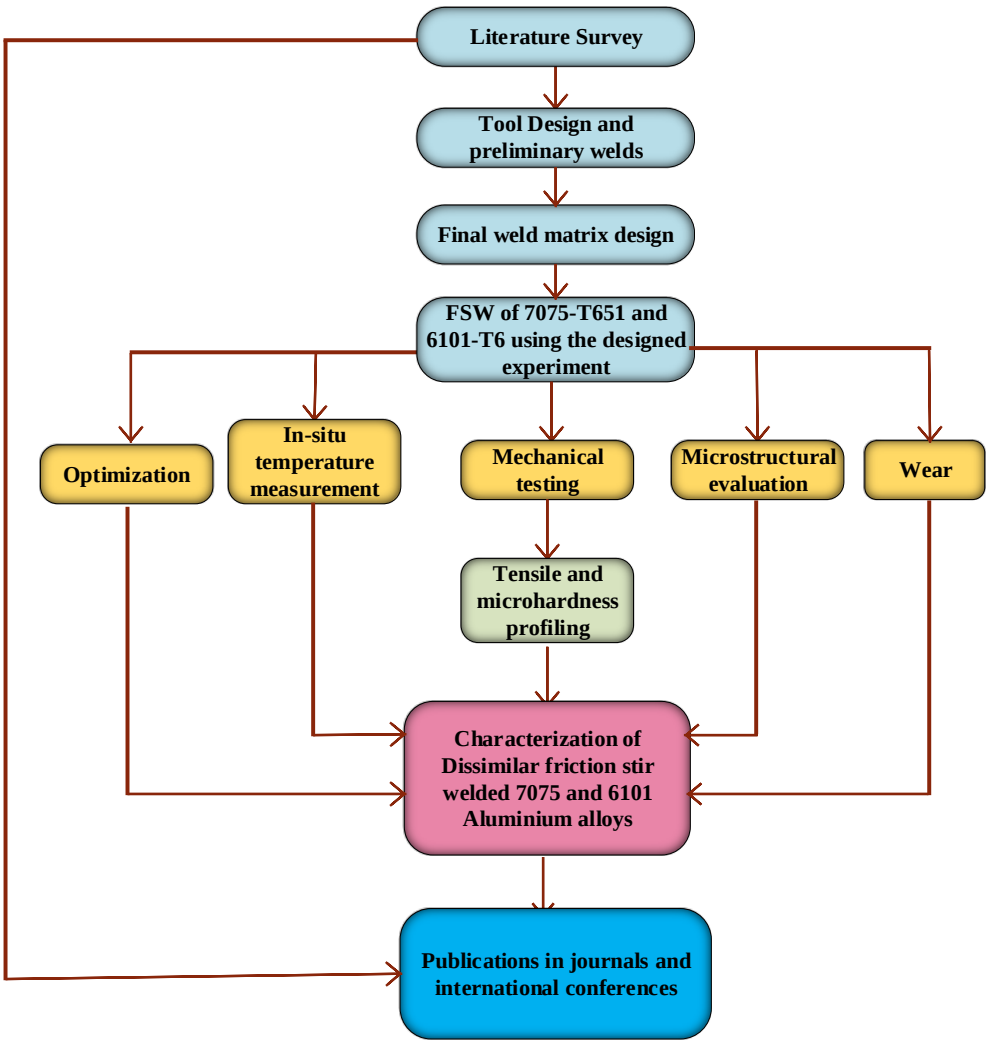

Figure 1.7 Schematic representation of the research work.

Chapter 1

This chapter contains the introduction as the main section. The subsections comprise background information about welding technology, the classification of welding, aluminium alloys, FSW of aluminium alloys, statement of the problem, the motivation for the study, and the significance of the study. The aim and objectives of the research work are also discussed in this chapter.

Chapter 2

This chapter contains all the peer-reviewed articles that have been published or accepted for publications in ISI/Scopus-indexed and DHE-approved journals. Seven journals articles are summarised in this chapter. Article 1 provides a critical review of the corrosion and wear in friction stir welded aluminium alloys including the direction of future research in this field. Article 2 covers in-process cooling in FSW of aluminium alloys. Article 3 discusses the optimisation of process parameters using Taguchi for the FSW of dissimilar aluminium alloys. Article 4 covers the effects of processing parameters on mechanical behaviour, and material flow and wear behaviour of friction stir welded 6101-T6 and 7075-T651 aluminium alloys. Article 5 presents the effects of processing parameters on temperature distributions, tensile behaviour, and microstructure in FSW of dissimilar aluminium alloys. Article 6 covers the tool rotational speed impact on temperature variations, mechanical properties, and microstructures of FSW of dissimilar high strength aluminium alloys. Article 7 discusses the impact of tool profiles on mechanical behaviour and material flow in FSW of dissimilar aluminium alloys.

Chapter 3

This chapter presents two articles published in peer-reviewed Scopus-indexed conferences. The one in section 3.2 is a review and analysis of the reported mechanical properties of friction stir welded aluminium alloys while the article in section 3.3 contains experimental data and an analysis including relevant conclusions to achieving the overall objectives of this research work.

Chapter 4

The findings of this research are summarised in this chapter. The recommendations for future work on the FSW of dissimilar 6101-T6 and 7075-T651 aluminium alloys are also given.

CHAPTER TWO

SUMMARY OF PUBLISHED AND ACCEPTED SCOPUS/ISI LISTED JOURNALS

2.1 INTRODUCTION

This chapter contains all the published and accepted articles submitted to journals listed in Scopus or ISI, and are accredited by the Department of Higher Education and Training (DHET) of South Africa. All the articles are in conformity with the respective journal formats and requirements.

The author of this thesis is the main contributor and the first author of all the published and submitted articles presented in the chapter. The literature survey, experiments and analysis of the results in all the articles were carried out by the author.

2.2 ARTICLE I

Wear and Corrosion Behaviour of Friction Stir Welded Aluminium Alloys- An Overview

Published in International Journal of Mechanical and Production Engineering Research and Development (IJMPERD). Vol. 9, Issue 3, Jun 2019, 967-982. (**Scopus- Indexed**)

In this article, an extensive review of wear and corrosion characteristics in similar and dissimilar joints of aluminium alloys welded via FSW was presented. The review captured the effects of

FSW on mechanical and electrochemical behaviour of friction stir welded aluminium alloys and the lifespan of the welds. Wear and corrosion being the two important degradation processes in metals, affect friction stir welded joints of aluminium alloys. Their effects are reviewed in the article.

Wear and corrosion were found to be influenced by various factors such as the microstructures of the weld joint, additions of alloys or reinforcements to the weld joints, processing parameters employed during the welding, electrochemical solutions or environments which the weld is subjected to, heat treatment, and grades of the aluminium alloys being joined together in similar or dissimilar welding. The types of corrosion and methods of wear and corrosion measurement were also captured in the review.

The review shows that corrosion and wear resistance is favoured by grain size reduction in the weld zone. Additions of alloys or reinforcements to the weld were revealed in the review to mitigate against corrosion susceptibilities and also improve wear resistance. The review further highlighted the significant impacts of process parameters on corrosion and wear behaviour of both similar and dissimilar friction stir welds. The article compared corrosion in similar friction stir welds of aluminium alloys to those of their parent metals and indicated that most welded joints in similar welds exhibit more resistance to corrosion and wear than the parent alloys. The review also indicates that corrosion characteristics of friction stir welded alloys demonstrate different degrees of corrosion resistance in different electrochemical media such as air, seawater or 3.5 % NaCl and EXCO solution. The corrosion behaviour of dissimilarly friction stir welded aluminium alloys was also examined, and the available literature revealed that the corrosion susceptibilities in dissimilar aluminium alloys differ as a result of different electrochemical compositions. The review also

touched on the effects of heat treatment on the corrosion characteristics of both similar and dissimilar aluminium alloys. It was found that RRA heat treatment performed on a welded joint considerably improves resistance to corrosion, especially SCC. PWAA was also found to reduce SCC.

New research questions were given in the article and gaps were identified in the tribological and electrochemical field on friction stir welded aluminium alloys for future explorations.

International Journal of Mechanical and Production Engineering Research and Development (IJMPERD)
ISSN(P): 2249-6890; ISSN(E): 2249-8001
Vol. 9, Issue 3, Jun 2019, 967-982
@TJPRC Pvt. Ltd.

WEAR AND CORROSION BEHAVIOUR OF FRICTION STIR WELDED ALUMINIUM ALLOYS- AN OVERVIEW

OLATUNJI P. ABOLUSORO[1*] & ESTHER T. AKINLABI [2]

[1,2]*Department of Mechanical Engineering Science, University of Johannesburg, Gauteng, Auckland Park, Kingsway Campus, Auckland Park, Johannesburg, South Africa*

[2]*Department of Mechanical Engineering, Covenant University Ota, Nigeria*

ABSTRACT

The need to enhance the integrity and durability of welds to minimize cost and material wastage has led to the demand for more understanding of weld degradation processes, such as wear due to mechanical loading and corrosion when the materials are operated under corrosive conditions. Corrosion and wear in friction stir welding of some aluminum alloys have been investigated separately, understanding how friction stir welds perform under wear and corrosion conditions are significant, so that the durability and lifetime of welds can be predicted and extended. This paper reviewed available literature concerning the development in tribological and corrosion behavior of friction stir welds of both similar and dissimilar aluminum alloys. The review also highlighted various forms of wear and corrosion and factors affecting their mechanism in friction stir welds of aluminum alloys. The review generally showed that corrosion and wear are significantly influenced by the processing parameters employed for the welding and the resulting microstructure and mechanical properties of the welds. The need for further studies on the synergistic or antagonistic effects of the combination of wear and corrosion on friction stir welding of aluminum alloys is also highlighted.

KEYWORDS: Aluminum Alloys, Corrosion, Friction Stir Welding & Wear

Received: Feb 26, 2019; **Accepted**: Mar 18, 2019; **Published**: May 20, 2019; **Paper Id.**: IJMPERDJUN2019105

Original Article

INTRODUCTION

Aluminum alloys are principal materials that have found usage in many industries as a result of its mechanical properties, structural virtues, fabrication, high resistance to corrosion, weldability. etc. (Elatharasan &Kumar, 2014; Vieira, Rocha, Papageorgiou, & Mischler, 2012). Among the various welding methods used to join metals together, especially low-temperature alloys like Aluminium, friction stir welding has emerged the most suitable today for processing Aluminium alloys. This is attributed to its numerous merits over conventional fusion welding techniques. Friction stir welding technology is a joining technique that made use of a tool rotating with a shoulder and pin deepened into the joint of the two materials to be welded and then traverse along the line to form the weld. Heat is produced by the frictional movements of the rotating tool on the joint workpiece. This heating result in plastic deformation of the material at high temperature. This welding technology has found applications in many industries and has been utilized to join Aluminium alloys both homogenous and heterogeneous alloys.(Givi & Asadi, 2014), (Hovanski, Carsley, Clarke, & Krajewski, 2015), (Padhy, Wu, & Gao, 2017),

During Friction stir welding of Aluminium and its alloys, the plasticization that occurs changes the welded joint microstructure and mechanical properties. These changes affect the mechanical and electrochemical

behavior of welds in terms of wear and corrosion.(Threadgill, Leonard, Shercliff, & Withers, 2009) The durability and lifetime of welds in mechanical devices critically depend on their corrosion and wear resistance (Esther T Akinlabi, Andrews Anthony, Stephen A, Akinlabi 2014). Corrosion and wear have been identified as a key factor responsible for material degradation. Many researchers have been attracted to the friction stir welding technology and of recent particular attention are being given to the wear and corrosion behavior aspects of the welded joints.

This review is aimed at presenting an overview of reported findings on wear and corrosion behavior of friction stir welding of Aluminium and its alloys, and the need for further research in the field.

CORROSION IN FRICTION STIR WELDING OF ALUMINIUM ALLOYS

Corrosion can be explained as the decay of metal following a chemical reaction with its immediate environments. (Givi & Asadi, 2014), (Ponthiaux, Wenger, & Pierre, 2012). Corrosion occurs in metals mainly through electrochemical means between the surface of the metal and the electrolyte. Corrosion in metals can occur in different forms. (Ponthiaux et al., 2012), (Kuiry, 2012), (Arora, Mukherjee, Grewal, Singh, & Dhindaw, 2014), Figure 1 shows different categories and forms of corrosion. A brief description of these forms of corrosion in metals is highlighted below.

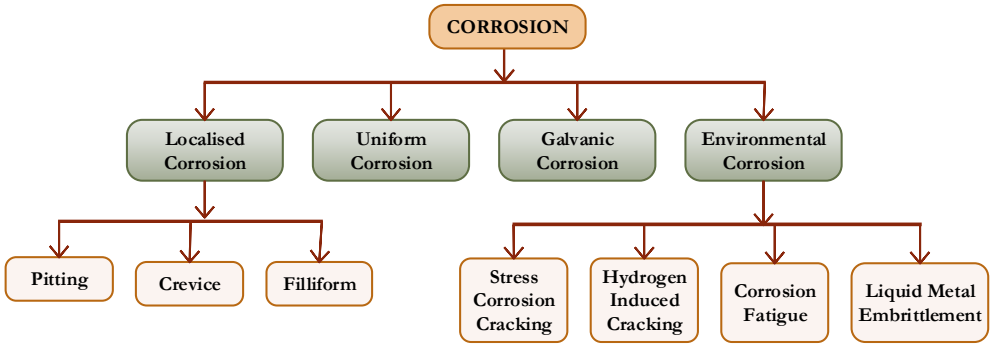

Figure 1: Schematic representation of corrosion and its different forms

- **General Attack/Uniform Corrosion**: This occurs when the entire surface of the metal structure is affected. This type of corrosion is easily predictable and therefore can be easily prevented.
- **Localized Corrosion**: This happens when only a portion of the metal surface is affected. Localized corrosion can be in the following forms.
- **Pitting Corrosion**: Created small holes in the metal surface. It happens in a localized area of the metal due to a broken layer of the protective oxide.
- **Crevice Corrosion**: This occurs when liquid stagnated in a crevice over a long period of time and reduction in Oxygen or acidic conditions of the environment. Examples include clamps, welded joints, and threaded portions
- **Filiform Corrosion**: This occurs when water gets under coatings e.g. paints, weakness.
- **Galvanic Corrosion**: This takes place when two metals having varying electrochemical potentials are found in an electrolyte such as salt water, the metals with greater potential is called anode and the other with lower potential acts as a cathode. An electrochemical reaction takes place between the metals causing the anode to dissolve or corrosion to occur. Galvanic corrosion occurrence depends on these three factors. These are; the presence of dissimilar electrochemical metals, electrical contacts of the metals and the presence of the metals in an electrolyte.

- **Environmental Cracking**: Stress from the environment, temperature and chemicals can make some metals to crack or fatigue or become brittle. This type of corrosion include:
- Stress corrosion cracking (SCC)
- Corrosion fatigue
- Hydrogen-induced cracking
- Liquid metal embrittlement.

Measurement of Corrosion

An Electrochemical measuring device is used to analyze results obtained from the corrosion test system. It performs open circuit potential measurements, electrochemical polarization, electrochemical impedance, yield corrosion potentials, current data and rate of materials removal own to corrosion. (Kuiry, 2012), (Ponthiaux et al., 2012).

The region of weldments that are prone to corrosion in most alloys is generally predictable. An example, very known to professionals is Austenitic stainless steel, where decay in welds occur own to chromium removal by the formation of chromium carbides in the heat affected zone (HAZ). (Donatus, 2017). For Aluminium alloys, it is not easy to predict the corrosion morphology of the weldments. Factors like thermomechanical treatments grain sizes, the composition of alloys, types of precipitates, characteristics of the near surface deformed layers and processing parameters influence the corrosion susceptibilities of the weldments (Donatus, 2017). Available works on the extent to which, these factors above influence corrosion is reviewed below.

Effects of Microstructure on Corrosion

Aluminium alloys consist of about eight series. The alloy in each series constitutes different alloy elements. The alloy elements are introduced to the parent metal to promote certain properties like mechanical, wear and resistance to corrosion. During friction stir welding of homogenous and heterogeneous aluminium alloys, these properties are altered. This is due to severe plastic deformation of the metals being joined together. Severe plastic deformation can result to chemical and microstructural changes. (Arora et al., 2014), (Bousquet, Poulon-Quintin, Puiggali, Devos, & Touzet, 2011), (Davoodi, Esfahani, & Sarvghad, 2016), (Chen, Li, & Hihara, n.d.).

Gharavi et al (Gharavi, Matori, Yunus, Othman, & Fadaeifard, 2015) investigated corrosion morphology and microstructure analysis of friction stir welding of AA6061-T6 Aluminium alloys. They revealed that the welding process affected the resistance to corrosion of the joint due to the degradation of intermetallic particles. They further show that by reducing the size of the grains in the weld region, the resistance to corrosion is reduced. Also, Chen et al (Chen et al., n.d.) in their investigation of mechanical properties, microstructure and corrosion of friction stir welding of 6061 Aluminium alloy, reported that corrosion is lowest in the stirred zone of the weld as a result of microstructural specimen orientation. Ralston et al (Ralston, Birbilis, & Davies, 2010) studied how grain size affects corrosion and concluded that corrosion resistance of smaller strain containing mainly large undissolved size is poor and that increase of strain leads to better resistance to corrosion. Similarly, Ralston et al (Ralston, Fabijanic, & Birbilis, 2011) in another study on high purity Aluminium alloy also concluded that corrosion tendency is high when the grain size increases and low when the size decreases. Bousquet et al (Bousquet et al., 2011) investigated the connection between hardness, corrosion susceptibilities, and microstructure, of AA2024-T3. They showed that the heat affected zone (HAZ) close to the thermomechanical

affected zone (TMAZ) has the highest susceptibilities to intergranular corrosion. This is due to the occurrence of unbroken line S^I (S) intergranular precipitates at the edges of the grain. In addition, the pitting corrosion observed was as a result of intermetallic fragmentation of the particles due to the stirring action of the tool during the welding. Davoodi et al (Davoodi et al., 2016) investigated corrosion and microstructure behaviour of FSW zone of aluminium AA5083/AA7023 dissimilar weld. Corrosion examination revealed that resistance to corrosion of weld areas lies in-between that of AA5083 and AA7023, and that AA5083 has comparatively lower volt potential than AA7023. They further added that corrosion begins at the weld boundary and the regions around intermetallic particles, especially in AA7023 side.

In a related development, the resistance to corrosion behavior of FSW of AA71080-T79 aluminium was studied by Wadeson et al. (Wadeson et al., 2006). Results obtained show that the boundary thermomechanically affected zone (TMAZ) was prone to corrosion. The report also indicates intergranular occurrence of localized corrosion. This was attributed to non-uniformity in the distribution of $MgZn_2$ precipitates in the TMAZ unlike the parent alloy that had its precipitates relatively uniform in distribution. Further influence of precipitates on corrosion behavior was revealed in the study of FSW of 2024 Al alloy by Wang et al (L. Wang, Hui, Zhou, Xu, & He, 2016). Microstructural evaluation of the alloy revealed the occurrence of two different phases of precipitates in the base alloy. Al_2CuMg and Al-Cu-Fe-Mn phase. The distribution of Mg in the first phase of the weld was not uniform with greater concentrations at the middle, which diminishes towards the edge of the particles.

Also, the corrosion susceptibilities of weldzone of a Friction Stir Welded joint of 2050 Al-Cu-Li alloy was studied by Proton et al (Proton et al., 2013). The outcome revealed that the weldzone was prone to inter and intragranular corrosion. This type of behaviour in corrosion was due to differences in microstructures noticed on a small dimension. Also, differences in corrosion characteristics of the weld zone noticed on a small scale were due to different behavior of corrosion from one end of the weld zone to another and also by a localization of the damage by corrosion attributed to the "Onion ring structure". (Ralston et al., 2011)

The relationship between microstructure and corrosion behavior might have been established from the above literature. However, a comprehensive understanding of the corrosion mechanism, grain refinement, and processing applicable to different grades of aluminium alloys is yet to be fully developed.

Effects of Additions of Alloys and Reinforcements

Effects of addition of alloys on corrosion behaviour in friction stir welding have been experimented. Recently, the corrosion behavior of Zn modified friction stir welding of Al-Mg alloys was investigated by Hou Longgang et al (Hou Longgang, Yu Jiajia, Zhang Di, Zhuang Linzhong, Zhou Li, 2017). Their results indicated that both maximum corrosion depth, and the dominating corrosion mode vary with increase in Zn content. The addition of Zn changes the corrosion from intergranular corrosion to pitting corrosion. In another research, Vijaya Kumar et al (Vijaya Kumar, Madhusudhan Reddy, & Srinivasa Rao, 2015) experimented the effect of Boron carbide (B_4C) addition on the corrosion susceptibilities of FSW of AA7075 alloy. They concluded that the B_4C nanoparticles addition significantly improved pitting corrosion of the weld. Furthermore, Kartsonakis et al, (Kartsonakis, Dragatogiannis, Koumoulos, Karantonis, & Charitidis, 2016) studied corrosion characteristics of dissimilar friction weld of (AA)6082-T6 and AA5083-H111 aluminium alloy. Multi-walled carbon nanotubes, cerium molybdate (CeMo) and titanium carbide reinforced with 2-mercaptobenzothiazole (MBT) were used as nanoadditives. The sample susceptibilities to corrosion with nanoadditives and that without nanoadditives were examined using electrochemical techniques. The outcome showed that the addition of CeMo and MBT as the FSW takes

place improved resistance to corrosion of the final metal. This was due to the accumulation of $(MoO4)^{-2}$ ions that emanate from the shell container to the outer surface of the two alloys and the development of stabilized complexes among the thiol groups of MBT and also due to the alloy of the metals stopping the entrance of chloride. In another study by Hatamleh et al (Hatamleh, Singh, & Garmestani, 2009) on corrosion susceptibilities of AA7075 Aluminium alloy during peened friction stir weld, the samples were brought under slow strain rate examination in 3.5% NaCl solutions. Observation showed no sign of stress corrosion cracking SCC or pitting corrosion on the welded sample during the slow strain rate test. However, exposure of the friction stirred welded plates to 3.5% NaCl solutions for 60 days showed pitting corrosion on the sample, but stressed corrosion cracking was not observed on any of the peened and unpenned samples. The results generally show that the rate of corrosion was small for all treated surface samples. Sizes and number of pits was larger on the unpenned surface and smaller on the shot peened surface.

Effects of Welding Parameters

Researchers have revealed that corrosion behavior of weldments could also be influenced by processing parameters like tool design, rotational and transverse speed etc. This is because, these factors influence the extent of mixtures, highest temperature attained, temperature gradient and the distribution of heat. (Arora et al., 2014), (Elatharasan & Kumar, 2014). The effects of process parameters and its influence on corrosion is reviewed in this section.

D'Urso et al (D'Urso, Giardini, Lorenzi, Cabrini, & Pastore, 2017) investigate the influence of the processing parameters on resistance to corrosion of friction stir welding of aluminium AA2024 and AA7075. The welding was carried out with varied processing parameters, like rotational speed and rate of feed. The corrosion behavior of welds was studied using local unconstrained corrosion potential evaluation to locate the anode and cathode regions of the welds. The outcome revealed that the lower hardness region has greater anodic free corrosion potential than the closest areas. The potential difference between the various regions of the welds results to galvanic corrosion of the less susceptible region. The anodic position and the region covered were determined by both the welding parameters and the alloy. In the case of AA2024, an intense pitting and crevice attack were observed while the AA7075 showed exfoliation corrosion on the rolling bands. Joining both alloys resulted in intense galvanic corrosion damage on the AA7075 in the lower hardness region. The decrease in hardness and the difference in electrochemical behaviour of the weld were caused by microstructural disruption of the alloys during the FSW. The authors concluded that the connections between process parameters and welds joint properties have led to the identification of the optimum welding conditions. Hassan et al (A. S. Hassan, Mahmoud, Mahmoud, & Khalifa, 2010) studied the corrosion morphology of dissimilar friction stir welding of A319 and A356AL alloy. Effects of welding and tool rotation speed including post-weld heat treatment (PWHT) on corrosion susceptibilities were also studied. Tool rotational speeds of 1800, 1400 and 1120 rpm with welding speeds of 112 and 80mm/min were used. The PWHT was carried out at duration of 12 hours with the temperature at 540^0C and then aged at 155 °C for a period of 6 hours. Corrosion resistance test of the welds was carried out by immersing it for 6 hours in a solution of sodium chloride (NaCl) and hydrogen peroxide (H_2O_2). The results indicate that both as welded and post weld heat treated samples exhibited higher resistance to corrosion than both base alloys. Resistance to corrosion of the weld portion was equally found to reduce when the tool rotational speed increase and/or when the welding speed reduces. In another study on effects of processing parameter on corrosion of FSW of AA2024-T345 by Jariyaboon et al (Jariyaboon et al., 2007), results obtained show that rotational speed determines the attack location in the weldment region. For low speed, corrosion attack mainly occurs in the stir zone whereas for higher speed it occurs in the heat affected zone. In

related research, Bousquet et al (Bousquet et al., 2011) results were in agreement with the above. Their result also indicates that corrosion susceptibility in the Heat Affected Zone (HAZ) was attributed to S^{I}-(S-Al_2CUMg) phase at the boundaries of the grains. Also Kang et al (Kang, Fu, Luan, Dong, & He, 2010) showed that pitting corrosion density and the extent of the attack was a bit greater in the shoulder area during FSW of AA2024-T3. They also observed that optimum welding parameters can improve resistance to corrosion of weldment. Also, Esmaily et al. (Esmaily et al., 2016) in their findings on the friction stir weld of AA6005-T6 alloy reported that the nugget zone is prone to pitting corrosion, but the range of the pitting corrosion attack in the nugget zone reduces with increase in number of friction stir passes. However, an increase in the number of friction stir passes induced pitting corrosion in the HAZ of the weld. Another outcome of research by Venkata subramanian et al (Venkatasubramanian, Mideen, & Jha, 2012)) on corrosion behavior of FSW of 2219 Aluminium alloy evaluated at different depth show that the upper surface of the welded zone has stronger corrosion resistance and it reduces with depth. Also, the stirred region was found to have better resistance to pitting corrosion than the parent metal and that the resistance to corrosion reduced with an increase in traverse speed for fixed tool rpm. Furthermore, higher tool rpm led to coarsening of the Al_2Cu precipitates, thereby increasing pitting corrosion in the nugget region. However, for friction stir welding of dissimilar alloys of Al and Cu, Esther and Andrews (Esther T Akinlabi, Andrews Anthony, 2014) reported that corrosion behavior improved as the rotational speed of the tool increased. In another related study Elatharasan & Kumar (Elatharasan & Kumar, 2014) evaluated corrosion resistance of FSW of AA7075 and found that HAZ of the weld showed the highest tendency to intergranular corrosion and that resistance to corrosion decreases with increase in the traverse speed.

It is obviously established that welding parameters influence to a considerable extent the corrosion susceptibilities of welds. More experimental findings to optimize these process parameters to achieve a reduction in corrosion rate for different friction stir welding of homogenous and heterogeneous aluminium alloys will still be of great benefits.

Corrosion in Welds and Their Parent Metals

Comparing the corrosion characteristics of base metal with their similar friction stir welded joints, de Abreu et al (de Abreu et al., 2017) studied multiple scale electrochemical structures of FSW of 7475-T651 and 2024 -T3 aluminium alloys. Their result shows higher corrosion in the stir zone of the weld compares to the two-parent metals. Galvanic coupling occurred with AA7475 acting as the anode and AA2024 as the cathode. Zn deposit reportedly occurred on the intermetallic particles of the AA2024 after a day. However, Wang (H. Wang, 2016) results on FSW of 7022 alloys showed that the corrosion in the base alloy is greater than that of the welded joints and that corrosion resistance optimum result was obtained at 400rpm and 30mm/min. This result was in agreement with Zhao et al's study on FSW of 6082 aluminium alloy corrosion performance. Also, Chen & Hihara (Chen, Li, & Hihara, n.d.) investigated FSW of 6061 Aluminium alloys and reported that FSW improved the corrosion resistance and that the heat affected zone had better corrosion resistance than other regions of the weld. This was in agreement with their separate studies on corrosion of FSW of AA5086 under the same electrochemical conditions. Contrarily Dudzik & Jurczak, (Dudzik & Jurczak, 2016), evaluation of the corrosion properties of FSW of AW7020 alloy in seawater revealed that the parent metal exhibit better corrosion in seawater condition than the friction stir welded joint which shows more susceptibilities to corrosion. Further comparison of parent metals to friction stir welded samples was also carried out by Corral et al (Corral, Trillo, Li, & Murr, 2000). They studied pitting corrosion and stress corrosion cracking of FSW of 5454 in O- and –H34 tempers. The welded joint was discovered to exhibit better resistance to pitting corrosion than the parent metal. Discontinuities defect that may be associated with

remnants boundaries of the base metal were noticed. These defects led to an increase in corrosion susceptibilities intermittently.

Corrosion in Different Electrochemical Solution

The corrosion behaviour of welded samples could be greatly influenced by the electrochemical conditions, in which it is used. Some authors have investigated corrosion of friction stir welded sample in various electrochemical solutions. Pao et al. (Pao, Gill, Feng, & Sankaran, 2001) studied crack growth of corrosion fatigue of FSW 7050 aluminium alloy in both air and 3.5% NACl solutions They reported that corrosion fatigue growth rate in air in the welded zone is a little greater than that of the base metals but in the heat affected zone, the fatigue is lower in both air and in the 3,5% NACl solutions. In related work, Zucchi (F. Zucchi, 2001) studied corrosion behavior of FSW of 5083 in 3.5% NACl and EXCO solution. The FSW showed higher resistance to corrosion in EXCO and lower pitting corrosion susceptibilities than the parent metal.

More studies could focus on the use of different electrochemical conditions depending on the area of applications of the weld.

Corrosion in Dissimilar FSW of Aluminum Alloys

Corrosion susceptibilities of FSW of dissimilar Aluminium alloys have been investigated by various researchers. Jayaraj et al (Jayaraj, Malarvizhi, & Balasubramanian, 2017) reported that interrelated microstructure could be noticed in the stir zone of FSW of dissimilar Aluminium alloys own to the mixing of the two alloys. The complex flow pattern of the stir zone gave rise to galvanic coupling, because of the differences in potential between the two metals. This makes studying corrosion in dissimilar metals imperative. LU. Donatus et al (LU.Donatusa, G.E.Thompsona, X.Zhoua, J.Wanga, A.Cassella, 2015) in another study examined corrosion behavior of dissimilar FSW of AA5083-0 and AA6082-T6 alloys. They established in their report that high welding speed increased proneness to corrosion and that the HAZ of the two alloys, the Mg_2Si particles distribution along the grain boundaries of the both alloys and the galvanic contacts of the two alloys were the cause of the weld corrosion susceptibilities. Corral et al's (Corral et al., 2000) outcome on the investigation of corrosion performance of FSW of 2024 and 2195 Aluminium alloys shows that both alloys exhibit nearly the same corrosion potentials with their FSW joint. In another corrosion investigation in dissimilar weld of aluminium alloy, Jariyaboon et al (Jariyaboon et al., 2006) established that the stirred zone of the friction stir welded AA2024 and AA7010 is prone to intergranular corrosion damage. However, Dilip et al (Dilip, Koilraj, Sundareswaran, Janaki Ram, & Koteswara Rao, 2010) in their findings on corrosion behavior of FSW of Aluminium alloys reported that the corrosion characteristics exhibited by the dissimilar friction stir welded joint of 2219 and 5083 was better than that of similar FSW of 2219 and 5083 and also better than the 2219 base materials. Furthermore, Ahmad et al (Ahmad, Ul-Hamid, & B.j, 2001) welded another dissimilar aluminum, alloys 5052 H34 and 7075-T6 and examined the corrosion behavior of the weld using potentiostat in two solutions 0.5% HCl and 0.5% NaOH. Tafel extrapolation and cyclic polarizations methods were employed to measure the specimen's resistance to pitting corrosion. The findings obtained showed that the best resistance to corrosion of welded joint was obtained in 0.5% NaOH compared to 0.5% HCl. The rate of corrosion of FSW joint was greater than base alloys in 0.5% NaOH, whereas it's lower than base alloys in 0.5% HCl. The Base metal alloys are more prone to pitting corrosion than the friction stir welded joint. The joint showed better resistance to corrosion in NaOH and HCl media. In related research, Wei & Gao (Wei, Liao, & Gao, 1998) investigated corrosion resistance of base Al-alloys 2024-T3 and 7075-T73 similar and dissimilar friction stir welded alloys in seawater (3.5% NaCl solution) at ambient

temperature using Potentiostat. The outcome of corrosion behaviour indicates that the parent alloys has higher corrosion resistance than the weld. This is due to particle content and secondary phases formed during stir welding that act as active zones to increase pits thereby promoting corrosion in seawater. Dissimilar welded Al2024-T3/Al7075-T73 showed higher susceptibilities to corrosion than the galvanic coupling of the same alloys. The potential and corrosion current density of dissimilar welded Al2024-T3/Al7075-T73 were given as -793.7 mV and 5.32 $\mu A.cm^{-2}$ respectively, whereas, galvanic coupling had potential equal to -653 mV with a current density of 1.0025 $\mu A.cm^{-2}$. It was also shown that the rate of corrosion of dissimilar weld was lower than that of similar welds of Al2024-T3 and Al7075-T73.

The literature survey in this section indicates that corrosion behavior of all dissimilar friction stir welded aluminium alloys is not homogenous. All the aluminium series have varying properties in terms of corrosion resistance and the type of corrosion attack suffered by the materials. Processing parameters and other factors equally play a role in determining corrosion morphology in friction stir weld of heterogenous aluminium alloys. Proper correlation of corrosion susceptibilities with properties exhibited in dissimilar aluminium alloys welded joints could be explored further.

Effects of Post-Weld Heat Treatment (PWHT)

Reports from various researchers have shown that post weld heat treatment has effects on corrosion characteristics. Vijaya Kumar et al. (Vijaya Kumar et al., 2015) performed retrogression and reaging (RRA) post-weld heat treatment on friction stir welded (FSWed) joint of AA7075 to determine the corrosion behavior. Their findings show appreciable improvement in pitting corrosion resistance. Stress corrosion cracking (SCC) is enhanced but with little loss in hardness. Post weld artificial aging (PWAA) method has been applied to some alloys to reduce stress corrosion cracking. Pao et al (Pao, P.S., Gill, S.J., Feng, C.R., and Sankaran, 2001) have shown the restoration of resistance to stress corrosion cracking in 7050-T7451 through PWAA for a 24hour at 121^0c after testing in a 3.5% NaCl solution. Sankaran et al (Sankaran, K.K., Smith, H.L., and Jata, 2002) in another study evaluated the corrosion susceptibilities of some Aluminium alloys after PWAA treatment. Their result showed that corrosion behavior of the welded joint is comparable to that of the parent metal. Similarly, Dunlavy and Jata (Dunlavy, M., and Jata, 2003) evaluated the corrosion fatigue behavior of the combination of the same alloy after PWAA. Their result showed that the fatigue strength of the welds decreased by half. Widener et al (Widener, Burford, Kumar, Talia, & Tweedy, 2007) also attempted to improve the corrosion performance of 7075 Aluminium alloy through a various combination of PWAA and starting temper. The 7075-T73 and 7075-T6 were passed through PWAA. They concluded that welding in T73 followed by PWAA performs better in terms of corrosion resistance than welding in T6 temper and aging to T73. They equally added that PWAA for about 4hours at 325^0F enhanced resistance to corrosion.

Research has shown that PWAA has the potential of restoring SCC. However, it has been reported that in some cases, it reduces resistance to exfoliation. RRA has equally been experimented but not widely.(Widener et al., 2007), (Leonard, 2000). More investigations on PWHT using RRA and PWAA to restore corrosion resistance still beckon on researchers.

WEAR

The response of friction stirred welded joint of Aluminium alloys to wear processes is important for the industrial application. Wear characteristics of friction stir welded joints has been reported by some researchers. The following sections examine the literature in this regard.

Wear Testing Method

Tribometer is an instrument that measures wear. The machine, basically controls mechanical loading, measure frictional force, normal force and evaluation of coefficient of friction (COF) with time and rate at which materials are removed (Kuiry, 2012).

Most of the main friction and wear tests were done via a ball-on-flat configuration in reciprocating sliding and with a pin on disk configuration in a one-directional sliding. Pin on disk wear testing is a technique of analyzing force of friction, frictional coefficient and rate at which wear takes place between two metals. (Syed Khaja N, Md Tousef a, Purna, B. C, Narendra Mohan, Vidhu Kampurath, 2016), (Ponthiaux et al., 2012), (Dinaharan & Murugan, 2011)

The effects of sliding velocities and contact load of the pin-on-disk machine on the rate of wear have been investigated. Wang and Zhang (A. Wang & Rack, 1991), (Zhang & Alpas, 1997), have reported that wear mechanism may change suddenly at particular sliding velocities and contact loads resulting to sudden increase on the rate of wear. Investigations by Glaeser and Ruff showed that Pin-on-disk was the most used wear test method followed by the pin-on-flat method. (Ludema & Bayer, 2012), (A. Wang & Rack, 1991).

Wear in Similar and Dissimilar Friction Stir Welding

Analysis of wear behaviour in similar and dissimilar friction stir welding available in literature have been reviewed below.

Seyed et al (Syed Khaja N, Md Tousef a, Purna, B. C, Narendra Mohan, Vidhu Kampurath, 2016) investigated wear behaviour in similar and dissimilar FSW of AA6061 and AA6082. The wear analysis results revealed that similar welds of AA6061 sample gave better resistance to wear in the welded zone than the other welds. However, dissimilar AA6061-AA6082 weld specimen gave better wear performance in the non-welded zone. Another study on wear behaviour of the same alloys above was carried out by Khaja et al (Khaja Naimuddin, Md, Vidhu, Asim Mohamad, & Ali, 2016). They studied the wear resistance of FSW joint of similar AA6061 and similar AA6082. The wear results obtained from each of the above were compared to that of dissimilar friction stir welded (FSWed) joint of the two alloys. They concluded that FSW of similar AA6061 materials is the most resistance to wear in comparison to similar FSW of AA6082 and dissimilar FSW of both metals. These results show agreement with Seyed et al (Syed Khaja N, Md Tousef a, Purna, B. C, Narendra Mohan, Vidhu Kampurath, 2016).

In related work, Dubey et al (Dubey, Kumar, & Yadav, 2017) investigated the wear characteristics and hardness for FSWed and unwelded portion of cast Al (4-10%) Cu alloy. They discovered that the highest hardness value was obtained at the middle of the nugget region followed by a systematic reduction across the (TMAZ) and the (HAZ). This was correlated with friction stir behaviour.

Effects of Additions of Reinforcements and Processing Parameter on Wear

Wear investigation on FSWded aluminium alloy with the addition of materials as reinforcement has also been carried out. Kalaiselvan and Murugan (Kalaiselvan & Murugan, 2013) studied wear behaviour of Aluminium 6061-B_4C composite. They reported that the occurrence of fine grain microstructure and B_4C particulates in the welded region improve the wear behaviour. In related research, Farahmand and Parvin (Farahmand Nikoo, Parvin, & Bahrami, 2017) investigated wear characteristics in aluminium AA6061-T6 reinforced with nano-particles Al_2O_3 during friction stir

welding and found atremendous improvement in wear resistance.

The effects of processing parameters on wear was reported by Dinaharan & Murugan (Dinaharan & Murugan, 2011). They investigated the influence of FSW parameters on sliding wear properties of AA6061/0-10wt and reported that the rate of wear reduces as tool rotational speed goes higher, but further rise in tool rotational speed could result to increase in rate of wear. A similar study was also performed by Adel et al (A. M. Hassan, Almomani, Qasim, & Ghaithan, 2012) however, their welding was carried out with SiC and graphite reinforced aluminium matrix composite. The wear behavour in relation to the welding parameters investigated revealed an increase in wear resistance of the weld at higher traverse speed and lower rotational speed. Pin profile on the wear characteristics was also studied. The results show that the square pin profile performs better than hexagonal and orthogonal pins investigated. In a related study, Mirjavadi et al (Mirjavadi et al., 2017) welded 5083 aluminium alloy reinforced with TiO_2 using FSW. The optimized parameter was processed from 1 to 4 passes. The wear behaviour investigated indicates a significant improvement in wear resistance for samples welded through four passes.

Temperature influence on the rate of wear for Aluminium silicon alloys has been investigated by Rajaram et al (Rajaram, Kumaran, & Rao, 2010). Their findings showed that the rate of wear decreases when the temperature decreases.

The available literature reviewed above on wear behaviour in FSW shows that welding parameters and additions of other elements as reinforcements to the aluminium matrix considerably affect the wear characteristics. In most cases, improvement is noticed in wear resistance of the reinforced aluminium alloy. Proper choice of operating welding parameters could also enhance wear resistance. More research efforts on wear characteristics of different aluminium composites and grades similarly and dissimilarly welded through FSW under different welding parameters will further broaden the knowledge-based on wear mechanism in FSWded aluminium alloys.

CONCLUSIONS

An overview of wear and corrosion mechanism in friction stir welding of aluminium alloy has been presented. The review highlighted various forms of corrosion mechanism and wear in friction stir welding. The review shows that the weld parameter is a key factor that influences corrosion and wears. Proper control of the weld parameters could help achieve the desired microstructural evolution for proper bonding and high resistance to corrosion and wears. Although the correlation between wear, corrosion, microstructure, mechanical properties, and welding parameters have been established in this reviewed. However, comprehensive knowledge and more understanding of the mechanism involved may still need to be explored. A considerable amount of works has been done separately on wear and corrosion of welded samples of various aluminium alloys, however, the combine effects of wear and corrosion on friction stir welding of aluminium alloys is yet to be fully reported. Findings from a separate experimental study of wear and corrosion may not be sufficient to evaluate the durability of weld, since most corrosion resistance elements are not wear resistance and vice versa. There is complexity in the results of combining wear and corrosion. Information from tribological (wear) behaviour without a corrosive medium and that of the electrochemical behaviour without wear is not adequate enough to fully predict the performance of friction stir welds. Friction and wear affect the susceptibilities of material to corrosion, and conversely corrosion influences the conditions of frictional wear. There is a synergy between wear and corrosion. Therefore; there is a need for further investigation on the combined effect of wear and corrosion in friction stir welding of aluminum alloys. More understanding of the mechanism of interactions of mechanical and electrochemical in friction stir welds will assist in predicting the performance and lifetime of welds.

REFERENCES

1. *Ahmad, Z., Ul-Hamid, A., & B.j, A. A. (2001). The corrosion behavior of scandium alloyed Al 5052 in neutral sodium chloride solution. Corrosion Science, 43(7), 1227–1243. https://doi.org/10.1016/S0010-938X(00)00147-5*
2. *Arora, H. S., Mukherjee, S., Grewal, H. S., Singh, H., & Dhindaw, B. K. (2014). Corrosion behaviour in friction stir processed and welded materials. In Advances in Friction-Stir Welding and Processing (pp. 295–328).*

   https://doi.org/10.1533/9780857094551.295
3. *Bousquet, E., Poulon-Quintin, A., Puiggali, M., Devos, O., & Touzet, M. (2011). Relationship between microstructure, microhardness and corrosion sensitivity of an AA 2024-T3 friction stir welded joint. Corrosion Science, 53(9), 3026–3034. https://doi.org/10.1016/j.corsci.2011.05.049*
4. *Chen, Z., Li, S., & Hihara, L. H. (n.d.). Microstructure, mechanical properties and corrosion of friction stir welded 6061 Aluminum Alloy. Hawaii Corrosion Laboratory, Department of Mechanical Engineering, University of Hawaii at Manoa, Honolulu, HI 96822, USA. https://doi.org/10.1017/CBO9781107415324.004*
5. *Corral, J., Trillo, E. A., Li, Y., & Murr, L. E. (2000). Corrosion of friction-stir welded aluminum alloys 2024 and 2195. Journal of Materials Science Letters, (19), 2117–2122. https://doi.org/10.1023/A:1026710422951*
6. *D'Urso, G., Giardini, C., Lorenzi, S., Cabrini, M., & Pastore, T. (2017). The Effects of Process Parameters on Mechanical Properties and Corrosion Behavior in Friction Stir Welding of Aluminum Alloys. In Procedia Engineering (Vol. 183, pp. 270–276). https://doi.org/10.1016/j.proeng.2017.04.038*
7. *Davoodi, A., Esfahani, Z., & Sarvghad, M. (2016). Microstructure and corrosion characterization of the interfacial region in dissimilar friction stir welded AA5083 to AA7023. Corrosion Science, 107, 133–144.*

   https://doi.org/10.1016/j.corsci.2016.02.027
8. *de Abreu, C. P., Costa, I., de Melo, H. G., Pébère, N., Tribollet, B., & Vivier, V. (2017). Multiscale Electrochemical Study of Welded Al Alloys Joined by Friction Stir Welding. Journal of The Electrochemical Society, 164(13), C735–C746.*

   https://doi.org/10.1149/2.0391713jes
9. *Dilip, J. J. S., Koilraj, M., Sundareswaran, V., Janaki Ram, G. D., & Koteswara Rao, S. R. (2010). Microstructural characterization of dissimilar friction stir welds between AA2219 and AA5083. Transactions of the Indian Institute of Metals, 63(4), 757–764. https://doi.org/10.1007/s12666-010-0116-8*
10. *Dinaharan, I., & Murugan, N. (2011). Influence of Parameters Friction Stir Welding on Sliding Wear Behavior of AA6061/0-10 wt.% ZrB2 in-situ Composite Butt Joints. Journal of Minerals and Materials Characterization and Engineering, 10(14), 1359–1377. https://doi.org/10.4236/jmmce.2011.1014107*
11. *Donatus, U. (2017). Corrosion Behaviour of Friction Stir Welded Aluminium Alloys: Unpredictability and Protection. Research & Development in Materials Science, 1–3. https://doi.org/10.12691/materials-2-3-1*
12. *Dubey, A. M., Kumar, A., & Yadav, A. K. (2017). Wear behaviour of friction stir weld joint of cast Al (4–10%) Cu alloy welded at different operating parameters. Journal of Materials Processing Technology, 240, 87–97.*

    https://doi.org/10.1016/j.jmatprotec.2016.09.003
13. *Dudzik, K., & Jurczak, W. (2016). Influence of Friction Stir Welding (FSW) on Mechanical and Corrosion Properties of AW-7020M and Aw-7020 Alloys. Polish Maritime Research, 23(3), 86–90. https://doi.org/10.1515/pomr-2016-0036*

14. *Dunlavy, M., and Jata, K. V. (2003). High-Cycle Corrosion Fatigue of Friction Stir Welded 7050-T7451. Friction Stir Welding and Processing, II, 91–98.*

15. *Elatharasan, G., & Kumar, V. S. S. (2014). Corrosion analysis of friction stir-welded aa 7075 aluminium alloy. Strojniski Vestnik/Journal of Mechanical Engineering, 60(1), 29–34. https://doi.org/10.5545/sv-jme.2012.711*

16. *Esmaily, M., Mortazavi, N., Osikowicz, W., Hindsefelt, H., Svensson, J. E., Halvarsson, M., Johansson, L. G. (2016). Corrosion behaviour of friction stir-welded AA6005-T6 using a bobbin tool. Corrosion Science, 111, 98–109. https://doi.org/10.1016/j.corsci.2016.04.046*

17. *Esther T Akinlabi, Andrews Anthony, S. A. A. (2014). Effects of processing parameters on the corrosion properties of dissimilar Friction Stir Welds of aluminium and copper. Transactions of Nonferrous Metal Society of China, 24(5), 1323–1330. https://doi.org/10.1111/1365-2664.12806*

18. *F. Zucchi, G. T. andV. G. (2001). Pitting and stress corrosion cracking resistance of friction stir welded AA 5083, 859, 853–859. https://doi.org/10.1002/1521-4176(200111)52:11<853::AID-MACO853>3.0.CO;2-1*

19. *Farahmand Nikoo, M., Parvin, N., & Bahrami, M. (2017). Al2O3-fortifed AA6061-T6 joint produced via friction stir welding: The effects of traveling speed on microstructure, mechanical, and wear properties. Proceedings of the Institution of Mechanical Engineers, Part L: Journal of Materials: Design and Applications, 231(6), 534–543.*

    https://doi.org/10.1177/1464420715602140

20. *Gharavi, F., Matori, K. A., Yunus, R., Othman, N. K., & Fadaeifard, F. (2015). Corrosion behavior of Al6061 alloy weldment produced by friction stir welding process. Journal of Materials Research and Technology, 4(3), 314–322.*

    https://doi.org/10.1016/j.jmrt.2015.01.007

21. *Al-Jalali, M. A. (2014). The Critical Temperature-Concentration Phase Diagrams in Some Kondo and Spin Glass Alloys. International Journal of Physics and Research (IJPR), 4, 9-24*

22. *Givi, M. K. B., & Asadi, P. (2014). Advances in Friction-Stir Welding and Processing. Advances in Friction-Stir Welding and Processing. https://doi.org/10.1016/C2013-0-16268-X*

23. *Hassan, A. M., Almomani, M., Qasim, T., & Ghaithan, A. (2012). Effect of processing parameters on friction stir welded aluminum matrix composites wear behavior. Materials and Manufacturing Processes, 27(12), 1419–1423. https://doi.org/10.1080/10426914.2012.700156*

24. *Hassan, A. S., Mahmoud, T. S., Mahmoud, F. H., & Khalifa, T. A. (2010). Friction stir welding of dissimilar A319 and A356 aluminium cast alloys. Science and Technology of Welding and Joining, 15(5), 414–422.*

    https://doi.org/10.1179/136217110X12720264008358

25. *Hatamleh, O., Singh, P. M., & Garmestani, H. (2009). Corrosion susceptibility of peened friction stir welded 7075 aluminum alloy joints. Corrosion Science, 51(1), 135–143. https://doi.org/10.1016/j.corsci.2008.09.031*

26. *Hou Longgang1, Yu Jiajia1, Zhang Di1, Zhuang Linzhong1,2, Zhou Li3, Z. J. (2017). corrosion behaviour of friction stir welding of Al-Mg-(Zn) Alloy. Rear Metals, Materials and Engineering, 16(9), 2437–2444.*

27. *Hovanski, Y., Carsley, J. E., Clarke, K. D., & Krajewski, P. E. (2015). Friction-Stir Welding and Processing, 67(5), 996–997. https://doi.org/10.1007/s11837-015-1397-5*

28. *Jariyaboon, M., Davenport, A. J., Ambat, R., Connolly, B. J., Williams, S. W., & Price, D. A. (2006). Corrosion of a dissimilar friction stir weld joining aluminium alloys AA2024 and AA7010. Corrosion Engineering, Science and Technology, 41(2), 135–142. https://doi.org/10.1179/174327806X107905*

29. *Jariyaboon, M., Davenport, A. J., Ambat, R., Connolly, B. J., Williams, S. W., & Price, D. A. (2007). The effect of welding parameters on the corrosion behaviour of friction stir welded AA2024-T351. Corrosion Science, 49(2), 877–909. https://doi.org/10.1016/j.corsci.2006.05.038*

30. *Jayaraj, R. K., Malarvizhi, S., & Balasubramanian, V. (2017). Electrochemical corrosion behaviour of stir zone of friction stir welded dissimilar joints of AA6061 aluminium–AZ31B magnesium alloys. Transactions of Nonferrous Metals Society of China (English Edition), 27(10), 2181–2192. https://doi.org/10.1016/S1003-6326(17)60244-9*

31. *Kalaiselvan, K., & Murugan, N. (2013). Dry sliding wear behaviour of Friction Stir Welded aluminum (6061)-B 4C composite. International Journal of Microstructure and Materials Properties, 8(3). https://doi.org/10.1504/IJMMP.2013.055386*

32. *Kang, J., Fu, R., Luan, G., Dong, C., & He, M. (2010). In-situ investigation on the pitting corrosion behavior of friction stir welded joint of AA2024-T3 aluminium alloy. Corrosion Science, 52(2), 620–626. https://doi.org/10.1016/j.corsci.2009.10.027*

33. *Kartsonakis, I. A., Dragatogiannis, D. A., Koumoulos, E. P., Karantonis, A., & Charitidis, C. A. (2016). Corrosion behaviour of dissimilar friction stir welded aluminium alloys reinforced with nanoadditives. Materials and Design, 102, 56–67. https://doi.org/10.1016/j.matdes.2016.04.027*

34. *Khaja Naimuddin, S., Md, T., Vidhu, K., Asim Mohamad, M., & Ali, Y. (2016). Analysis of Wear Behaviourof the Friction Stir Welded Jointswith Varying Track Diametersfor Non-Welded and Welded Samples. Indian Journal of Science and Technology, 9(41). https://doi.org/10.17485/ijst/2016/v9i41/100936*

35. *Kuiry, S. (2012). Evaluation of Wear-Corrosion Synergy Through Tribocorrosion Studies. Bruker, 1–24.*

36. *Leonard, A. J. (2000). Corrosion Resistance of Friction Stir Welds in Aluminum Alloys 2014A-T651 and 7075-T651. 2nd International Friction Stir Welding Symposium, june, 26–28.*

37. *LU.Donatusa, G.E.Thompsona, X.Zhoua, J.Wanga, A.Cassella, K. B. (2015). Corrosion susceptibility of dissimilar friction stir welds of AA5083 and AA6082 alloys. Material Characterization, 107, 85–97.*

38. *Cicek, V., & Ozdemir, M. (2013). Aqueous Corrosion Inhibition Studies of Aluminum 2024, 6061, and 7075 Alloys by Oxyanion Esters of α-Hydroxy Acids and Their Salts. International J. of Applied and Natural Sciences (IJANS), 2(2), 9-16.*

39. *Ludema, K. C., & Bayer, R. G. (2012). Tribological Modeling for Mechanical Designers. ASTM International, (STP 1105). https://doi.org/10.1520/STP1105-EB*

40. *Mirjavadi, S. S., Alipour, M., Emamian, S., Kord, S., Hamouda, A. M. S., Koppad, P. G., & Keshavamurthy, R. (2017). Influence of TiO2 nanoparticles incorporation to friction stir welded 5083 aluminum alloy on the microstructure, mechanical properties and wear resistance. Journal of Alloys and Compounds, 712, 795–803.*

    https://doi.org/10.1016/j.jallcom.2017.04.114

41. *Padhy, G. K., Wu, C. S., & Gao, S. (2017). Friction stir based welding and processing technologies - processes, parameters, microstructures and applications: A review. Journal of Materials Science and Technology, 34, 1–38. https://doi.org/10.1016/j.jmst.2017.11.029*

42. *Pao, P.S., Gill, S.J., Feng, C.R., and Sankaran, K. K. (2001). Effects of Weld Microstructure on Fatigue Crack Growth in Friction Stir Welded Al 7050. TSM Aluminium 2001, 265–279.*

43. Ponthiaux, P., Wenger, F., & Pierre, J. (2012). Tribocorrosion: material behaviour under combined conditions of corrosion and mechanical loading. Corrosion Resistance, (May 2014), 81–106. https://doi.org/10.5772/35634

44. Proton, V., Alexis, J., Andrieu, E., Delfosse, J., Lafont, M. C., & Blanc, C. (2013). Characterisation and understanding of the corrosion behaviour of the nugget in a 2050 aluminium alloy Friction Stir Welding joint. Corrosion Science, 73, 130–142. https://doi.org/10.1016/j.corsci.2013.04.001

45. Rajaram, G., Kumaran, S., & Rao, T. S. (2010). High temperature tensile and wear behaviour of aluminum silicon alloy. Materials Science and Engineering A, 528(1), 247–253. https://doi.org/10.1016/j.msea.2010.09.020

46. Ralston, K. D., Fabijanic, D., & Birbilis, N. (2011). Effect of grain size on corrosion of high purity aluminium. In Electrochimica Acta (Vol. 56, pp. 1729–1736). https://doi.org/10.1016/j.electacta.2010.09.023

47. Sankaran, K.K., Smith, H.L., and Jata, K. (2002). Pitting Corrosion Behavior of Friction Stir Welded 7050-T74 Aluminum Alloy. Trends in Welding Research, APRIL, 284–286.

48. Syed Khaja N, Md Tousef a, Purna, B. C, Narendra Mohan, Vidhu Kampurath, Y. A. (2016). Wear behaviour of welded and non-welded samples of friction stir welding of similar and dissimilar joints of aluminium alloys (aa .... wear behaviour of welded and non-welded samples of friction stir welding of similar and dissimilar joints of aluminium. International Jounal of Mechanical Engineering and Technology., 7(June), pp289-299.

49. Threadgill, P. L., Leonard, A. J., Shercliff, H. R., & Withers, P. J. (2009). Friction stir welding of aluminium alloys. International Materials Reviews, 54(2), 49–93. https://doi.org/10.1179/174328009X411136

50. Venkatasubramanian, G., Mideen, A. S., & Jha, A. K. (2012). Corrosion Behavior Of Aluminium Alloy Aa2219 − T87 Welded Plates in Sea Water. ISSN:0974-6846 Indian Journal of Science and Technology, 5(11), 3578–3584.

51. Nagaral, M., Auradi, V., & Ravishankar, M. K. (2013). mechanical behaviour of aluminium 6061 alloy reinforced with al2o3 & graphite particulate hybrid metal matrix composites. International Journal of Research in Engineering & Technology (IJRET) Vol, 1, 193-198.

52. Vieira, A. C., Rocha, L. A., Papageorgiou, N., & Mischler, S. (2012). Mechanical and electrochemical deterioration mechanisms in the tribocorrosion of Al alloys in NaCl and in NaNO3solutions. Corrosion Science, 54(1), 26–35. https://doi.org/10.1016/j.corsci.2011.08.041

53. Vijaya Kumar, P., Madhusudhan Reddy, G., & Srinivasa Rao, K. (2015). Microstructure and pitting corrosion of armor grade AA7075 aluminum alloy friction stir weld nugget zone – Effect of post weld heat treatment and addition of boron carbide. Defence Technology, 11(2), 166–173. https://doi.org/10.1016/j.dt.2015.01.002

54. Wadeson, D. A., Zhou, X., Thompson, G. E., Skeldon, P., Oosterkamp, L. D., & Scamans, G. (2006). Corrosion behaviour of friction stir welded AA7108 T79 aluminium alloy. Corrosion Science, 48(4), 887–897.

    https://doi.org/10.1016/j.corsci.2005.02.020

55. Wang, A., & Rack, H. J. (1991). Transition wear behavior of SiC-particulate- and SiC-whisker-reinforced 7091 Al metal matrix composites. Materials Science and Engineering A, 147(2), 211–224. https://doi.org/10.1016/0921-5093(91)90848-H

56. Wang, H. (2016). Analysis on the Corrosion Performance of Friction Stir Welding Joint of 7022 Aluminum Alloy. International Journal of Electrochemical Science, 11, 6933–6942. https://doi.org/10.20964/2016.08.09

57. Wang, L., Hui, L., Zhou, S., Xu, L., & He, B. (2016). Effect of corrosive environment on fatigue property and crack propagation behavior of Al 2024 friction stir weld, 26, 2830–2837. https://doi.org/10.1016/S1003-6326(16)64411-4

58. *Wei, R. P., Liao, C.-M., & Gao, M. (1998). A transmission electron microscopy study of constituent-particle-induced corrosion in 7075-T6 and 2024-T3 aluminum alloys. Metallurgical and Materials Transactions A, 29(4), 1153–1160.*

    https://doi.org/10.1007/s11661-998-0241-8

59. *Widener, C. a., Burford, D. a., Kumar, B., Talia, J. E., & Tweedy, B. (2007). Evaluation of Post-Weld Heat Treatments to Restore the Corrosion Resistance of Friction Stir Welded Aluminum Alloy 7075-T73 vs. 7075-T6. Materials Science Forum, 539–543, 3781–3788. https://doi.org/10.4028/www.scientific.net/MSF.539-543.3781*

60. *Zhang, J., & Alpas, A. T. (1997). Transition between mild and severe wear in aluminium alloys. Acta Materialia, 45(2), 513–528. https://doi.org/10.1016/S1359-6454(96)00191-7*

2.3 ARTICLE II

In-Process cooling in Friction Stir Welding of Aluminium Alloys- An Overview

Published *in Lecture Note in Mechanical Engineering*. 435-444. 2019. (**Scopus indexed**) https://doi.org/10.1007/978-981-13-8297-0_45

This is a review article on the available literature on cooling processes during FSW of aluminium alloys. The thermal cycle set up during FSW often leads to precipitates coarsening with resultant reduction in the mechanical properties of the weld joint. Various efforts made by researchers to improve the mechanical properties through in-process cooling were reviewed in this article. The article highlighted various cooling media such as water, compressed air, cryogenic, ice, liquid nitrogen and their effects on mechanical properties and corrosion. It was discovered that all the cooling media generally improves the mechanical properties. However, submerged welding in water was found to give better weld tensile strength. The review also showed that the variation of the hardness profile across the welding zone does not depend on the cooling medium employed but vary according to the aluminium grades welded. In-process cooling effects on the corrosion behaviour of friction stir welded aluminium alloys was also captured in the review. The available literature showed that underwater welds are more resistant to corrosion than naturally cooled welds. In-process cooling was also found to result in better fine grain structures compared to naturally cooled welds. The review further linked the improvement in mechanical properties of in-process cooled welds to these microstructural changes.

The article identified some research gaps for possible further studies.

In-Process Cooling in Friction Stir Welding of Aluminium Alloys—An Overview

Olatunji P. Abolusoro and Esther T. Akinlabi

Abstract Friction stir welding (FSW) is a welding technique that has found extensive use in the joining of aluminium alloys for many applications. During FSW welding, severe plastic deformation occurs due to the stirring actions of the tool which generates heat on the workpiece. The thermal cycle set up at the weld region causes deterioration of precipitates by coarsening or dissolutions. The resultant mechanical properties of the weld region, therefore, become lesser than that of the base metal. Efforts have been made by various researchers to address this challenge through in-process cooling using different cooling fluids such as cryogenic, slush ice, water, compressed air and liquified nitrogen to control the temperature during FSW so as to enhance the mechanical behavior of the welds. The in-process cooling approach was generally reported to have improved the mechanical and corrosion behavior of welded joints as a result of fine and stable microstructures obtained at the weld zone. This paper reviewed the research efforts in this direction. The authors and their investigations and findings have been briefly summarized and the influence of these cooling media on tensile, microstructures and corrosion behavior has been highlighted. The overall aim of this review paper is to provide comprehensive requisite knowledge of the current state of research on in-process cooling in FSW of aluminium alloys with a view to exposing further areas of research interest in this aspect of FSW.

Keywords Aluminium · Friction stir welding · In-process cooling · Microstructures · Tensile strength

O. P. Abolusoro (✉) · E. T. Akinlabi
Department of Mechanical Engineering Science, University of Johannesburg, Kingsway Campus, 524, Auckland Park, Johannesburg, Gauteng 2006, South Africa
e-mail: abolusoroolatunji@yahoo.com

M. Awang et al. (eds.), *Advances in Material Sciences and Engineering*, Lecture Notes in Mechanical Engineering,
https://doi.org/10.1007/978-981-13-8297-0_45

1 Introduction

Friction stir welding is a modern solid-state welding method that started in 1991 at the welding institute in UK. It has been used extensively to weld low-temperature alloys such as aluminium, magnesium copper etc. Recent development has seen this welding technology being used to join steel, plastics, and other materials. However today, it has been predominantly used to join aluminium alloys. FSW involves a rotating tool made up of shoulder with a protruded part known as the pin. During welding, the tool is pressed against the workpiece surface to be joined. As the tool rotates and traverses the workpiece joint surface, heat is produced by the frictional movements of the rotating tool on the workpiece. This heat softened the material interface and plastically deformed the workpiece joint region and melted them together. Although FSW heat input is generally not high, the thermal cycle that occurred during welding could lead to coarsening or dissolution of grain precipitates [1–8]. The consequence of this grain reorientations is that the three major zones of the weld i.e. nugget zone (NZ), heat affected zone (HAZ) and thermo-mechanically affected zone (TMAZ) become softened thereby lowering the tensile strength of the joints than those of the base materials. Therefore, for the joints to be more efficient, temperature control during the welding becomes imperative. Various cooling media to control temperature during FSW of aluminium alloys have been investigated by researchers. Such media apart from the natural cooling air, include water, liquid nitrogen, cryogenic, compressed air and ice. In process cooling in friction stir welding with water can be done by immersing the rotating tool and the workpiece in water as shown in Fig. 1 [3–6, 8–13]. In some cases, the water may be sprinkled between the rotating tool and the workpiece interface [7, 12, 14, 15]. The temperature control achieved through in-process cooling during friction stir welding affects the microstructural evolutions and grain refinement of the joint. These changes considerably depend on the type of cooling media employed [10]. Figure 2 shows typical surface morphologies of in-process cooling in friction stir welding of 2014Al-T6 using the same process parameter for air cooled and water-cooled welds. In-process cooling in friction stir welding of aluminium alloys have recently attracted the attention of researchers in view of the importance of aluminium as one of the most widely used engineering materials in industries. This paper reviewed the available literatures on in-process cooling of friction stir welded joints of aluminium alloys.

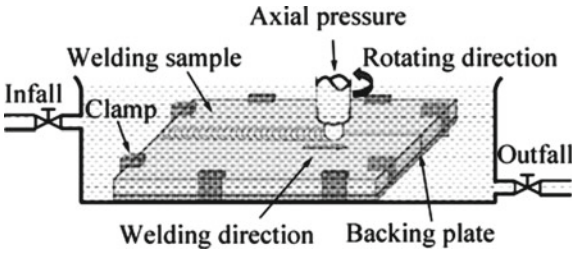

Fig. 1 Schematic diagram of underwater friction stir welding [3]

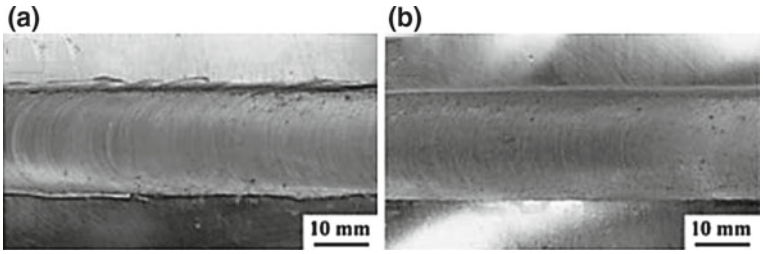

Fig. 2 Surface morphologies of FSW 2014Al-T6 using the same process parameter. **a** Air cooled weld, **b** water cooled weld [10]

1.1 Investigations and Findings

Investigations and findings from various authors have been summarized in this section. Table 1 contains various authors, their focus, findings and conclusions on in-process cooling in FSW.

2 Summary

Based on the focus, findings and conclusions of the authors as highlighted in Table 1, the cooling effects of the various media considered on tensile strength, hardness, microstructures and corrosion can be summarized below.

2.1 Cooling Effects on Tensile Strength

Most of the effects of water cooling in FSW investigated were carried out by submerged or underwater welding [3–6, 8–13] however, very few cases of water being sprayed on the tool-workpiece interface and water heat sink were also reported [7, 12, 14, 15]. Most of the author's findings agreed and confirmed that tensile strength is enhanced by in-process water cooling. Other cooling methods like compressed air and liquid nitrogen, slush ice, rock salt with ice were also reported to enhance tensile strength in FSW of aluminium alloys. However, water and ice were reported to perform better than the other cooling media [14, 18]. This was generally attributed to the reduction of heat generated due to the cooling media during the welding which led to discontinuous smaller grain sizes of precipitates and narrow heat affected zones. Although many of the author's findings and conclusions followed this trend but there are few reports on tensile behavior of underwater FSW of some aluminium alloys on the contrary [10].

Table 1 Summary of findings on in-process cooling in friction stir welding of aluminium alloy

References	Authors	Focus	Findings and conclusions
[9]	N. D. Ghetiya and K. M. Patel	FSW of AA2014-T4 aluminium alloy fully immersed in water. Experiment and modeling	Box-Behnken experimental designs and ANOVA (Analysis of variables) used agreed with the experimental outcome of improvement of 75% in the tensile strength of base materials of the friction stir aluminium alloy fully immersed in water. This was attributed to discontinuous smaller grain sizes of precipitates
[10]	Z. Zhang, B. L. Xia, Z. Ma	FSW of 2014-T6 aluminium alloy done underwater and air-cooling conditions	Low hardness zone was observed in both cooling methods at the advancing and retrieving sides of the weld. Tensile strength of the natural air-cooled welds increased as the welding speed goes higher, however, cooling underwater has no influence on the tensile and hardness properties of the welds
[3]	H. J. Liu, H. J. Zhang, Y. X. Huang, L. Yu	Mechanical behaviour of submerged friction stir welding of 2219 aluminium alloy	Improvement of tensile strength was observed, however, plasticity degenerates. Hardness was lower in the submerged welding at the nugget zone but greater in other zones
[14]	C. Sharma, D. K. Dwivedi, P. Kumar	Tensile behavior of friction stirs welded AA7039 with natural air-cooling during welding and cooling employing water, liquified nitrogen and compressed air	Hardness was higher with the three in-process cooling media. However, water cooling performed better in tensile strength than the other two cooling methods and those without in-process cooling. All the cooling processes generally alter the fracture locations to nugget zone from heat affected zone

(continued)

Table 1 (continued)

References	Authors	Focus	Findings and conclusions
[4]	H. J. Zhang, H. J. Liu, L. Yu	Cooling effects of water on heat affected zone of underwater FSW of 2219-T6 aluminium alloy	Water improves the hardness of the HAZ. This was due to a reduction in precipitate hardening and narrow zone as a result of the cooling effects of water
[5]	Y. Zhao, K Yan, S. Jiang, S. Yang, Z. Lu	Under water and air-cooling friction stir welding of 6013 and AZ31 aluminium alloy and magnesium alloy respectively	The joint integrity of welds with water cooling was better than that of air cooling. However, the hardness in the air was higher than that of water
[6]	Z. Zhang, Z. Y. Ma, B. L. Xiao	Effects of high speed on the mechanical behaviour of FSW of 2219-T6 under in-process water and air-cooled conditions	The welds produced under both cooling conditions were good at high speed. However, air cooling led to lower hardness zone while water cooling had no significant effects on hardness. The tensile behavior of water-cooled welds was slightly better and the post weld artificial aging used improved the hardness for all the joints at all welding speeds. This was due to the formation of Al_2Cu_2 in the low hardness and stir zone
[7]	W. F. Xu, J. S. Yao, J. H. Liu, G. H. Luan, D. L. Chen	Enhancing ductility and strength through in-process water and air cooling of FSW of 2219 aluminium alloy	Water cooling enhanced the ductility and strength of the welds but lowered the hardness of the weld than those obtained in air cooling
[8]	S. Sree Sabari, S. Malarvizhi, V. Balasubramanian	Rotational speed influence and underwater cooling behaviour of FSW of AA2519-T87	Higher tensile strength was observed at lower rotational speed in water submerged welds. This was due to a reduction in heat produced, greater grain boundary of precipitates and narrow hardness spread zone

(continued)

Table 1 (continued)

References	Authors	Focus	Findings and conclusions
[11]	H. J. Liu, H. J. Zhang, L. Yu	Welding speed influence on the mechanical and microstructural behavior of water submerged friction stir welding of 2219 aluminium alloy	High welding speed led to the degeneration of precipitates at TMAZ which resulted to narrow and soft zone with higher hardness value. Tensile tests of welds at lower welding speed fractured at heat affected zone while those at higher speeds fractured at TMAZ
[12]	S. Sinhmar, D. K. Dwivedi	Corrosion and mechanical behaviour of sprayed water and natural air-cooled during friction stir welding of 2014 aluminium alloy	Water cooled welds exhibit greater hardness at HAZ than natural air-cooled welds. Tensile and yield strength, as well as resistance to corrosion, were also higher in the water-cooled welds than the air-cooled welds. This was due to discontinuous smaller grain sizes of precipitates in the weld zone
[15]	Q. Wang, Y. Zhao, K. Yan, S. Lu	Corrosion study of water submerged friction stir welding of 7055 aluminium alloy	Underwater joint exhibit better resistance to corrosion than the normal joint and the base metal. This was attributed to blockage of corrosion path.in the underwater joint as a result of $MgCu_2$ distributions in the matrix
[13]	Deepti Jaiswala, Ratnesh Kumar, Raj Singhb, Sunil Pandey, Rajesh Prasad	Cooling media effects on mechanical behavior of FSW of 1060 aluminium alloy	The optimum parameter used for air-cooled welding was also applied for underwater welding. There was improvement in the impact and tensile strength. This was due to narrow HAZ resulting from heat reduction by the cooling water

(continued)

Table 1 (continued)

References	Authors	Focus	Findings and conclusions
[16]	Jamshidi Aval Hamed	Heat input influence during FSW and post-weld aging time on mechanical behavior and microstructure of AA7075-AA5086	Heat sink made of copper with water tunnels to rapidly cooled the workpiece during the FSW was used. The result showed an increase in tensile strength, decrease in residual stresses, smaller grain size and narrowed softened region compared to samples without heatsink cooling
[17]	Khosro Bijanrostami and Reza Vatankhah Barenji	Effects of submerged friction stir welding of 6061-7075 on hardness and grain size. Experiment and modeling	The empirical model used predicted the experimental values obtained considerably. Fine grain size and greater hardness were obtained at reduced rotational speed and higher travel speed. The grain boundaries mechanism and its influenced dislocations were attributed to this behavior
[18]	Ashish Jacob, Sachin Maheshwari, Arshad Noor Siddiquee and Namrata Gangi	Enhancement of strength and microstructure through in process cooling using water, slush ice, and crushed ice added with rock salt during FSW of 7475	The cooling led to substantially fine grains at the stir zone and significantly increased mechanical behavior of the weld. Ice water cooling gave exceptionally stable microstructures
[19]	L. Fratini, G. Buffa, R. Shivpuri	In process cooling effects on mechanical and microstructural behavior of AA7075 during FSW using water as cooling medium	The cooling improved joint strength and narrowed the softened zone. There was a slight difference in hardness between the naturally cooled and water-cooled welds
[20]	M. Jariyaboon, A. J. Davenport, R. Ambat, B. J Connolly, S. W. Williams, D. A. Price	Cryogenic cooling effects on corrosion behavior of FSW AA7010-T7651	Intergranular corrosion occurred at HAZ with and without cooling but cooling narrowed the HAZ. Cryogenic cooling has no influence on anodic reaction but showed greater cathodic reaction in the nugget zone

2.2 Effects on Hardness

The effects of in-process cooling on hardness profile have not been fully established from the reviewed literature. Hardness depends on the type of aluminium alloys being joined together and materials movement and mixing during the welding. The hardness across the three zones of the weld varies irrespective of cooling methods employed.

2.3 Effects on Corrosion

Better corrosion resistance was equally reported to have been observed in underwater friction stir welds than the natural air-cooled friction stirs welds. The same reasons for better tensile strength and hardness have been ascribed to this [12, 15]. However, increase in cathodic reactivity was reported in cryogenic cooling [20].

2.4 Effects on Microstructures

Analysis of cooling effects on microstructure during friction stir welding revealed the evolution of fine grain structures with smaller sizes in the nugget zone as a result of cooling brought about by the water during plastic deformation of the materials at the joint interface [3–18].

3 Conclusions

An overview of in-process cooling in friction stir welding of aluminium alloys have been discussed in this paper. Underwater or sprayed water, heat sink with water, compressed air, cryogenic and liquid nitrogen cooling during friction stir welding and their effects on tensile strength, hardness, microstructures and corrosion resistance of welded joints have been highlighted. The reports from various authors considered in this review affirmed the improvement in mechanical properties and corrosion of welds carried out with in-process cooling and therefore made it a desirable process for improving friction stir weld joints of low temperature alloys like aluminium. The improvement on mechanical behavior was generally linked to inhibition of coarsening of strengthening precipitates by the various cooling media. The heat input to the weld region as a result of the cooling is just sufficient enough for the required bonding and therefore hindered abnormal grain growth that could result from high heat input. However, the effects of this on wear and corrosion has not been fully reported. Also, the in-process cooling applications to high temperature alloys in friction stir

welding still calls for investigations. Future research could focus more on wear and corrosion behavior of the in-process cooling welds. This is a gap that seems yet to be fully reported. Investigations on effects of other cooling media different from the ones discussed above on mechanical properties, microstructures, wear and corrosion behaviour of different grades and series of aluminium alloys for both similar and dissimilar FSW could be explored. The research could also be extended not only to other low-temperature alloys such as copper, magnesium etc. but also to high-temperature alloys like steel.

References

1. Akinlabi ET, Akinlabi SA (2012) Effect of heat input on the properties of dissimilar friction stir welds of aluminium and copper. Am J Mater Sci 2(5):147–152
2. Takayama Y, Akutsu Y, Choshiro N, Kato H, Watanabe H (2010) Temperature measurement during friction stir welding of dissimilar aluminum alloys, pp 0–5
3. Liu HJ, Zhang HJ, Huang YX, Yu L (2010) Mechanical properties of underwater friction stir welded 2219 aluminum alloy. Trans Nonferrous Met Soc China (English Ed) 20(8):1387–1391
4. Zhang HJ, Liu HJ, Yu L (2012) Effect of water cooling on the performances of friction stir welding heat-affected zone. J Mater Eng Perform 21(7):1182–1187
5. Zhao Y, Jiang S, Yang S, Lu Z, Yan K (2016) Influence of cooling conditions on joint properties and microstructures of aluminum and magnesium dissimilar alloys by friction stir welding. Int J Adv Manuf Technol 83(1–4):673–679
6. Zhang Z, Xiao BL, Ma ZY (2015) Enhancing mechanical properties of friction stir welded 2219Al-T6 joints at high welding speed through water cooling and post-welding artificial ageing. Mater Charact 106:255–265
7. Xu WF, Liu JH, Chen DL, Luan GH, Yao JS (2012) Improvements of strength and ductility in aluminum alloy joints via rapid cooling during friction stir welding. Mater Sci Eng A 548:89–98
8. Sree Sabari S, Malarvizhi S, Balasubramanian V (2016) Characteristics of FSW and UWFSW joints of AA2519-T87 aluminium alloy: effect of tool rotation speed. J Manuf Process 22:278–289
9. Ghetiya ND, Patel KM (2015) Prediction of tensile strength and microstructure characterization of immersed friction stir welding of aluminium alloy AA2014-T4. NOPR NISCAIR Publ Res J Indian J Eng Mater Sci IJEMS 133–140
10. Zhang Z, Xiao BL, Ma ZY (2014) Influence of water cooling on microstructure and mechanical properties of friction stir welded 2014Al-T6 joints. Mater Sci Eng A 614:6–15
11. Liu HJ, Zhang HJ, Yu L (2011) Effect of welding speed on microstructures and mechanical properties of underwater friction stir welded 2219 aluminum alloy. Mater Des 32(3):1548–1553
12. Sinhmar S, Dwivedi DK (2017) Enhancement of mechanical properties and corrosion resistance of friction stir welded joint of AA2014 using water cooling. Mater Sci Eng A 684:413–422
13. Jaiswal D, Kumar R, Singh R, Pandey S, Prasad R (2014) Influence of cooling media on mechanical properties of friction stir welded 1060 aluminium alloy, no 4, pp 54–57
14. Sharma C, Dwivedi DK, Kumar P (2012) Influence of in-process cooling on tensile behaviour of friction stir welded joints of AA7039. Mater Sci Eng A 556:479–487
15. Wang Q, Zhao Y, Yan K, Lu S (2015) Corrosion behavior of spray formed 7055 aluminum alloy joint welded by underwater friction stir welding. Mater Des 68:97–103
16. Hamed JA (2017) Effect of welding heat input and post-weld aging time on microstructure and mechanical properties in dissimilar friction stir welded AA7075–AA5086. Trans Nonferrous Met Soc China (English Ed) 27(8):1707–1715

17. Bijanrostami K, Vatankhah Barenji R (2017) Underwater dissimilar friction stir welding of aluminum alloys: elucidating the grain size and hardness of the joints. Proc Inst Mech Eng Part L J Mater Des Appl 1–13
18. Jacob A, Maheshwari S, Siddiquee AN, Gangil N (2018) Improvements in strength and microstructural behaviour of friction stir welded 7475 aluminium alloy using in-process cooling. Mater Res Express 5(1):1–12
19. Fratini L, Buffa G, Shivpuri R (2010) Mechanical and metallurgical effects of in process cooling during friction stir welding of AA7075-T6 butt joints. Acta Mater 58(6):2056–2067
20. Jariyaboon M, Davenport AJ, Ambat R, Connolly BJ, Williams SW, Price DA (2010) Effect of cryogenic cooling on corrosion of friction stir welded AA7010-T7651. Anti-Corros Methods Mater 57(2):83–89

2.4 ARTICLE III

Optimization of Process Parameters using Taguchi for Friction Stir Welding of Dissimilar Aluminium Alloys

Published *in Lecture Note in Mechanical Engineering* 2019. (**Scopus indexed**)

This article examined the two major process parameters which mostly influence the mechanical properties of welds in friction stir welding. These parameters are welding speed and rotational speed, and the article presented optimisation of these parameters and their contributions to obtaining welds with high integrity in the friction stir welding of 6101-T6 and 7075-T651 aluminium alloys. Taguchi Minitab software of experimental design with L_{16} orthogonal array was employed to optimise the parameters. Rotational speed of 1550rpm and a welding speed of 20mm/min were established to give the highest hardness at the NZ whereas 950rpm and 50mm/min rotational and welding speed respectively were found to produce the highest UTS. The article further presented the analysis of variance (ANOVA) of the parameters and gave rotational speed as the most significant parameter influencing the attainment of optimum tensile strength, and gave welding speed as the parameter with higher influence on hardness.

Optimization of Process Parameters Using Taguchi for Friction Stir Welding of Dissimilar Aluminum Alloys

Olatunji P. Abolusoro and Esther T. Akinlabi

Abstract Friction stir welding (FSW) is a major welding system employed to join aluminum alloys. This welding method is governed by so many variable parameters. These parameters control the quality and reliability of the welds. This paper gives attention to the optimization of two most prominent of these variable parameters which are the rotational speed and the travel speed of the tool through Taguchi technique of design of experiments. The friction stir welding was done on the 7075-T651 and 6101-T6 aluminum alloys with L_{16} orthogonal array of Taguchi method for the welding trials. 1550 rpm and 20 mm/min rotational speed and travel speed, respectively, were established to produce the maximum hardness at the nugget zone, while 950 rpm and 50 mm/min gave the optimum conditions for the ultimate tensile strength. The analysis of variance (ANOVA) gave rotational speed as the parameter with highest influence for achieving optimum tensile strength but gave tool travel speed in the case of hardness optimization.

Keywords Friction stir welding · Hardness · Taguchi technique · Ultimate tensile strength

1 Introduction

Introduction FSW is a system of welding that utilized a tool with shoulder and a probe which produce heat due to its frictional rotation on the workpiece. The heat plasticized the material at the interface of the joint thus enabling the tool pin to penetrate and stir the materials together and form bonding [1, 2]. This technology was invented in 1991 and has been successfully used to weld aluminum alloys in aerospace, marine, automobile, and spacecrafts applications. The use of FSW has now been extended to other alloys such as magnesium, copper, steel, and composites [2–4]. There are factors that influence the integrity of the welds produced in FSW. These factors include among others, tool rotational speed, tool geometry, travel speed, the spindle tilt angle, axial

O. P. Abolusoro (✉) · E. T. Akinlabi
Department of Mechanical Engineering Science, University of Johannesburg, Johannesburg, South Africa
e-mail: abolusoroolatunji@yahoo.com

S. S. Emamian et al. (eds.), *Advances in Manufacturing Engineering*, Lecture Notes in Mechanical Engineering, https://doi.org/10.1007/978-981-15-5753-8_19

force, and plunge depth [5]. Many researchers have reported the impact of these factors on mechanical properties and microstructures of welds [6–9]. Optimizations of these parameters, therefore, become important to save time and cost of experiments and to obtain high quality of welds. Researchers have employed various methods of optimizing these parameters [10, 11] Prominent among them is the Taguchi technique which has found tremendous usage for optimizations. Taguchi is an experimental design method for systematic design and analysis of experimental output for quality characteristics. Many research works on Taguchi optimization technique in FSW have been reported. For instance, Elanchezhian et al. [12] used a mathematical model to optimize the parameters of the FSW of AA8081 and 6062 considering the impact and tensile strength performance. Taguchi L_9 orthogonal array and ANOVA were used to arrive at the optimum conditions. Similarly, Prasad and Namola [13] used ANOVA optimization technique to optimize the processing parameters of FSW of AA5083 and 6061 with experimental design of Taguchi L_9 orthogonal array. Hardness and ultimate tensile strength (UTS) were used as the outputs to determine the optimum parameter. Ugrasan et al. [14] also optimized the parameters using L_9 orthogonal array Taguchi method for FSW of 6061 and 7075 aluminum alloys. The UTS and Vickers hardness were utilized to evaluate the optimized and significant parameters. Panda et al. [15] employed Taguchi method to optimize welding speed, tool pin geometry, and tool rotational speed using the tensile strength of the welds. Their result indicates that welding speed is a significant factor influencing the tensile strength. Jayaraman et al. [16] employ ANOVA and signal-to-noise ratio to obtain the optimum welding conditions for FSW of cast aluminum alloys. The tensile strength was correlated with non-linear regression model created which was discovered to be helpful in the prediction of the tensile strength. Gomathisankar et al. [17] used a complex proportional assessment (COPRAS) model to optimize tool rotational and travel speeds, tilt angle, and dwell time. L_9 Taguchi orthogonal array was designed for the experiment. Confirmation test was later carried out for the outcome verification. Some researchers have established that the tool rotational and travel speed are the most important factors that influence the quality of welds obtained in FSW [18–21]. These two factors are therefore considered for optimization in this work. Generally, selection of optimum conditions where a parameter is varied and others held constant is difficult. It involves large number of experiments which is time- and money-consuming. Taguchi experimental design method has been developed to address this challenge. This work, therefore, employ the Taguchi design of experiment with L_{16} orthogonal array to optimize tool rotational and travel speed in the friction welding of 7075-T651 and 6101-T6 aluminum alloys.

Multiple performance characteristics optimization requires an overall evaluation of the signal-to-noise ratio. This is necessary as a result of differences in S/N which may be higher for a performance characteristic and correspondingly lower in another.

2 Experimental Procedures

The elemental components of the parent alloys (6101-T6 and 7075-T651) and their mechanical properties are illustrated in Tables 1 and 2, respectively.

The two aluminum alloys (7075-T651 and 6101-T6) were cut into 130 mm × 60 mm each and arranged in butt configuration for the welding. The 6101-T6 was kept on the advancing side, while the 7075-T651 was on the retreating side. Threaded pin welding tool used was fabricated with H13 mild steel made up of shoulder diameter of 22 mm, pin length of 5.6 mm, root pin diameter of 7.5 mm, and pin mouth diameter of 5.5 mm. Tool rotational speed and travel speed were selected as welding variables to be optimized. Other parameters for instance plunge depth and tilt angle were held constant at 2° and 0.2 mm, respectively. The experiment was designed using Taguchi technique at four levels for each of the two parameters under considerations. This gave an L_{16} orthogonal array as shown in Table 3. The welding was carried out based on this experimental design, and the mean including the signal-to-noise ratio were evaluated. Three tensile samples were cut according to ASTM E8 standard from the center of each weld for testing. The average ultimate tensile strength for each parameter was evaluated and shown in Table 3. The Vickers hardness test was carried out perpendicular to the welding directions. A 300 kgf was applied for 15 s during the test, and about 27 indentations were taken on each sample. The average hardness values in the nugget zone of the weld were also evaluated and shown in Table 7.

Table 1 Elemental components

Alloy	Si	Cu	Fe	Mn	Mg	Ti	Cr	Zn	Al
6101-T6	0.53	0.01	0.14	0.002	0.600	0.008	0.001	0.003	Others
7075-T651	0.40	1.70	0.50	0.300	2.40	0.20	0.22	5.50	Others

Table 2 Mechanical properties

Alloy	Tensile strength (MPa)	Ultimate tensile strength (MPa)	Elongation (%)
6101-T6	172	180	21
7075-T651	462	575	18

Table 3 Tensile test results

S. No.	Rotational speed (rpm)	Traverse speed (mm/min)	Ultimate tensile strength (MPa)
1	950	20	138.41
2	950	50	143.39
3	950	80	142.97
4	950	110	154.00
5	1250	20	141.85
6	1250	50	143.79
7	1250	80	66.98
8	1250	110	147.57
9	1550	20	141.31
10	1550	50	145.41
11	1550	80	144.73
12	1550	110	146.80
13	1850	20	137.14
14	1850	50	135.46
15	1850	80	141.88
16	1850	110	118.21

3 Results and Discussion

3.1 Ultimate Tensile Strength

The results obtained for the ultimate tensile strength (UTS) for each parameter are given in Table 3. The results show that highest UTS was obtained at 950 rpm tool rotational speed and 110 mm/min tool traverse speed, while the lowest UTS occurred at 1850 rpm and 110 mm/min.

3.1.1 Analysis of Variance (ANOVA)

In this work, larger is better approach was employed for the signal-to-noise ratio since maximum UTS is desired in any welding joint. Values of F in the ANOVA table shown in Table 4 show the impact of the variable process parameters to achieve the peak UTS, while values of P show uncontrollable factors probability known as noise. Maximum F and minimum P is the optimization target. Any variable parameter below 5% is taken as a significant parameter. The F values in Table 4 indicate that the rotational speed of the tool has a greater influence on tensile strength. It contributes about 63%, while the travel speed contributes 37%. The response to mean and signal-to-noise ratio (S/N) evaluated using the larger is better approach are presented in Tables 5 and 6, respectively. The main effects for mean and S/N are illustrated in

Table 4 Analysis of variance (ANOVA)

Source	DF	Adj SS	Adj MS	*F*-Value	*P*-Value
Rotational speed	1	45.31	45.31	0.10	0.759
Traverse speed	1	28.67	28.67	0.06	0.807
Error	13	6001.84	461.68		
Total	15	6075.82			

Table 5 Response for means

Level	Rotational speed	Traverse speed
1	144.7	139.7
2	125.0	142.0
3	144.6	124.1
4	133.2	141.6
Delta	19.6	17.9
Rank	1	2

Table 6 Response for signal-to-noise ratios

Level	Rotational speed	Traverse speed
1	43.20	42.90
2	41.52	43.04
3	43.20	41.47
4	42.47	42.98
Delta	1.68	1.58
Rank	1	2

Figs. 1 and 2, respectively. The interactions between the means and *S*/*N* for the two processing parameters accessed for optimizations, i.e., the welding tool rotational and travel speed are demonstrated in Figs. 3 and 4 for the means and signal-to-noise ratios, respectively.

3.1.2 Response Optimization for the UTS.

The response optimization for the rotational and travel speed for the UTS can be deduced from Tables 5 and 6 for mean and signal-to-noise ratio, respectively, and also from main effects plot for mean in Fig. 1 and *S*/*N* ratio effects plot in Fig. 2. The analysis gave 950 rpm rotational speed and 50 mm/min traverse speed as the optimized parameters. The mean and signal-to-noise ratio interactions with the two factors and four levels were illustrated in Figs. 3 and 4, respectively.

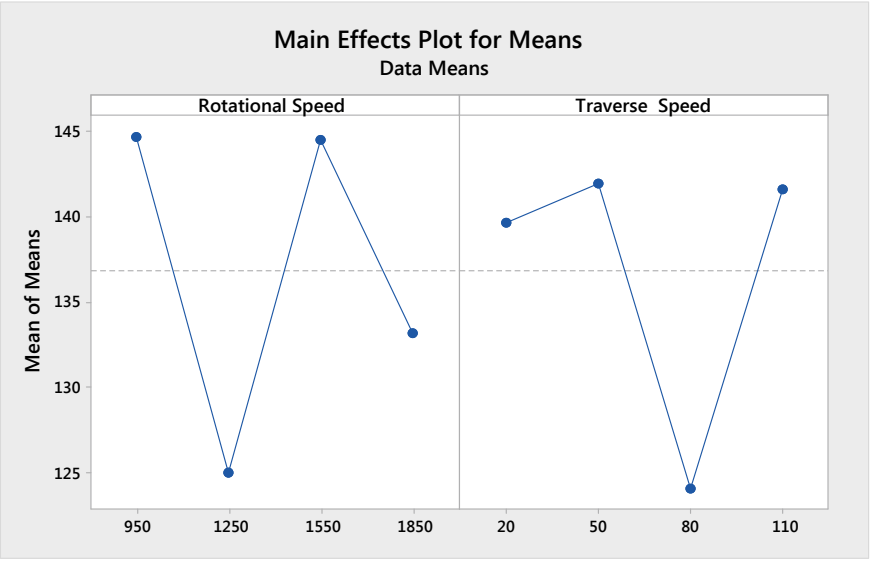

Fig. 1 Main effects plot for *means*

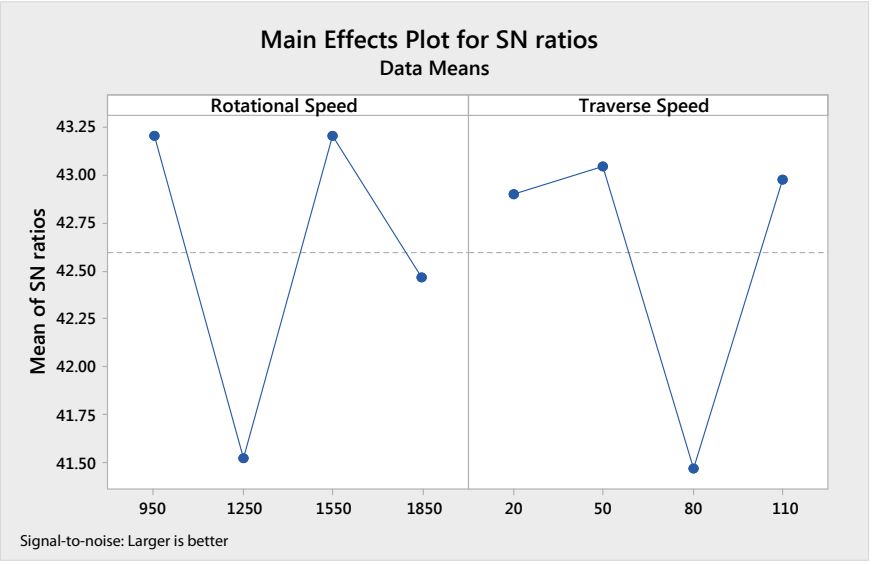

Fig. 2 Main effects plot for S/N ratios

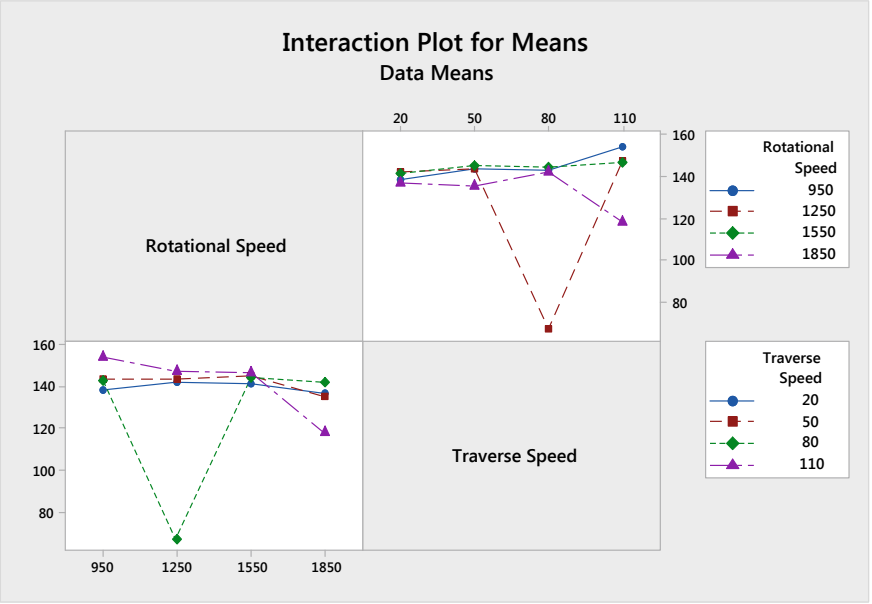

Fig. 3 Interaction plot for means

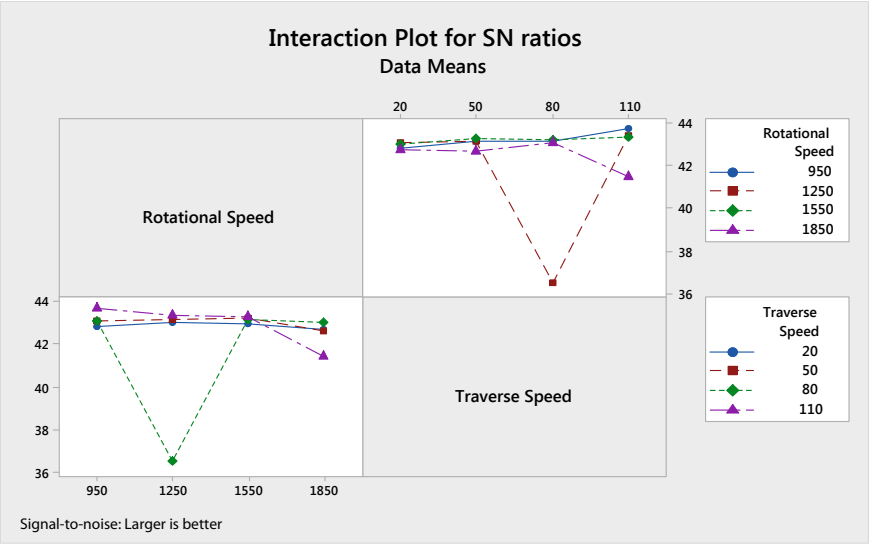

Fig. 4 Interaction plot for *S/N ratios*

Table 7 Hardness test results

S. No.	Rotational speed (rpm)	Traverse speed (mm/min)	Hardness (HV)
1	950	20	120.31
2	950	50	81.48
3	950	80	111.71
4	950	110	118.44
5	1250	20	98.51
6	1250	50	104.41
7	1250	80	74.56
8	1250	110	105.44
9	1550	20	121.08
10	1550	50	124.36
11	1550	80	126.64
12	1550	110	107.71
13	1850	20	100.43
14	1850	50	99.85
15	1850	80	133.26
16	1850	110	65.18

3.2 Hardness

Hardness The average hardness values taken at the weld nugget zone for each parameter are presented in Table 7. 1550 rpm and 80 mm/min rotational and traverse speed, respectively, gave the highest Vickers hardness at the nugget zone.

3.2.1 Analysis of Variance (ANOVA)

The ANOVA analysis outcome is shown in Table 8. Since hardness is ability of material to resist plastic deformation, the larger the better approach is used to evaluate the *S*/*N* which is presented in Table 8. The contribution of the rotational speed to the hardness at the nugget zone is insignificant, while the travel speed contributes

Table 8 Analysis of variance (ANOVA)

Source	DF	Adj SS	Adj MS	*F*-Value	*P*-Value
Rotational speed	1	0.10	0.097	0.00	0.988
Traverse speed	1	111.89	111.888	0.27	0.612
Error	13	5400.02	415.386		
Total	15	5512.00			

Table 9 Response table for means

Level	Rotational speed	Traverse speed
1	107.99	110.08
2	95.73	102.53
3	119.95	111.54
4	99.68	99.19
Delta	24.22	12.35
Rank	1	2

Table 10 Response table for signal-to-noise ratio (*S*/*N*)

Level	Rotational speed	Traverse speed
1	40.56	40.79
2	39.54	40.12
3	41.56	40.74
4	39.7	39.71
Delta	2.02	1.08
Rank	1	2

majorly to the hardness results. The response to mean and *S*/*N* taking the larger is better approach are given in Tables 9 and 10, respectively. The main effects for mean and *S*/*N* are illustrated in Figs. 5 and 6, respectively. The interactions between the

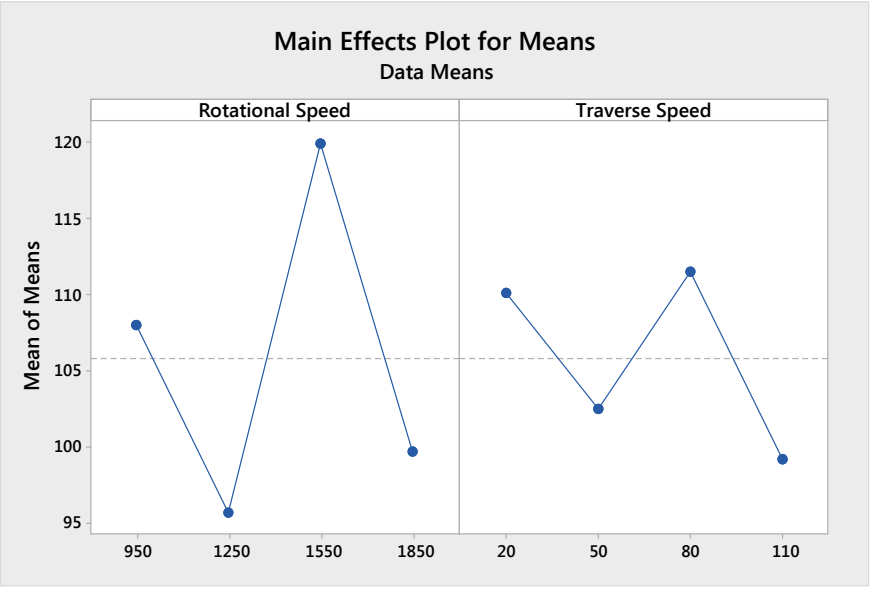

Fig. 5 Main effects plots for means

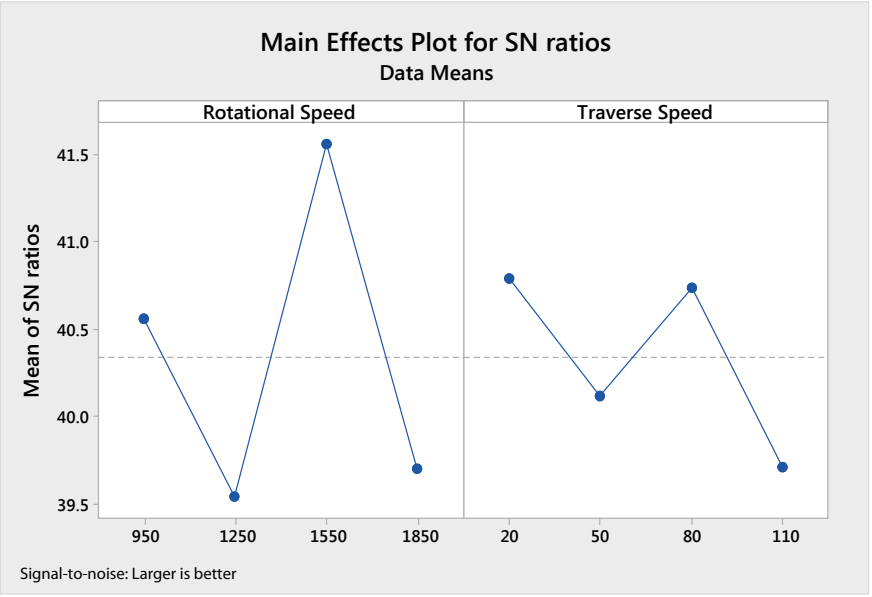

Fig. 6 Main effects plot for *S*/*N ratios*

two processing parameters considered for the optimizations are illustrated in Fig. 7 for the means while that of the *S*/*N* is shown in Fig. 8.

3.2.2 Response Optimization for Hardness

The response optimization for the rotational and travel speed for the hardness as analyzed from the *S*/*N* response and main effect plots in Fig. 6 gave the optimized parameters as 1550 rpm rotational speed and 20 mm/min traverse speed.

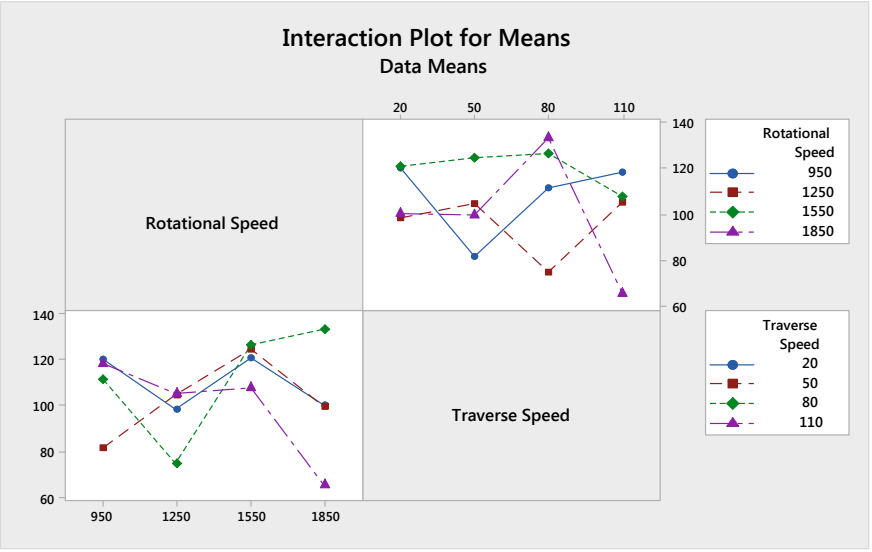

Fig. 7 Interaction plot for means

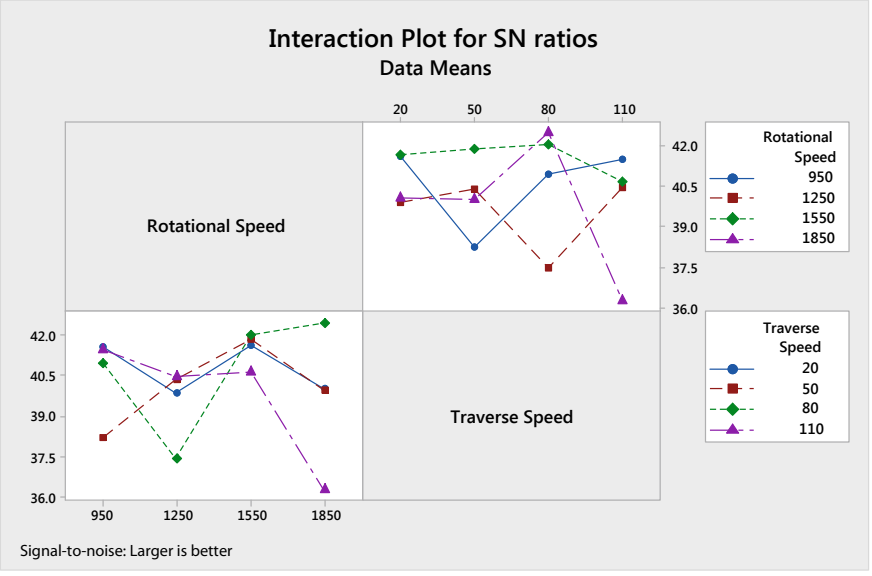

Fig. 8 Interaction plot for the *S/N ratios*

4 Conclusions

- The optimum rotational speed and travel speed for achieving maximum UTS are 950 rpm and 50 mm/min, respectively.
- The percentage contributions of the rotational speed toward attaining optimum UTS is 63% while that of transverse speed is 37%.
- Maximum hardness was obtained at an optimum rotational speed of 1550 rpm and 20 mm travel.
- The travel speed is the predominant factor toward attaining optimum hardness. The rotational speed contribution is very insignificant.

References

1. Nandan R, DebRoy T, Bhadeshia HKDH (2008) Recent advances in friction-stir welding—process, weldment structure and properties. Prog Mater Sci https://doi.org/10.1016/j.pmatsci.2008.05.001
2. Kumar K, Kailas SV (2008) The role of friction stir welding tool on material flow and weld formation. Mater Sci Eng, A. https://doi.org/10.1016/j.msea.2007.08.013
3. Mishra A (2018) Friction stir welding of dissimilar metal: a review. Int J Res Appl Sci Eng Technol. https://doi.org/10.22214/ijraset.2018.1237
4. Abolusoro OP, Akinlabi ET (2019) Wear and corrosion behaviour of friction stir welded aluminium alloys—an overview. Int J Mech Prod Eng Res Dev (IJMPERD) 9:967–982
5. Shah PH, Badheka VJ (2017) Friction stir welding of aluminium alloys: an overview of experimental findings—process, variables, development and applications. Proc Inst Mech Eng Part L J Mater Des Appl. https://doi.org/10.1177/1464420716689588
6. RajKumar V, VenkateshKannan M, Sadeesh P, Arivazhagan N, Devendranath Ramkumar K (2014) Studies on effect of tool design and welding parameters on the friction stir welding of dissimilar aluminium alloys AA 5052–AA 6061. Procedia Eng. https://doi.org/10.1016/j.proeng.2013.11.019
7. Abnar B, Kazeminezhad M, Kokabi AH (2015) Effects of heat input in friction stir welding on microstructure and mechanical properties of AA3003-H18 plates. Trans Nonferrous Met Soc China (English Edition). https://doi.org/10.1016/S1003-6326(15)63826-2
8. Palanivel R, Koshy Mathews P, Dinaharan I, Murugan N (2014) Mechanical and metallurgical properties of dissimilar friction stir welded AA5083-H111 and AA6351-T6 aluminum alloys. Trans Nonferrous Met Soc China (English Edition). https://doi.org/10.1016/S1003-6326(14)63028-4
9. Rao RV, Senthil Kumar M (2018) Experimental investigation on effect of welding parameters on the friction stir welding of AA 6061. Mater Today: Proc 5:12265–12272. https://doi.org/10.1016/j.matpr.2018.02.205
10. Farzadi A, Bahmani M, Haghshenas DF (2017) Optimization of operational parameters in friction stir welding of AA7075-T6 aluminum alloy using response surface method. Arab J Sci Eng 42:4905–4916. https://doi.org/10.1007/s13369-017-2741-6
11. Prasad MVRD, Kumar Namala K (2018) Process parameters optimization in friction stir welding by ANOVA. Mater Today: Proc 5:4824–4831. https://doi.org/10.1016/j.matpr.2017.12.057
12. Elanchezhian C, Vijaya Ramnath B, Venkatesan P, Sathish S, Vignesh T, Siddharth RV et al (2014) Parameter optimization of friction stir welding of AA8011-6062 using mathematical method. Procedia Eng. https://doi.org/10.1016/j.proeng.2014.12.308

13. Nourani M (2011) Taguchi optimization of process parameters in friction stir welding of 6061 aluminum alloy: a review and case study. Engineering 03:144–155. https://doi.org/10.4236/eng.2011.32017
14. Ugrasen G, Bharath G, Sagar R, Shivu PR, Keshavamurthy R (2018) Science direct optimization of process parameters for Al6061-Al7075 alloys in friction stir welding using Taguchi's technique. Mater Today Proc 5, 3027–3035. https://doi.org/10.1016/j.matpr.2018.01.103
15. Panda MR, Mahapatraand SS, Mohanty CP (2015) Parametric investigation of friction stir welding on AA6061 using taguchi technique. Mater Today Proc. https://doi.org/10.1016/j.matpr.2015.07.177
16. Jayaraman M, Sivasubramanian R, Balasubramanian V, Lakshminarayanan AK (2009) Optimization of process parameters for friction stir welding of cast aluminium alloy A319 by Taguchi method. J Sci Ind Res
17. Gomathisankar M, Gangatharan M, Pitchipoo P (2018) A novel optimization of friction stir welding process parameters on aluminum alloy 6061–T6. Mater Today Proc 5:14397–14404. https://doi.org/10.1016/j.matpr.2018.03.025
18. Saravanan V, Rajakumar S, Muruganandam A (2016) Effect of friction stir welding process parameters on microstructure and mechanical properties of dissimilar AA6061-T6 and AA7075-T6 aluminum alloy joints. Metallogr Microstruct Anal 5:476–485. https://doi.org/10.1007/s13632-016-0315-8
19. Kalemba-Rec I, Kopyściański M, Miara D, Krasnowski K (2018) Effect of process parameters on mechanical properties of friction stir welded dissimilar 7075–T651 and 5083–H111 aluminum alloys. Int J Adv Manuf Technol. https://doi.org/10.1007/s00170-018-2147-y
20. Pattanaik AK, Pradhan S, Panda SN, Bagal DK, Pal K, Patnaik D (2018) Effect of process parameters on friction stir spot welding using grey based taguchi methodology. Mater Today Proc 5:12098–12102. https://doi.org/10.1016/j.matpr.2018.02.186
21. Abolusoro OP, Akinlabi ET (2019) Experimental investigation of tool pin geometry and process parameter influence on the mechanical property of friction stir welded 6101-T6 and 7075-T651 Aluminium alloys, IOP conference series. J Phys 1378:032077. https://doi.org/10.1088/1742-6596/1378/3/032077

2.5 ARTICLE IV

Effects of Processing Parameters on Mechanical, Material Flow and Wear Behaviour of Friction Stir Welded 6101-T6 and 7075-T651 Aluminium Alloys

Published in *Manufacturing Review*, vol 7, 1-14, 2020. (**Scopus-indexed**) https://doi.org/10.1051/mfreview/2019026

FSW was performed between dissimilar 6101-T6 and 7075-T651 aluminium alloys with five parameters (1250rpm/20mm/min, 1250 rpm/65mm/min, 1250rpm/110mm/min, 1550rpm/110mm/min and 1850rpm/110mm/min) chosen for the experiment. The effects of these parameters on mechanical properties, wear and material flow patterns, were investigated and reported in the article. The mechanical testing of the prepared tensile specimen showed that failure occurred at the HAZ of the 6101-T6 on the advancing side of the butt-welding configuration. The SEM fractographs of the fractured surfaces revealed a fibrous structure with dimples which is typical of a ductile material. Necking occurred before the specimen fractured which indicated a gradual crack propagation process. The article also reported the effects of tool welding and rotational speed on the tensile strength, hardness, wear, and material mixing patterns. It was found that the UTS decreases as the rotational speed increases. However, the contrary was observed in the case of the welding speed. The UTS increases with an increase in welding speed. This implies that higher welding speed and lower rotational speed produce better tensile strength. The hardness on the other hand varied across the three zones of the welds for all the parameters with a welding speed of 65mm/min giving a maximum average hardness of 122.62Hv at the NZ while the rotational speed of 1850rpm gave the highest hardness of 122.46Hv at the NZ.

The wear behaviour examined at the various welding speeds showed that the highest wear rate took place at the highest welding speed of 110mm/min but occurred at medium rotational speed of 1550rpm. The article revealed that the wear behaviour of the NZ in relation to the hardness at the zone for all the parameters employed, confirmed the reports of some authors that hardness and wear rate are inversely related.

Furthermore, the article also touched on the material mixing pattern for all the parameters. An onion ring structure was observed for welds done with 1250rpm/65mm/min and 1250rpm/110mm/min whereas a lamellae flow structure was observed for 1250rpm/20mm/min and 1550rpm/110mm/min.

Manufacturing Rev. **7**, 1 (2020)

https://doi.org/10.1051/mfreview/2019026

Manufacturing Review
Available online at:
https://mfr.edp-open.org

RESEARCH ARTICLE OPEN ACCESS

Effects of processing parameters on mechanical, material flow and wear behaviour of friction stir welded 6101-T6 and 7075-T651 aluminium alloys

Olatunji P. Abolusoro* and Esther T. Akinlabi

Department of Mechanical Engineering Science, University of Johannesburg, Johannesburg, South Africa

Received: 12 October 2019 / Accepted: 26 November 2019

Abstract. Dissimilar friction stir welding (FSW) between 6101-T6 and 7075-T651 aluminium alloys was conducted. Three different parameters each were investigated for rotational speed and travel speed, and the effects of these parameters on the tensile behaviour, hardness and wear were evaluated. The results indicate that the ultimate tensile strength increases with an increase in the feed rate. However, the increase in rotational speed decreases the ultimate tensile values. The fractured analysis of the tensile samples shows similarities in the fractured pattern as all the samples failed at heat affected zone close to the 6101-T6 alloy. The hardness varies across the heat affected zones and nugget zone both at constant rotational speed and welding speeds. The highest resistance to wear occurred at 65 mm min^{-1} and 1850 rpm welding speed and rotational speed respectively while better material mixing was achieved at the nugget zone of the welds at 1250 rpm and 110 mm/min.

Keywords: Aluminium alloys / friction stir welding / mechanical properties / process parameters / wears

1 Introduction

One of the best technologies that have been identified to join low-temperature alloys especially aluminium is the friction stir welding (FSW). This welding technology emanated in 1991 and have been successfully employed to join aluminium alloy in many applications such as in marine, military, automotive and aerospace industries. The FSW utilized a rotating tool which has a pin and a shoulder. When this tool rotates on a workpiece, friction occurred which generates the heat needed to plasticized the material at the joint interface, permitting the stirring of the material by the rotating tool pin. The pressure from the tool shoulder and the mixing of materials by the tool bonded the workpiece interface together [1–8]. The heat generated during FSW alters the mechanical properties of the weld through microstructural modifications. This modification is often influenced by the processing parameter employed for the welding [8–10]. It has, therefore, become imperative to understand the influence of these parameters on the quality of welds. Particular attention has been given to the study of the relationship between mechanical properties and process parameters by researchers. Asadi and Givi [11] established how process parameters such as feed rate and tool rotational speed as well as tool profile affect the mechanical behaviour of welds. Tool rotational speed effects on tensile behaviour have been reported by some authors. For example, Lombard et al. [12] optimized the process parameters of friction stir welded 5083-H321 aluminium alloy in order to minimise defects and maximise fatigue life. Eleven parameters of combinations of rotational and traverse speeds were used. The tensile results obtained show that 200 rpm rotational speed and 85 mm/min travel speed gave the highest tensile value of 313 Mpa. The study portrayed that the major processing parameter affecting tensile strength is the rotational speed. Min-Su Han et al. [13] however reported that excess rotational speed could generate defects and improper joining. Prabha et al. [14] also investigated the influence of tool rotational speed on the tensile strength of 5083 aluminium alloy and concluded that rotational speed of 1120 rpm gave the best tensile results out of two other speeds of 1400 and 1800 rpm used. Aydin et al. [15] also identified tool rotational speed as a significant FSW variable which affects the rate of strain and the process of recrystallization. Ghosh et al. [16] reported an improvement in joint strength of FSW of dissimilar A356 and 6061 aluminium alloys welded with low travel and rotational speeds. In addition, Hariharan and Nimal [17] joined AA6061 and AA7075 aluminium alloys via FSW using a computerized numerical control machine. They reported an optimized tool rotational speeds of 1250 rpm and travel speed of 120 mm/min to give a defect free welds. Also,

* e-mail: abolusoroolatunji@yahoo.com

Table 1. Chemical composition of the welded aluminium alloys.

Alloy	Si	Cu	Fe	Mn	Mg	Ti	Cr	Zn	Al
6101-T6	0.53	0.01	0.14	0.002	0.600	0.008	0.001	0.003	Others
7075-T651	0.40	1.70	0.50	0.300	2.40	0.20	0.22	5.50	Others

Table 2. Mechanical properties of the welded alloys.

Alloy	Tensile strength (MPa)	Ultimate tensile strength (MPa)	Elongation (%)
6101-T6	172	200	15
7075-T651	462	575	11

Table 3. Rotational speeds and travel speeds.

Rotational speed (rpm)	Travel speed (mm min^{-1})
1250	20
1250	65
1250	110
1550	110
1850	110

Danielos and Pantelis [18] reported a good material mixing and mechanical properties at 950 rpm and 47.5 mm/min rotational and travel speed respectively in the FSW of 6082 and 7075-T651 aluminium alloys. Another work by Cole et al. [19] on FSW of 7075 and 6061 revealed an improvement in the joint strength at lower heat input. A similar work carried out by Guo et al. [20] shows that an increase in the welding speed which led to heat input reduction produced a higher UTS. Koilraj et al. [21] predicted mechanical strength of FSW of some aluminium alloys using Taguchi method. Rajkumar et al. [22] equally revealed that there exists a range of tool rotational speed where weld quality can be guaranteed. This demonstrates the possibilities of optimizing these process parameters of FSW in order to obtain high weld quality. Elangova et al. [23] showed the relationship between high welding speed and heat input. Heat input affects the metallurgical evolution that occurred during welding. And therefore, affect the strength across the zones of the weld. On this basis, an appropriate combination of the feed rate and the rotational speed of the tool can be said to be a significant factor for FSW control that determines the mechanical properties of the welded joint. Another significant factor affecting good mechanical strength, good material mixing and bonding in dissimilar aluminium friction stir welding is the relative positions of the alloys during the welding [18,24]. For instance, Guo et al. [20] noted a better material mixing condition at the nugget zone of the weld when the softer alloy (6061) is placed on the advancing side while the harder one (7075) is kept on the retreating side during the FSW of both alloys. Some reseachers have also reported that the thermal profile generated along the weld and the material movement and flow pattern are influenced by which of the dissimilar materials are kept on the advancing or retreating side of the welds [25]. Wear behaviour in some friction stir welded alloys have also been investigated by some researchers. Won Bae Lee et al. [26] investigated wear characteristics of FSW AZ91 magnesium alloy reinforced with silicon particles. Their result showed that better resistance to wear occurred at the welded zone compares to the parent metals. Palanivel et al. [27] established an empirical relationship between process parameters and wear resistance in the FSW of AA5083H111-AA6351-T6 alloys. Their result indicates that resistance to wear increases as tool rotational and welding speed increases to a certain extent after which the reverse occurred. This finding was in agreement with Dinaharan et al. [28] study on wear behaviour of FSW of AA6061/0-10wt% ZrB_2 composites. Seyed et al. [29] studied wear behaviour of similar and dissimilar FSW of AA6082 and AA6061 alloy. Their report indicates that similar welds of AA6061 gave superior wear resistance at the nugget zone to those of similar weld of AA6082 and dissimilar welds of both alloys. However, the dissimilar welds performed better at non-welded zone. This result was in agreement with similar investigations on the wear of FSW of AA6061 and AA6082 carried out by Khaja et al. [30]. The influence of Process parameters often differs in dissimilar friction stir welding of aluminium alloys and have not been fully studied. This work is an effort to give more understanding of the process as it relates to mechanical properties, material flow and wear behaviour in dissimilar welding of aluminium alloys.

2 Experimental procedure

2.1 Sample's chemical composition and properties

The elemental composition and mechanical properties of the welded alloys are shown in Tables 1 and 2, respectively.

2.2 Process parameters

The rotational and travel speeds used for the experiments are shown in Table 3. The parameters were chosen based on the optimized parameters on similar work reported in the literature [31]. The rotational and the travel speeds range were carefully selected to cover below and above the reported optimized values.

2.3 Experimental procedure

2.3.1 Welding set up

The aluminium plates 6101-T6 and 7075-T651 with a thickness of 6 mm to be welded were cut into pieces of 60 mm × 100 mm each. The edges to be joined were milled to allow proper lapping when placed in the welding position. The surface especially the areas to be welded were cleaned with very smooth emery paper to remove oxide layers that might have been formed on the surfaces of the alloys. Acetone was further used to clean the surface to remove dirt and oil or grease. A cylindrical tapered tool having shoulder diameter of 22 mm, probe length 5.65 mm, with root and mouth diameter of 7.3 mm and 5.5 mm, respectively as shown in Figure 1a and b was used for the welding. The welding was carried out with a two-tonne numerical welding machine manufactured by ETA Technology Ltd, Bangalore, India (Fig. 2a). The plates were arranged in butt configuration with the 6101-T6 placed on the advancing side (AS) while the 7075-T651 alloy was placed on the retreating side (RS). The plates were clamped in this arrangement for the welding as shown in Figure 2b. The welding was performed in the rolling directions of the plates. The welding parameters shown in Table 3 were utilized for the welding. Other parameters used are plunge depth of 0.15 mm and tool tilt angle of 2°.

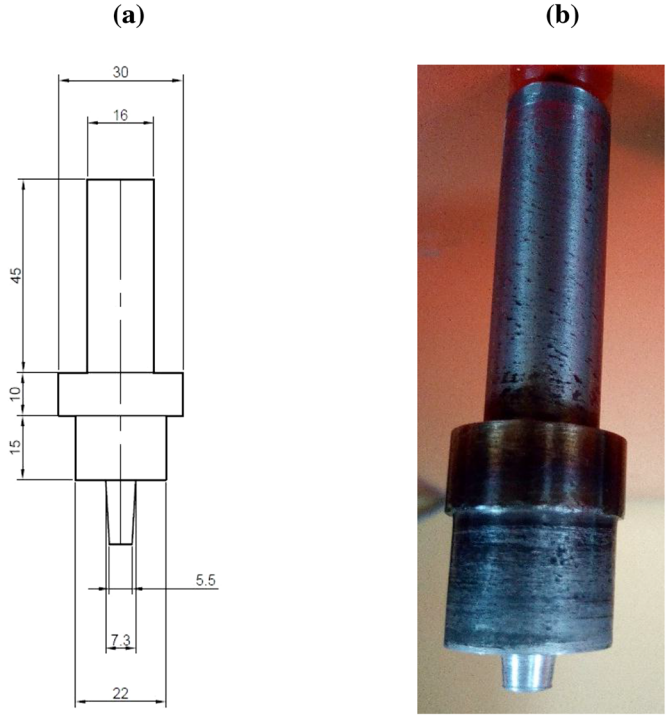

Fig. 1. Tapered threaded tool (a) schematic diagram (b) picture.

2.3.2 Mechanical testing of the welds

Three tensile samples from each weld as shown in Figure 3 were cut perpendicularly to the weld following ASTM E8 standard specifications for mechanical strength evaluation. The tensile testing was carried out as a function of tool rotational and travel speeds using Instron testing machine. SEM fractography analysis was done on the tensile tested samples.

Fig. 3. Tensile samples evaluated.

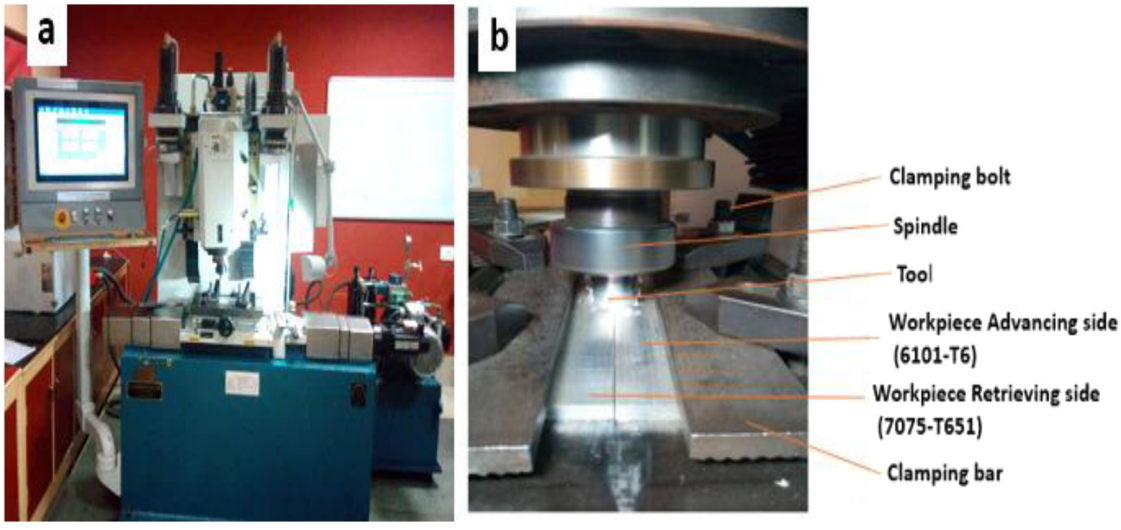

Fig. 2. (a) Welding equipment. (b) Welding arrangement.

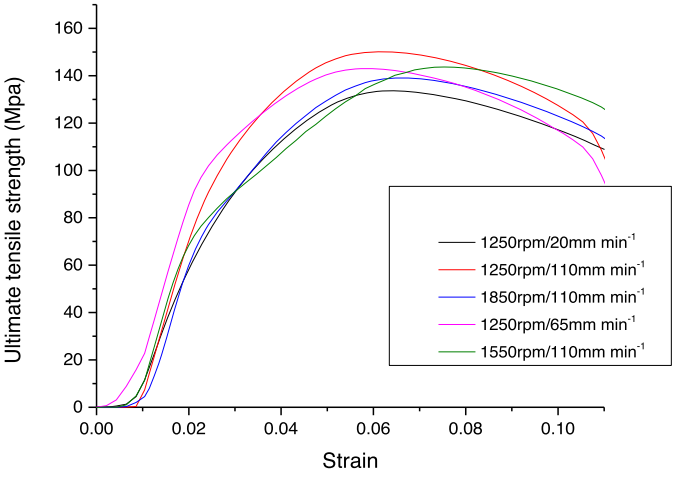

Fig. 4. Graph of stress vs strain at different process parameters.

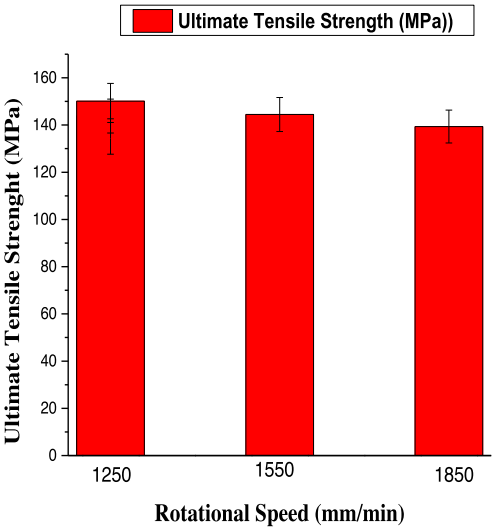

Fig. 5. Effects of rotational speed on ultimate tensile Strength with error bars at 95% confidence level.

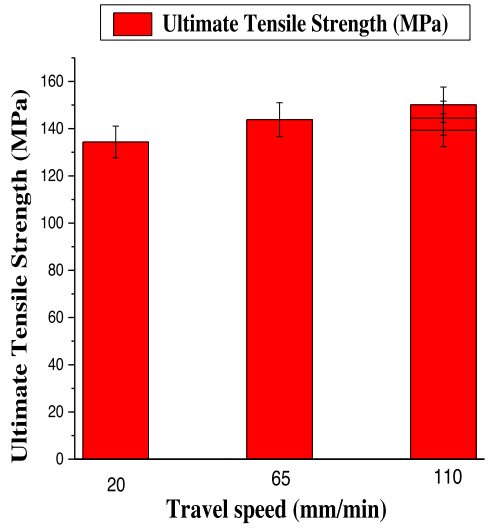

Fig. 6. Effects of travel speed on ultimate tensile strength with error bars at 95% confidence level.

2.3.3 Hardness testing

The hardness test was profiled across the welding direction. Vickers hardness testing equipment was used. 300 kgf load was applied with a dwelling time of 15 s and 26 indentations were made on each sample at 1 mm interval.

2.3.4 Wear testing

The wear specimen measured 6 mm × 6 mm × 10 mm were cut from the nugget zone of the weld. A ball on disc machine of model E52100 with alloy steel ball of 6.35 mm diameter equipped with MFTI7 software was employed for the wear test under dry sliding conditions and at an ambient temperature of 25°C in accordance with ASTM G99 standard. A load of 20N at a sliding distance of 3 mm for 300 s and velocity of 3 mm/s were used. The worn surface analysis was carried out using a scanning electron microscope (SEM).

3 Results and analysis

3.1 Tensile analysis

The average stress-strain relationships obtained for all the process parameters are shown in Figure 4. While the effect of rotational speed and travel speed are respectively shown in Figures 5 and 6. The detailed analysis of the results are fully discussed in this section.

3.1.1 Effect of rotational speed on tensile behaviour

The average values of the three tensile samples evaluated for each of the process parameters were plotted for the three different rotational speeds used in the study as shown in Figure 5. The rotational speed of 1250 rpm at a travel speed of 110 mm min^{-1} gave the highest ultimate tensile strength of 150 MPa. The result shows that the ultimate tensile strength reduces with an increase in rotational speed. This can be attributed to more heat input into the weld from the frictional heat generated by the tool as the rotational speed increases. This trend was also observed by Mohammed et al. [32] and Izabela et al. [33] with similar reasons given. The thermal cycle set up at the weld region own to heat input from the tool rotational speed becomes higher as the rotational speed increases. This causes deterioration of precipitates by coarsening or dissolutions at the welding zone and consequently lowers grain bonding thereby reducing the resultant mechanical properties of the weld [8,18,19].

3.1.2 Effect of travel speed on tensile behaviour

At constant rotational speeds of 1250 rpm and varying travel speed, the ultimate tensile values increases as the travel speed increases. This is illustrated in Figure 6. The

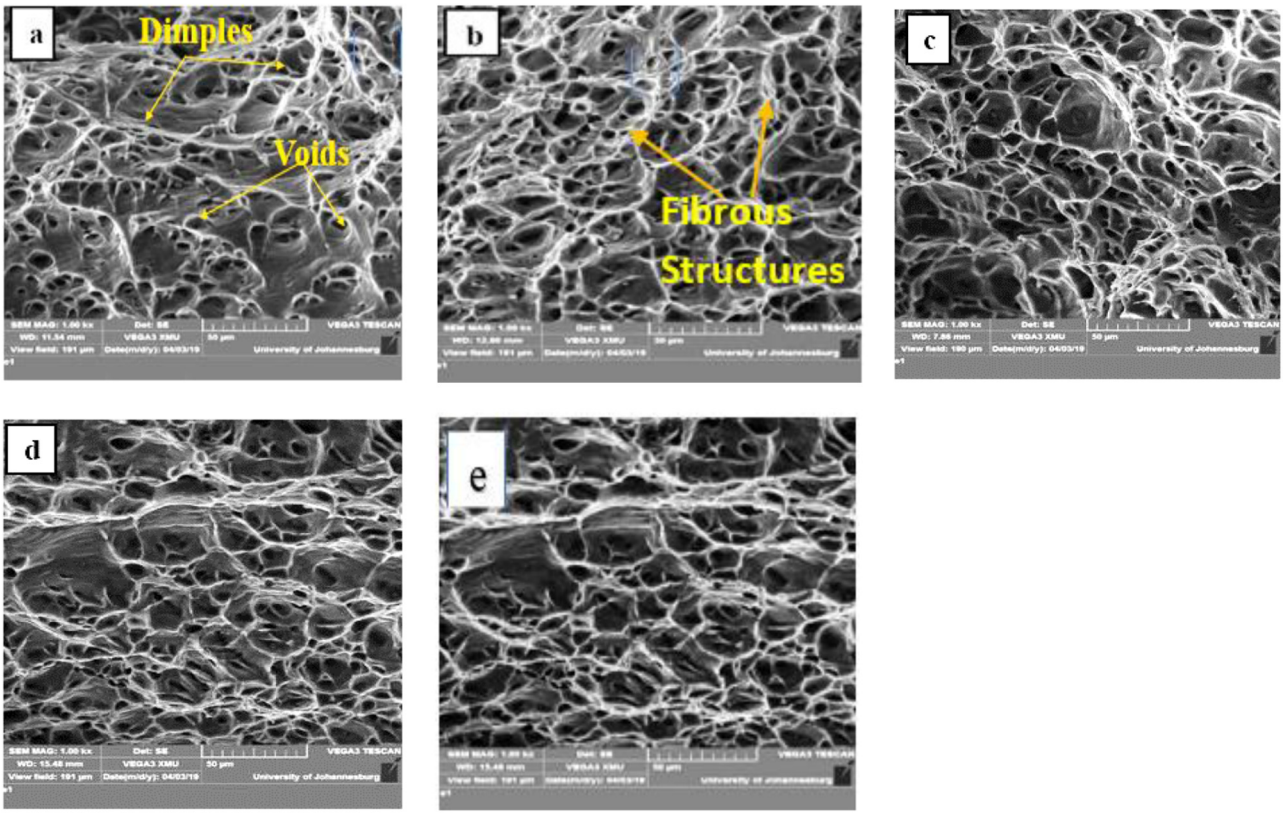

Fig. 7. Fractographs of the tensile tests fractured surfaces. (a) 1250 rpm at 20 mm min^{-1}. (b) 1250 rpm at 65 mm min^{-1} (c) 1250 rpm at 110 mm min^{-1}. (d) 1550 rpm at 110 mm min^{-1} (e) 1850 rpm at 110 mm min^{-1}.

travel speed of 110 mm min^{-1} being the highest used gave the highest ultimate tensile value of 150 MPa. This is as a result of less heat input into the weld due to less dwelling time of the tool rotation on the alloys as the travel speed increases. Higher travel speeds have been correlated to low heat input into the weld which led to faster cooling rates of the welded joints thereby promoting greater grain boundaries of precipitates which favours better mechanical properties [18,34].

3.1.3 Fracture analysis of the tested samples

All the samples tested for tensile evaluations failed at the heat affected zone (HAZ) close to the 6101-T6 alloy placed on the advancing side during the welding. This can be attributed to the lower ultimate tensile strength possess by the 6101-T6 parent alloy compare to the other 7075-T651 alloy dissimilarly welded to it. The none failure of the material at the nugget zone suggest that proper material mixing and bonding occurred considerably within the range of rotational and travel speeds deployed for this study. Similar reasons were given by Daniolos and Pantelis [18]. The fractographs taken and shown in Figure 7a–e exhibits similarities in structures due to the fracture of the welds at the heat affected zone of the advancing side alloy for the range of rotational and travel speeds considered. The fractured samples also indicate that there was appreciable plastic deformation and necking before failure took place. Fibrous features with appreciable lip region at the outer boundary of the final fracture were noticeable. These fibrous features indicate that the crack propagation occurred slowly. The cracking pattern also exhibited what is termed equiaxed dimples with prominent cup and cone features, typical behaviour of ductile materials.

3.2 Hardness analysis

3.2.1 Hardness at different welding speeds

The hardness tests carried out on both parent alloys gave 60.01 and 178.8 Hv for 6101-T6 and 7075-T651, respectively. The hardness profile is shown in Figure 8 and the average hardness values obtained at different welding zones across the three welding speeds are shown in Figure 10. The hardness values obtained at the heat affected zone (HAZ) of the RS were lower than that of the parent alloy 7075-T651 at the RS. The subjection of the alloy to thermal cycle at that region during the welding could result in the dissolution of precipitates of the alloy leading to reduction of the hardness. The maximum average hardness value of 126.96 Hv as illustrated in Figure 10 was obtained at the HAZ of the retreating side and occurred at the travel speed of 110 mm min^{-1} which is the highest welding speed employed. The less dwelling time of the tool as it traverses on the workpiece joint interface at the 110 mm min^{-1} welding speed promote better grain refinement at the region and may account for highest

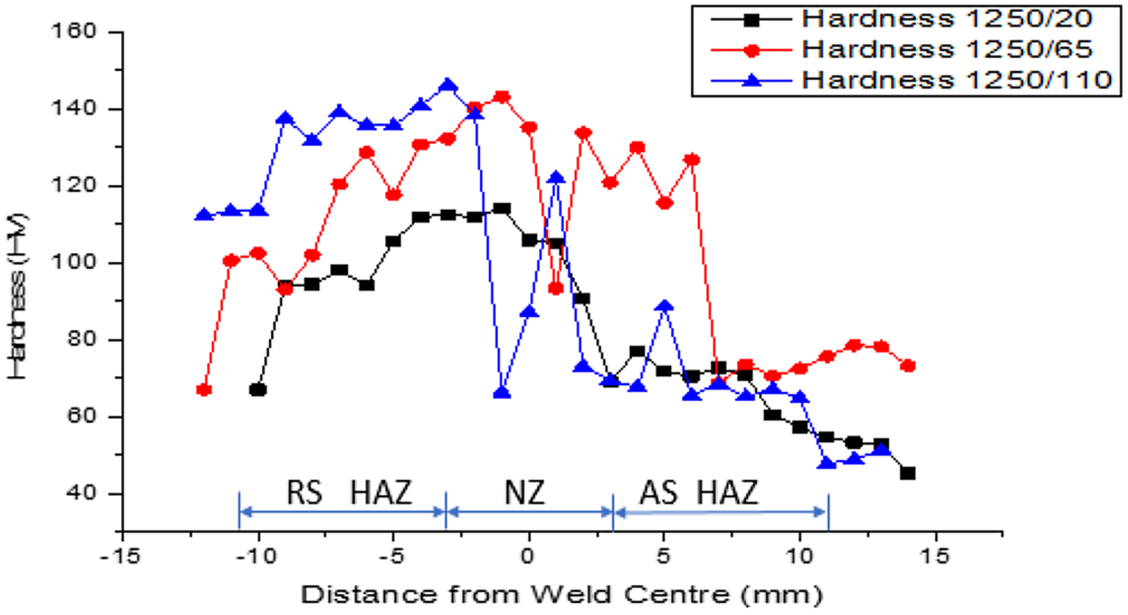

Fig. 8. Hardness profile at varying welding speed.

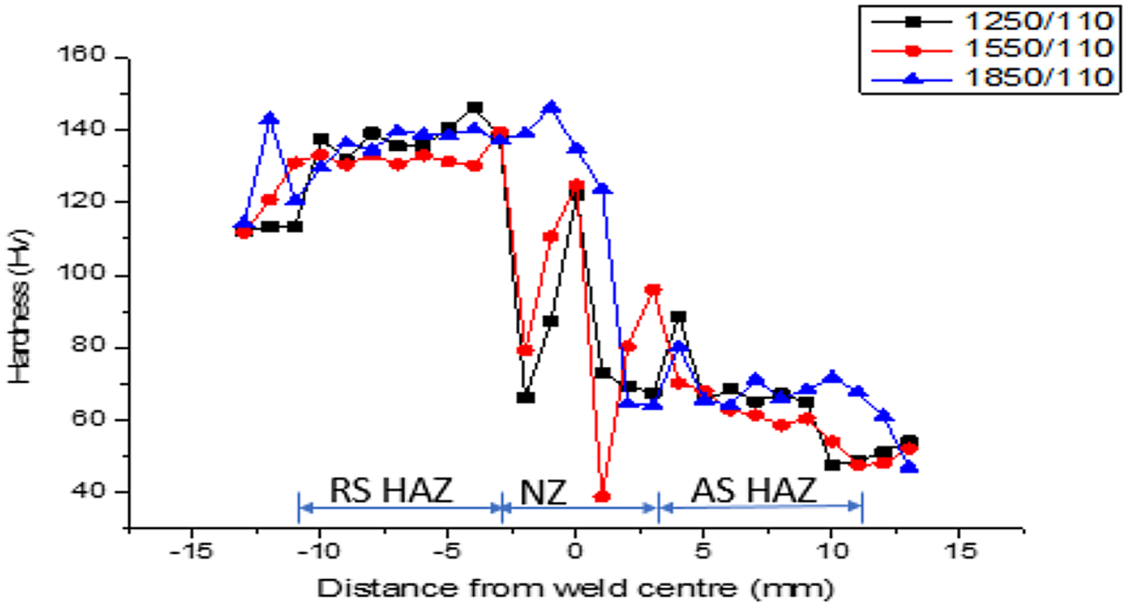

Fig. 9. Hardness profile at varying rotational speed.

values of hardness obtained at that particular welding speed at the HAZ of the RS. At lower welding speeds, the thermal impact is felt more and development of coarse precipitates may occur resulting to decrease in hardness. At the nugget zone (NZ), the average hardness values at different welding speed were generally lower than the hardness of the 7075-T651 parent alloy but are higher than that of 6101-T6 parent alloy. This is due to the mixing of both alloys at this region. The hardness at the NZ increased to a maximum of 122.62 HV as the welding speed increases to 65 mm/min and drastically dropped to 83.56 HV with further increase in welding speed to 110 mm min^{-1}. The variation in the average hardness values in the NZ at different welding speed is due to inhomogeneous mixing of material compositions and distribution at the zone which could result to the dissolution of strengthening precipitates and hence lowering the hardness values in the zone as noticed at welding speeds of 20 mm and 110 mm min^{-1}. The same transformation observed in the NZ took place in the HAZ of the advancing side. The average hardness value in the region at 20 mm/min was 60.97 HV which moved up to 81.88 HV at 65 mm/min before dropping to 58.71 HV at the welding speed of 110 mm min^{-1}. There is little or no difference between the average hardness values obtained at the HAZ of the AS and that of the parent alloy 6101-T6 at the AS. This may be due to the high thermal conductivity

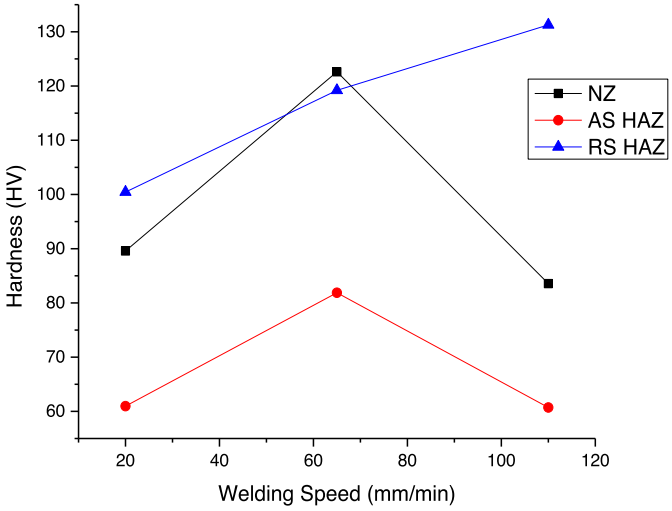

Fig. 10. Average hardness values at the NZ, AS HAZ and RS HAZ for the three different welding speed.

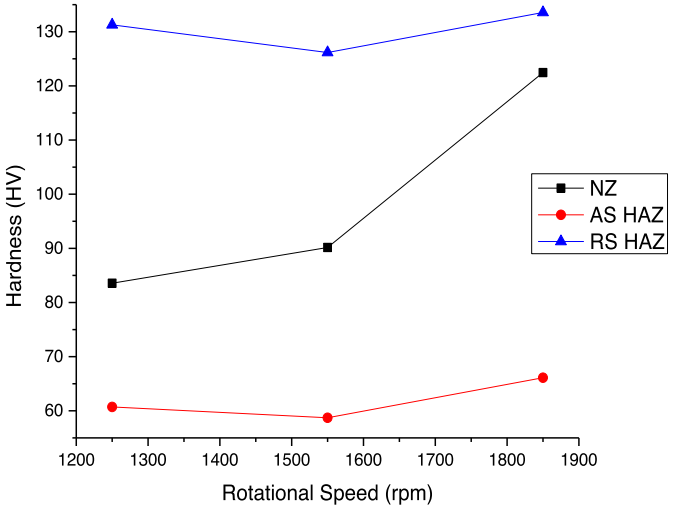

Fig. 11. Average hardness values at the NZ, AS HAZ and RS HAZ for the three different rotational speed.

of the alloy which promotes heat dissipation from the welding process to the surrounding thereby reducing thermal stress set up in the region during welding. Lower values of average hardness recorded at a welding speed of 20 mm min^{-1} on the AS sides of the HAZ can be linked to precipitate coarsening due to slower traversing of the tool on the workpiece. Although higher traversing speed of 110 mm min^{-1} also led to lower average hardness values on AS of the HAZ. This suggests that there is a range of welding speed within which optimum hardness values can be obtained within the region.

3.2.2 Hardness at different rotational speeds

The hardness profile as shown in Figure 9 exhibit similar pattern of transformation across the RS of the HAZ, the NZ and the AS of the HAZ for the three different rotating speeds at a constant welding speed of 110 mm min^{-1}. At the HAZ of the RS, the hardness values were highest but drop abruptly at the NZ. The least value of hardness at the NZ occurred at the rotation speed of 1550 rpm. This may be due to little void at the weld centre own to improper bonding of the transported grains at that point. Also, from Figure 11 at the HAZ of the RS, the average value of hardness is 131.27 HV at 1250 rpm. This value decreases to 126.96 HV as the rotational speed increase to 1550 rpm and became maximum with 133.56 HV at 1850 rpm. All the hardness values at the RS of the HAZ are lower than that of the parent alloy on the RS. Similar behaviour was observed for HAZ of the AS with an average hardness value of 60.71 HV at 1250 rpm which decreases to 58.41 HV at 1550 rpm and rose slightly up to 66.11 HV at 1850 rpm. However, these values do not differ considerably from that of the parent alloy at the advancing side own to the high thermal conductivity of the alloy as explained earlier on in Section 3.2.1. A slightly different pattern was observed in NZ. The average hardness value increases as the tool rotational speed increases within the range of 83.56 HV at 1250 rpm to 122.46 HV at 1850 rpm. The general drop in hardness values on both sides of the HAZ at 1550 rpm may not be unconnected with poor material mixing and coarsening of the precipitates at the zones during the welding.

3.3 Wear behaviour

MFTI7 software of the tribometer used generates the wear volume, depth and coefficient of friction while the wear rate and the wear resistance were calculated using equation (1) [35,36]. Table 4 shows the summary of the results obtained for the wear test for each processing parameter employed.

$$\text{Wear rate } (\text{mm}^3/\text{Nm}) = \frac{\text{Wear volume}}{\text{Applied force} \times \text{Sliding distance}} \times 1000 \quad (1)$$

3.3.1 Wear rate at different welding speeds

The wear profiling as obtained from the tribometer software for the samples at different welding speeds are shown in Figure 16A a (i, ii), b (i, ii), and c (i, ii). The coefficient of friction (COF) responses of the weld at different welding speeds is shown in Figure 13. The COF at the three different welding speeds employed did not show a clear difference as the wear process progresses. The wear rate obtained at the different welding speeds for the samples A–C as shown in Table 4 is much lower than those of the parent materials. The relationship between the welding speeds and wear rate as illustrated in Figure 14 indicate that there was a reduction in the wear rate as the welding speed increases to 65 mm min^{-1}. However, a further increase in the speed to 110 mm min^{-1} resulted in appreciably high wear rate. This observation agreed with earlier findings by Palanivel et al. [23] and Dinaharan et al. [24]. The lowest wear rate at 65 mm min^{-1} can be ascribed to better material mixing and grain refinement at the

Table 4. Summary of wear results obtained for different parameters.

Denotation	Rotational speed (rpm)/ welding speed (mm min^{-1})	Weight of sample before testing (g)	Weight of sample after testing (g)	Weight loss (g)	Wear depth (mm)	Wear volume × E^{-2} (mm^3)	Wear rate × E^{-4} (mm^3 Nm^{-1})
A	1250/20	4.3829	4.3825	0.004	0.04607	3.443031	1.9128
B	1250/65	4.3611	4.3609	0.002	0.0895	2.679846	1.4888
C	1250/110	4.4723	4.4721	0.002	0.06762	6.813473	3.7853
D	1550/110	3.9141	3.9138	0.003	0.05050	7.141568	3.9675
E	1850/110	3.8586	3.8584	0.002	0.05675	3.098608	1.7215
6101-T6	–	3.5621	3.562	0.001	0.06057	9.483394	5.2686
7075-T6	–	4.7118	4.7119	0.001	0.10227	7.524306	4.1802

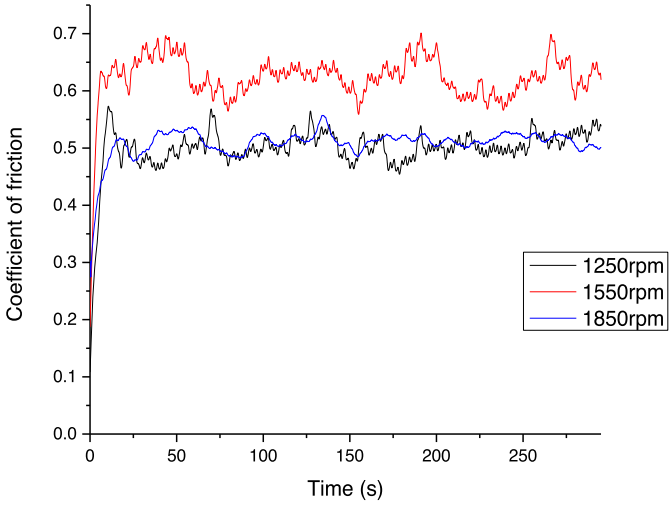

Fig. 12. Coefficient of friction responses at different tool rotational speed.

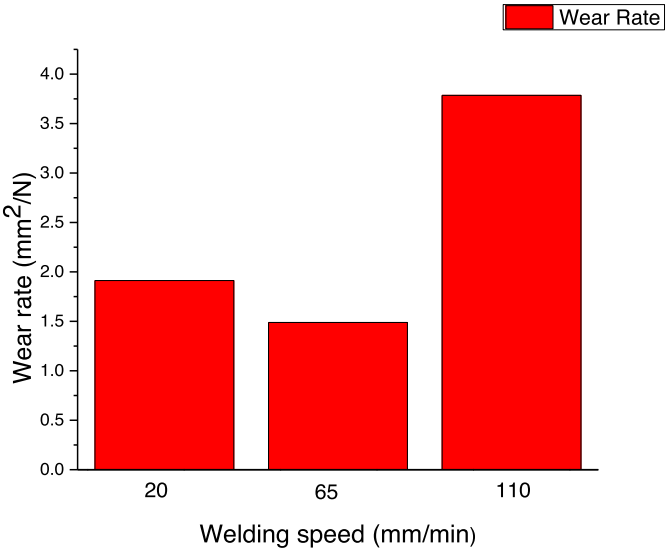

Fig. 14. Wear rate at different welding speeds.

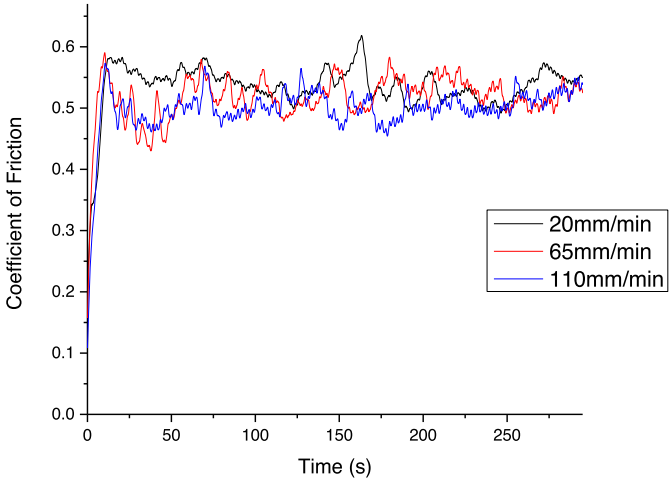

Fig. 13. Coefficient of friction responses at different welding speed.

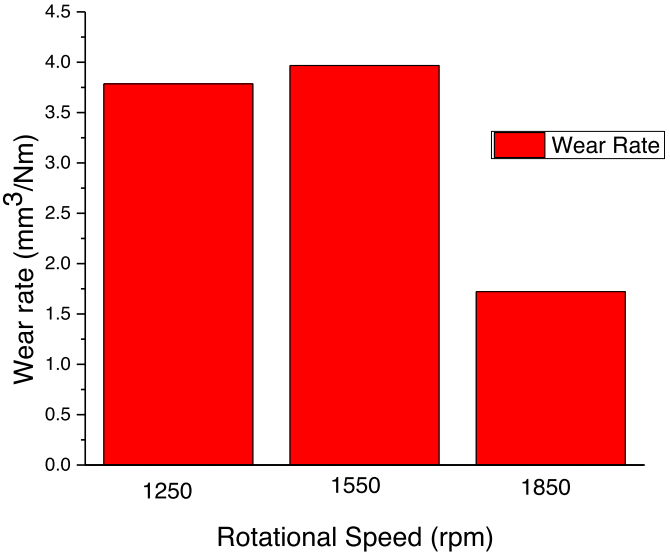

Fig. 15. Wear rate at different rotational speeds.

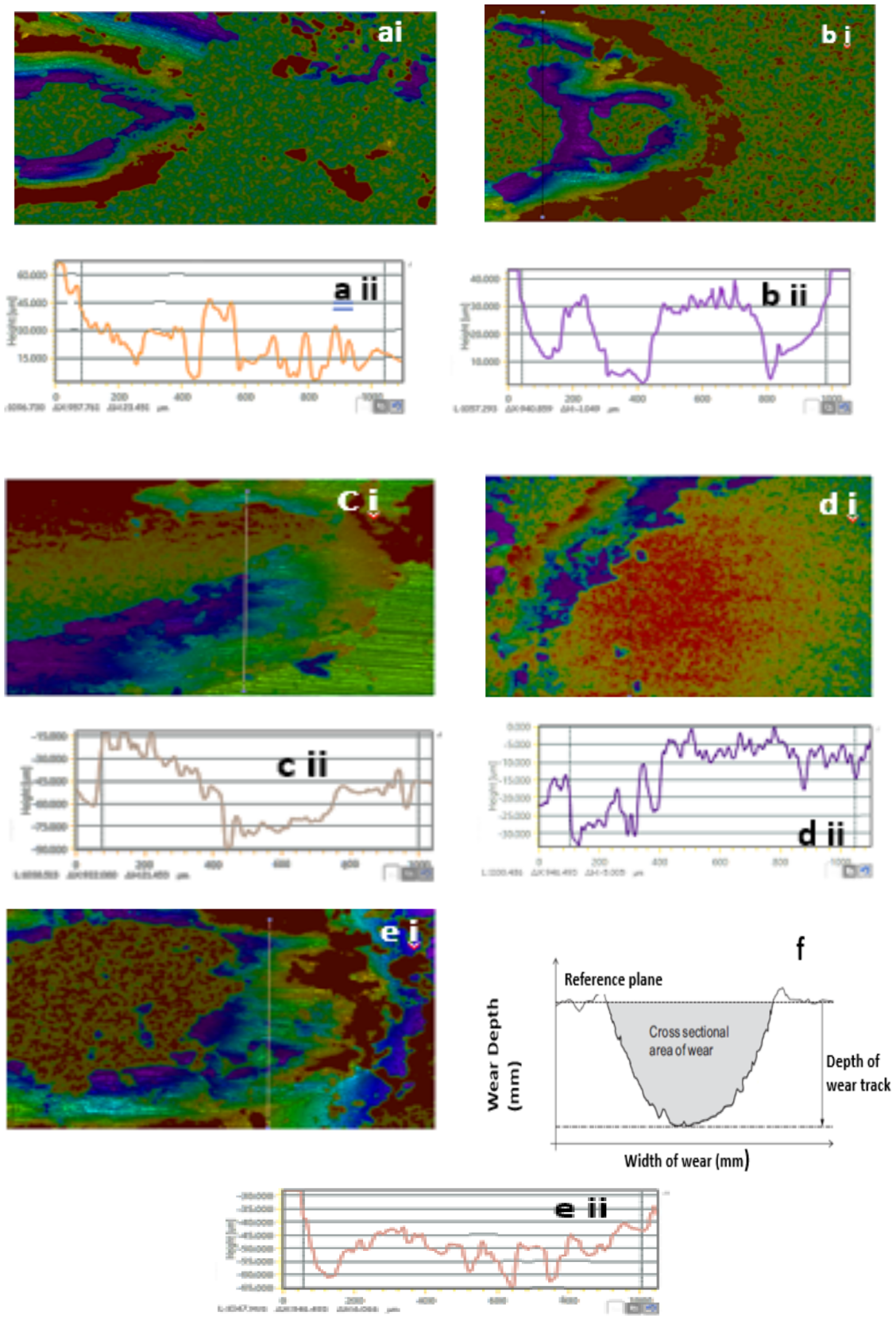

Fig. 16. Wear profiling (ai) and (aii) for sample A. (bi) and (bii) for sample B. (ci) and (cii) for sample C. (di) and (dii) for sample D. (ei) and (eii) for sample E. (f) Illustration of wear profile.

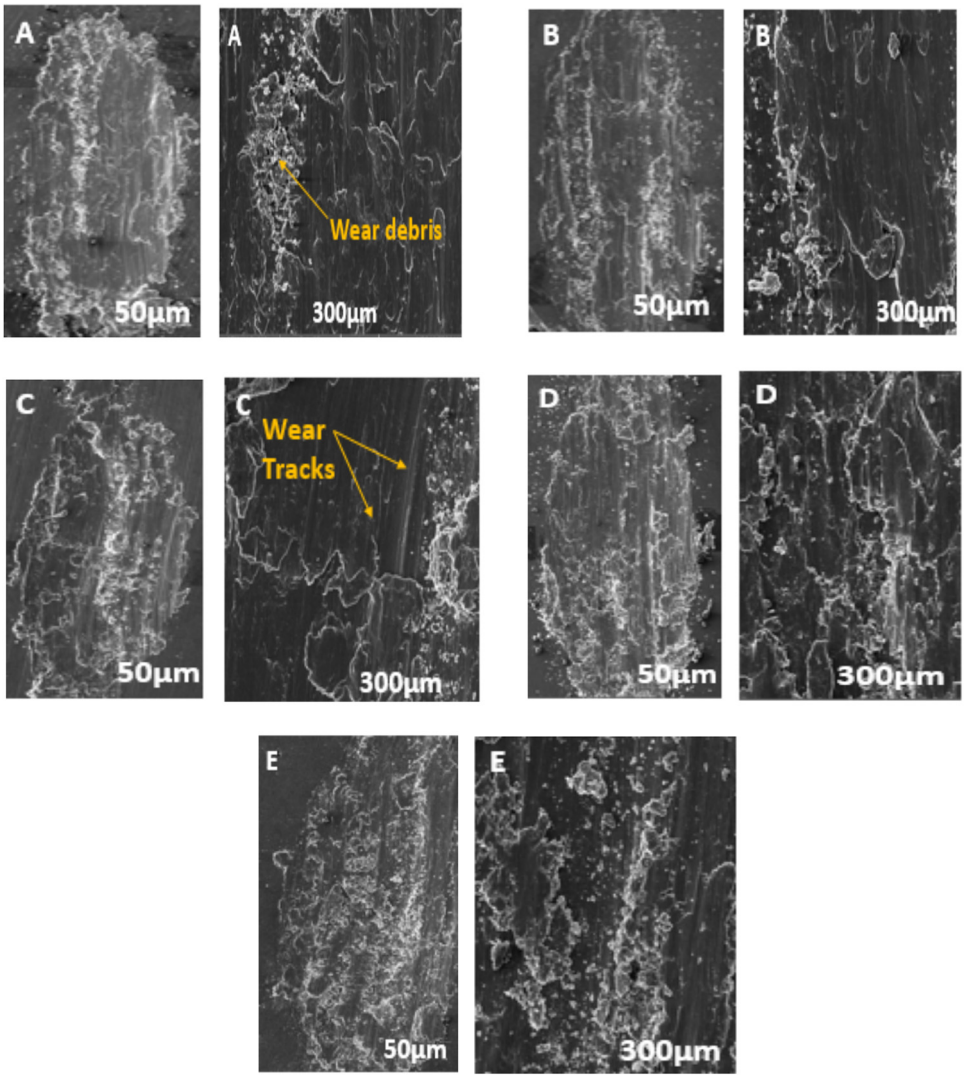

Fig. 17. SEM micrograph of wear tracks for sample A–E at different magnifications.

nugget zone. This finding also reflects in the high hardness values obtained at the nugget zone of the sample as illustrated in the hardness profile shown in Figure 9. This was in agreement with Gopi et al. [37] and Umasankar et al. [38] who affirmed that wear rate is inversely proportional to the hardness. The SEM micrographs of the samples at a different speed as indicated in Figure 17A–C similarly exhibit narrow and shallow grooves attributed to a lower coefficient of friction due to abrasion from entrapped debris and asperities on the hard counterbody.

3.3.2 Wear rate at different rotational speeds

The wear profiling as obtained from the tribometer software for the samples at different rotational speeds are shown in Figure 16 ci, c ii, di, d ii, e i and e ii. Calculated wear rates for the samples at different rotational speeds are shown in C, D and E in Table 4. The coefficient of friction responses of the welds at different rotational speed as shown in Figure 12 indicate that the coefficient of friction was highest at the rotational speed of 1550 and minimum at 1250 rpm. The wear rate as observed in Figure 15 was highest in D at 1550 rpm. All these imply that more wear took place at the rotational speed of 1550 rpm than the other two rotational speeds of 1250 and 1850 rpm. The high COF and wear rate observed at that speed is an indication of low resistance to wear. This is also evident in the hardness profile shown in Figure 9. The hardness values dropped at the nugget zone. The same zone where the wear test was carried out. This is another confirmation that hardness is inversely proportional to wear rate as reported by some authors [24,25]. The wear rate at the three rotational speeds studied was generally lower than those of the two parent metals. This can be attributed to grain refinement and proper material mixing and cohesion at the nugget zones own to thermal cycle impact from the welding process. The SEM micrographs at the different rotational speeds studied are shown in Figure 17C–E. The micrographs generally show mild adhesion mechanism with evidence of grooves but very narrow and shallow.

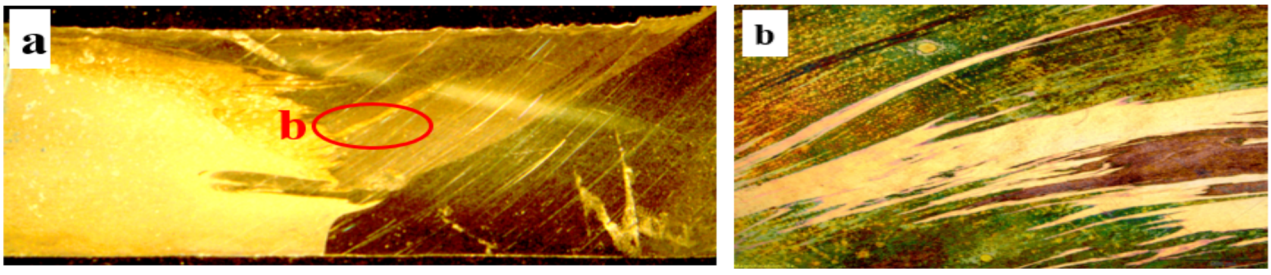

Fig. 18. Material flow at 1250 rpm and 20 mm/min (a) Macrograph (b) microstructures at 20X.

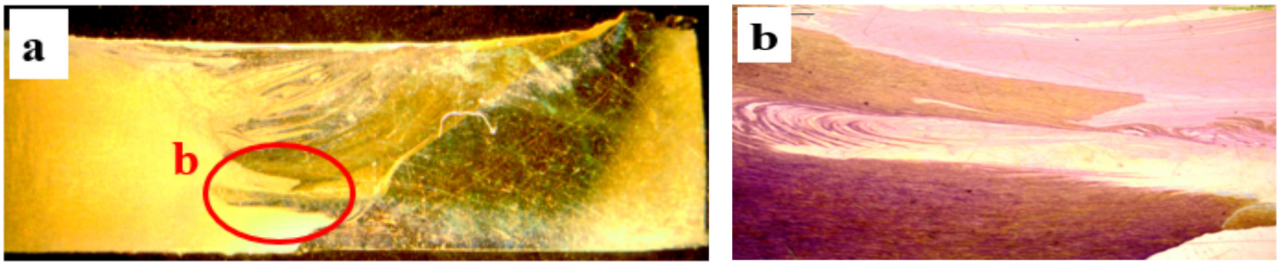

Fig. 19. Material flow at 1250 rpm and 65 mm/min (a) Macrograph (b) microstructures at 20X.

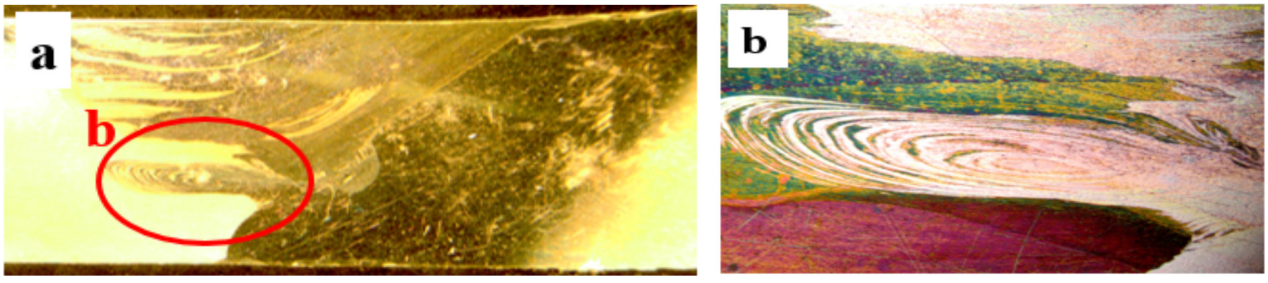

Fig. 20. Material flow at 1250 rpm and 110 mm/min (a) Macrograph (b) microstructures at 20X.

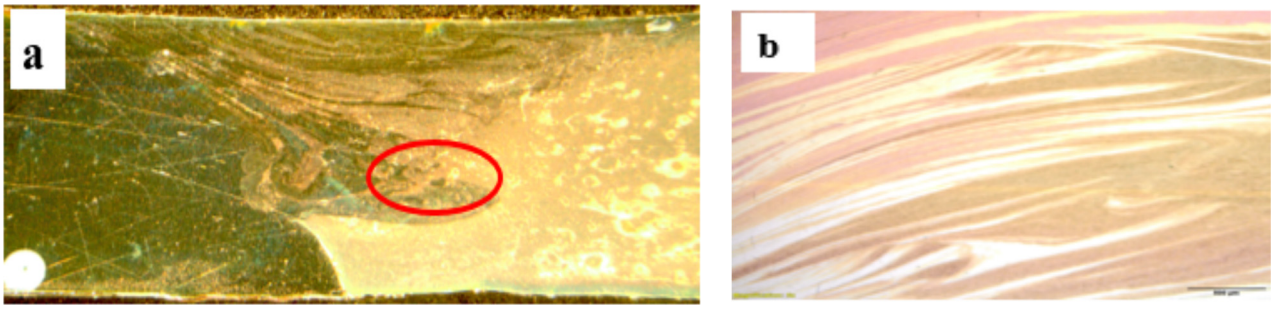

Fig. 21. Material flow at 1550 rpm and 110 mm/min (a) Macrograph (b) microstructures at 20X.

3.3.3 Microstructures

The macrostructures and microstructures of each parameters obtained through an optical microscope are presented in Figures 18–22. The circled portions in Figures 18a, 19a, 20a, 21a and 22a are named "b" and are all magnified to 20X to give Figures 18b, 19b, 20b, 21b and 22b, respectively.

The macrographs for all the samples demonstrated non-uniformity in the material transportation from the upper weld region to the lower region as shown in Figures 18a, 19a, 20a, 21a and 22a. This may be attributed to variations in the contact area of the tool pin with the materials due to the tapered tool pin geometry used for the welding [39]. The weck's reagent used revealed 7075-T651 as a lighter colour

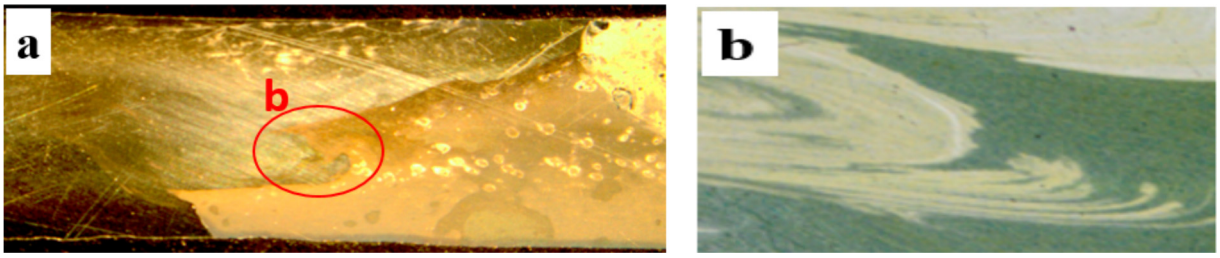

Fig. 22. Material flow at 1850 rpm and 110 mm/min (a) Macrograph (b) microstructures at 20X.

while 6101-T6 is shown as a darker colour. The microstructures generally demonstrate appreciable material mixing at the nugget zone which promotes good bonding and disallowed the materials from fracturing at the welding joint during the tensile testing as explained earlier in Section 3.1.3. However, more layers of materials from the 6101-T6 on the advancing side of the weld seems to be swept more into the 7075-T651 on the retreating side at the weld at 1250 rpm and 110 mm/min (Fig. 20a). The mixing pattern of the alloys at the nugget zone at this parameter as observed in Figure 20b demonstrates alternate layers of the materials in a circular form which is often described as the "onion ring structures". These appreciable mixing and material flow pattern at the nugget zone of the weld could be correlated to the highest tensile value obtained at that parameter as given in Section 3.1.1 compared to the other parameters. On the contrary, at 1850rpm and 110 mm/min, considerable materials transportation and mixing was not properly achieved. Only the circled portion of the 6101-T6 materials as shown in Figure 22a could be observed to extend into the 7075-T651 material compared to the other welds. This may be attributed not only to the higher rotational speed used but also due to the high traversing speed employed together for the weld which may not permit systematic interfacial mixing as the tool traverse faster on the joint interface of the alloys [39,40]. This also accounts for the lowest tensile value obtained at that parameter compared to other parameters used. The microstructures taken at the circled portion of the nugget zone of the micrographs revealed onion ring flow structures for 1250 rpm/65 mm/min and 1250 rpm/110 mm/min and alternate lamellae flow pattern for 1250 rpm/20 mm/min and 1550 rpm/110 mm/min.

4 Conclusion

- The ultimate tensile values for dissimilar welds of 6101-T6 and 7075-T651 have been found to decrease as the rotational speed increases but increase with an increase in travel speeds. These show that higher travel speed and lower rotational speed promote sound mechanical properties of the friction stir welded 6101-T6 and 7075-T651 aluminium alloys.
- All the tensile samples failed at the HAZ of the 6101-T6 alloy. The none failure of the material at the nugget zone indicates that good material mixing and bonding occurred considerably within the range of rotational and travel speeds deployed for this study.
- The hardness at the HAZ of both alloys was lower than those of their respective parent alloys. However, the hardness at the NZ was higher than that of the 6101-T6 parent alloy but lower than that of 7075-T651 parent alloy at all the rotational and welding speeds considered. Wear rate reduces as the welding speed increases. However, beyond a certain speed, the wear rate begins to increase. The highest resistance to wear was obtained at 65 mm/min welding speed.
- The wear rate increases as the tool rotational speed increase to a level but reduce with a further increase in the rotational speed. The highest resistance to wear was obtained at a rotational speed of 1850 rpm.

5 General comments

A systematic relationship between tool rotational speed, traverse speed, wear behaviour, material flow and mechanical properties of friction stir welded 61010-T6 and 7075-T651 aluminium alloys have been established in this study. The observed correlation agrees with some findings in the literature on other dissimilar friction stir welding of aluminium alloys, This has widened the scope and understanding of dissimilar friction stir welding of aluminium alloys for lightweight industrial applications. However in-situ temperature measurement could not be carried out during the experiment for better understanding of the effects of the welding parameters on the thermal cycle set up and the accompanied microstructural modifications and mechanical behaviour.

References

1. W.M. Thomas ED, J.C. Nicolas, M.G. Needham, P. Murch, C. D. Templesmith, US Patent Application. 1995; No. 546031
2. W.M. Thomas ED, J.C. Nicolas, M.G. Needham, P. Murch, C. D. Templesmith, Int. patent Application. 1991. No.PCT/GB92/02203
3. R.S. Mishra, Z.Y. Ma, Friction stir welding and processing, Mater. Sci. Eng. **50** (2005) 1–78
4. G. Buffa, L. Donati, L. Fratini, L. Tomesani, Solid-state bonding in extrusion and FSW: Process mechanics and analogies, J. Mater. Process. Technol. **177** (2006) 344–7

5. P.H. Shah, V.J. Badheka, Friction stir welding of aluminium alloys: An overview of experimental findings – Process, variables, development and applications, Proc. Inst. Mech. Eng. Part L J. Mater. Des. Appl. **233** (2017) 1191–1226
6. T.A. Esther, A. Andrews, A.A. Stephen, Effects of processing parameters on the corrosion properties of dissimilar Friction Stir Welds of aluminium and copper, Trans. Nonferrous Met. Soc. China **24** (2014) 1323–1330
7. M. Sivashanmugam, S. Ravikumar, T. Kumar, V. Seshagiri Rao, D. Muruganandam, A review on friction stir welding for aluminium alloys. In: *Proceedings of the International Conference on Frontiers in Automobile and Mechanical Engineering – 2010, FAME-2010, IEEE, New Jersey*, 2010
8. S. Bocchi, M. Cabrini, G. D'Urso, C. Giardini, S. Lorenzi, T. Pastore, The influence of process parameters on mechanical properties and corrosion behaviour of friction stir welded aluminium joints, J. Manuf. Process. **35** (2018) 1–15
9. P. Cavaliere, A. De Santis, F. Panella, A. Squillace, Effect of welding parameters on mechanical and microstructural properties of dissimilar AA6082-AA2024 joints produced by friction stir welding, Mater. Des. **30** (2009) 609–616
10. P. Olatunji Abolusoro, E.T. Akinlabi. In-Process Cooling in Friction Stir Welding of Aluminium Alloys-An Overview. In: Al. MA et, editor. Advances in Material Sciences and Engineering, Lecture Notes in Mechanical Engineering, Springer Nature Singapore Pvt. Ltd., Berlin, 2020, 435–444
11. M.K.B. Givi, P. Asadi, Advances in Friction-Stir Welding and Processing (Elsevier, Amsterdam, 2014), 1–756
12. H. Lombard, D.G. Hattingh, A. Steuwer, M.N. James, Optimising FSW process parameters to minimise defects and maximise fatigue life in 5083-H321 aluminium alloy, Eng. Fract. Mech. **75** (2008) 341–54
13. M.S. Han, S.J. Lee, J.C. Park, S.C. Ko, Y.B. Woo, S.J. Kim, Optimum condition by mechanical characteristic evaluation in friction stir welding for 5083-O Al alloy, Trans. Nonferrous Met. Soc. China **19** (2009) 17–22
14. K.A. Prabha, P.K. Putha, B.S. Prasad, Effect of tool rotational speed on mechanical properties of aluminium alloy 5083 weldments in friction stir welding, Mater. Today Proc. **5** (2018) 18535–18543
15. H. Aydin, A. Bayram, U. Esme, Y. Kazancoglu, O. Guven, Application of Grey Relation Analysis (Gra) and Taguchi Method for the Parametric Optimization of Friction Stir Welding (Fsw) Process, Appl. Grey. Relat. Anal. **44** (2010) 205–11
16. M. Ghosh, K. Kumar, S.V. Kailas, A.K. Ray, Optimization of friction stir welding parameters for dissimilar aluminum alloys, Mater. Des. **31** (2010) 3033–3037
17. R. Hariharan, R.J. Golden Renjith Nimal, Friction stir welding oof dissimilar aluminium alloys (6061&7075) by using computerized numerical control machine, Middle-East J. Sci. Res. **20** (2014) 601–605
18. N.M. Daniolos, D.I. Pantelis, Microstructural and mechanical properties of dissimilar friction stir welds between AA6082-T6 and AA7075-T651, Int. J. Adv. Manuf. Technol. **88** (2017) 2497–505
19. E.G. Cole, A. Fehrenbacher, N.A. Duffie, M.R. Zinn, F.E. Pfefferkorn, N.J. Ferrier, Weld temperature effects during friction stir welding of dissimilar aluminium alloys 6061-t6 and 7075-t6, Int. J. Adv. Manuf. Technol. **71** (2014) 643–652
20. J.F. Guo, H.C. Chen, C.N. Sun, G. Bi, Z. Sun, J. Wei, Friction stir welding of dissimilar materials between AA6061 and AA7075 Al alloys effects of process parameters. Mater Des. **56** (2014) 185–192
21. M. Koilraj, V. Sundareswaran, S. Vijayan, S.R. Koteswara Rao, Friction stir welding of dissimilar aluminium alloys AA2219 to AA5083 – Optimization of process parameters using Taguchi technique, Mater. Des. **42** (2012) 1–7
22. S. Rajakumar, V. Balasubramanian, Establishing relationships between mechanical properties of aluminium alloys and optimised friction stir welding process parameters, Mater. Des. **40** (2012) 17–35
23. K. Elangovan, V. Balasubramanian, M. Valliappan, Influences of tool pin profile and axial force on the formation of friction stir processing zone in AA6061 aluminium alloy, Int. J. Adv. Manuf. Technol. **38** (2008) 285–295
24. D.A. Dragatogiannis, E.P. Koumoulos, I.A. Kartsonakis, D.I. Pantelis, P.N. Karakizis, C.A. Charitidis, Dissimilar Friction Stir Welding Between 5083 and 6082 Al Alloys Reinforced With TiC Nanoparticles, Mater. Manuf. Process. **31** (2016) 2101–2114
25. D.A. Dragatogiannis, D. Kollaros, P. Karakizis, D. Pantelis, J. Lin, C. Charitidis, Friction Stir Welding between 6082 and 7075 Aluminum Alloys Thermal Treated for Automotive Applications, Mater. Perform. Charact. **8** (2019)
26. L. Won-Bae, L. Chang-Yong, K. Myoung-Kyun, Y. Jung-I1, K. Young-Jig, Y. Yun-Mo JS-B, Microstructures and wear property of friction stir welded AZ91Mg/SiC particle reinforced composite, Compos. Sci. Technol. **66** (2006) 1513–1520
27. R. Palanivel, P.K. Mathews, N. Murugan, I. Dinaharan, Prediction and optimization of wear resistance of friction stir welded dissimilar aluminium alloy, Proc. Eng. **38** (2012) 578–584
28. M.N.I. Dinaharan, Influence of friction stir welding parameters on sliding wear behaviour of AA6061/0-10 wt.% ZrB2 in-situ composite butt joints, J. Miner. Mater. Charact. Eng. **10** (2011) 1359–77
29. N. Syed Khaja, Md. A. Tousef, B.C. Purna, N. Mohan, Y.A. Vidhu Kampurath, Wear behaviour of welded and non-welded samples of friction stir welding of similar and dissimilar joints of aluminium alloys, Int. J. Mech. Eng. Technol. **7** (2016) 289–299
30. S. Khaja Naimuddin, T. Md, K. Vidhu, M. Asim Mohamad, Y. Ali, Analysis of Wear Behaviourof the Friction Stir Welded Jointswith Varying Track Diametersfor Non-Welded and Welded Samples, Indian J. Sci. Technol. **9** (2016) 41
31. G. Swaminathan, S. Sathiyamurthy, Experimental Study of Mechanical and Metallurgical Properties of Friction Stir Welded Dissimilar Aluminum Alloys, Int. J. Mech. Prod. Eng. Res. Dev. **8** (2018) 1049–1058
32. M.M. Abd Elnabi, A.B. Elshalakany, M.M. Abdel-Mottaleb, T.A. Osman, A.A. El Mokadem, Influence of friction stir welding parameters onmetallurgical and mechanical properties ofdissimilar AA5454-AA7075 aluminum alloys, J. Mater. Res. Technol. **8** (2019) 1684–1693
33. I. Kalemba-Rec, M. Kopyscianski, D. Miara, K. Krasnowski, Effect of process parameters on mechanical properties of friction stir welded dissimilar 7075-T651 and 5083-H111 aluminum alloys, Int. J. Adv. Manuf. Technol. **97** (2018) 2767–2779

34. S. Rajakumar, C. Muralidharan, V. Balasubramanian, Influence of friction stir welding process and tool parameters on strength properties of AA7075-T6 aluminium alloy joints, Mater. Des. **32** (2011) 535–549
35. A.K. Shrivastava, K.K. Singh, A.R. Dixit, Tribological properties of Al 7075 alloy and Al 7075 metal matrix composite reinforced with SiC, sliding under dry, oil lubricated, and inert gas environments, Proc. Inst. Mech. Eng. Part J. J. Eng. Tribol. **232** (2018) 693–698
36. F. Alshmri, H.V. Atkinson, S.V. Hainsworth, C. Haidon, S.D. A. Lawes, Dry sliding wear of aluminium-high silicon hypereutectic alloys, Wear **313** (2014) 106–116
37. V. Gopi, R. Sellamuthu, S. Arul, Measurement of hardness, wear rate and coefficient of friction of surface refined Al-Cu alloy, Proc. Eng. **97** (2014) 1355–1360
38. U. Das, R. Das, V. Toppo, Wear behaviour study of Friction Stir Welded Dissimilar Metals: AA6101-T6 and AA6351-T6 Aluminium Alloys, IOP Conf. Ser. Mater. Sci. Eng. **377** (2018)
39. R. Palanivel, P. Koshy Mathews, N. Murugan, I. Dinaharan, Effect of tool rotational speed and pin profile on microstructure and tensile strength of dissimilar friction stir welded AA5083-H111 and AA6351-T6 aluminum alloys, Mater. Des. **40** (2012) 7–16
40. S. Ravikumar, V. Seshagiri Rao, R.V. Pranesh, Effect of Process Parameters on Mechanical Properties of Friction Stir Welded Dissimilar Materials between AA6061-T651 and AA7075-T651 Alloys, Int. J. Adv. Mech. Eng. **4** (2014) 101–114

Cite this article as: Olatunji P. Abolusoro, Esther T. Akinlabi, Effects of processing parameters on mechanical, material flow and wear behaviour of friction stir welded 6101-T6 and 7075-T651 aluminium alloys, Manufacturing Rev. **7**, 1 (2020)

2.6 ARTICLE V

Effects of Processing Parameters on Temperature Distributions, Tensile Behaviour, and Microstructure of Friction Stir Welding of Dissimilar Aluminium Alloys

Published *in Lecture Note in Mechanical Engineering* 2019. (**Scopus-indexed**)

This article reported on how the processing parameters employed in the FSW of 6101-T6 and 7075-T651 aluminium alloys impacted on the temperature distributions, the tensile strength and the microstructural changes in the welds.

Four rotational and welding parameters (1250rpm/50mm/min, 1550rpm/50mm/min, 1850rpm/50mm/min, 1850rpm/50mm/min) were selected for welding with in-situ temperature measurements. The temperature profile observed across all the parameters indicate that the temperature distribution varies in both alloys. This was ascribed to variations in the thermal conductivities of both base metals. Higher values of temperatures were recorded in the 7075-T651on the retreating side than in the 6101-T6 on the advancing side of the welds. The temperature profile generally showed that the temperature increases and attains a peak at the middle of the weld as the welding progresses. The article also reported the effect of the rotational and traverse speed of the tool on the temperature distributions. The temperature was found to increase as the rotational speed increases but decreases as the welding speed increases. The higher temperature obtained at higher rotational speed was attributed to higher frictional effects of the tool on the rotating workpiece which resulted in high heat generation. Also, the lower temperature observed at higher speed was ascribed to less dwelling time of the tool on the workpiece due to faster movement of the tool on the workpiece joints.

The microstructural observation of the weld indicated that enough heat needed for plasticisation and bonding occurred at the joint interface. Lamellae material flow behaviour was observed in all the welds. This research article also showed that large volumes of material transportation occurred at 1850rpm and 50mm/min rotational and traverse speeds respectively. However full penetration of the alloy into one another was observed more at a rotational speed of 150rpm and traverse speed of 50mm/min.

The UTS values at higher rotational speeds were found to be lower than those at lower rotational speeds. The contrary was noticed in the traverse speed. The UTS increases as the traverse speed increases.

Effects of Processing Parameters on Temperature Distributions, Tensile Behaviour and Microstructure of Friction Stir Welding of Dissimilar Aluminium Alloys

Olatunji P. Abolusoro and Esther Titilayo Akinlabi

Abstract Research has shown that there is a correlation between process parameters, temperature variations, tensile strength, microstructures and the durability of the welds obtained in friction stir welding (FSW). The need to institute this correlation is crucial in order to achieve a weld free of defects and having sound mechanical behaviours for industrial applications. This work examines process parameters effects on variations of weld temperature, tensile strength and microstructures in dissimilar FSW of 6101-T6 and 7075-T651 aluminium alloys with a plate thickness of 6 mm. The welding was done with rotational speeds of 1250, 1550 and 1850 rpm and traverse speeds of 50 and 110 mm/min. The results obtained indicate that processing parameters significantly affect the temperature distributions in the weld. Increase in rotational speed increases the temperature but cause a decrease in tensile strength. While the increase in travel speed cause a reduction in temperature which results to increase in the tensile strength. Highest tensile strength of 143 MPa was obtained at 1250 rpm and 50 mm/min but better mixing of both materials was achieved at 1550 rpm and 50 mm/min.

Keywords Aluminium · Friction stir welding · Temperature · Processing parameters

1 Introduction

One of the metals that are broadly used in many engineering applications is aluminium. The extensive use of this alloy emanates from its properties. One of which is its high strength to weight ratio. FSW is a technology that has been in use for joining both similar and dissimilar aluminium alloys. The unique advantages of this

O. P. Abolusoro (✉) · E. T. Akinlabi
Department of Mechanical Engineering Science, University of Johannesburg, Johannesburg 2006, South Africa
e-mail: abolusoroolatunji@yahoo.com

E. T. Akinlabi
Department of Mechanical Engineering, Covenant University, Ota, Ogun State, Nigeria

S. Vijayan et al. (eds.), *Trends in Manufacturing and Engineering Management*,
Lecture Notes in Mechanical Engineering,
https://doi.org/10.1007/978-981-15-4745-4_64

welding technology which include non-requirements of filler metals as the case in non-solid state welding technology and environmentally friendly have endeared it to its wide usage in industries for joining aluminium alloys [1–3]. There are parameters that govern the friction stir welding process. Two most prominent of these factors are the rotation and travel speed of the tool pin on the workpiece. These two parameters affect largely the heat generated during the welding and consequently affect temperature distributions, tensile and microstructures of the weld [4–7]. Aissani et al. [8] reported the influence of process parameters on tensile behaviour. Lombard et al. [9] optimized the rate of feed and rotation of tool effects on tensile strength and concluded that tool rotational speed impact more on tensile behaviour. Many other researchers have reported the relationship between these factors, tensile and microstructures [10–14] Also, the influence of these processing parameters on temperatures distributions have been examined by some researchers. Umasanka and Vijay studied the relationship between tool rotational speed, mechanical impact strength and temperature on AA6101-T6 and AA6351-T6 alloys welded using FSW. Their result indicates that temperature goes higher with an increase in rotational speed and that the impact strength depends on the pressure and the duration of impact [15]. Yoshima et al. welded dissimilar ADC12 and AA6061 alloy and examined the temperature distributions during the welding. The temperature measurements were done at various offset values. Their results indicate that temperature goes higher with an increase in tool offset and the temperature at any point depends on its distance from the welding tool which generates the heat [16]. Modelling of temperature distributions in FSW of one of the chosen alloys for this work (AA7075) has been attempted. Kandasamy et al. analyzed temperature changes in FSW of AA7075 aluminium alloy using finite element approach. The temperature measurement was done using k-type thermocouple on the workpiece and hand infrared thermometer on the tool. Their result demonstrated close agreement with the experimental values obtained [17]. Many researchers have utilized various approaches to investigate temperature changes during FSW. Some of these methods include thermal cameras, thermocouple inserted in the welding tool or in the workpiece [18–22]. Other methods like ultrasound and neutron-based techniques have also been used [23, 24]. However, the most commonly used method observed in literature is that of a thermocouple embedded in workpiece [15, 16, 25, 26]. This particular method was employed in this study. Thermocouple positions have also been reported to affect the accuracy of temperatures measured. While close proximity of the thermocouple to the rotating tool pin or the stir zone gives a better estimate of the weld temperature, the likely destruction of the thermocouple wires as the pin progresses limits the use of this method [15]. Hence in this study, the thermocouple was embedded in the workpiece in an area close to the heat-affected zone. Although numerous researches on FSW of dissimilar aluminium alloys have been carried out, however, welding parameter's relationship with microstructures, tensile and temperature variations especially on FSW of 7075-T651 and 6101-T6 have not been fully reported. This paper, therefore, presents this relationship for more understanding.

2 Experimental Procedures and Processing Parameters

2.1 Elemental Composition and Properties of the Sample

Dissimilar aluminium alloys 6101-T6 and 7075-T651 were used for the experiment. The elemental constituents of the two materials are indicated in Table 1 while Table 2 shows the mechanical properties.

2.2 Process Parameters

Three tool rotational speeds and two feed rates were engaged in this study as presented in Table 3.

2.3 Experimental Procedures

The tool for the experiment was fabricated using high carbon steel H13. It has shoulder diameter of 22 mm with a tapered pin profile of big diameter 7.3 mm, small diameter 5.5 mm and pin length of 5.6 mm as illustrated in Fig. 1. The two alloy plates of 7075-T651 and AA6101-T6 were cleaned and arranged in butt configuration with AA6101-T6 on the advancing side and 7075-T651 on the retreating side as illustrated in Fig. 2. The FSW was performed along the rolling direction of the two alloy samples with the tilt angle at 2^0. Two thermocouple wires were embedded in the workpiece 2 mm away from the welding zone on both sides of the plates and are placed 40 mm apart. The thermocouples were connected to a temperature data capturing machine for in-process temperature measurements. The thermocouple arrangement is shown in Fig. 3. Four different experiments were carried out using the parameters shown in Table 3. Three tensile samples cut according to ASTM E8 standard were tested for each weld and the average for each weld taken for evaluation. The microstuctural analysis was done on the nugget zone of each weld using an optical microscope.

Table 1 Elemental constituents of the two materials

Alloy	Si	Fe	Cu	Mn	Mg	Cr	Zn	Ti	Al
6101-T6	0.53	0.14	0.01	0.002	0.600	0.001	0.003	0.008	Others
7075-T651	0.40	0.50	1.70	0.300	2.40	0.22	5.50	0.20	Others

Table 2 Mechanical properties of the alloy

Alloy	Tensile strength (Mpa)	Ultimate tensile strength (Mpa)	Elongation (%)	Thermal conductivity (W/m °C)
6101-T6	172	180	15	167
7075-T651	462	575	11	130

Table 3 Processing parameters

Rotational speed (rpm)	Travel speed (mm/min)
1250	50
1550	50
1850	50
1850	110

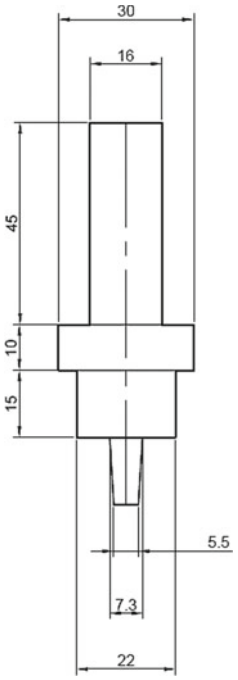

Fig. 1 Schematic diagram of the welding tool

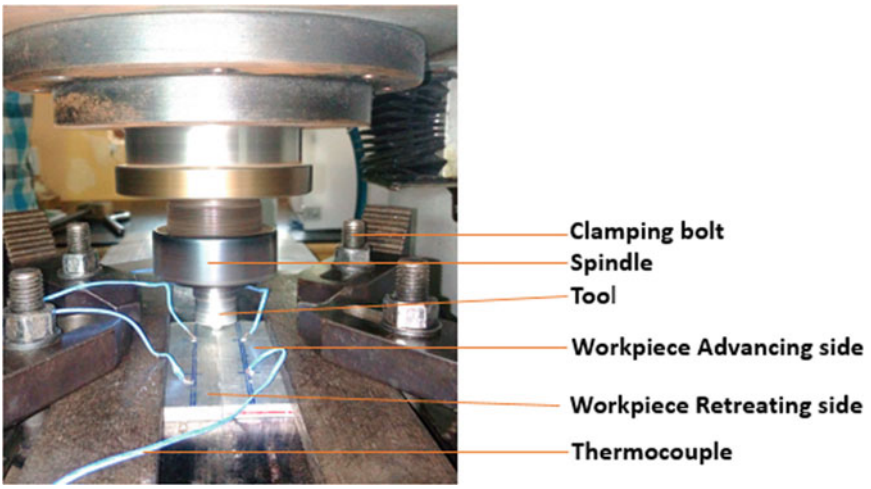

Fig. 2 Workpiece retreating side

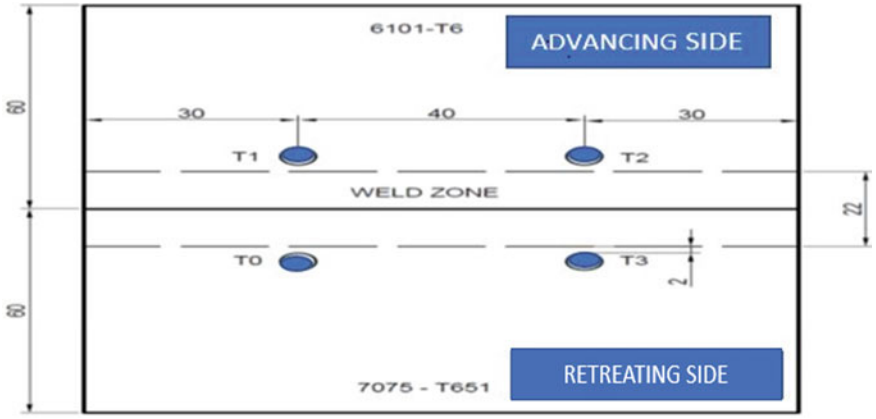

Fig. 3 Schematic diagram of the thermocouple arrangements T0, T1, T2, T3 on the alloy plates

3 Results and Discussion

3.1 Weld Appearance

The weld joints were carefully observed after the welding and were found to be externally free form defects although little flashes are noticed in some of the welds as shown in the photograph in Fig. 4.

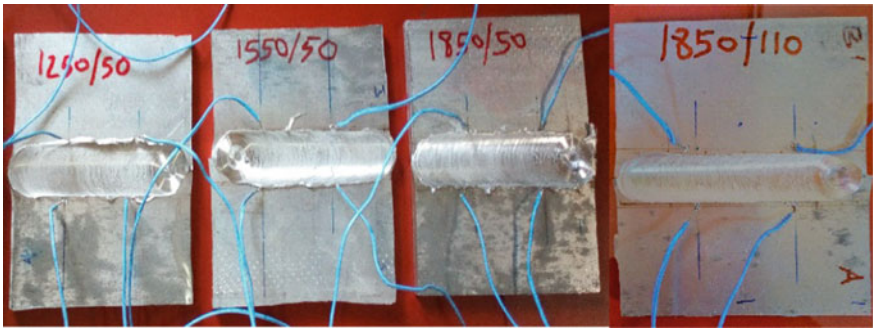

Fig. 4 Welded plates with embedded thermocouple

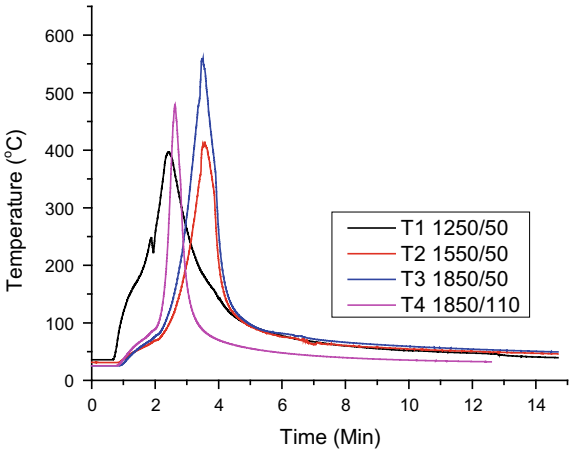

Fig. 5 The highest temperature profile of the processing parameters used

3.2 Temperature Profile of the Weld

Heat is produced as a consequence of the friction between the workpiece and the rotating tool. This generated heat influenced the thermo-mechanical welding process and impact on the mechanical behaviours of the joints. The highest heat takes place at the workpiece and rotating tool interface. The temperature profile of the welding process with time is presented in Fig. 5. The temperatures recorded at the 6101-T6 side of the weld which is the advancing side were lower than those at the 7075-T651 side which is the retreating side. This is as a result of different thermal conductivity influence of the welded plates. The 6101-T6 alloy on the advancing side of the welds has a higher thermal conductivity than 7075-T651 placed on the retrieving side. This implies that the rate of heat transfer and heat losses is higher in 6101-T6 than in 7075-T651, hence the aluminium alloy 7075-T651 on the retreating side retains more heat than 6101-T6 and therefore gave higher temperature values than the 6101-T6 alloys during the welding. The temperature profile also indicates that the temperature

generally increases as the welding progresses and get to the peak in the middle of the weld.

3.3 Effects of Tool Rotational Speed on the Temperature Distribution

The highest temperature of about 560 °C was recorded at a rotational speed of 1850 rpm while the least was about 365 °C at a rotational speed of 1250 rpm. The temperature generally increases across the studied samples as the tool rotational speed increases. This is due to higher heat generation as the rotating tool speed goes higher own to increase in frictional movement between the rotating tool and the workpiece.

3.4 Effects of Welding Speed on the Temperature Distribution

Varying the travel speed also influenced the temperature distributions. At 1850 rpm and 50 mm/min, the highest temperature recorded was 560 °C while at 110 mm/min travel speed with the same rotational speed of 1850 rpm, the highest temperature was 480 °C. The lower temperature recorded at the higher travel speed could be as a result of less heat generated own to less dwelling time of the rotating tool as it moves faster on the workpiece. While the higher temperature obtained at the lower travel speed was due to more dwelling time of the rotating tool as it moves slower on the workpiece. Also, the ratio of the rotational speed to the welding speed of the tool decreases from 37 to 17 rpm min/mm as the speed rises from 50 mm/min to 110 mm/min. This decrease in the ratio leads to a reduction in heat input and consequently lowers the temperature of the weld.

3.5 Tensile Behaviour of the Welds at Constant Travel Speed

At a steady travel speed of 50 mm/min, the ultimate tensile strength reduces as the rotational speed rises. This is shown in Fig. 6. This emanates from more heat generated as the rotational speed increases as shown in the temperature profile in Fig. 5. The excessive heat cause deterioration of the precipitates at the welding zone which leads to poor grain bonding and consequently decreases the mechanical strength.

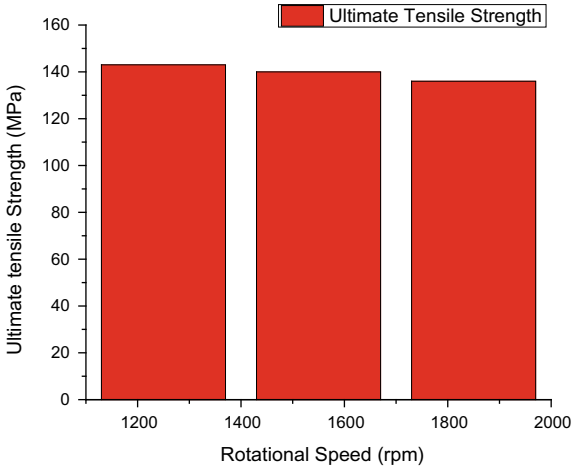

Fig. 6 Effect of rotational speed on ultimate tensile strength

3.6 Tensile Behaviour of the Welds at Constant Rotational Speed

At a steady rotational speed of 1850 rpm, the rising of feed rate from 50 to 110 mm/min causes the ultimate tensile strength to increase by 4 MPa. The increase follows a drop in the temperature as shown in Fig. 5. This implies that there was an improvement in grain bonding as the temperature drops and consequently an improvement in the ultimate tensile strength of the joint. This is shown in Fig. 7.

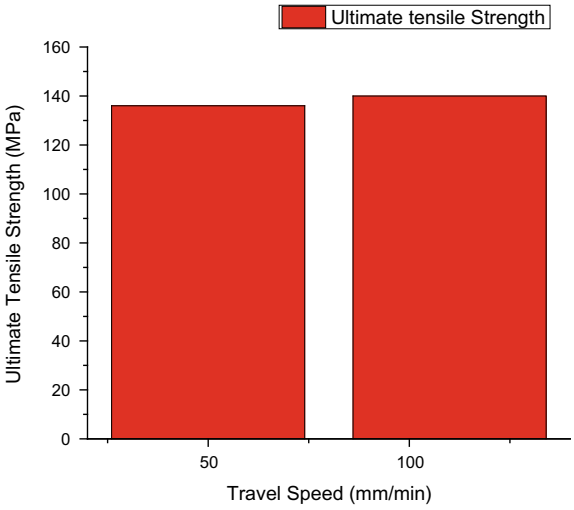

Fig. 7 Effect of travel speed on the ultimate tensile strength

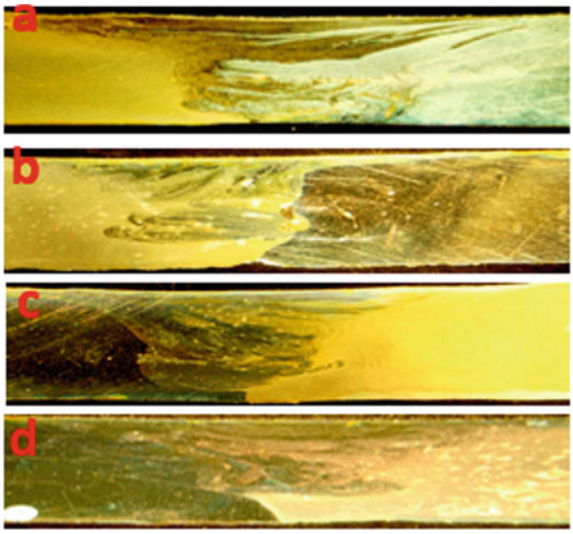

Fig. 8 Macrographs of the welded zone. **a** 1250 rpm/50 mm/min, **b** 1550 rpm/50 mm/min, **c** 1850 rpm/50 mm/min, **d** 1850 rpm/110 mm/min

3.7 Macrostructure and Microstructure of the Welds

The macrographs of all the welds (Fig. 8a–d) show that there was sufficient heat for plasticization for all the welds. The welds exhibited onion ring structures at all the rotational speed. Lamellae structure pattern of material flow was observed in all the parameters. Larger material movement is observed at the 1850 rpm and 110 mm/min. However, full penetration of the alloys into one another occurred more at 1550 rpm and 50 mm/min rotational speed and feed rate respectively.

The microstructure varies across the length and the breath of the weld and can be divided into unmixed, mechanically mixed and mixed regions as reported by some authors [27–29]. The unmixed region is observed close to the tool shoulder areas. Fine-grain structure is observed here as shown in Figs. 9a, 10a, 11a and 12a as a result of dynamic recrystallization during the welding. The mechanically mixed region (Figs. 9b, 10b, 11b and 12b) is the interface region of both alloys at the fusion zone. It contains the microstructures of both alloys. Weck's reagent etchant used revealed 7075-T651 as a lighter colour and the 6101-T6 as brown colour. At the mixed region, the tool pin stirring mechanism moved plastically deformed materials in alternate layers of 7075-T651 and 6101-T6 to form lamellae structural pattern (Figs. 9c, 10c, 11c and 12c.

Material penetration of the aluminium alloy into each other was highest at 1550 rpm and 50 mm/min rotational speed and travel speed, respectively.

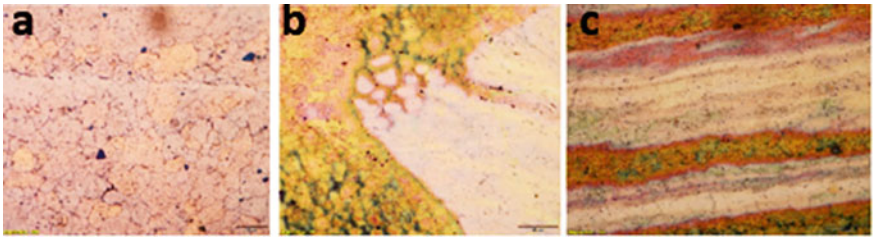

Fig. 9 Microstructures of weld nugget zone at 100× for 1250 rpm/50 mm/min, **a** unmixed, **b** mechanically mixed, **c** mixed regions

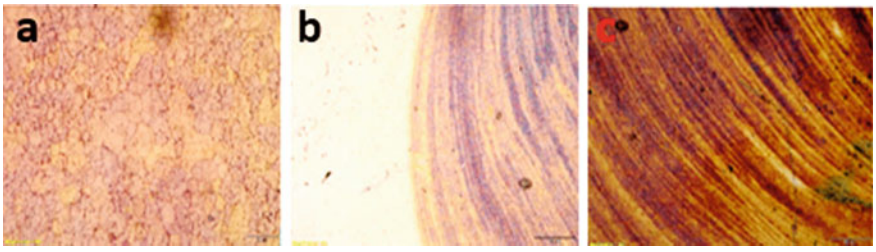

Fig. 10 Microstructures of weld nugget zone at 100× for 1550 rpm/50 mm/min, **a** unmixed, **b** mechanically mixed, **c** mixed regions

Fig. 11 Microstructures of weld nugget zone at 100× for 1850 rpm/50 mm/min, **a** unmixed, **b** mechanically mixed, **c** mixed regions

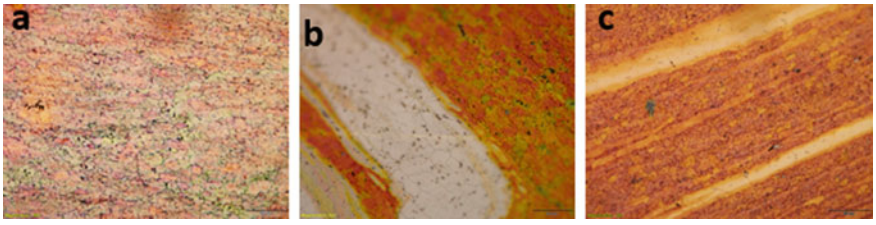

Fig. 12 Microstructures of weld nugget zone at 100× for 1850 rpm/110 mm/min, **a** unmixed, **b** mechanically mixed, **c** mixed regions

4 Conclusions

Conclusions from the results obtained are as follows:

1. Increase in the tool rotational speed result in an increase in the temperature generated during the welding process.
2. Increase in travel speed decreases the temperature.
3. Temperature profile varies relative to welding time
4. Tensile strength decreases as the tool rotational speed increases.
5. There is an increase in tensile strength as the welding speed increases.
6. Material distributions in the welding zone are not even. The volume of material swept into one another was more in 1850 rpm at a welding speed of 110 mm/min. However, the highest penetration of the alloy into one another occurred at the 1550 rpm rotational speed and at the welding speed of 50 mm/min.

Acknowledgements The authors appreciate the head and all the scholars of the Friction stir laboratory of the India Institute of Technology Kharagpur where this experiment was carried out and to the University of Johannesburg South Africa for sponsorship.

References

1. Padhy GK, Wu CS, Gao S (2017) Friction stir based welding and processing technologies - processes, parameters, microstructures, and applications: a review. J Mater Sci Technol 34:1–38
2. Sidhu MS, Chatha SS (2012) Friction stir welding—process and its variables: a review. Int J Emerg Technol Adv Eng 2(12):275–279
3. Abolusoro OP, Akinlabi ET (2019) Wear and corrosion behaviour of friction stir welded aluminium alloys—an overview. Int J Mech Prod Eng Res Dev 9(3):967–982
4. Mishra RS, Mahoney MW, Sato Y, Hovanski Y (2016) Friction stir welding and processing VIII
5. Silva ACF, De Backer J, Bolmsjö G (2017) Temperature measurements during friction stir welding. Int J Adv Manuf Technol 88(9–12):2899–2908
6. Khandkar MZH, Khan JA, Reynolds AP (2003) Prediction of temperature distribution and thermal history during friction stir welding: input torque based model. Sci Technol Weld Join 8(3):165–174
7. Yan F, Zhang Y, Fu X, Li Q, Gao J (2019) A new calculating method of frictional heat and its application during friction stir welding. Appl Therm Eng 153(January):250–263
8. Givi MKB, Asadi P (2014) Advances in friction-stir welding and processing
9. Lombard H, Hattingh DG, Steuwer A, James MN (2008) Optimising FSW process parameters to minimize defects and maximize fatigue life in 5083-H321 aluminium alloy. Eng Fract Mech 75(3–4):341–354
10. Prabha KA, Putha PK, Prasad BS (2018) Effect of tool rotational speed on mechanical properties of aluminium alloy 5083 weldments in friction stir welding. Mater Today Proc 5(9):18535–18543
11. Aydin H, Bayram A, Esme U, Kazancoglu Y, Guven O (2010) Application of grey relation analysis (Gra) and Taguchi method for the parametric optimization of friction stir welding (FSW) process. Appl Grey Relat Anal 44(4):205–211

12. Abd Elnabi MM, Elshalakany AB, Abdel-Mottaleb MM, Osman TA, El Mokadem AA (2019) Influence of friction stir welding parameters on metallurgical and mechanical properties of dissimilar AA5454-AA7075 aluminum alloys. J Mater Res Technol 8(2):1684–1693
13. Rajakumar S, Balasubramanian V (2012) Establishing relationships between mechanical properties of aluminium alloys and optimized friction stir welding process parameters. Mater Des 40:17–35
14. Kumar SR, Rao VS, Pranesh RV (2014) Effect of welding parameters on macro and microstructure of friction stir welded dissimilar butt joints between AA7075-T651 and AA6061-T651 alloys. Procedia Mater Sci 5:1726–1735
15. Das U, Toppo V (2018) Effect of tool rotational speed on temperature and impact strength of friction stir welded joint of two dissimilar aluminum alloys. Mater Today: Proc 5:6170–6175
16. Takayama Y, Akutsu Y, Choshiro N, Kato H, Watanabe H (2010) Temperature measurement during friction stir welding of dissimilar aluminum alloys, pp 0–5
17. Kandasamy J, Sairam J, Hussain MM (2018) ScienceDirect ICMPC_2018 comparative analysis of temperature variation in friction stir welding. Mater Today Proc 5:18798–18804
18. Sun YF, Fujii H, Sato Y, Morisada Y (2019) Friction stir spot welding of SPCC low carbon steel plates at extremely low welding temperature. J Mater Sci Technol 35:733–741
19. Silva-Magalhães A, De Backer J, Martin J, Bolmsjö G (2019) In-situ temperature measurement in friction stir welding of thick section aluminium alloys. J Manuf Process 39:12–17
20. Hamilton C, Dymek S, Sommers A (2010) Characteristic temperature curves for aluminum alloys during friction stir. Weld J
21. Covington JL, Robison W, Webb BW (2006) Experimental characterization of tool heating during friction stir welding. Mech Eng 179–184
22. Buffa G, Donati L, Fratini L, Tomesani L (2006) Solid state bonding in extrusion and FSW: Process mechanics and analogies. J Mater Process Technol 177(1–3):344–347
23. Feng Z et al (2007) In situ neutron diffraction measurements of temperature and stresses during friction stir welding of 6061-T6 aluminium alloy. Sci Technol Weld Join 12(4):298–303
24. Fehrenbacher A, Duffie NA, Ferrier NJ, Pfefferkorn FE, Zinn MR (2014) Effects of tool-workpiece interface temperature on weld quality and quality improvements through temperature control in friction stir welding. Int J Adv Manuf Technol 71(1–4):165–179
25. Upadhyay P, Reynolds AP (2010) Effects of thermal boundary conditions in friction stir welded AA7050-T7 sheets. Mater Sci Eng A 527(6):1537–1543
26. Miles M, Karki U, Hovanski Y (2014) Temperature and material flow prediction in friction-stir spot welding of advanced high-strength steel. JOM 66(10):2130–2136
27. Palanivel R, Koshy Mathews P, Murugan N, Dinaharan I (2012) Effect of tool rotational speed and pin profile on microstructure and tensile strength of dissimilar friction stir welded AA5083-H111 and AA6351-T6 aluminum alloys. Mater Des 40:7–16
28. Ouyang JH, Kovacevic R (2002) Material flow and microstructure in the friction stir butt welds of the same and dissimilar aluminum alloys. J Mater Eng Perform
29. Shigematsu I, Kwon YJ, Suzuki K, Imai T, Saito N (2003) Joining of 5083 and 6061 aluminum alloys by friction stir welding. J Mater Sci Lett

2.7 ARTICLE VI

Tool Rotational Speed Impact on Temperature Variations, Mechanical Properties and Microstructures of Friction Stir Welding of Dissimilar High Strength Aluminium Alloys

Published in *The Brazilian Society of Mechanical Science and Engineering.* DOI: 10.1007/s40430-020-2259-9. **(ISI-listed).**

In this article, the effects of tool rotational speed on temperature profile, mechanical properties and microstructures of friction stir welded 6101-T651 and 7075-T651 aluminium alloys in butt configurations were reported.

Three different rotational speeds of 1250rpm, 1550rpm and 1850rpm at a constant traverse speed of 50mm/min were investigated in the study. In-situ temperature measurements were taken on both sides of the welds using thermocouples connected to Labview software. Each parameter gave a different temperature profile due to different amounts of heat generated from different rotational speeds. The highest temperature profile recorded on the advancing and retreating sides of the welds varied for each parameter. While the highest occurred on the advancing side in the 1550rpm, the highest occurred on the retreating side at the 1250rpm and 1850rpm. Non-uniformity in heat transfer as a result of differences in thermal conductivities of the base materials leading to different heat absorption and transfer rates, has been attributed to this behaviour.

The article also related the temperature profile obtained for each parameter to the tool rotational speeds. The temperature increases with an increase in the rotational speed giving rise to the highest temperature of 550^0C at the highest rotational speed of 18550rpm. The UTS of the welds was found to decrease as the rotational speed increases. Fractographic analysis of the tested tensile samples revealed that necking took place before failure. Equiaxed dimples with voids were

noticeable on the fractured surfaces. The fractured surfaces are characterised by fibrous structural patterns which indicate the ductile nature of the welded alloys. The article also reported on the microstructures of the welds NZ which formed three regions namely mixed, mechanically mixed, and unmixed regions. The unmixed region experienced tool rotational impact during the welding which caused grain refinement and recrystallisation. The mixed and mechanically mixed regions contained the microstructures of both alloys. The microstructures showed lamellae patterns of flow and in some cases the formation of onion ring structures was noticeable.

Journal of the Brazilian Society of Mechanical Sciences and Engineering (2020) 42:176
https://doi.org/10.1007/s40430-020-2259-9

TECHNICAL PAPER

Tool rotational speed impact on temperature variations, mechanical properties and microstructure of friction stir welding of dissimilar high-strength aluminium alloys

Olatunji P. Abolusoro[1] · Esther T. Akinlabi[2] · Satish V. Kailas[3]

Received: 9 August 2019 / Accepted: 26 February 2020

Abstract
Temperature variations during friction stir welding result from the heat generated by the frictional action of a rotating tool on the workpiece. This temperature distribution affects the mechanical behaviour and ultimately the quality of welds produced. The study of the correlations between process parameter, temperature, mechanical properties and microstructure has become imperative in order to promote welds devoid of defects and possessing sound mechanical properties and to establish a temperature feedback control for effective components designs for industrial applications. This work studied the impact of tool rotational speed on temperature profile, mechanical behaviour and microstructure of friction stir welding of dissimilar aluminium alloy 6101-T6 and 7075-T651. Processing parameters of three different rotational speeds with values 1250 rpm, 1550 rpm and 1850 rpm and a constant travel speed of 50 mm/min were employed. The temperature profile was measured with one end of thermocouple wires embedded in the plates and the other end connected to a data capturing software device. The temperature profile indicates that the temperature rises with time and is higher at the retreating sides than at the advancing side of the weld. The tensile test results show that the ultimate tensile strength decreases as the temperature increases. Microstructural observations of weld zone revealed non-uniformity in material flow. However, more material penetration into each other occurred more at 1550 rpm.

Keywords Aluminium alloys · Friction stir welding · Mechanical properties · Temperature

1 Introduction

Friction stir welding (FSW) is a welding technique that has gained wide use in the welding of low-temperature alloys especially aluminium alloys. The welding process involves the use of a rotating tool on a workpiece leading to the generation of heat which plasticized and stirred the workpiece joint together in a completely solid-state welding. There are various parameters that determine the quality of the weld. Such parameters include tilt angle, axial force, travel speed, plunge depth, rotational speed, tool pin geometry, temperature distribution, etc. These factors affect the heat generated and the plasticization and flow of the materials during friction stir welding and consequently affect the mechanical properties and quality of the weld [1–4]. Studies have indicated a direct link between weld temperature and mechanical behaviour of a friction stir weld joint. Microstructural evolution, defects, corrosion, wear and mechanical properties are all direct consequences of temperature distributions during welding and are often determined by processing parameters employed during the welding [5–10]. Microstructural changes during FSW has been reported by various researchers [11–16]. Precipitate dissolution and coarsening including precipitate-free formation regions have been identified in the weld zone [17, 18]. The formation of these microstructural changes has also been linked to processing parameters such as feed rate and tool rotational speed [11, 19, 20]. Tool rotational speed has been established as one of the important process variables in FSW. This particular variable affects

Technical Editor: Lincoln Cardoso Brandao.

✉ Olatunji P. Abolusoro
abolusoroolatunji@yahoo.com

[1] Department of Mechanical Engineering Science, University of Johannesburg, Johannesburg, South Africa

[2] Department of Mechanical Engineering, Covenant University, Ota, Nigeria

[3] Department of Mechanical Engineering, Indian Institute of Science, Bangalore, India

Published online: 17 March 2020

the strain rate behaviour of the recrystallization process [21]. Researchers have reported that there is an optimal tool rotational speed range within which quality welds can be achieved [22]. Lombard et al. [23] employed eleven combinations of tool feed rate and rotational speed for systemic optimization. Their report showed that the maximum tensile strength of 313 MPa at a rotational speed of 200 rpm was achieved. In a related study, Aruna et al. [24] studied three tool rotational parameters impact on the mechanical strength of FSW of 5083 aluminium alloy. They concluded that the rotating speed of 1200 rpm yielded the maximum UTS. Izabela et al. [25] also studied the effects of tool rotational speed on the FSW of 7075-T651 and 5083-H111 aluminium alloys. They reported that better material mixing was obtained at higher rotational speed but the mechanical properties reduce as the rotational speed goes up. However, Min-Su-Han et al. [26] in their report revealed that excessively high temperature from high welding speed could result in defects and poor mechanical properties. Umasanka and Vijay [27] studied the correlation between temperature, rotational speed and mechanical strength of FSW of 6101-T6 and 6351-T6 alloys. The results indicate that there is a corresponding increase in temperature as the rotational speed increases. The mechanical impact strength of the weld varies with the duration of impact and pressure. Prasad et al. [28] also studied the effect of the rotational speed of 100 rpm and 1000 rpm on microstructural changes and creep properties of low-temperature FSW of P91 steel. The welding temperature was measured at the tooltip, and the result revealed that temperature control is essential for a reduction in microstructural degradation during welding. Silva et al. [29] investigated the temperature variation during FSW of 6082 aluminium alloy with 20 mm thickness. The temperatures were measured at three different positions around the tool. The results show that the highest temperature of 607 °C was obtained from the thermocouple placed at the transition from the shoulder to the pin, while the lowest occurred at the pin's tip. Kandasamy et al. [30] also investigated the temperature generated both on the tool and the workpiece during FSW of 7075 alloys. The maximum temperature obtained was compared with simulated results and was found to be in close agreement. Temperature measurements with high accuracy during FSW are often difficult to carry out through validation of the experiment. This is as a result of severe plastic deformation that occurs and could damage the thermocouple at the hottest region which is the interface between the rotating tool and the workpiece where the temperature is expected to be measured [6, 31]. Many researchers have utilized several approaches to measure or predict temperature during FSW. Some of these approaches include the use of thermal cameras and thermocouple embedded in tool [32–34]. Others include infrared thermometers, ultrasound, neutron-based methods [9, 31] and thermocouples embedded in the workpiece [27, 35, 36]. The most commonly employed among these methods in literature is the use of thermocouples embedded in the workpiece at close proximity to the rotating pin area [37]. However, this approach also has the disadvantage of having the thermocouple destroyed during the passage of the rotating tool [9]. Thermocouple placed at the surface of the plates to be welded would give a higher temperature than those placed behind the plates particularly when the materials for backing plates possess high thermal conductivity. These make different positions of thermocouple found in various studies [6, 38]. In this work, the thermocouple used was embedded into the workpiece at a proximity to the heat affected zone. It is pertinent to point out that tool rotational speed on workpiece generates the needed heat for FSW and cause temperature changes. Its influence often differs in FSW of dissimilar alloys. Although considerable amount of studies has been done on effects of tool rotational speed on the tensile strength of some friction stir welded aluminium alloys, however, majority of the works focused only on the relationship between the tool rotational speed and the tensile strength of the weld. Only very few attempts have been made to establish the relationship between the tool rotational speed, the generated temperature during the welding, the microstructures and material flow pattern and the mechanical properties of the friction stir welded aluminium alloys. The correlations between these factors are very significant in welding process control for industrial applications and are yet to be reported on friction stir dissimilar welding of 6101-T6 and 7075-T651 aluminium alloys. This study, therefore, focuses on how the tool rotational speed causes variations in temperatures and how these variations affect the microstructure, material flow and mechanical properties of dissimilar FSW of 7075-T651 and 6101-T6 aluminium alloys. These aluminium alloys have been selected in view of their high strength-to-weight ratio, corrosion resistance, high thermal and electrical conductivity which have made them strategic and important materials in aerospace and automobile applications.

2 Experimental procedures

2.1 Sample's chemical composition and properties

The elemental composition and the mechanical properties obtained from the tested samples of the alloys are shown in Tables 1 and 2.

2.2 Process parameters

The fixed travel speed and the different rotational speed of the tool employed for the experiment are given in Table 3. These parameters were chosen based on trial runs carried out

Table 1 Chemical composition of the welded aluminium alloys (%wt)

Alloy	Si	Cu	Fe	Mn	Mg	Ti	Cr	Zn	Al
6101-T6	0.53	0.01	0.14	0.002	0.600	0.008	0.001	0.003	Others
7075-T651	0.40	1.70	0.50	0.300	2.40	0.20	0.22	5.50	Others

Table 2 Mechanical properties of the welded alloy

Alloy	Tensile strength (MPa)	Ultimate tensile strength (MPa)	Elongation (%)	Thermal conductivity (W/m*°C)
6101-T6	172	180	21	167
7075-T651	462	575	18	130

Table 3 Rotational speeds and travel speeds

Rotational speed (rpm)	Travel speed (mm/min)
1250	50
1550	50
1850	50

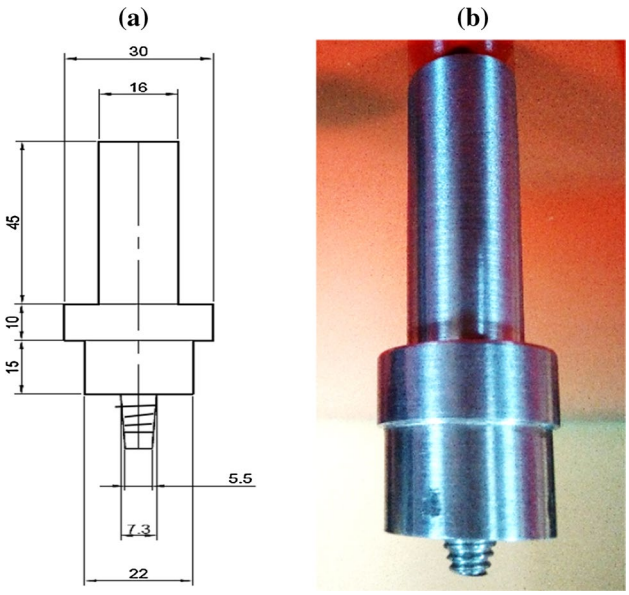

Fig. 1 **a** Schematic diagram of the tool. **b** Photograph of the tool

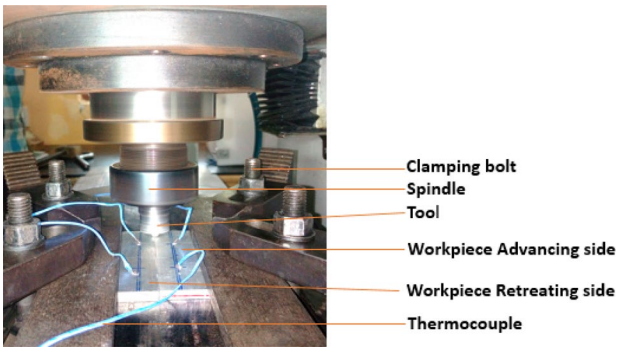

Fig. 2 Experimental setup and welding arrangements

prior to this experiment. Five different tool rotational speeds (950 rpm, 1250 rpm, 1550 rpm, 1850 rpm and 2150 rpm) at two different travel speeds of 50 mm/min and 80 mm/min were carefully selected around the optimized values from the literature [39] for the trial runs. The welds from the rotational speeds of 950 rpm and 2150 rpm at both travel speeds of 50 mm/min and 80 mm/min were found to develop root defects, an indication of too low heat input and too high heat input, respectively. The tool rotational speeds of 1250 rpm, 1550 rpm and 1850 rpm at the travel speed of 50 mm/min gave defect-free welds. These three parameters were therefore selected to carry out this study. The details of the procedure followed are given in Sect. 2.3.

2.3 Experimental procedures

The two aluminium alloys to be welded were properly cleaned to remove dirt and oxide layers that might have been formed on the surface. The tool of pin length 5.65 mm with a root diameter of 7.3 mm and pin mouth diameter of 5.5 mm and a shoulder diameter of 22 mm as shown in Fig. 1a, b was used for the experiment. The experiment was carried out with a 100 kN numerical welding machine designed and manufactured by IISc, Bangalore, and ETA Technology Ltd, Bangalore, India. The experimental setup and the welding arrangement for the study are shown in Fig. 2. The two alloys were clamped in butt configuration with the 6101-T6 placed on the advancing side (AS), while the 7075-T651 was placed on the retreating side (RS). The advancing side is that side of the weld in which the rotating tool movement and the traversing direction is the same. Here, the solid materials are transformed into semi-solid or plasticized and flow around the tool pin rotating at the interface of the two materials to be joined. The retreating side, on the other hand, is the side of the weld where the direction of tool rotation is opposite to the traversing direction. Here, the plasticized materials from the advancing side retreated and get cooled. The four ends of the thermocouple wires used were embedded at four different points in the plates, two on each side of the plate at about 2 mm away from the weld boundaries as shown in Fig. 3. The other four ends were connected to

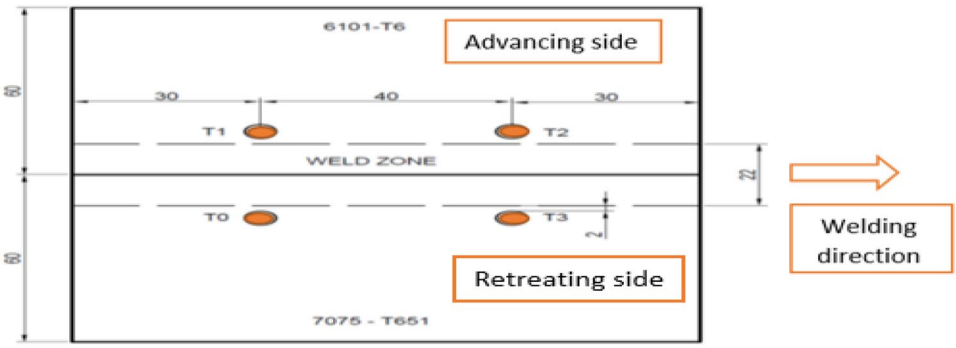

Fig. 3 Thermocouple arrangements

Fig. 4 Prepared tensile samples

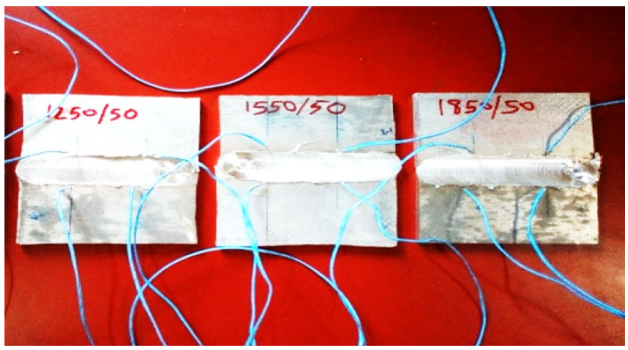

Fig. 5 Welded samples

Labview evaluation software for temperature data capturing and analysis. The friction stir welding was performed at three different parameters shown in Table 3. The specimens for tensile testing were prepared in accordance with ASTM E8 as shown in Fig. 4. Three tensile specimens were tested for each processing parameter, and the average ultimate tensile strength values for each were taken for evaluation.

3 Results and discussion

3.1 Weld appearance

Careful observations of the welds after the welding as shown in Fig. 5 revealed that the welds are externally free from defects although, very little flashes could be noticed in the welds.

3.2 Temperature profile

The profile of the highest temperatures obtained during the welding for each of the parameters as shown in Fig. 6 indicate that the temperature rises with time and attained a maximum at the middle of the welding. Each welding parameter exhibits different temperature profiles at the retreating and the advancing side of the weld. This is as a result of different amount of heat generated during the welding which

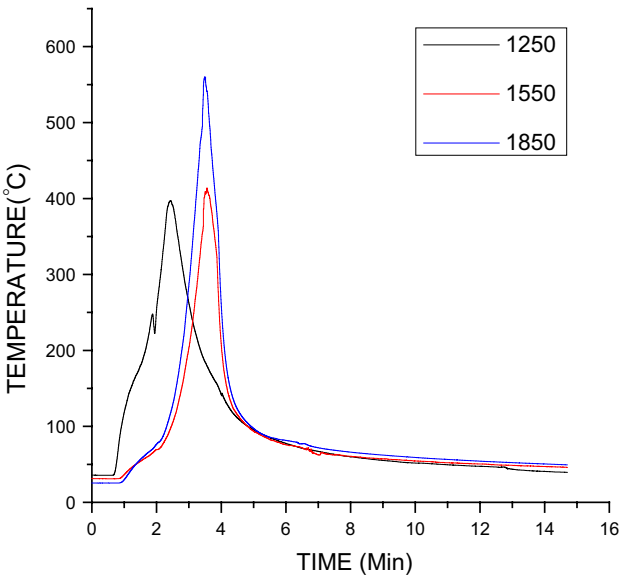

Fig. 6 Highest temperature profile of the three different welding parameters

emanates from different processing parameters employed. At the 1250 rpm, the highest temperature at the advancing side is 366 °C which is lower than 397 °C obtained at the retreating side. This is shown in Fig. 7. However, at 1550 rpm, as shown in Fig. 8, the advancing side highest temperature is

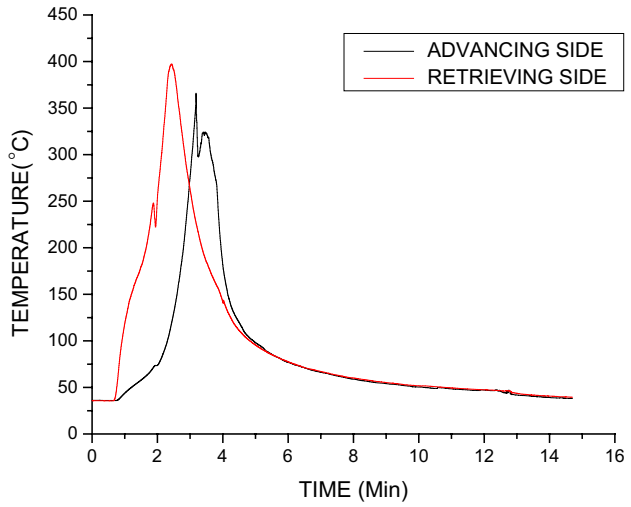

Fig. 7 Temperature profile at 1250 rpm for advancing and retreating side

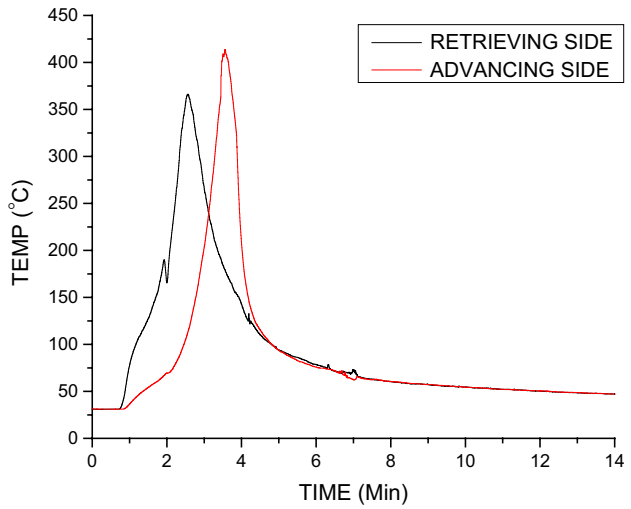

Fig. 8 Temperature profile at 1550 rpm for advancing and retreating side

414 °C which is higher than 366 °C obtained at the retreating side. This could be due to absorption of part of the heat generated by the latent heat of the alloy at the retreating side of the weld and the heat loss rate on the advancing side seems to be much lower than the rate of heat absorbed at the retreating side. However, as the rotational speed increases to 1850 rpm, the highest temperature obtained at the 6101-T6 side and 7075-T651 sides is 471 °C and 560 °C, respectively. This is shown in Fig. 9. This means that temperature variations at the 1250 rpm and 1850 rpm exhibit similarity in behaviour as the highest temperature at the 7075-T651 on the retreating side is greater than that of 6101-T6 on the advancing side for both parameters. The variations in these

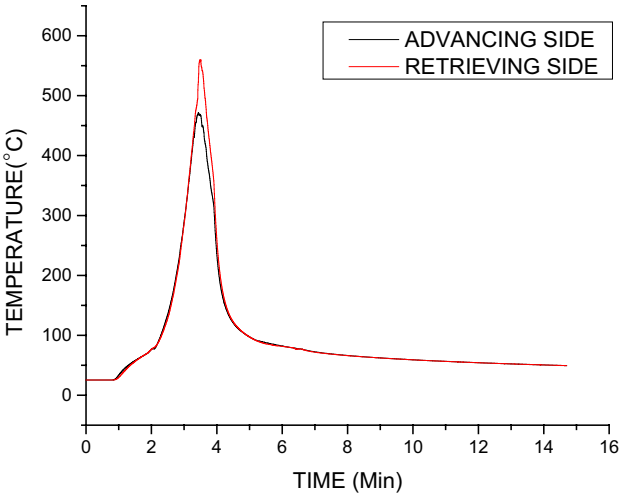

Fig. 9 Temperature profile at 1850 rpm for advancing and retreating side

temperature profiles at the advancing and retreating sides can be attributed to inhomogeneous heat distributions and transferred as a result of differences in the thermal conductivity of both alloys. The thermal conductivity of 6101-T6 is higher than that of 7075-T651; hence, heat transfer occurred faster in 6101-T6 than in 7075-T651. This also implies that the rate of heat losses in the 6101-T6 is higher than that of 7075-T651 and consequently leads to lower temperature obtained at the advancing side of the welds.

3.3 Effects of rotational speed on the temperature

The heat generated during friction stir welding results from the frictional effects of the rotating tool on the workpiece. The temperature measured indicates that the highest temperature of about 550 °C was obtained at a tool rotational speed of 1850 rpm. The lowest recorded occurred at a rotational speed of 1250 rpm. The temperature considerably increases across the weld samples as the rotating tool speed increases as shown in Fig. 10. This is due to greater frictional effects of the rotating tool on the workpiece as the rotational speed increases leading to a higher amount of heat generation and consequently raising the weld temperature.

3.4 Effects of rotational speed on tensile behaviour

The tool's rotation on the workpiece considerably affects the tensile behaviour of the welds. As the rotational speed of the tool goes higher, there is a corresponding reduction in the tensile strength of the welds. This is shown in Fig. 11. The highest ultimate tensile strength of 143 MPa was obtained at the lowest rotational speed of the tool. This can be ascribed to more heat input into the system when the rotational speed increases. The

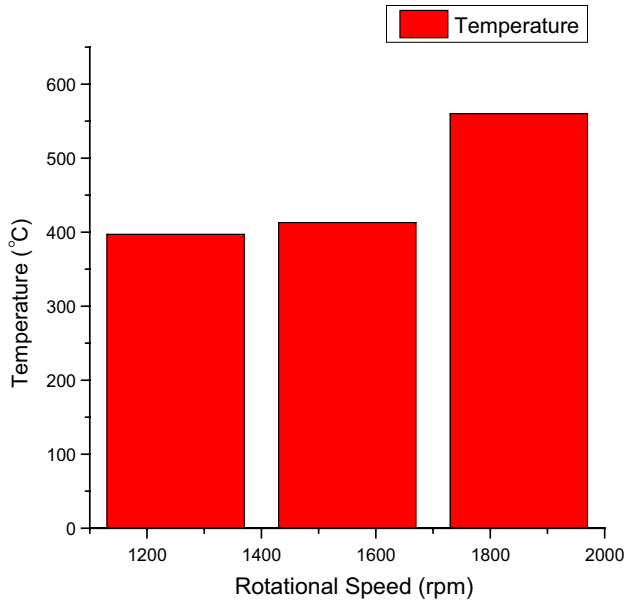

Fig. 10 Effect of rotational speed on temperature

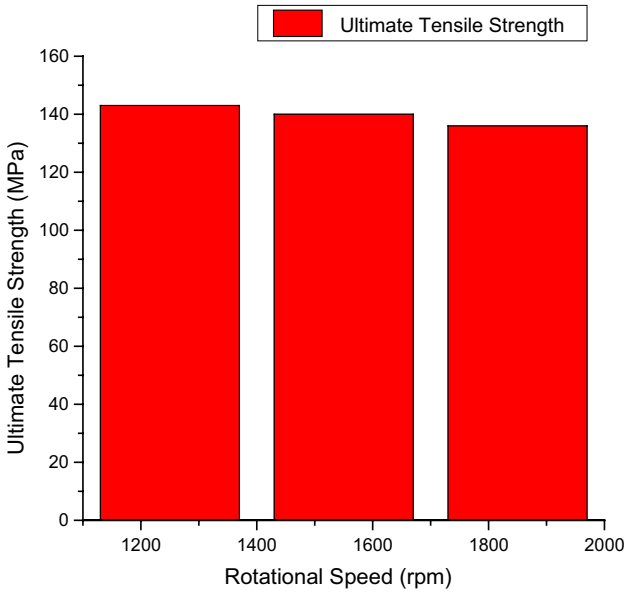

Fig. 11 Effect of rotational speed on tensile strength

increase in heat input causes microstructural changes in the weld region. The strengthening precipitates become coarsened leading to lower grain bonding which consequently reduced the tensile strength of the welds.

3.5 Temperature distribution effects on tensile behaviour

The heat produced during friction stir welding emanates from the friction between the tools rotating on the stationary workpiece. The produced heat affects plasticization, transfer and mixing of materials at the stir zone. These further determine the microstructural development at the joint interface and consequently affect the mechanical behaviour of the joints. The tensile test results obtained as shown in Fig. 12 indicate that the highest ultimate tensile strength of 143 MPa occurred at the lowest weld temperature. As the temperature increases due to the increase in tool rotational speed, there is a decrease in the ultimate tensile strength across the welds. This decrease could be as a result of coarsening or dissolution of precipitates at the weld zone due to higher heat generation which results in weak bonding at the weld zone. The little differences observed in the ultimate tensile strength across the welds at different temperature changes indicate that the amount of changes in heat generated in the welds due to tool rotational speed changes is not sufficient enough to cause significant coarsening and precipitates dissolution at the weld zone, hence, the little changes in the ultimate tensile strength of the weld.

3.6 Tensile test analysis

The average tensile test results for the three welded samples along with both base metals are shown in Fig. 13. The results revealed that the ultimate tensile strengths of all the welds were lesser than those of the parent metals. The percentage elongations for the welds were also

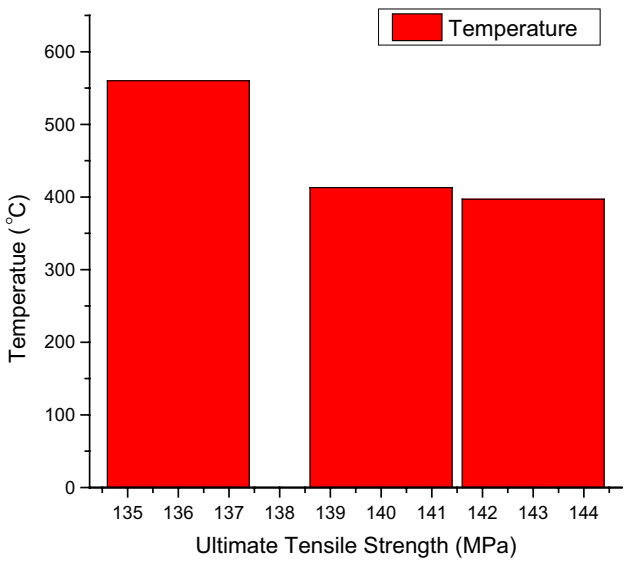

Fig. 12 Effect of temperature on tensile strength

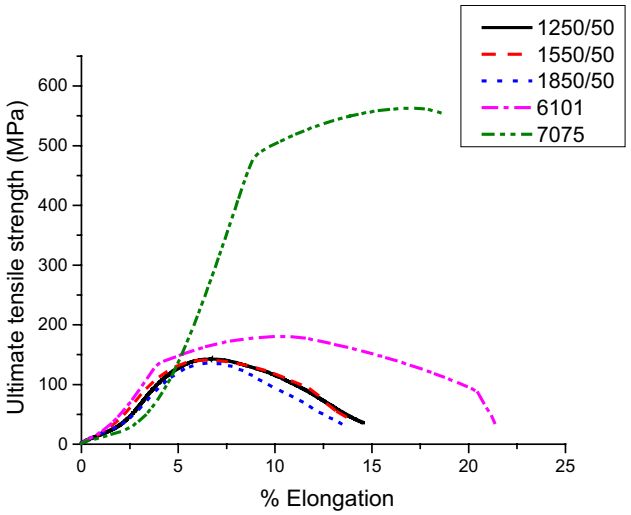

Fig. 13 Graph of ultimate tensile strength against percentage elongation

Table 4 Weld efficiency at different rotational speeds

Process parameter (rpm/mm/min)	Ultimate tensile strength (MPa)	Efficiency of welds in %
1250/50	143	79
1550/50	140	77
1850/50	136	75

found to be lower than those of the base metals. The joint efficiencies of the welds calculated as the ratio of the ultimate tensile strength of the welds to that of 6101-T6 base metals expressed in percentage are shown in Table 4. The efficiency of the weld reduces as the temperature increases due to the increase in rotational speed.

3.7 Fracture analysis

The mode of fracture of the tensile specimens observed revealed that the fracture took place at the heat affected zone (HAZ) close to the 6101-T6 side as shown in Fig. 14a–d. This can be attributed to its lower mechanical strength compared to 7075-T651. Also, the microstructural reorientations of the grains at that section lead to the formation of coarse precipitates with the resultant reduction in mechanical properties as a result of heat. The non-failure of the alloys at the weld zone is an indication of proper material mixing and bonding of the dissimilar metals for all the parameters employed. Considerable necking before failure was observed in all the tested specimen of the welds as shown in Fig. 14 b–d. This implies that the material undergoes extensive plastic deformation before the fracture occurred. This behaviour is synonymous with ductile materials like aluminium alloys. The fractographs of the tensile specimens are shown in Fig. 15a–e. All the fractographs of the three process parameters utilized as shown in Fig. 15a–c significantly show similarities in the fracture pattern. This is due to the failure of all the samples at the heat affected zone of the 6101-T6 side of the welds. The fractographs equally revealed that plastic deformation and necking occurred before the material fractured. This is evident in the fracture morphology of the tested specimens which are generally characterized by fibrous features, an indication that the crack propagation occurred slowly. Equiaxed dimples with voids are noticeable (Fig. 15a–d) which is a typical behavioural pattern of ductile materials. The dimples are structures emanated from the nucleation, growth and coalescence of voids. These voids are formed as a result of the inhomogeneous rate of deformation

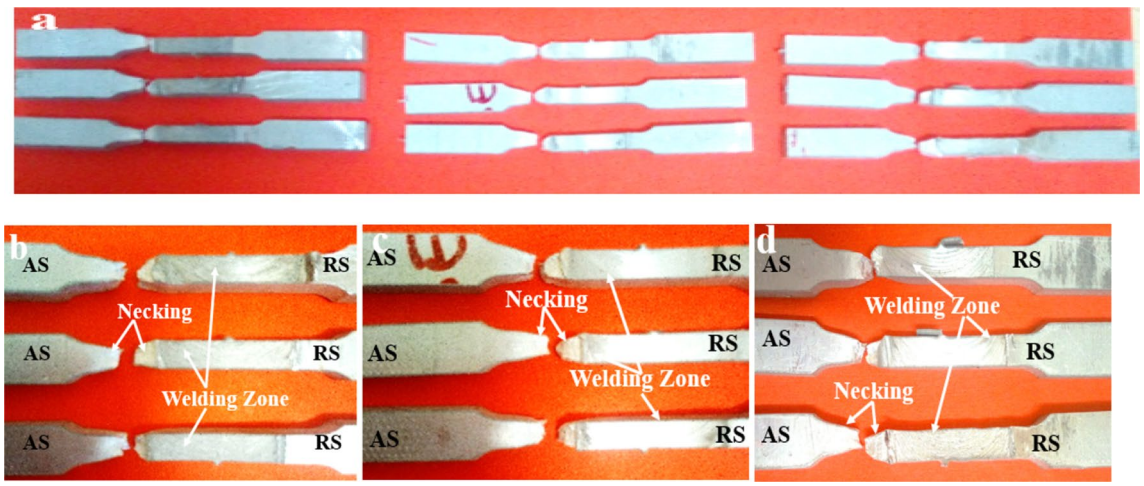

Fig. 14 Fractured specimen. **a** All the tested specimen. **b** 1250 rpm. **c** 1550 rpm. **d** 1850 rpm

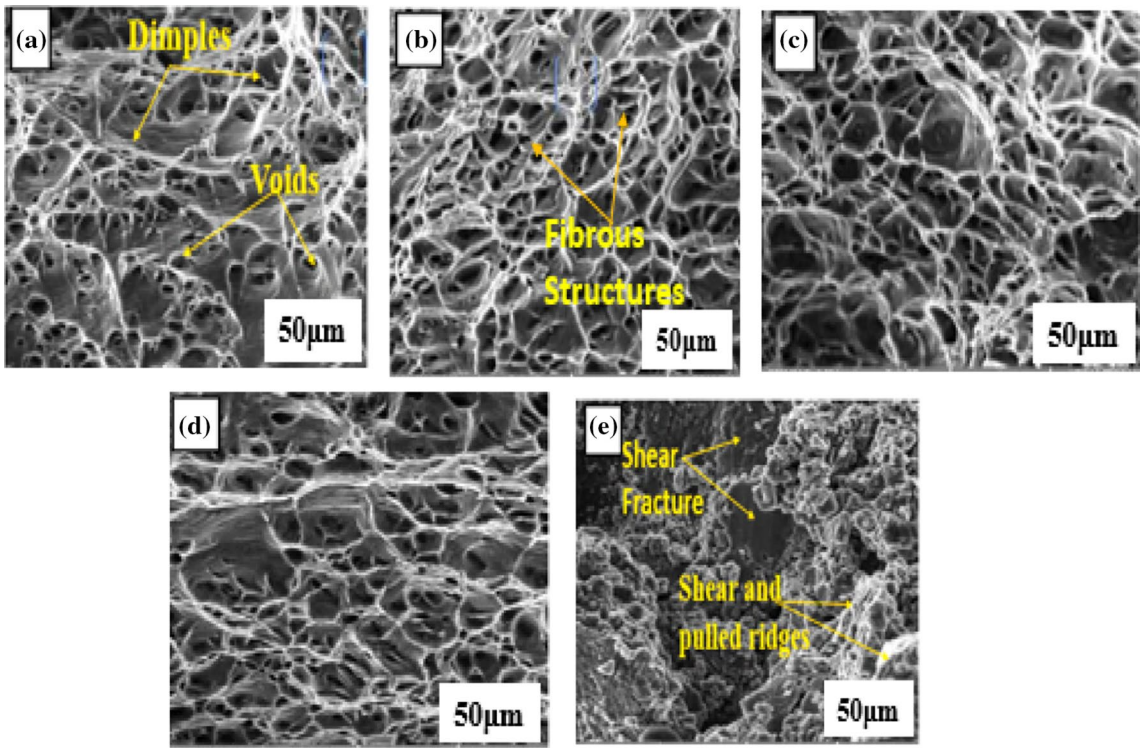

Fig. 15 SEM fractographs of the tensile tests fractured surfaces at 1.00k× for **a** 1250 rpm at 50 mm/min. **b** 1550 rpm at 50 mm/min. **c** 1850 rpm at 50 mm/min. **d** Base material 6101-T6. **e** Base material 7075-T651

in the material under the applied load. The growth and coalescence of these voids controlled the fractured behaviour. When these voids grow to critical sizes relative to the spacing in-between them, a local plastic instability developed leading to the formation of macroscopic flaws which resulted in the fracture. The 6101-T6 base material has the highest percentage of elongation. The ultimate tensile strength was much higher than those of the welded samples; however, it is far below that of the 7075-T651, and the fracture pattern observed in the 6101-T6 alloy (Fig. 15d) is similar to those obtained for the welded samples. This is due to the failure of the welded samples at the 6101-T6 side. 7075-T651 exhibits the highest ultimate tensile strength although the percentage elongation was a little lower than the other base metal of 6101-T6. The fracture pattern of the 7075-T651 did not demonstrate appreciable necking before failure. This indicates lower ductility compared to the other base metal. The cracking features as shown in Fig. 15e indicate a transgranular mode of cracking accompanied by shear and pulled fractures.

3.8 Hardness

The microhardness was profiled across the welding direction at 1-mm interval. The hardness values varied across the three zones of the weld, i.e. heat affected zone (HAZ), nugget zone (NZ) and thermo-mechanically affected zone (TMAZ) and exhibited similar transformation pattern across the three parameters used in this study as shown in Fig. 16. At the 7075-T651 side which is the retreating side on the left of the NZ, the microhardness increases from base metal towards the HAZ and became maximum at the TMAZ just before the NZ. This is due to grain refinement as a result of heat experienced at the zone. At the NZ, the microhardness values droped drastically. This can be attributed to inhomogeneity in the composition of the welding zone brought about by material mixing during the

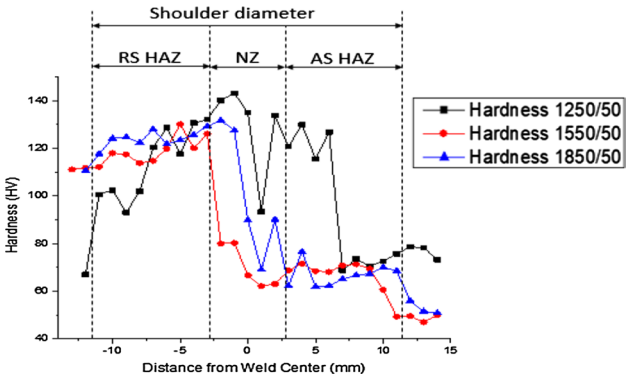

Fig. 16 Hardness profile of the three rotational speeds

FSW and coarsening of precipitates at this region which reduces hardness. At the HAZ of the advancing side which is the 6101-T6 on the right side of the NZ in Fig. 16, the hardness values further droped as expected. This is as a result of dissolutions of strengthening precipitates of the alloy in this zone. The highest hardness values at NZ and both sides of the HAZ were obtained at the rotational speed of 1250 rpm. This is due to better grain refinement at these zones as the tool generates a significant amount of heat needed for grain cohesion than the other two parameters with higher temperatures. Further analysis of the hardness variations across the three zones of the welds is shown in Fig. 17. The average hardness values evaluated from the welding zones of all the parameters demonstrate similarity in behaviour. At the NZ, the highest average hardness value of 122.62 HV was obtained at the rotational speed of 1250 rpm. As the speed increases to 1550 rpm, there is a drastic drop in the hardness value, but it moved up again as the tool rotational speed goes up to 1850 rpm. At the HAZ of the AS, the same pattern with the NZ was exhibited. The average hardness value of 81.88 HV was the highest and also occurred at 1250 rpm but droped a little at 1550 rpm and then moved slightly higher at 1850 rpm. At the HAZ of the retreating side, the highest average microhardness value of 119.2 was obtained and occurred also at the same 1250 rpm. A decrease in the value was equally noticed as the tool rotational speed increases to 1550 rpm and moved up again as the speed increases to 1850 rpm. The drop in average hardness at 1550 rpm across the three zones could probably be as a result of coarsening of the strengthening precipitates due to more heat input from the higher rotational speed. Although a further increase in the rotational speed to 1850 rpm caused a little rise in the average hardness across the zones, it might be as a result of improvement in the material movement at that rotational speed.

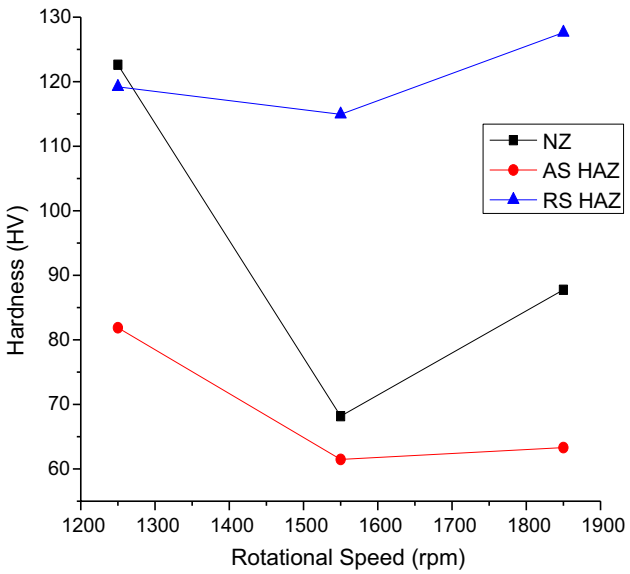

Fig. 17 Average hardness values at NZ, AS HAZ and RS HAZ of the three rotational speeds

3.9 Microstructure

The mixing and dilution of the two dissimilar alloys at the joint interface during the welding occurred as a result of the rotational effect of the tool. Although the weld dilution could not be ascertained in this study, however, the mixing pattern and material flow at the different rotational speed employed have been revealed through the macrostructure and microstructural observations of the weld zones. The macrostructures as shown in the macrographs in Figs. 18a, 19a and 20a revealed that there is sufficient heat for plasticization of the joint interface at all the three tool rotational speeds. Transformation of materials across the depth joint is not uniform as a result of varying contact area own to the tapered pin used. However, more material interaction occurred at the 1250 rpm rotational speed than in the 1550 rpm and 1850 rpm.

The microstructures vary across the length and breadth of the weld zone and generally formed three types of regions which agree to the findings of some researchers on dissimilar FSW of aluminium alloys [40–44]. The regions can be classified into mixed flow, mechanically mixed and unmixed region. The unmixed region is found at the uppermost part of the joint close to the tool shoulder region (Figs. 18c, 19c, 20c). The heat emanated from the tool rotating mechanism on the workpiece impacts on the microstructures of the region which becomes refined in grain structures leading to the occurrence of dynamic recrystallization during the welding. The mechanically mixed region contains microstructure of both 6101-T6 and 7075-T651 aluminium alloys (Figs. 18d, 19d, 20d). The Weck's reagent etchant revealed 7075-T651 as a lighter colour and 6101-T6 as a darker colour. Full penetration of the aluminium alloys into each other was not accomplished in all the welds. However, substantial materials were swept into each other at the tool rotational speeds of 1250 rpm and 1550 rpm. Onion ring structures of material flow were visible in 1550 rpm and 1850 rpm. This is shown in Figs. 19b and 20b. The mixed region like the mechanically mixed region also contains the microstructures of both alloys. Here, the alloys flow into each other in alternate layers in lamellae structural pattern as shown in Figs. 18e, 19e and 20e. The SEM microstructure of the weld zones for all the welds is given in Fig. 21a–c. Interfacial and alternate layered flow structure occurred in all the zones.

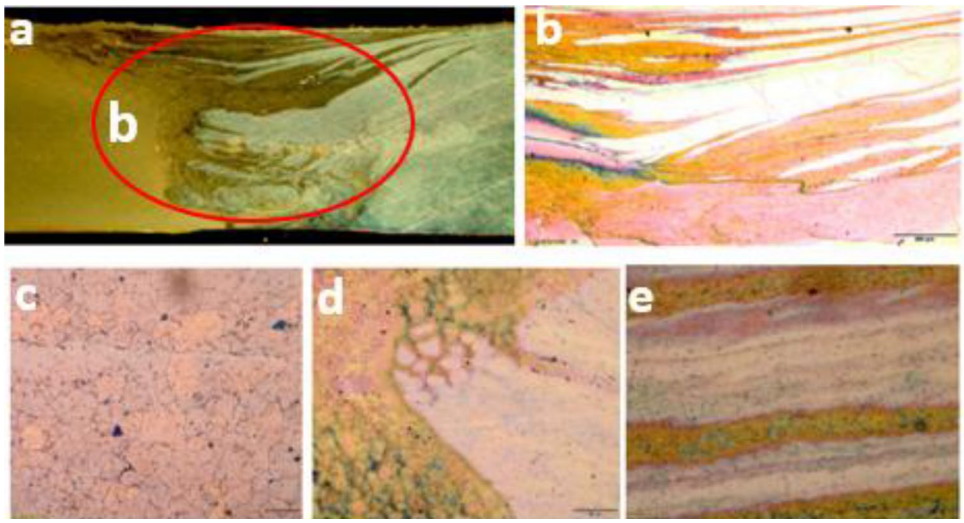

Fig. 18 Optical images of material flow pattern and microstructures of weld nugget zone at 100× for 1250 rpm. **a** Macrograph of the joint, **b** material flow pattern, **c** unmixed, **d** mechanically mixed, **e** mixed regions

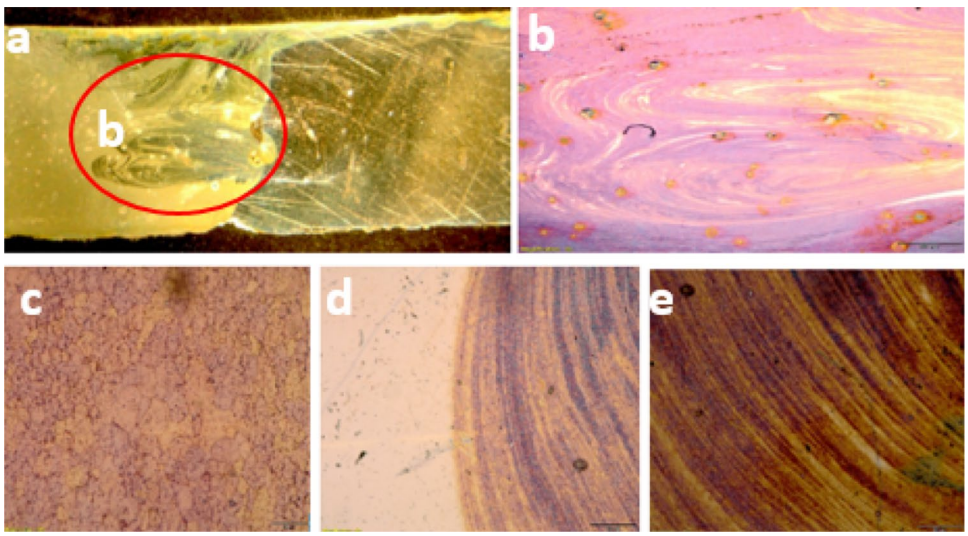

Fig. 19 Optical images material of flow pattern and microstructures of weld nugget zone at 100× for 1550 rpm. **a** Macrograph of the joint, **b** material flow pattern, **c** unmixed, **d** mechanically mixed, **e** mixed regions

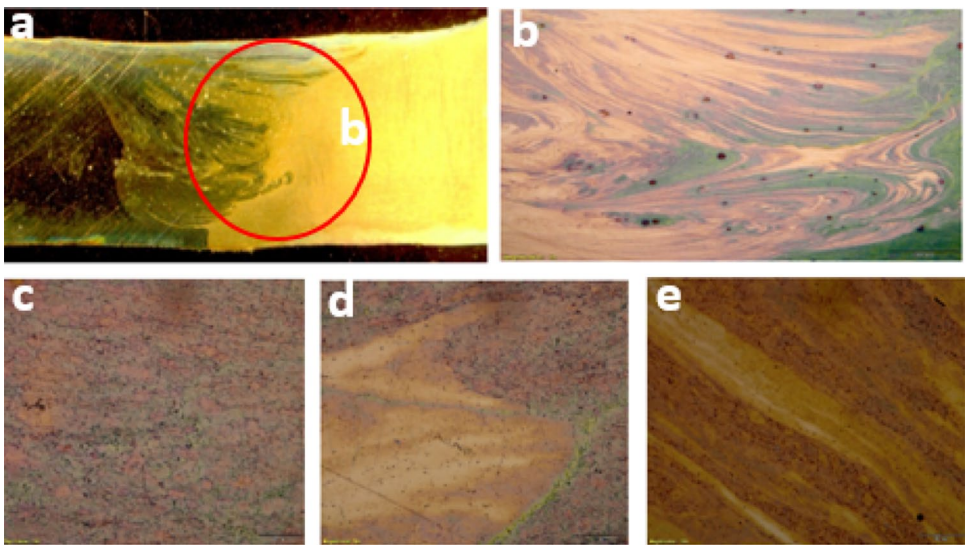

Fig. 20 Optical images of material flow pattern and microstructures of weld nugget zone at 100× for 1850 rpm. **a** Macrograph of the joint, **b** material flow pattern, **c** unmixed, **d** mechanically mixed, **e** mixed regions

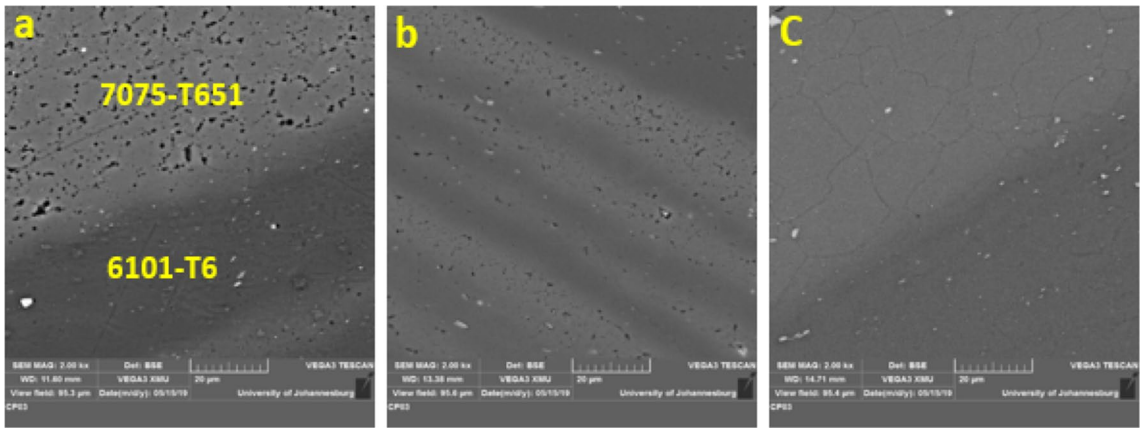

Fig. 21 SEM microstructures of mixed region at 20 µm. **a** 1250 rpm, **b** 1550 rpm, **c** 1850 rpm

4 Conclusion

The experimental study above has further established the relationship between temperature distributions in friction stir welding and the resulting mechanical properties and microstructures. Conclusions from these relationships can be drawn as follows:

1. The temperature is directly proportional to the rotational speed of the tool. An increase in the speed of rotation of the tool leads to an increase in temperature.
2. The lower temperature at a considerable range during the friction stir welding favours improvement in tensile strength of the joints.
3. Higher temperature beyond the optimum value during the friction stir welding decreases the mechanical properties.
4. The little differences observed in the ultimate tensile strength across the welds indicate that 300 rpm tool rotational speed differences may not be sufficient to cause significant changes in the ultimate tensile strength of the weld.
5. The observed temperature profile of the welding revealed that temperature increases with time and attained its peak in the middle of the welding.
6. Material distributions in the welding zone are not even. The volume of material swept into one another was more in 1250 rpm. However, the highest penetration of the alloy into one another occurred at the 1550 rpm rotational speed.

References

1. Sidhu MS, Chatha SS (2012) Friction stir welding—process and its variables: a review. Int J Emerg Eng Technol Adv Eng 2(12):275
2. Bagheri Hariri M, Gholami Shiri S, Yaghoubinezhad Y, Mohammadi Rahvard M (2013) The optimum combination of tool rotation rate and travelling speed for obtaining the preferable corrosion behaviour and mechanical properties of friction stir welded AA5052 aluminium alloy. Mater Des 50:620–634
3. Mishra RS, Ma ZY (2005) Friction stir welding and processing. Mater Sci Eng R. https://doi.org/10.1016/j.mser.2005.07.001
4. Padhy GK, Wu CS, Gao S (2018) Friction stir based welding and processing technologies—processes, parameters, microstructures and applications: a review. J Mater Sci Technol 34:1–38
5. Abolusoro PO, Akinlabi ET (2019) Wear and corrosion behaviour of friction stir welded aluminium alloys—an overview. Int J Mech Prod Eng Res Dev 9:967–982
6. Silva ACF, De Backer J, Bolmsjö G (2017) Temperature measurements during friction stir welding. Int J Adv Manuf Technol 88:2899–2908
7. Khandkar MZH, Khan JA, Reynolds AP (2003) Prediction of temperature distribution and thermal history during friction stir welding: input torque based model. Sci Technol Weld Join 8:165–174
8. Tang J, Shen Y (2016) Numerical simulation and experimental investigation of friction stir lap welding between aluminium alloys AA2024 and AA7075. J Alloys Compd. https://doi.org/10.1016/j.jallcom.2016.01.138
9. Fehrenbacher A, Duffie NA, Ferrier NJ, Pfefferkorn FE, Zinn MR (2014) Effects of tool–workpiece interface temperature on weld quality and quality improvements through temperature control in friction stir welding. Int J Adv Manuf Technol 71:165–179
10. Bie J, Liu Y-L, Zhang Z (2008) Effect of processing parameters on temperature distributions in friction stir welding. Suxing Gongcheng Xuebao J Plast Eng 15(3):212–217
11. Hassan KAA, Prangnell PB, Norman AF, Prince DA, Williams SW (2003) Effect of welding parameters on nugget zone microstructure

and properties in high strength aluminium alloy friction stir welds. Sci Technol Weld Join. https://doi.org/10.1179/136217103225005480
12. Rhodes CG, Mahoney MW, Bingel WH, Spurling RA, Bampton CC (1997) Effects of friction stir welding on microstructure of 7075 aluminium. Scr Mater. https://doi.org/10.1016/S1359-6462(96)00344-2
13. Bisadi H, Tavakoli A, Tour Sangsaraki M, Tour Sangsaraki K (2013) The influences of rotational and welding speeds on microstructures and mechanical properties of friction stir welded Al5083 and commercially pure copper sheets lap joints. Mater Des. https://doi.org/10.1016/j.matdes.2012.06.029
14. Sato YS, Kokawa H, Enomoto M, Jogan S (1999) Microstructural evolution of 6063 aluminium during friction-stir welding. Metall Mater Trans A Phys Metall Mater Sci. https://doi.org/10.1007/s11661-999-0251-1
15. Rodrigues DM, Loureiro A, Leitao C, Leal RM, Chaparro BM, Vilaça P (2009) Influence of friction stir welding parameters on the microstructural and mechanical properties of AA 6016-T4 thin welds. Mater Des. https://doi.org/10.1016/j.matdes.2008.09.016
16. Abolusoro PO, Akinlabi ET (2020) In-process cooling in friction stir welding of aluminium alloys—an overview. In: Awang M et al (eds) Advances in material sciences and engineering. Lecture notes in mechanical engineering. Springer, Singapore, pp 435–444. https://doi.org/10.1007/978-981-13-8297-0_45
17. Jata KV, Sankaran KK, Ruschau JJ (2000) Friction-stir welding effects on microstructure and fatigue of aluminium alloy 7050-T7451. Metall Mater Trans A Phys Metall Mater Sci. https://doi.org/10.1007/s11661-000-0136-9
18. Mahoney MW, Rhodes CG, Flintoff JG, Spurling RA, Bingel WH (1998) Properties of friction-stir-welded 7075 T651 aluminum. Metall Mater Trans A 29(7):1955–1964
19. Lotfi AH, Nourouzi S (2014) Effect of welding parameters on microstructure, thermal, and mechanical properties of friction stir welded joints of Aa7075-T6 aluminium alloy. Metall Mater Trans A Phys Metall Mater Sci. https://doi.org/10.1007/s11661-014-2235-z
20. Guo JF, Chen HC, Sun CN, Bi G, Sun Z, Wei J (2014) Friction stir welding of dissimilar materials between AA6061 and AA7075 Al alloys effects of process parameters. Mater Des. https://doi.org/10.1016/j.matdes.2013.10.082
21. Aydin H, Bayram A, Esme U, Kazancoglu Y, Guven O (2010) Application of grey relation analysis (Gra) and Taguchi method for the parametric optimization of friction stir welding (FSW) process. Appl Grey Relat 44:205–211
22. Rajakumar S, Balasubramanian V (2012) Establishing relationships between mechanical properties of aluminium alloys and optimised friction stir welding process parameters. Mater Des 40:17–35
23. Lombard H, Hattingh DG, Steuwer A, James MN (2008) Optimising FSW process parameters to minimise defects and maximise fatigue life in 5083-H321 aluminium alloy. Eng Fract Mech 75:341–354
24. Prabha KA, Putha PK, Prasad BS (2018) Effect of tool rotational speed on mechanical properties of aluminium alloy 5083 weldments in friction stir welding. Mater Today Proc 5(24):18535–18543
25. Kalemba-Rec I, Kopyściański M, Miara D, Krasnowski K (2018) Effect of process parameters on mechanical properties of friction stir welded dissimilar 7075-T651 and 5083-H111 aluminium alloys. Int J Adv Manuf Technol. https://doi.org/10.1007/s00170-018-2147-y
26. Han MS, Lee SJ, Park JC, Ko SC, Woo Y Bin, Kim SJ (2009) Optimum condition by mechanical characteristic evaluation in friction stir welding for 5083-O Al alloy. Trans Nonferrous Met Soc China (Engl Ed). https://doi.org/10.1016/S1003-6326(10)60238-5
27. Das U, Toppo V (2018) Effect of tool rotational speed on temperature and impact strength of friction stir welded joint of two dissimilar aluminum alloys. Mater Today Proc 5:6170–6175
28. Kalevala PR, Akram J, Misra M, Ramachandran D, Gabbita JR (2016) Low-temperature friction stir welding of P91 steel. Def Technol 12:285–289
29. Silva-magalhães A, Backer J De, Martin J, Bolmsjö G (2019) In-situ temperature measurement in friction stir welding of thick section aluminium alloys. J Manuf Process Elsevier 39:12–17
30. Schmale J, Fehrenbacher A, Shrivastava A, Pfefferkorn FE (2016) Calibration of dynamic tool–workpiece interface temperature measurement during friction stir welding. Meas J Int Meas Confed 88:331–342
31. Feng Z, Hubbard CR, David SA, Brown DW, An K, Clausen B et al (2007) In situ neutron diffraction measurements of temperature and stresses during friction stir welding of 6061-T6 aluminium alloy. Sci Technol Weld Join 12:298–303
32. Hamilton C, Dymek S, Sommers A (2010) Characteristic temperature curves for aluminum alloys during friction stir welding. Weld J 89:189s–194s. https://doi.org/10.1016/j.ijmachtools.2008.02.001
33. Buffa G, Donati L, Fratini L, Tomesani L (2006) Solid-state bonding in extrusion and FSW: process mechanics and analogies. J Mater Process Technol 177:344–347
34. Covington JL, Robison W, Webb B (2005) Experimental characterization of tool heating during friction stir welding. ASM Proceedings of the International Conference: Trends in Welding Research, pp 179–184
35. Takayama Y, Akutsu Y, Choshiro N, Kato H, Watanabe H (2010) Temperature measurement during friction stir welding of dissimilar aluminum alloys, pp 1829–1834
36. Miles M, Karki U, Hovanski Y (2014) Temperature and material flow prediction in friction-stir spot welding of advanced high-strength steel. JOM 66:2130–2136
37. Upadhyay P, Reynolds AP (2010) Effects of thermal boundary conditions in friction stir welded AA7050-T7 sheets. Mater Sci Eng A 527:1537–1543
38. Fehrenbacher A, Smith CB, Duffie NA, Pfefferkorn FE, Ferrier NJ, Zinn MR (2013) Combined temperature and force control for robotic friction stir welding. J Manuf Sci Eng 136:021007. https://doi.org/10.1115/1.4025912
39. Swaminathan G, Sathiyamurthy S (2018) Experimental study of mechanical and metallurgical properties of friction stir welded dissimilar aluminium alloys. Int J Mech Prod Eng Res Dev 8(1):1049–1058
40. Palanivel R, Koshy Mathews P, Murugan N, Dinaharan I (2012) Effect of tool rotational speed and pin profile on microstructure and tensile strength of dissimilar friction stir welded AA5083-H111 and AA6351-T6 aluminium alloys. Mater Des 40:7–16
41. Shigematsu I, Kwon YJ, Suzuki K, Imai T, Saito N (2003) Joining of 5083 and 6061 aluminium alloys by friction stir welding. J Mater Sci Lett. https://doi.org/10.1023/A:1022688908885
42. Ouyang JH, Kovacevic R (2002) Material flow and microstructure in the friction stir butt welds of the same and dissimilar aluminium alloys. J Mater Eng Perform 11:51–63
43. Abolusoro PO, Akinlabi ET (2019) Experimental investigations of tool pin geometry and process parameter influence on mechanical property of friction stir welded 6101-T6 and 7075-T651 aluminium alloys. In: International conference on engineering for sustainable world, 2019, p 1378
44. Abolusoro PO, Akinlabi ET (2020) Effects of processing parameters on mechanical, material flow and wear behaviour of friction stir welded 6101-T6 and 7075-T651 aluminium alloys. Manuf Rev 7:1

2.8 ARTICLE VII

Impact of Tool Profile on Mechanical Behaviour and Material Flow in Friction Stir Welding of Dissimilar Aluminium Alloys

Published *in Material Science and Engineering Technology,* 2020. DOI 10.1002/mawe.202000002 **(ISI-listed).**

Tool profile is known to affect the manner in which the materials at the joint interface of friction stir welded materials interacts. This in turn affects the mechanical properties of the welded joints. This research article presented the influence of tool pin geometry on tensile strength, hardness and material flow characteristics in the FSW between 6101-T6 and 7075-T651 aluminium alloys. Tapered threaded and tapered unthreaded tool pins were investigated in this article. Three tool rotational speeds of 950rpm, 1550rpm and 1850rpm at a constant welding speed of 20mm/min were considered for each tool and a comparison was made in the performance of both tools under each of the parameters in terms of its UTS, hardness of the NZ, and material flow behaviour.

The findings revealed that both tools exhibit similarities in their tensile strength behaviour. The UTS increases as the rotational speed increases to medium speed. However, the UTS drops with further increase in the rotational speed to 1850rpm. This was ascribed to coarsening of the precipitates at the joint interface which causes poor bonding as a result of higher heat input from the high rotational speed of 1850rpm. The tensile values obtained from welds with the threaded pin are higher than those obtained from the unthreaded pin. The article also reported on the variation in hardness profiles across the HAZ and NZ of all the welds from both tools. Material flow pattern examined from all the welds in both tools were equally reported. Non-uniformity in material transportations were observed from all the welds in both tools. Partial material mixing

occurred in the unthreaded tool at 950rpm which resulted in the formation of voids. The material mixed better in the threaded tool pin at lower rotational speed than in the unthreaded tool pin. However, at medium speed, the material seems to flow more into one another in the unthreaded tool pin than in the threaded tool pin. At the highest speed of 1850rpm, both tools demonstrate considerable similar mixing behaviours. The differences in the material mixing patterns in both tools were attributed to the geometry of the tool pin.

Impact of tool profile on mechanical behavior and material flow in friction stir welding of dissimilar aluminum alloys

Einfluss des Werkzeugprofils auf mechanisches Verhalten und Materialfluss beim Rührreibschweißen unterschiedlicher Aluminiumlegierungen

O.P. Abolusoro[1], E.T. Akinlabi[1], S.V. Kailas[2]

The tool pin geometry used in friction stir welding of any material affects the transportation and mixing of the materials at the joint interface during the welding process. This further affects the mechanical properties of the joint. Tapered threaded and unthreaded tool pin profiles were investigated in this research work. The relationship between the material mixing characteristics and mechanical properties of each pin profile were evaluated. The results indicate that more materials mixing occurred in the nugget zone of the welds at lower rotational speed with the threaded tool pin than the unthreaded tool pin. However, at medium rotational speed, more volume of materials was swept into each other better in the unthreaded tool pin than the threaded pin. The tensile strengths of welds with the threaded tool pin were higher than the unthreaded tool pin. Although the two tool pins exhibit similarities in hardness variations across the weld zones however, higher average values of hardness were obtained at the nugget zone for welds performed with the tapered threaded tool pin. These could be as a result of better material mixing and higher opposition to grain dislocations across the dividing lines in the welds from the threaded tool pin.

Keywords: Friction stir welding / material flow / mechanical properties / tool pin geometry / aluminum alloys

Schlüsselwörter: Rührreibschweißen / Materialfluss / mechanische Eigenschaften / Werkzeugstiftgeometrie / Aluminiumlegierungen

1 Introduction

Friction stir welding as a welding (FSW) method was recently developed to join particularly low temperature alloys which are often difficult to weld with conventional non-solid-state welding techniques. It is a process whereby a tool which is essentially made up of a shoulder and a pin is designed to rotate on the workpiece joint interface. The friction between the workpiece and the rotating tool shoulder produce heat. This heat softens the materials at the workpiece joint interface causing the ro-

[1] Department of Mechanical Engineering Science, University of Johannesburg, JOHANNESBURG, REPUBLIC OF SOUTH AFRICA
[2] Department of Mechanical Engineering, Indian Institute of Science, BANGALORE, REPUBLIC OF INDIA

Corresponding author: O.P. Abolusoro, Department of Mechanical Engineering Science, University of Johannesburg, JOHANNESBURG, REPUBLIC OF SOUTH AFRICA,
E-Mail: abolusoroolatunji@yahoo.com

tating pin to penetrate, stir and mixes the plasticized materials to produce bonding [1–3]. This technology has become a very suitable method for joining aluminum alloys [4]. The quality of welds obtained from FSW is influenced by the tool pin geometry, rotational and travel speed, tilt angle and axial force [5, 6]. Principal among these factors is the tool pin geometry which is being investigated in this work. It is established that FSW joints formation is controlled by the flow of materials and temperature variations across the weld which is influenced by the tool pin profile and processing parameters [7, 8]. Tool pin geometry affects material transportations and mixing and significantly influence the mechanical properties of weld joints [9, 10]. Various research works on different pin designs and their effects on mechanical properties and material flow pattern have been carried out. For instance, better mechanical properties, defect free and fine grain structures were obtained with a square pin in similar and dissimilar FSW of some aluminum alloys [11–13]. Similarly, comparative analysis of welds carried out with square, octagonal and hexagonal tool pin profile revealed the highest tensile strength with the square pin [14]. However, in another development, the mechanical properties obtained in welds with conical pin have been found to perform better than the square pin [15].

Chamfered shoulder with rounded frustum shape end pin has also been reported to give superior quality weld compared to cylindrical pin [16]. However, cylindrical threaded pin with 3 flat surfaces and groove produced higher tensile strength than the other tools [17]. Heat generated and material flow in FSW have been attributed to the tool shoulder and pin profile employed for the welding [9, 18]. FSW of AA7075 aluminum alloy with triangular three grooves, and square tool pin gave welds free of defects due to better flow of materials than tapered threaded and conical platforms which gave voids in the welds [19]. Threaded and unthreaded tool pin investigated using computational fluid dynamics (CFD) revealed vertical pressure slope in the threaded tool which performs better than the unthreaded [20, 21]. Material flow pattern studied through a tracer embedded in the weld flow path during FSW revealed that plasticized material flow around the probe region is influenced by the tool pin thread [22–24]. An efficient tool for FSW must possess a shape with enough stirring ability and simple enough for easy production and minimization of cost. Although contemporary works in literature have indicated that pin profile affects mechanical properties, microstructures and material flow behavior in FSW, however, a comparative study on basic tool profile effects on mechanical behavior and material movements during FSW especially of dissimilar aluminum alloys still demands attention. This is due to variations in mechanical and metallurgical behavior as well as thermal stability and material transportation pattern of various aluminum alloys grades during FSW. This study, therefore, is an attempt to investigate tapered threaded and unthreaded tool pin effects on mechanical behavior and material flow pattern in the friction stir welding of 6101-T6 and 7075-T651 aluminum alloys.

2 Experimental procedures

The alloys 7075-T651 and 6101-T6 with the indicated elemental compositions and mechanical properties were used for the experiment, *Tables 1, 2*.

The plates were cut into 130 mm × 60 mm and welded along the rolling directions of the alloys. A two-tonne ETA Technology machine was used to carry out the welding. Two different tool pins (tapered threaded and tapered unthreaded) fabricated from H13 steel were employed for the welding. Both tools have 22 mm shoulder diameter, 5.5 mm pin mouth diameter and 7.5 mm pin root diameter with a pin length of 5.6 mm and 0.5 mm thread

Table 1. Elemental components of the welded alloys.

Alloy	Si	Cu	Fe	Mn	Mg	Ti	Cr	Zn	Al
6101-T6	0.53	0.01	0.14	0.002	0.600	0.008	0.001	0.003	rest
7075-T651	0.40	1.70	0.50	0.300	2.40	0.20	0.22	5.50	rest

Table 2. Mechanical properties of the welded alloys.

Alloy	Tensile strength (MPa)	Ultimate tensile strength (MPa)	Elongation (%)
6101-T6	172	180	21
7075-T651	462	575	18

pitch for the threaded tool pin, *Figure 1*. The 6101-T6 alloy was placed on the advancing side while 7075-T651 was on the retreating side. Three parameters were used for both tools, *Table 3*. (AS) The tilt angle was kept at 2^0 while the plunge depth was at 0.15 mm throughout the experiment. (RS) Three tensile samples from welds of each parameter were prepared in line with ASTM E8 standard for evaluation, *Figure 2*. The hardness was profiled perpendicular to the welding directions with about 27 indentations taken on each sample. Macrographs and microstructures of all the samples were studied using optical microscope.

Figure 2. Tensile samples.

Figure 1. Tools (a) Threaded (b) Unthreaded.

Table 3. Processing parameters employed for the experiment.

S/N	Rotational speed (min^{-1})	Travel speed (mm/min)
1	950	20
2	1550	20
3	1850	20

3 Results and discussion

3.1 Tensile strength and tool geometry effects

The stress-strain behavior for all the parameters for both unthreaded and threaded tool pins are illustrated, *Figures 3, 4*. The average ultimate tensile values obtained in both tools demonstrates similarities in behavior across the three welding parameters. The tensile strength for both tools increases

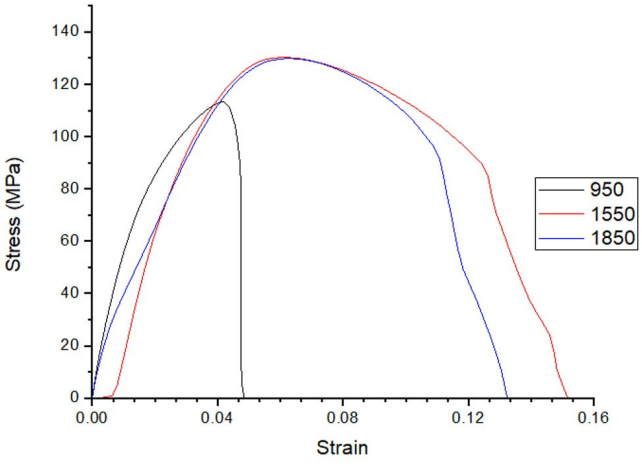

Figure 3. Stress/strain graph for unthreaded tool.

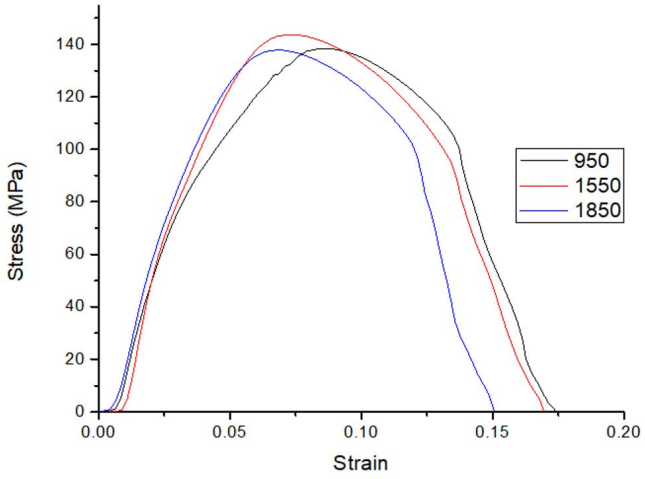

Figure 4. Stress/strain graph for threaded tool.

as the rotational speed increases from 950 min^{-1} (lowest rotational speed) to 1550 min^{-1} (medium rotational speed) but decrease slightly as the rotational speed further increase to 1850 min^{-1} (highest rotational speed) in both tools. The highest tensile strength of 143 MPa was achieved with the threaded tool at the medium rotational speed, *Figure 5*. The decrease in tensile value observed at the highest rotational speed is due to greater thermal cycle set up in the weld which led to coarsening of the precipitates and poor bonding. The tensile value obtained for each parameter is generally higher in threaded tool than the unthreaded tool, Figure 5. This can be attributed to better material mixing by the tool thread which promotes resistance of the grains to boundary dislocations [25].

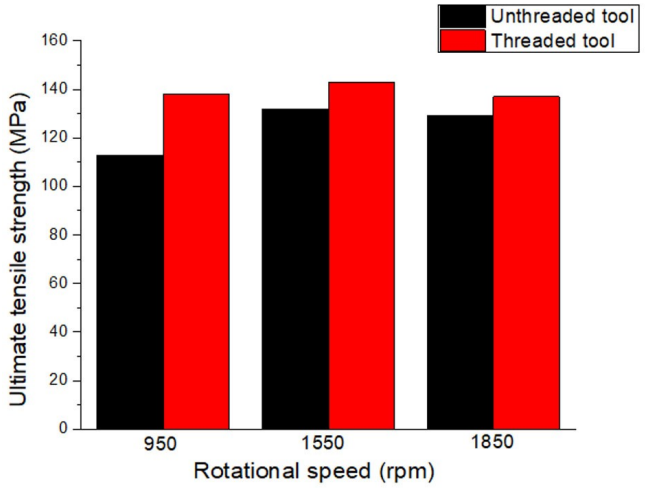

Figure 5. Ultimate tensile strength for threaded and unthreaded tools.

3.2 Hardness and tool geometry effects

The hardness varies across the welding zones in all the parameters in both threaded and unthreaded tools. (HAZ) The hardness values at the heat affected zone of the advancing side (6101-T6) of the weld are the lowest while those at the retreating side as expected were the highest for all the parameters in both tools, *Figures 6, 7*. (NZ) The average hardness at the nugget zones increase as the rotational speed increases to 1550 min^{-1} but drop at 1850 min^{-1} in both tools though slightly in the un-

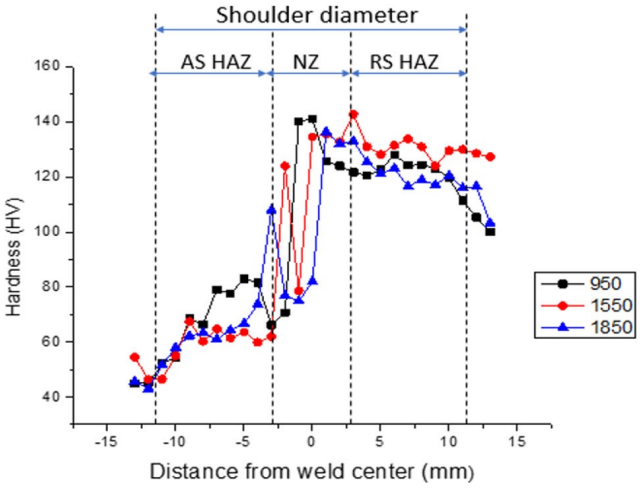

Figure 6. Hardness profiles for threaded tool welds.

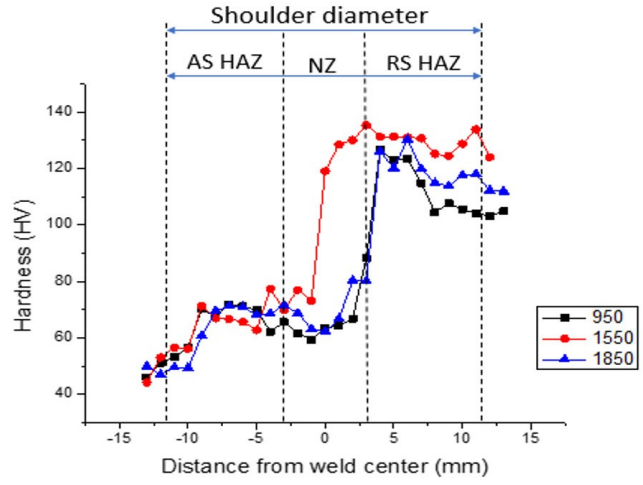

Figure 7. Hardness profile for unthreaded tool welds.

threaded tool. The average hardness at the nugget zone of the welds was considerably higher in the threaded tool than the unthreaded tool, *Figures 8, 9*. This is due to better material transportations and mixing from the tool pin thread which promotes greater grain bonding and hardened precipitates.

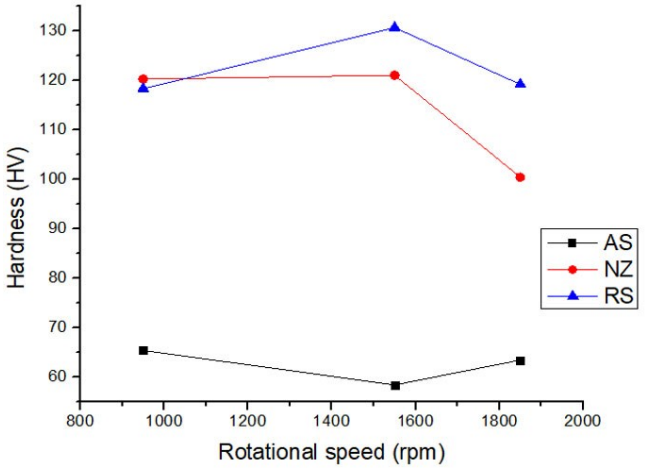

Figure 8. Average hardness values at the NZ, AS HAZ and RS HAZ for threaded tool welds.

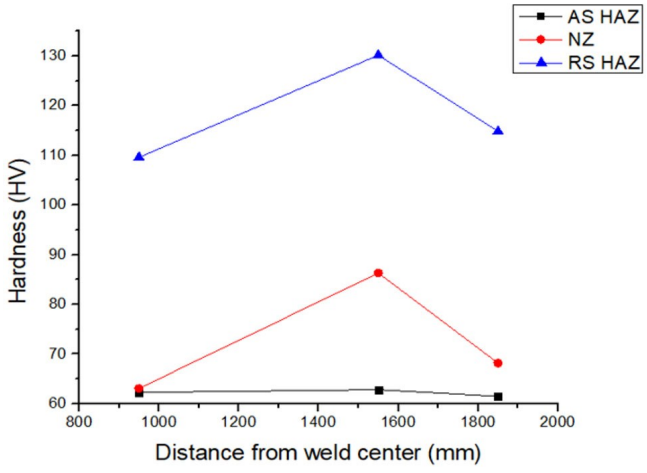

Figure 9. Average hardness values at the NZ, AS HAZ and RS HAZ for unthreaded tool welds.

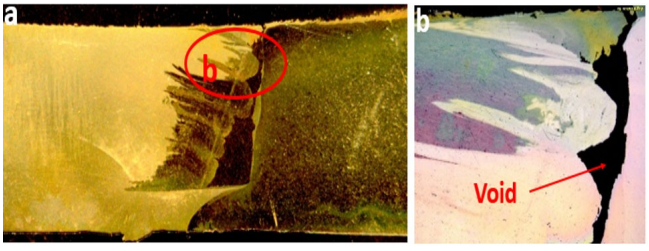

Figure 10. Material flow at 950 min^{-1} for unthreaded tool pin. (a) Macrograph (b) Microstructures at 20X.

3.3 Material flow pattern

Optical microscope was used to study the material mixing and flow pattern in both tools for all the parameters, *Figures 10–15*. The figures demonstrate that materials transportation from top to the bottom of the welds is not uniform due to variations in contact area resulting from the tool pin geometry. The weck's reagent used revealed 7075-T651 as the lighter color while the 6101-T6 as the darker color. At 950 min^{-1}, the unthreaded tool pin macrograph shows partial mixing and blending which resulted in wormhole or void, Figure 10a, b. This can be at-

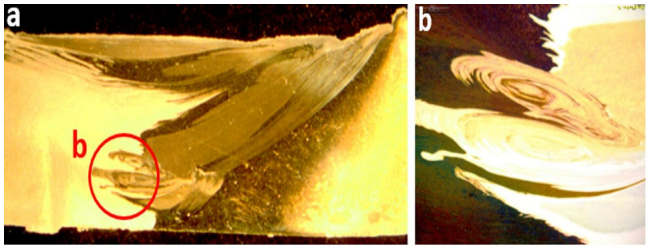

Figure 11. Material flow at 950 min^{-1} for threaded tool pin. (a) Macrograph (b) Microstructures at 20X.

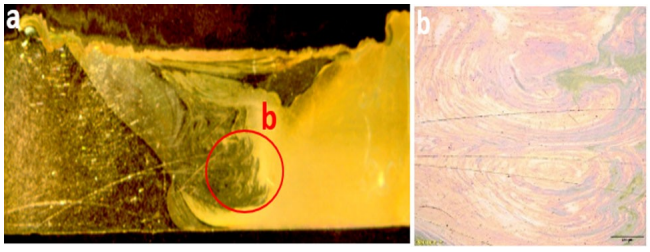

Figure 12. Material flow at 1550 min^{-1} for unthreaded tool pin. (a) Macrograph (b) Microstructures at 20X.

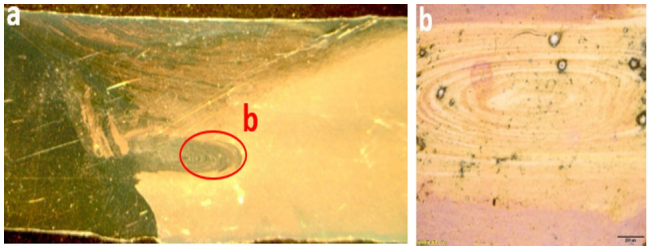

Figure 13. Material flow at 1550 min^{-1} for threaded tool pin. (a) Macrograph (b) Microstructures at 20X.

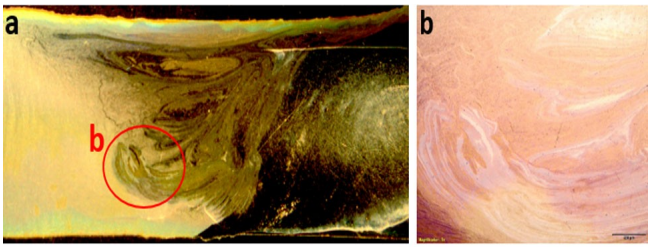

Figure 14. Material flow at 1850 min^{-1} for unthreaded tool pin. (a) Macrograph (b) Microstructures at 20X.

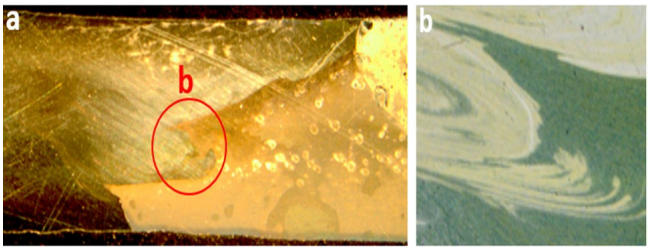

Figure 15. Material flow at 1850 min^{-1} for threaded tool pin. (a) Macrograph (b) Microstructures at 20X.

tributed to less interaction between the pin and material as a result of less area of contact which cause nonuniformity in material flow [26]. More material mixing was observed in the same parameter for the threaded tool, Figure 11a. This is due to the thread on the tool pin which promote more material interaction and sweeping of the alloys into each other. Little onion ring structures were noticed at higher magnification of the circled portions, Figure 11b. At 1550 min^{-1}, more mixing and material transportations seem higher in the unthreaded tool than the threaded tool, Figures 12a, 13a. However, onion ring structures are visible in both tools, Figures 12b, 13b. At 1850 min^{-1}, the material flow in both the threaded and the unthreaded tools are not uniform. However, more volume of material from the advancing side seems to be swept into the retreating side towards the end of the depth of the weld for the unthreaded tools than the threaded tool, Figures 14a, 15a. This could be due to promotion of sticking over sliding conditions which promote more heat and material plasticization during the welding. Higher magnification of the circled portions revealed some similarities in material mixing, Figures 14b, 15b.

4 Conclusion

- The ultimate tensile strength (UTS) is maximum at medium rotational speed in both unthreaded and threaded tool pins.
- The threaded tool pin performs better in tensile strength than the unthreaded tool pin.
- The average hardness values in the heat affected zone (HAZ) and nugget zone (NZ) were higher in threaded than the unthreaded tool pin.
- Better material mixing was noticed in threaded tool at lower rotational speed, however, at medium rotational speed more materials appears to be swept into one another in the unthreaded tool than the threaded tool. But at higher speed, both tools exhibit similar mixing pattern to a considerable extent. These variations resulted from the inhomogeneous mixing of the materials from top to the bottom of the weld in both tools.

5 References

[1] A.K. Kadian, P. Biswas, *J. Manuf. Process.* **2017**, *26*, 382.
[2] M.A. Hussain, N.Z. Khan, A.N. Siddiquee, Z. A. Khan, *Mater. Today Proc.* **2018**, *2*, 5.
[3] O.P. Abolusoro, E.T. Akinlabi, *Int. J. Mech. Prod. Eng. Res. Dev.* **2019**, *9*, 967.
[4] R.K.R. Singh, C. Sharma, D.K. Dwivedi, N. K. Mehta, P. Kumar, *Mater. Des.* **2011**.
[5] S. Ravikumar, V. Seshagiri Rao, R.V. Pranesh, *Int. J. Adv. Mech. Eng.* **2014**, *4*, 101.
[6] R.A. Kumar, M.R. Thansekhar, *Adv. Mater. Res.* **2014**, *586,* 984.
[7] R. Nandan, T. DebRoy, H.K.D.H. Bhadeshia, *Prog. Mater. Sci.* **2008**.
[8] F. Gratecap, G. Racineux, S. Marya, *Int. J. Mater. Form.* **2008**.
[9] K. Kumar, S.V. Kailas, *Mater. Sci. Eng. A.* **2008**.
[10] K. Palani, C. Elanchezhian, B. Vijaya Ramnath, G.B. Bhaskar, E. Naveen, *Mater. Today Proc.* **2018**, *5*, 24515.
[11] K. Elangovan, V. Balasubramanian, M. Valliappan, *Mater. Manuf. Process.* **2008**, *23*, 251.
[12] S.M. Bayazid, H. Farhangi, A. Ghahramani, *Procedia Mater. Sci.* **2015**, *11*, 12.

[13] J. Marzbanrad, M. Akbari, P. Asadi, S. Safaee, *Metall. Mater. Trans. B Process Metall. Mater. Process. Sci.* **2014**.
[14] R. Palanivel, P. Koshy Mathews, N. Murugan, I. Dinaharan, *Mater. Des.* **2012**, *40*, 7.
[15] C.N. Suresha, B.M. Rajaprakash, S. Upadhya, *Mater. Manuf. Process.* **2011**, *26*, 1111.
[16] K.P. Mehta, V.J. Badheka, *Trans. Nonferrous Met. Soc. China.* **2017**, 27.
[17] M. Raturi, A. Garg, A. Bhattacharya, *Eng. Fail. Anal.* **2019**, *96*, 570.
[18] E.T. Akinlabi, *J. Mater. Eng. Perform.* **2012**.
[19] M. Yuqing, K. Liming, L. Fencheng, C. Yuhua, X. Li, *Int. J. Adv. Manuf. Technol.* **2017**, *88*, 949.
[20] G. Chen, H. Li, G. Wang, Z. Guo, S. Zhang, Q. Dai, X. Wang, G. Zhang, Q. Shi, *Int. J. Mach. Tools Manuf.* **2018**, *124*, 12.
[21] M. Ilangovan, S. Rajendra Boopathy, V. Balasubramanian, *Def. Technol.* **2015**, *11*, 174.
[22] K. Colligan, *Weld. J.* **1999**, 229.
[23] Y.N. Zhang, X. Cao, S. Larose, P. Wanjara, *Can. Metall. Q.* **2012**, *51*, 250.
[24] J.A. Querin, H.A. Rubisoff, J.A. Schneider, in *ASM Proc. Int. Conf. Trends Weld. Res.*, **2009**, 108.
[25] O.P. Abolusoro, E.T. Akinlabi, *J. Phys.: Conf. Ser.* **2019**, 1378 032077.
[26] O.P. Abolusoro, E.T. Akinlabi, *Manufacturing Rev.* **2020**, *7*, 1.

Received in final form: February 16th 2020

CHAPTER THREE

PEER REVIEWED SCOPUS- INDEXED INTERNATIONAL CONFERENCE PAPERS

3.1 INTRODUCTION

A summary of peer-reviewed international conference publications indexed in SCOPUS are presented in this chapter.

3.2 ARTICLE I

Experimental Investigations of Tool Pin Geometry and Process Parameter Influence on Mechanical Property of Friction Stir Welded 6101-T6 and 7075-T651 Aluminium Alloys

Presented at the 3rd International Conference on Engineering for Sustainable World (ICESW) in May 2019 at Ota Nigeria.

Published *in Journal of Physics Conference Series, IOP Publishing* 1378 (2019) 032077 doi:10.1088/1742-6596/1378/3/032077. (**Scopus indexed**)

This article presents the influence of tool pin geometry and welding parameters on the mechanical behaviour of FSW in 6101-T6 and 7570-T651 aluminium alloys of 6mm thickness in butt configuration. The influence of travel and rotational speed on tensile behaviour of the weld joints were studied. The effects of tool pin designs, namely tapered threaded and tapered unthreaded pin on the tensile strength of the welds, were equally investigated in the article. It was established that the tensile strength of the welds decreases as the tool rotational speed increases. However, the

contrary was observed in the case of travel speed. The tensile strength increases as travel speed increases. This particular trend was noticed in all the welds of both the tapered threaded and tapered unthreaded tool pins. The article also reported on how the pin geometry affects the tensile behaviour of the welds. It was found that welds performed with the tapered threaded tool pin gave higher tensile strength values than those from the tapered unthreaded tool pin. These higher values of UTS obtained with the threaded tool was attributed to more homogenous material movement and mixing at the NZ of the weld due to the threaded pin.

Experimental Investigations of Tool Pin Geometry and Process Parameter Influence on Mechanical Property of Friction Stir Welded 6101-T6 and 7075-T651 Aluminium Alloys

Experimental Investigations of Tool Pin Geometry and Process Parameter Influence on Mechanical Property of Friction Stir Welded 6101-T6 and 7075-T651 Aluminium Alloys

Olatunji P Abolusoro[1*] and Esther T Akinlabi[2]

[1, 2] Department of Mechanical Engineering Science, University of Johannesburg, Gauteng, South Africa.
[2] Department of Mechanical Engineering, Covenant University, Ota, Ogun State, Nigeria
* Corresponding Author; abolusoroolatunji@yahoo.com

Abstract-
One of the variables that significantly affect the joint integrity of welds carried out with friction stir welding (FSW) is the tool pin geometry. This particular factor considerably affects the mechanical properties, joint size and microstructural evolution of the weld. The extent to which tool geometry affects the mechanical behaviour of welds under different processing parameters needs to be fully understood in order to achieve highly reliable joints for various industrial applications. This work is, therefore, an attempt at, investigating tool pin geometry and processing parameters effects on the mechanical behaviour and stability of friction stir welds through joining of 6101-T6 and 7075-T651 aluminium alloys via FSW. Two pin designs named tapered unthreaded and tapered threaded were used for this study. The result obtained shows that low rotational speed and high welding speed promote the tensile strength of the welded alloys and that welds carried out with the tapered threaded tool gave higher tensile values than the tapered unthreaded.

Keywords: Mechanical properties, tensile strength, tool geometry, friction stir welding

1. Introduction

Friction stir welding is a system of welding categorized under solid state form of welding where a tool made up of pin and shoulder rotates on the joint interface of the workpiece to be joined, producing heat in the process thereby causing plasticization of the materials. The pin stirring mechanism mixes the plasticized interface materials together and produces bonding as the tool traverse the joint line [1], [2], [3], [4], [5]. Friction stir welding has become the most suitable technique for joining aluminium alloys [6], [7], [8]. The mechanical properties and general quality of welds produced from FSW are often affected by a number of variables. Principal among them are the geometry or profile of the tool pin and their rotational and travel speed [9], [10], [11]**.** Material movement and temperature distributions are often influenced by the tool pin design and the tool movements, consequently, the microstructural development and the mechanical qualities of the weld are also affected [12], [13]. The design of an efficient tool for friction stir welding required that the tool shape be simple enough to minimize cost and must possess adequate stirring ability to produce good welds. Many researchers have therefore been attracted to the investigations of tool profile effects on the performance of friction stir welded materials especially aluminium alloys. Chent et al [14] used computational fluid dynamics (CFD)to investigate the effects of threaded and unthreaded tool pin on material flow. They noted that threaded tool pin geometry performs better through the formation of vertical pressure slope. This was in agreement with Illangova et al's studies [15]. Reza-E-Rabby et al [16] investigated pin thread effects on weld performance of FSW of AA 6061-T651. Their report

indicated that flat threaded tool pin largely excludes defects unlike the threaded tool with flat and without a flat. Elangovan et al [17] obtained sound mechanical properties and welds free from defects by using square pin under medium rotational speed to friction stir weld AA6061. Bayazid et al [18] equally employed cylindrical, triangle and square pin tool to weld 7075 alloy. They observed that cylindrical and square pin gave various defects but welds obtained with square pin tool were defects free. Colligan investigated material flow pattern during FSW by embedding a tracer into the weld path. He reported that the tool thread influenced the full flow of plasticized materials around the probe [19]. Zhang et al [20] and Querin et al [21] in their separate investigations confirmed that tool profile significantly affects material movement and heat supplied to the weld. Aval [22] studied the effects of tool pin profile on mechanical behaviour and microstructure development of 6082 and 7075 aluminium alloys welded through friction stir method. They observed that square frustrum pin gave homogenous mixing of the two metals. Madhav et al [23] in their study on FSW of AA6061 and AA7075 reported that cylindrical threaded pin having 3 flat surfaces and cylindrical groove demonstrated better tensile strength than the other tools used. In a related study, Palanivel et al [24] welded AA5083-H111 and AA6351-T6 via FSW using five different tool pin geometry to investigate their effects on microstructure and tensile strength. They revealed that the straight square pin design produced the highest strength. Processing parameters influence on some FSW of aluminium alloys has also been reported. Aissani [25] demonstrated how processing parameter mostly pin profile and tool rotational speed affect the tensile strength of welded aluminium alloys via friction stir. Lombard et al [26] employed eleven parameters of tool travel and rotational speed combinations for optimization. Their results showed that the highest value of 313MPa was obtained at 200rpm and 80mm/min rotational and travel speed respectively. Ghosh et al [27] reported better joint strength for dissimilar weld of A356 and 6061 aluminium alloys at an optimized tool rotational and travel speed. Rajakumar et al [28] demonstrated the existence of a range of tool rotational speed within which weld quality can be ascertained. Although works in contemporary literature indicate that pin profile, tool rotational and travel speed affects microstructure, defects and mechanical behaviour of welds, however, a comparative analysis of basic tool geometry, rotational and travel speed for dissimilar welding of aluminium alloys is yet to be fully reported. The welding of dissimilar aluminium alloys using friction stir welding method still demand special attention own to variation in mechanical strength, the thermal stability of the base materials, material movement pattern and metallurgical properties. This work, therefore, seeks to investigate the effect of tool pin design and welding variables such as travel speed and rotational speed of the tool on the mechanical behaviour of FSW of 6101-T6 and 7075-T651 aluminium alloys.

2 Experimental procedures

2.1 Sample's Elemental Composition and Properties

The elemental compositions of the two alloys are presented in table 1**.**

Table 1: chemical components of the welded alloys

Alloy	Si	Cu	Fe	Mn	Mg	Ti	Cr	Zn	Al
6101-T6	0.53	0.01	0.14	0.002	0.600	0.008	0.001	0.003	Others
7075-T651	0.40	1.70	0.50	0.300	2.40	0.20	0.22	5.50	Others

2.2 Welding set up

The FSW was carried out on aluminium alloys 6101-T6 and 7075-T651 of 6mm thickness each. Prior to the welding, the alloys were cut into pieces of about 130mm × 60mm each. The edges to be joined were milled to allow proper lapping and positioning for welding. The surface areas of both alloys were cleaned with emery paper and washed with acetone to remove oxide layer deposits and oil or grease on the alloy surfaces. Two tools with cylindrical tapered pins, one threaded and the other unthreaded both having 22mm shoulder diameter, pin root diameter of 7.5mm and pin mouth diameter of 5.5mm as presented in figure 1 (a) and (b) and figure 2 (a) and (b) were investigated for this work. The plates to be joined were positioned in butt configuration. The 6101-T6 was kept on the advancing side while the 7075-T651 was located on the retrieving side. The two alloys were clamped in this arrangement for the welding as shown in figure 3. The welding took place in the rolling direction of the alloys. The five variable parameters employed for this work are shown in table 2. Other process parameters remained constant. These include tilt angle of 2^0 and plunge depth of 0.15mm. Five welds were carried out with each tool using the processing parameters shown in table 2. Three tensile samples each were cut from each weld for evaluation following ASTM standard E8 as presented in figure 4. The ultimate tensile strengths of the parent materials are shown in table 3.

(a) **(b)**

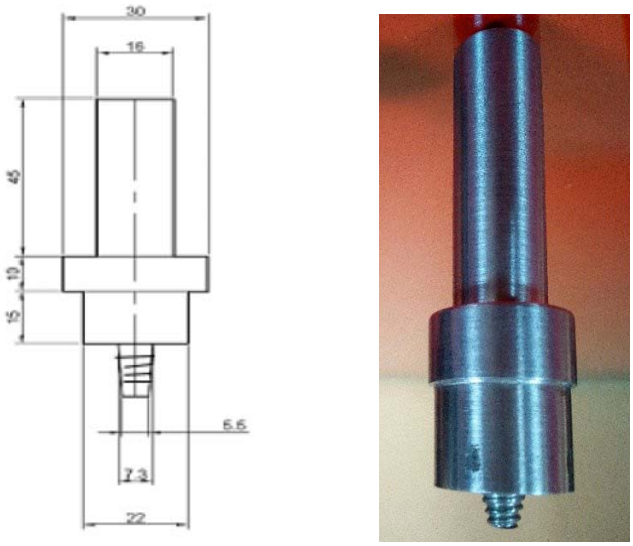

Figure 1: Diagram of cylindrical tapered threaded tool (a) Schematic (b) picture

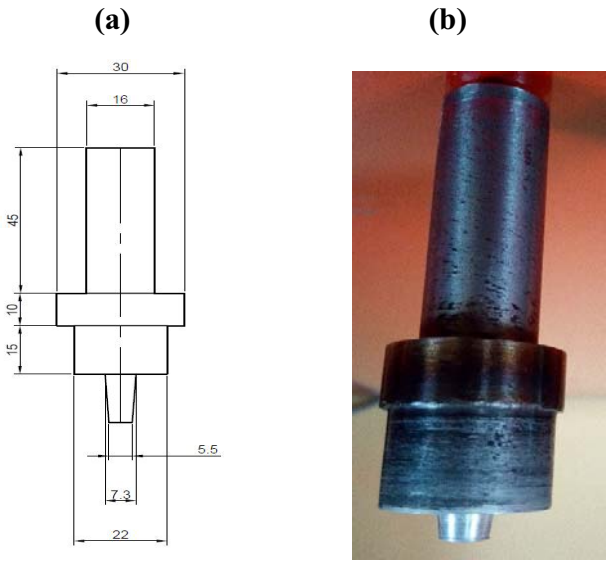

Figure 2: Diagram of cylindrical tapered unthreaded tool (a) Schematic (b) picture

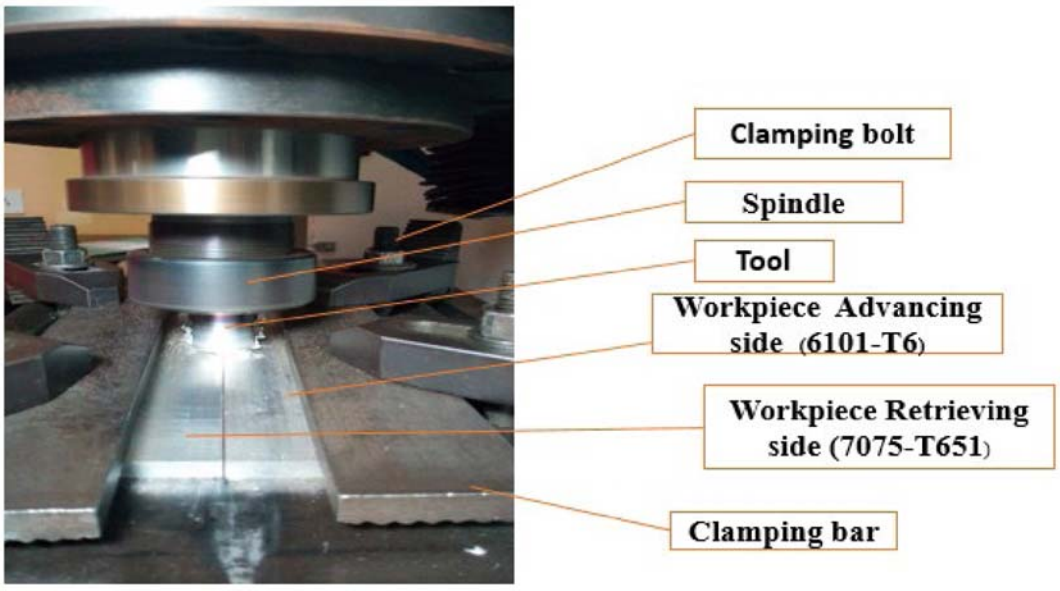

Figure 3: Welding arrangement

Table 2: Processing parameters

S/N	Rotational speed (rpm)	Travel speed (mm/min)
1	1550	50
2	1550	80
3	1550	110
4	1250	110
5	1850	110

Table 3: Mechanical properties of the welded alloy

Alloy	Tensile Strength (MPa)	Ultimate Tensile Strength (MPa)	Elongation (%)
6101-T6	172	180	21
7075-T651	462	575	18

3 Results and Discussion

Three samples each as shown in figure 4 were cut from the welds upon which the tensile tests were carried out. The average values of the ultimate tensile strengths obtained for all the welding variables used are shown in table 4.

Figure 4: Tensile samples from weld of each parameter for both tools

Table 4: Processing parameters and corresponding ultimate tensile strength values for threaded and unthreaded tool pins.

S/N	Rotational Speed (rpm)	Travel Speed (mm/min)	Ultimate Tensile Strength (MPa) (Threaded Tool)	Ultimate Tensile Strength (MPa) (Unthreaded Tool)
1	1550	50	140	140
2	1550	80	144	142
3	1550	110	147	144
4	1250	110	155	148
5	1850	110	142	139

3.1 Effects of Rotational Speed on the tensile behaviour of the welds from both tools

The tensile behaviour similarly varies across all the rotational speeds at a constant travel speed of 110mm/min in both tools used for the experiment. The tensile strength generally decreases as the rotational speed increases as shown in figure 5. This can be ascribed to increase in the heat supplied to the weld when the rotational speed increases. The higher thermal cycle set up in the weld causing microstructural reorientations at the three regions of the thermomechanical affected zone (TMAZ), heat affected zone (HAZ) and the nugget zone (NZ) of the weld. Coarsening of the precipitates occurred at greater rotational speed but at lesser rotational speed, greater grain boundary of precipitates took place which promotes high tensile strength.

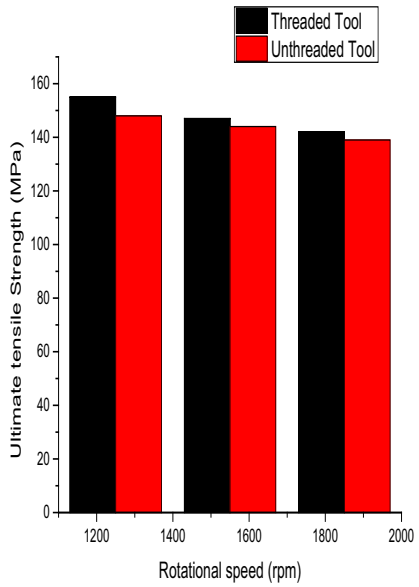

Figure: 5

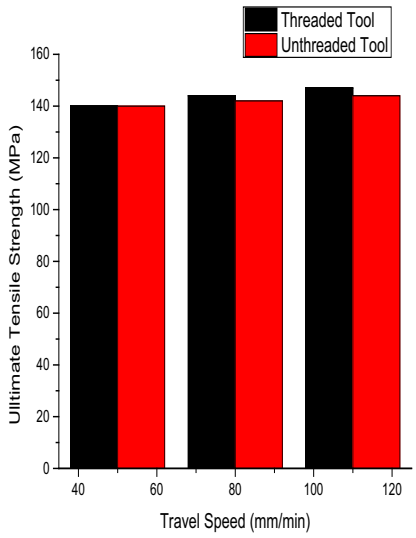

Figure: 6

Figure 5: Effects of rotational speed on the ultimate tensile strength of both threaded and unthreaded tool pin.

Figure 6: Effects of travel speed on the ultimate tensile strength of both threaded and unthreaded tool pin.

3.2 Influence of travel speed on the tensile behaviour of the welds from both tools

Both tools exhibited similar behaviour across the varied speeds at constant tool rotational speed of 1550rpm. Although both tools demonstrate the same tolerance to tensile strength at 50mm/min travel speed however, the tensile strength decreases as the travel speed increases as shown in fig. 5 and 6. This is due to less tool dwelling time on the workpiece at higher travel speeds. This implies that less heat is impacted into the weld as the tool travel faster on the workpiece. Also, part of the heat emanating from the tool is absorbed as latent heat for plasticization. The resulting less heat promotes grain bonding at the joint interface of the weld and consequently promotes the tensile strength of the joint leading to greater values obtained as the speed increases.

3.3 Effects of pin profile on Tensile behaviour.

The Ultimate tensile strength obtained for both the threaded and the unthreaded tools at constant travel speed and constant rotational speed exhibited similarities. However, the ultimate tensile values obtained for the threaded tool pin are higher than those of the unthreaded pin for all the processing parameters as shown in table 4 except at 1550rpm and 50mm/min where the values are the same. The highest ultimate tensile strength of 155MPa was recorded for the threaded tool. The better performance of the threaded tool pin over the unthreaded can be attributed to homogenous material mixing and enhancement of resistance to grain boundary dislocations own to the threads on the pin.

4 Conclusions

Conclusions can be drawn based on this experiment as follows

1. Both the threaded and the unthreaded tool pin developed, are suitable for friction stir welding of aluminium alloys.
2. Rotational speed increase during the friction stir welding does not promote tensile properties in both tools. However, increase in travel speed favours increase in ultimate tensile strength.
3. The threaded tool pin performs better than the unthreaded tool pin in terms of tensile strength.

Reference

[1] Kadian, A.K. and Biswas, P. (2017) Effect of tool pin profile on the material flow characteristics of AA6061. Journal of Manufacturing Processes, **26**, 382–92. https://doi.org/10.1016/j.jmapro.2017.03.005

[2] Azmal Hussain, M., Zaman Khan, N., Noor Siddiquee, A. and Akhtar Khan, Z. (2018) Effect of Different Tool Pin Profiles on the Joint Quality of Friction Stir Welded AA 6063. Materials Today: Proceedings, https://doi.org/10.1016/j.matpr.2017.11.680

[3] Jadhav, G.C. and Dalu, R.S. (2014) Friction Stir Welding – Process Parameters and its Variables: A Review. International Journal Of Engineering And Computer Science, **3**.

[4] Sidhu, M.S. and Chatha, S.S. (2012) Friction Stir Welding – Process and its Variables : A Review. **2**.

[5] Akinlabi, E.T., Andrews, A. and Akinlabi, S.A. (2014) Effects of processing parameters on corrosion properties of dissimilar friction stir welds of aluminium and copper. Transactions of Nonferrous Metals Society of China (English Edition), The Nonferrous Metals Society of China. **24**, 1323–30. https://doi.org/10.1016/S1003-6326(14)63195-2

[6] J. Brian Jordon, Harish Rao, Robert Amaro, P.A. (2019) CHAPTER 1 Introduction to Fatigue in Friction Stir Welding 1.1. *Fatigue in Friction Stir Welding*, 1–8.

[7] Ranjan, R., Carlos, A., Miranda, D.O., Hui, S., Walbridge, S. and Gerlich, A. (2019) Fatigue analysis of friction stir welded butt joints under bending and tension load. *Engineering Fracture Mechanics*, **206**, 34–45.

[8] Akinlabi, E.T., Andrews, A. and Akinlabi, S.A. (2014) Effects of processing parameters

on corrosion properties of dissimilar friction stir welds of aluminium and copper. Transactions of Nonferrous Metals Society of China (English Edition), **24**, 1323–30. https://doi.org/10.1016/S1003-6326(14)63195-2

[9] Lim, S., Kim, S., Lee, C.G. and Kim, S. (2004) Tensile behaviour of friction-stir-welded A356-T6/Al 6061-T651 bi-alloy plate. Metallurgical and Materials Transactions A: Physical Metallurgy and Materials Science, **35 A**, 2837–43. https://doi.org/10.1007/s11661-004-0231-4

[10] Kumar, R.A. and Thansekhar, M.R. (2014) Effects of Tool Pin Profile and Tool Shoulder Diameter on the Tensile Behaviour of Friction Stir Welded Joints of Aluminium Alloys. Advanced Materials Research, **984–985**, 586–91. https://doi.org/10.4028/www.scientific.net/amr.984-985.586

[11] Ravikumar, S., Seshagiri Rao, V. and Pranesh, R. V. (2014) Effect of Process Parameters on Mechanical Properties of Friction Stir Welded Dissimilar Materials between AA6061-T651 and AA7075-T651 Alloys. International Journal of Advanced Mechanical Engineering, **4**, 101–14. https://doi.org/10.1016/j.matdes.2014.10.065

[12] Leal, R.M., Galvão, I., Loureiro, A. and Rodrigues, D.M. (2015) Effect of friction stir processing parameters on the microstructural and electrical properties of copper. International Journal of Advanced Manufacturing Technology, **80**, 1655–63. https://doi.org/10.1007/s00170-015-7141-z

[13] Leal, R.M., Leitão, C., Loureiro, A., Rodrigues, D.M. and Vilaça, P. (2008) Material flow in heterogeneous friction stir welding of thin aluminium sheets: Effect of shoulder geometry. Materials Science and Engineering A, **498**, 384–91. https://doi.org/10.1016/j.msea.2008.08.018

[14] Chen, G., Li, H., Wang, G., Guo, Z., Zhang, S., Dai, Q. et al. (2018) Effects of pin thread on the in-process material flow behaviour during friction stir welding: A computational fluid dynamics study. International Journal of Machine Tools and Manufacture, **124**, 12–21. https://doi.org/10.1016/j.ijmachtools.2017.09.002

[15] Ilangovan, M., Rajendra Boopathy, S. and Balasubramanian, V. (2015) Effect of tool pin profile on microstructure and tensile properties of friction stir welded dissimilar AA 6061–AA 5086 aluminium alloy joints. Defence Technology, **11**, 174–84. https://doi.org/10.1016/j.dt.2015.01.004

[16] Reza-E-Rabby, M., Tang, W. and Reynolds, A.P. (2018) Effects of thread interruptions on tool pins in friction stir welding of AA6061. Science and Technology of Welding and Joining, **23**, 114–24. https://doi.org/10.1080/13621718.2017.1341363

[17] Elangovan, K., Balasubramanian, V. and Valliappan, M. (2008) Effect of tool pin profile and tool rotational speed on mechanical properties of friction stir welded AA6061 aluminium alloy. Materials and Manufacturing Processes, **23**, 251–60. https://doi.org/10.1080/10426910701860723

[18] Bayazid, S.M., Farhangi, H. and Ghahramani, A. (2015) Effect of Pin Profile on Defects of Friction Stir Welded 7075 Aluminum Alloy. **11**, 12–6. https://doi.org/10.1016/j.mspro.2015.11.013

[19] Colligan, K. (1999) Material flow behaviour during friction welding of aluminium. Welding Journal, 229–37.

[20] Zhang, Y.N., Cao, X., Larose, S. and Wanjara, P. (2012) Review of tools for friction stir welding and processing. Canadian Metallurgical Quarterly, **51**, 250–61. https://doi.org/10.1179/1879139512Y.0000000015

[21] Querin, J.A., Rubisoff, H.A. and Schneider, J.A. (2009) Effect of weld tool geometry on friction stir welded Ti-6AI-4V. *ASM* Proceedings of the International Conference: Trends in Welding Research, p. 108–12. https://doi.org/10.1361/cp2008twr108

[22] Jamshidi Aval, H. (2015) Influences of pin profile on the mechanical and microstructural behaviours in dissimilar friction stir welded AA6082-AA7075 butt Joint. Materials and Design, **67**, 413–21. https://doi.org/10.1016/j.matdes.2014.11.055

[23] Raturi, M., Garg, A. and Bhattacharya, A. (2019) Joint strength and failure studies of dissimilar AA6061-AA7075 friction stir welds: Effects of tool pin, process parameters and preheating. Engineering Failure Analysis, **96**, 570–88. https://doi.org/10.1016/j.engfailanal.2018.12.003

[24] Palanivel, R., Koshy Mathews, P., Murugan, N. and Dinaharan, I. (2012) Effect of tool rotational speed and pin profile on microstructure and tensile strength of dissimilar friction stir welded AA5083-H111 and AA6351-T6 aluminium alloys. Materials and Design, **40**, 7–16. https://doi.org/10.1016/j.matdes.2012.03.027

[25] Givi, M.K.B. and Asadi, P. (2014) Advances in Friction-Stir Welding and Processing. Adv. Frict. Weld. Process. https://doi.org/10.1016/C2013-0-16268-X

[26] Lombard, H., Hattingh, D.G., Steuwer, A. and James, M.N. (2008) Optimising FSW process parameters to minimise defects and maximise fatigue life in 5083-H321 aluminium alloy. Engineering Fracture Mechanics, **75**, 341–54. https://doi.org/10.1016/j.engfracmech.2007.01.026

[27] Ghosh, M., Kumar, K., Kailas, S. V. and Ray, A.K. (2010) Optimization of friction stir welding parameters for dissimilar aluminium alloys. *Materials and Design*, **31**, 3033–7. https://doi.org/10.1016/j.matdes.2010.01.028

[28] Rajakumar, S. and Balasubramanian, V. (2012) Establishing relationships between mechanical properties of aluminium alloys and optimised friction stir welding process parameters. *Materials and Design*, **40**, 17–35. https://doi.org/10.1016/j.matdes.2012.02.054

3.3 ARTICLE II

Review and Analysis of Mechanical Properties of Friction Stir Welds of High Strength Aluminium Alloys

Presented at the 3rd International Conference on Engineering for Sustainable World (ICESW) in May 2019 at Ota Nigeria.

Published *in Journal of Physics Conference Series, IOP Publishing* 1378 (2019) 032077 doi:10.1088/1742-6596/1378/4/042045 (**Scopus indexed**)

This article reviewed available research on the evolving tensile properties of friction stir welded high strength aluminium alloys, especially the 7075 alloy which is the most widely used of the seven series. This article presented the average values of reported UTS, YS and % elongation of friction stir welded 7075 alloys. Comparative analysis was carried out among the reported mechanical properties, and the relationship between the tensile behaviour, plate thickness, temper, and heat treatment conditions of similar and dissimilar friction stir welded 7075 alloys was established. The analysis showed that the temper condition influenced the mechanical behaviour of both similarly and dissimilarly welded joints. It was observed that similar welding in T6 and T651 temper conditions yield better efficiencies than dissimilar welding at these temper conditions with other series of aluminium alloys. The article also revealed that the thickness of the welded plates had no significant effect on the UTS, YS and % elongation of the welds. The paper equally revealed the range of temperatures within which PWHT could be carried out to maximize the tensile property of the weld. The article further highlighted the reliability of FSW technology for joining 7075 aluminium alloys at various tempers or heat treatment conditions.

Review and Analysis of Mechanical Properties of Friction Stir Welds of High Strength Aluminium Alloys

Review and Analysis of Mechanical Properties of Friction Stir Welds of High Strength Aluminium Alloys

Olatunji P Abolusoro[1*] and Esther T Akinlabi[1,2]

[1, 2] Department of Mechanical Engineering Science, University of Johannesburg, Gauteng, South Africa.
[2] Department of Mechanical Engineering, Covenant University, Ota, Ogun State, Nigeria
* Corresponding Author; abolusoroolatunji@yahoo.com,

Abstract
There have been significant advancements of recent in the studies of friction stir welding of high strength Aluminium alloys. These studies cover developments in the welded joint properties of these alloys. This paper reviews some available literature on evolving mechanical properties of friction stir welding of high strength aluminium alloys especially those of 7075 aluminium alloy which happens to be the most versatile member of the high strength aluminium alloy group. This review is aimed at establishing a correlation between the tensile behavior, plate thickness and temper conditions of the 7075 alloy when joined by friction stir welding (FSW) in both similar and dissimilar joints with other metals. The average values of reported ultimate tensile strength, yield strength, and percentage elongation have been calculated and presented. Comparative analysis was made between the tensile properties at different temper designation and plate thickness. The analysis revealed that temper conditions significantly affect the mechanical properties of both the similar and the dissimilar joints and that similar welding at T6 and T651 temper conditions gave higher weld efficiencies than dissimilar welding with other groups in the aluminium series. However plate thickness have little or no influence on the ultimate tensile behaviour, yield strength and elongation of the welds. The review also indicates that there is a range of temperature between which post weld heat treatment (PWHT) could be performed in order to obtain maximum tensile property This paper is a significant approach to enhance high performance joining techniques and the reliability or otherwise of friction stir welding technology to join 7075 aluminium alloys under different heat treatment or temper conditions of the alloys for better industrial applications.

Keywords: Aluminium alloy, Friction stir welding, Mechanical strength and temper

1. Introduction
High strength aluminium alloys are naturally the 7000 series of aluminium alloy. The major alloying elements utilized in this series is zinc. When this is combined with little quantity of magnesium, the resulting alloy is a high strength, heat treatable alloy. A prominent and most commercially utilized member of this group is the 7075 [1], [2], [3], [4]. The use of these alloys is ever increasing due to their desirable properties. These properties include; high strength comparable to those of many sheets of steel and with a higher strength to weight ratio than steel, high fatigue strength and considerably good resistance to corrosion [5], [6]. These unique characteristics have made this alloy gained wide acceptabilities in applications such as the aerospace, marine, automotive and defense industries [7]. 7075 aluminium alloy is weldable and is available in different temper conditions depending on the area of applications.

There have been numerous research efforts on this alloy aimed at exploring its potentials for better utilization. One of such researches is on similar and dissimilar friction stir joining of the alloys. Friction stir welding is a joining technique recently advanced to join two materials together. Friction stir welding utilized a rotating tool made up of shoulder with a protruded part known as a pin. When the rotating tool is brought into contact with the workpiece, friction is generated which softens the workpiece. The stirring action of the rotating pin at the joint interface of the workpiece caused plastic deformation, material flow and mixing of the two materials which solidifies at the trailing edge of the tool to form the weld. Friction stir welding technology has been successfully utilized to weld aluminium and high strength aluminium alloys in particular and it remains one of the best ways of joining aluminium alloys. [8], [9], [10]. Significant amount of investigations have been done by researchers on the influence of factors such as tool rotational and welding speed, tilt angle, plunge depth and axial force on the friction stir welded joints of high strength aluminium alloys under different conditions such as corrosion and mechanical strength which consist of tensile, wear, hardness, fatigue, impact and bending tests [11], [12], [13]. However, only a few reports are available on the influence of various temper conditions on the mechanical properties of friction stir welded joints of similar and dissimilar high strength aluminium alloys. These reports include those of Yan et al [14] that studied the influence of temper conditions (W, T6, and T7) on mechanical properties of friction stir welded AA7050 alloy. Their result showed that welds in W temper conditions gave the highest ultimate tensile strength, elongation and yield strength than those welded in T6 and T7 condition. Given et al [15] also studied the influence of different temper state of O and T6 on mechanical behaviour and microstructure of FSW of AA7075. The authors revealed that welds carried out in T6 temper conditions produced greater ultimate tensile strength and yield strength than welds in O temper state. However, there is a considerable reduction in elongation in T6 compared to those of O temper state. Also, Shama et al [16]. investigated the mechanical properties and microstructure of FSW of AA7039 under three pre-weld temper state of T6, W and O. They reported that welds in W conditions showed considerably greater yield strength and elongation than those in T6 and O conditions, but exhibit similarity to T6 and O in terms of ultimate tensile strength. Another study on temper conditions impact on FSW was carried out by Lin et al [17]. They investigated the effects of initial temper conditions T6 and T4 on tensile properties, hardness, and microstructure of FSW of 7055 alloys. They reported that joints in T6 temper exhibited slightly lower hardness in the weld zone than those in T4 conditions. However, the UTS, YS, and elongation obtained in T4 joints are higher than those of T6 joints.

The few available findings reviewed above specifically studied the temper influence on mechanical properties of high strength aluminium alloys. However, these findings are not sufficient enough for a comprehensive understanding of the influence of initial temper conditions on the mechanical properties of similar and dissimilar FSW of these high strength aluminium alloys especially the most widely utilized of the group which is the 7075 alloy. It has, therefore, become very essential to look into other works from various authors on FSW of 7075 alloys with a view to harness their findings on mechanical properties and relate it with the various tempers and other alloys differently employed in their studies.

This review, therefore, presents an analysis of the various documented values of mechanical property precisely the tensile behaviour obtained under different temper conditions, plate thickness and post weld heat treatment in both similar and dissimilar FSW of high strength aluminium alloy 7075. This is to further deepen the knowledge based on FSW of this alloy for

better understanding by researchers and manufacturers that would result in greater industrial applications.

2 Mechanical properties

This section captures the summary of reported ultimate tensile strength (UTS), yield strength (YS), and elongations of the pre-weld 7075 alloy and the friction stir welded alloy at different temper conditions as well as their analysis.

2.1 Tensile Strength

Tensile testing is a method widely used by researchers to evaluate the mechanical behavior of materials. Mechanical properties of 7075 alloy at different temper condition is indicated in table 1. While those from findings on FSW of 7075 aluminium alloys under different temper conditions, plate thickness, and post weld artificial aging and heat treatment from various authors have been summarized in table 2 to 8 as follows:

Table 1: Mechanical properties of 7075 alloy at different temper conditions

Temper condition	Ultimate tensile strength (MPa)	Yield Strength (MPa)	Elongation (%)
T6	570	350	10
T651	575	462	18
T7	505	305	13

Table 2: Tensile Results for Similar and Dissimilar welds with 7075-T7

Ref	Other Aluminium alloys welded with 7075-T7	Material thickness (mm)	Ultimate Tensile Strength (Mpa)	Yield Strength (Mpa)	Weld elongation (%)
[18]	AA2024	1.0	451	388	10.0
[19]	AA2024	3.1	477	316	13.8
[20]	AA2024-T3	9.5	--	398	--
[21]	AA2024	2.5.	476	--	--
[22]	AA2024	6.0	480	--	--
[23]	7050	6.35	473	--	6.1
		Average	**471.4**	**367.33**	**9.96**
[24]	Similar	8.0	458	--	--
[25]	Similar	8.0	346	227	4.6
		Average	**402**	**227**	**4.6**

Table 3: Tensile Results for Similar Welds with 7075-T6

Ref	Material thickness (mm)	Ultimate Tensile Strength (MPa)	Yield Strength (MPa)	Weld elongation (%)
[26]	5.0	311	-	-
[27]	5.0	567	480	8.2
[28]	20	401	322	-
[29]	20.0	415	255	8.1
[30]	6.0	450	-	-
[31]	4.0	370	-	-
[32]	5.0	462	-	-
[33]	6.35	468	312	7.5
[34]	7.0	450	325	7.0
[35]	10	350	--	6.5
	Average	**424.40**	**338.80**	**7.46**

Table 4: Tensile Results for Dissimilar Welds with 7075-T6

Ref	Other Materials welded with 7075-T6	Material thickness (mm)	Ultimate Tensile Strength (MPa)	Yield Strength (MPa)	Weld elongation (%)
[36]	2024	2.5	572	503	11.0
[37]	2014AT651	6.35	443	--	15
[38]	AA2024	4.0	434.7	---	2.2
[39]	6061-T6	5.0	209	-	-
[40]	2024-T4	4.0	381	302	9.6
[41]	AA6063	5.0	154	-	-
[42]	AA2024	5.0	341	-	-
		Average	**362.1**	**402.5**	**9.45**

Table 5: Tensile Results for Similar Welds with 7075-T651

Ref	Material thickness (mm)	Ultimate Tensile Strength (MPa)	Yield Strength (MPa)	Weld elongation (%)
[43]	6.0	568	404	19.9
[44]	6.0	563	-	11
[45]	6.3	468	312	7.5
[46]	6.35	473	-	3.1
[47]	5.0	402.9	-	3.6
[48]	12.0	335	394	12.0
[49]	6.0	425	--	_--
[50]	6.5	262	--	8.66
[51]	10.0	424	--	6
[51]	16.0	330	--	8
[45]	6.35	525	365	15.0
[52]	12.0	394	335	12.0
	Average	**430.83**	**362**	**9.70**

Table 6: Tensile Results for Dissimilar Weld with 7075-T651

Ref	Other Materials Welded with 7075-T651	Material thickness (mm)	Ultimate Tensile Strength (MPa)	Yield Strength (MPa)	Weld elongation (%)
[53]	2024-T351	6.35	435	290	13.0
[54]	5754-H111	5.0	239	-	-
[55]	5083-H111	6.0	371	308	9.9
[44]	6082-T6	6.0	193	-	4.0
[56]	6061-T6	6.0	485	-	-
		Average	**344.60**	**299**	**8.96**

Table 7: Tensile Results for Post Weld Artificial Aging (PWAA) of Similar welds of 7075-T651

Ref	Material thickness (mm)	Heat treatment condition	Ultimate tensile Strength (Mpa)	Yield Strength (Mpa)	Weld elongation (%)
[30]	6.35	RRA 5 min at 220^0	354	263	---
[45]	6.35	24 Hrs at 121^0C	447	312	3.5
[46]	6.35	PWAA to T6	364	-	6.1
[46]	6.35	PWAA to T7	349	--	6.1
[46]	6.35	PWAA to T73	357	---	6.1
[46]	6.35	121^0C for 7Hrs + FSW+121^0C for 24Hrs	428	---	4.9
[46]	6.35	121^0C for 7Hrs + FSW+163^0C for 27Hrs	373	-	4.0
[46]	6.35	121^0C for 7Hrs + FSW+163^0C for 17Hrs	347	-	3.7

Table 8: Tensile Results for Post Weld Heat Treatment (PWHT) of Dissimilar welds of 7075-T6

Ref	Other materials welded with 7075-T6	Material thickness (mm)	Heat treatment condition	Ultimate tensile Strength (Mpa)	Yield Strength (Mpa)	Weld elongation (%)
[57]	2024-T4	4.0	PWHT at 170^0C for 12Hrs	443	322	5.6

[57]	2024-T4	4.0	PWHT at 170^0C for 16Hrs	448	334	6.7
[57]	2024-T4	4.0	PWHT at 170^0C for 20Hrs	429	318	7.1

2.2 Analysis of Reported mechanical properties

2.2.1 Effects of temper conditions on ultimate tensile strength and elongation

2.2.1.1 T7 Temper Condition

The average UTS obtained for similar friction stir welding of 7075-T7 is 402MPa. This indicates a weld efficiency of 79.6%. The weld efficiency is a measure of the ratio of the average UTS to that of the base alloy expressed in percentage. Welding of this alloy with other aluminium alloys shows higher average values of 471MPa with a corresponding 9.96% elongation representing a weld efficiency of 93.2% which is higher than those of similar welds. There is no sufficient information from similar welds reported in the literature as reviewed in table 2 to justify why higher UTS was obtained in dissimilar welds. However, the overaged conditions of T7 temper 7075 alloys could be a factor when similarly welded together. The results obtained generally implies that the performance of the welds in both similar and dissimilar joints with other metals is considered reliable. This further affirm the effectiveness of FSW technology in joining high strength aluminium alloys.

2.2.1.2 T6 Temper Condition

Under T6 temper condition, the average values obtained for similar welds is 424MPa translating to an efficiency of 74.4%. The dissimilar average UTS value is 362MPa indicating an efficiency of 63.52% which is lower than that of similar welds. This could be attributed to the low strength of the other base alloys joined to the 7075-T6 which are mainly from group 2 and 6 series of aluminium alloys as reported by the various authors.

2.2.1.3 T651 Temper Condition

Welds in this temper show average UTS value of 430MPa and efficiency of 74.8% respectively when similarly welded. These are higher than the average UTS of 344MPa and efficiency of 59.8% obtained for dissimilar welds. This could also be due to lower strength of the dissimilar metals joined to the 7075-T651 alloy. The dissimilar metals as shown in table 6 are alloys from group 2, 5 and 6 of the aluminium series. Thus, failure is likely to occur on the side of these low strength alloys leading to decrease in UTS and weld efficiency.

2.2.2.1 Effects of heat treatments

The effects of heat treatments on the high strength aluminium alloy can be grouped into two, viz: PWAA and PWHT. This has been briefly explained in the next section.

2.2.2.2 Effects of PWAA

PWAA reported in table 7 for T651 temper condition indicate that the artificial aging of the welded joints affects the tensile behaviour of the welds. The aging temperature and the number of hours the weld was soaked in heat can increase or decrease the mechanical strength. The tensile strength obtained ranges from 347MPa to 354MPa which translate to between 60.3% to 61.6% which are lower than those obtained from as weld condition. Although the overall aim of PWAA on high strength aluminium alloys is not to increase the strength but rather to improve exfoliation and stress corrosion cracking.

2.2.2.3 Effects of PWHT

PWHT reported in table 8 was done by only one author. While the PWHT increase the tensile strength at heat soaking time of 16 hours, the tensile strength reduced when the soaking time is further increased to 20 hours. This indicates that there is a range of temperature between which PWHT could be carried out on dissimilar FSW of high strength aluminium alloys to maximize the mechanical properties.

2.3 Effects of Plate thickness on the UTS

The results of the UTS, YS, and elongations presented in table 2 to 8 show no correlation with the thickness of the plates joined. Both high and low UTS values were obtained under different thickness, indicating no particular trend. Thus, the UTS, YS and the elongation of the welded alloys as seen in the reported results from various authors are independent of the alloy thickness used for the experiment.

3 Conclusions

Conclusions from this literature survey and analysis can be drawn as follows:

- The temper conditions of the 7075 aluminium alloy before welding significantly affects the tensile strength of the weld both in similar joint or dissimilar joint with other metals.
- FSW remains a reliable technique of joining 7075 alloys at all temper conditions
- Similar welds of the 7075 alloy at T6 and T651 temper conditions exhibit better tensile behaviour than the dissimilar welds.
- There is a range of temperature between which PWHT could be performed in order to obtain maximum tensile property.

References

[1] Feng LI, J., wei PENG, Z., Xing LI, C., Qiang JIA, Z., Jing Chen, W & Qiao ZHENG, Z. (2008) Mechanical properties, corrosion behaviors and microstructures of 7075 aluminium alloy with various aging treatments. Transactions of Nonferrous Metals Society of China (English Edition), **18**, 755–62. https://doi.org/10.1016/S1003-6326(08)60130-2

[2] S. Pysz , M. Maj, E.C. (2014) High-Strength Aluminium Alloys and Their Use in Foundry Industry of Nickel Superalloys. Archives ofFoundry Engineering, **vol 14**, 77–76.
[3] Ikumapayi, O.M. & Akinlabi, E.T. (2019) Experimental data on surface roughness and force feedback analysis in friction stir processed AA7075 – T651 aluminium metal composites. Data in Brief, Elsevier Ltd. **23**, 103710. https://doi.org/10.1016/j.dib.2019.103710
[4] Ikumapayi, O.M. & Akinlabi, E.T. (2019) Efficacy of α - β grade titanium alloy powder (Ti–6Al–2Sn–2Zr–2Mo–2Cr–0.25Si) in surface modification and corrosion mitigation in 3.5% NaCl on friction stir processed armour grade 7075-T651 aluminum alloys—insight in defence applications . Materials Research Express, IOP Publishing. **6**, 076546. https://doi.org/10.1088/2053-1591/ab1566
[5] Olatunji P. Abolusoro & Esther T. Akinlabi. (2019) Wear and Corrosion Behaviouror of Friction Stir Welded Aluminium Alloys- An Overview. International Journal of Mechanical and Production Engineering Research and Development (IJMPERD*)*, **Vol. 9**, 967–982.
[6] Akinlabi, E.T., Andrews, A. & Akinlabi, S.A. (2014) Effects of processing parameters on corrosion properties of dissimilar friction stir welds of aluminium and copper. Transactions of Nonferrous Metals Society of China (English Edition), **24**, 1323–30. https://doi.org/10.1016/S1003-6326(14)63195-2
[7] Rambabu, P., Prasad, N.E. & Kutumbarao, V. V. (2017) Aerospace Materials and Material Technologies. https://doi.org/10.1007/978-981-10-2143-5
[8] Padhy, G.K., Wu, C.S. & Gao, S. (2017) Friction stir based welding and processing technologies - processes, parameters, microstructures and applications: A review. Journal of Materials Science and Technology, **34**, 1–38. https://doi.org/10.1016/j.jmst.2017.11.029
[9] Sidhu, M.S. & Chatha, S.S. (2012) Friction Stir Welding – Process and its Variables : A Review. **2**. International Journal of Emerging Technology and Advanced Engineering
[10] Shah, P.H. & Badheka, V.J. (2017) Friction stir welding of aluminium alloys: An overview of experimental findings – Process, variables, development and applications. Proceedings of the Institution of Mechanical Engineers, Part L: Journal of Materials: Design and Applications,. https://doi.org/10.1177/1464420716689588
[11] Bagheri Hariri, M., Gholami Shiri, S., Yaghoubinezhad, Y. & Mohammadi Rahvard, M. (2013) The optimum combination of tool rotation rate and traveling speed for obtaining the preferable corrosion behavior and mechanical properties of friction stir welded AA5052 aluminum alloy. Materials and Design, **50**, 620–34. https://doi.org/10.1016/j.matdes.2013.03.027
[12] Goloborodko, A., Ito, T., Yun, X., Motohashi, Y. & Itoh, G. (2004) Friction Stir Welding of a Commercial 7075-T6 Aluminum Alloy : Grain Refinement , Thermal Stability and Tensile Properties. **45**, 2503–8.
[13] Urso, G.D., Giardini, C., Lorenzi, S. & Cabrini, M. (2017) ScienceDirect ScienceDirect The influence of process parameters on mechanical properties and The influence of process mechanical properties corrosion behaviour of parameters friction stir on welded aluminum joints and corrosion behaviour of friction stir . **00**.
[14] Dixit, V., Mishra, R.S., Lederich, R.J. & Talwar, R. (2007) Effect of initial temper on mechanical properties of friction stir welded Al-2024 alloy. Science and Technology of

Welding and Joining, **12**, 334–40. https://doi.org/10.1179/174329307x197593
[15] Ipekoğlu, G., Erim, S. & Çam, G. (2014) Effects of temper condition and post weld heat treatment on the microstructure and mechanical properties of friction stir butt-welded AA7075 Al alloy plates. International Journal of Advanced Manufacturing Technology, **70**, 201–13. https://doi.org/10.1007/s00170-013-5255-8
[16] Sharma, C., Dwivedi, D.K. & Kumar, P. (2014) Influence of pre-weld temper conditions of base metal on microstructure and mechanical properties of friction stir weld joints of Al-Zn-Mg alloy AA7039. Materials Science and Engineering A, **620**, 107–19. https://doi.org/10.1016/j.msea.2014.09.094
[17] Lin, H., Wu, Y. & Liu, S. (2018) Impact of initial temper of base metal on microstructure and mechanical properties of friction stir welded AA 7055 alloy. Materials Characterization, **146**, 159–68. https://doi.org/10.1016/j.matchar.2018.09.043
[18] Tweedy, B., Allen, C. & Kumar, B. (2005) Design, Analysis and Testing of Friction Stir Welded Thin Sheet 2024 and 7075 Aluminum Alloys. Aeromat Conference Presentation, Orlando, FL,.
[19] Kumar, B., Widener, C., Cope, D & Tweedy, B. (2005) Effects Post Weld Aging on the Fatigue Crack Growth Rate, Corrosion Characteristics and Weld Microstructure of Al 2024 and 7075 Alloys. Aeromat 2005 Conference Presentation, Orlando, FL,.
[20] Bar, H. (2001) Effect of Friction Stir Welding on Dynamic Properties of AA2024-T3 and AA7075-T7351. 196–200.
[21] Russell, S.G., Tester, M., Nichols, E., Cleaver, A. & Maynor, J. (2001) Static, Fatigue and Crack Growth Behavior of Friction Stir Welded 7075-T6 and 2024-T3 Aluminum Alloys,. Friction Stir Welding and Processing, Indianapolis, *IN*, p. 93–104.
[22] Klæstrup Kristensen, J., Dalle-Donne, C., Ghidini, T., Mononen, J.T., Norman, A. Pietras, A., Russell, M., & Slater, S. (2004) Properties of Friction Stir Welded Joints in Aluminum Alloys 2024, 5083, 6082/6060 and 7075. Proceedings of the 5th International Friction Stir Welding Symposium, Sponsored by TWI, Ltd, Metz, France,.
[23] Lumsden, J., Pollock, G. & Mahoney, M.W. (2009) The Effect of Thermal Treatments on the Corrosion Behavior of Friction Stir Welded 7050 and 7075 Aluminum Alloys. Materials Science Forum, **426**–**432**, 2867–72. https://doi.org/10.4028/www.scientific.net/msf.426-432.2867
[24] Reynolds, A.P., Lockwood, W.D. & Seidel, T.U. (2009) Processing-Property Correlation in Friction Stir Welds. Materials Science Forum, **331**–**337**, 1719–24. https://doi.org/10.4028/www.scientific.net/msf.331-337.1719
[25] Kumar, P.V., Reddy, G.M. & Rao, K.S. (2015) ScienceDirect Microstructure , mechanical and corrosion behavior of high strength AA7075 aluminium alloy friction stir welds e Effect of post weld heat treatment. Defence Technology, **11**, 362–9.
[26] Suresha, C.N., Rajaprakash, B.M. & Upadhya, S. (2011) A study of the effect of tool pin profiles on tensile strength of welded joints produced using friction stir welding process. Materials and Manufacturing Processes, **26**, 1111–6. https://doi.org/10.1080/10426914.2010.532527
[27] Azimzadegan, T. & Serajzadeh, S. (2010) An investigation into microstructures and mechanical properties of AA7075-T6 during friction stir welding at relatively high rotational speeds. Journal of Materials Engineering and Performance, **19**, 1256–63. https://doi.org/10.1007/s11665-010-9625-1
[28] Yuqing, M., Liming, K., Fencheng, L., Yuhua, C. & Li, X. (2017) Effect of tool pin-tip

profiles on material flow and mechanical properties of friction stir welding thick AA7075-T6 alloy joints. International Journal of Advanced Manufacturing Technology, **88**, 949–60. https://doi.org/10.1007/s00170-016-8882-z

[29] Mao, Y., Ke, L., Chen, Y., Liu, F & Xing, L. (2018) Inhomogeneity of microstructure and mechanical properties in the nugget of friction stir welded thick 7075 aluminum alloy joints. Journal of Materials Science and Technology, **34**, 228–36. https://doi.org/10.1016/j.jmst.2017.11.039

[30] El-Nasr, A. (2010) Mechanical Properties and Fracture Behavior of Friction Stir Welded 7075-T6 Al Alloy. Journal of Engineering and ..., **3**, 147–61.

[31] Mohammadi-pour, M., Khodabandeh, A., Mohammadi-pour, S. & Paidar, M. (2016) Microstructure and mechanical properties of joints welded by friction-stir welding in aluminum alloy 7075-T6 plates for aerospace application. Rare Metals, 1. https://doi.org/10.1007/s12598-017-0971-0

[32] Farzadi, A., Bahmani, M. and Haghshenas, D.F. (2017) Optimization of Operational Parameters in Friction Stir Welding of AA7075-T6 Aluminum Alloy Using Response Surface Method. Arabian Journal for Science and Engineering, **42**, 4905–16. https://doi.org/10.1007/s13369-017-2741-6

[33] Mahoney, M.W., Rhodes, C.G., Flintoff, J.G., Bingel, W.H. & Spurling, R.A. (2007) Properties of friction-stir-welded 7075 T651 aluminum. Metallurgical and Materials Transactions *A*, **29**, 1955–64. https://doi.org/10.1007/s11661-998-0021-5

[34] Cavaliere, P. and Squillace, A. (2005) High temperature deformation of friction stir processed 7075 aluminium alloy. Materials Characterization **55**, 136–42. https://doi.org/10.1016/j.matchar.2005.04.007

[35] Paglia, C.S., Carroll, M.C., Pitts, B.., Reynolds, T & Buchheit, R.G. (2009) Strength, Corrosion and Environmentally Assisted Cracking of a 7075-T6 Friction Stir Weld. Materials Science Forum,. https://doi.org/10.4028/www.scientific.net/msf.396-402.1677

[36] Cavaliere, P., Cerri, E & Squillace, A. (2005) Mechanical response of 2024-7075 aluminium alloys joined by Friction Stir Welding. Journal of Materials Science,. https://doi.org/10.1007/s10853-005-0474-5

[37] Leonard, A.J. (2000) Corrosion Resistance of Friction Stir Welds in Aluminum Alloys 2014AT651 and 7075-T651. Proceedings of the 2nd International Friction Stir Welding Symposium, Sponsored by TWI, Ltd, Gothenburg, Sweden,.

[38] Bocchi, S., Cabrini, M., D'Urso, G., Giardini, C., Lorenzi, S. & Pastore, T. (2018) The influence of process parameters on mechanical properties and corrosion behavior of friction stir welded aluminum joints. Journal of Manufacturing Processes, Elsevier B.V. **35**, 1–15. https://doi.org/10.1016/j.jmapro.2018.07.012

[39] Saravanan, V., Rajakumar, S. & Muruganandam, A. (2016) Effect of Friction Stir Welding Process Parameters on Microstructure and Mechanical Properties of Dissimilar AA6061-T6 and AA7075-T6 Aluminum Alloy Joints. Metallography, Microstructure, and Analysis, **5**, 476–85. https://doi.org/10.1007/s13632-016-0315-8

[40] SAFARBALI, B., SHAMANIAN, M. & ESLAMI, A. (2018) Effect of post-weld heat treatment on joint properties of dissimilar friction stir welded 2024-T4 and 7075-T6 aluminum alloys. Transactions of Nonferrous Metals Society of China (English Edition), **28**, 1287–97. https://doi.org/10.1016/S1003-6326(18)64766-1

[41] Bayazid, S.M., Farhangi, H. & Ghahramani, A. (2015) Investigation of Friction Stir

Welding Parameters of 6063-7075 Aluminum Alloys by Taguchi Method. Procedia Materials Science, **11**, 6–11. https://doi.org/10.1016/j.mspro.2015.11.007

[42] Srinivas, B. and Devaraju, A. (2018) ScienceDirect Investigation of Velocity ratios on Mechanical and Microstructural Characterization of Friction Stir Welded Dissimilar 2024 and 7075 Aluminium Alloy. *Materials Today: Proceedings*, Elsevier Ltd. **5**, 19250–4. https://doi.org/10.1016/j.matpr.2018.06.282

[43] Xu, W., Li, Z. and Sun, X. (2017) Effect of Welding Speed on Mechanical Properties and the Strain-Hardening Behavior of Friction Stir Welded 7075 Aluminum Alloy Joints. *Journal of Materials Engineering and Performance*, **26**, 1938–46. https://doi.org/10.1007/s11665-017-2618-6

[44] Daniolos, N.M. and Pantelis, D.I. (2017) Microstructural and mechanical properties of dissimilar friction stir welds between AA6082-T6 and AA7075-T651. *International Journal of Advanced Manufacturing Technology*, **88**, 2497–505. https://doi.org/10.1007/s00170-016-8965-x

[45] Mahoney, M.W., Rhodes, C.G., Flintoff, J.G., Spurling, R.A. and Bingel, W.H. (1998) Properties of friction-stir-welded 7075 T651 aluminum. *Metallurgical and Materials Transactions A: Physical Metallurgy and Materials Science*, **29A**, 1958–65. https://doi.org/10.1007/s11661-998-0021-5

[46] Research, N. (2004) Corrective Measures to Restore Corrosion Resistance Following Friction Stir Welding. *CWL Publishing Enterprises, Inc, Madison*, **2004**, 352.

[47] Li, D., Yang, X., Cui, L., He, F. and Zhang, X. (2015) Investigation of stationary shoulder friction stir welding of aluminum alloy 7075-T651. *Journal of Materials Processing Tech*, Elsevier B.V. **222**, 391–8. https://doi.org/10.1016/j.jmatprotec.2015.03.036

[48] Sivaraj, P., Kanagarajan, D. and Balasubramanian, V. (2014) Effect of post weld heat treatment on tensile properties and microstructure characteristics of friction stir welded armour grade AA7075-T651 aluminium alloy. *Defence Technology*, Elsevier Ltd. **10**, 1–8. https://doi.org/10.1016/j.dt.2014.01.004

[49] Reimann, M., Goebel, J. and Santos, J.F. (2017) Microstructure and mechanical properties of keyhole repair welds in AA 7075-T651 using refill friction stir spot welding. **132**, 283–94.

[50] Shah, P.H. and Badheka, V. (2016) An experimental investigation of temperature distribution and joint properties of Al 7075 T651 friction stir welded aluminium alloys. **23**, 543–50. https://doi.org/10.1016/j.protcy.2016.03.061

[51] Rao, T.S., Reddy, G.M. and Rao, S.R.K. (2015) Microstructure and mechanical properties of friction stir welded AA7075 − T651 aluminum alloy thick plates. *Trans Nonferrous Met Soc China*, **25**, 1770–8. https://doi.org/10.1016/S1003-6326(15)63782-7

[52] Sivaraj, P., Kanagarajan, D. and Balasubramanian, V. (2014) Fatigue crack growth behaviour of friction stir welded AA7075-T651 aluminium alloy joints. Trans Nonferrous Met Soc China, **24**, 2459–67. https://doi.org/10.1016/S1003-6326(14)63371-9

[53] Kumar, K.S.A., Murigendrappa, S.M. & Kumar, H. (2017) A Bottom-Up Optimization Approach for Friction Stir Welding Parameters of Dissimilar AA2024-T351 and AA7075-T651 Alloys. *JMEPEG*, **26**, 3347–67. https://doi.org/10.1007/s11665-017-2746-z

[54] Kasman, Ş. & Yenier, Z. (2014) Analyzing dissimilar friction stir welding of AA5754/AA7075. International Journal of Advanced Manufacturing Technology, **70**, 145–56. https://doi.org/10.1007/s00170-013-5256-7

[55] Kalemba-Rec, I., Kopyściański, M., Miara, D. & Krasnowski, K. (2018) Effect of process parameters on mechanical properties of friction stir welded dissimilar 7075-T651 and 5083-H111 aluminum alloys. International Journal of Advanced Manufacturing Technology,. https://doi.org/10.1007/s00170-018-2147-y

[56] Hariharan, R., Golden, R.J & Nimal, R. (2013) Friction Stir Welding Of Dissimilar Aluminium Alloys (6061 and 7075) By Using Computerized Numerical Control Machine. Middle-East Journal of Scientific Research, **14**, 1752–6. https://doi.org/10.5829/idosi.mejsr.2013.14.12.7

[57] Safarbali, B., Shamanian, M. & Eslami, A. (2018) Effect of post-weld heat treatment on joint properties of dissimilar friction stir welded 2024-T4 and 7075-T6 aluminum alloys. Trans Nonferrous Met Soc China, **28**, 1287−1297. https://doi.org/10.1016/S1003-6326(18)64766-1

CHAPTER FOUR

CONCLUSIONS AND RECOMMENDATIONS

4.1 INTRODUCTION

The findings presented in this thesis are part of the research work aimed at widening the scope and application of FSW to aluminium alloys in industries through the characterisation of friction stir welded 6101-T6 and 7075-T651 aluminium alloys. The experimental and theoretical observations and analysis presented in the journals and conferences developed from this research are summarised in section 4.2. Recommendations for future work resulting from the research work are also highlighted in section 4.3 of the chapter.

4.2 CONCLUSIONS

The conclusions drawn from this study are as follows:

Tool pin geometry

i. The welds carried out with a tapered threaded tool pin yielded better mechanical properties than with a tapered unthreaded tool pin.

ii. Better material mixing was accomplished with the use of a threaded tool pin than with an unthreaded tool pin.

Optimization

i. The optimum combinations of tool rotational and welding speed to achieve maximum UTS are 950rpm and 50mm/min respectively.

ii. Optimum hardness values at the NZ was achieved at 1550rpm tool rotational speed and 20mm/min travel speed.

iii. The rotational speed is the predominant variable towards achieving optimum UTS, while the travel speed is the significant predominant factor for obtaining optimum hardness.

Temperature Variations

i. The temperature variations during the welding are affected by processing parameters, most significantly rotational speed. An increase in tool rotational speed increases the temperature of the weld.

ii. The weld temperature increases with time and reaches maximum at the middle of the weld.

Mechanical properties

i. Processing parameters were also established to influence the mechanical behaviour of the welds. Lower rotational speed and higher welding speed favour better mechanical properties of the welds.

ii. Tensile failures occurred at the HAZ of the 6101-T6 alloy on the advancing of the weld.

Wear behaviour

i. The wear rate of the NZ depends on the processing parameters. Resistance to wear increases with an increase in welding speed but decreases with an increase in rotational speed.

ii. The wear resistance was highest at the medium welding speed.

Microstructures

i. Three distinct regions comprising unmixed, mixed and mechanically mixed regions were observed in the NZ of the welds.

ii. Material mixing, the volume of material flowing into one another, and the mixing pattern are functions of the process parameters employed.

iii. The material flow pattern was characterised by onion ring structures and lamellae structural flow patterns.

4.3 RECOMMENDATIONS

Based on the findings presented in this work, the following future research studies are recommended:

1. The mechanical properties of welded joints could be further ascertained by carrying out other mechanical testing such as impact and fatigue tests on the welds.
2. The reported joint efficiency of the welds could be improved upon by carrying out PWHT on the welds.
3. Tool pin geometries other than the tapered threaded and unthreaded tool pins investigated in this work could also be explored to further establish the tool pin profile best suited for joining the two alloys.

4. A model for further analysis of the temperature distributions during the welding and the prediction of the heat transfer in the three welding zones of NZ, TMAZ and HAZ could be developed with the aid of suitable software. The measured in-situ temperature reported in this work could be used to validate the model.
5. XRD analysis of the NZ to study the phase changes in the dissimilar welded region of the alloys should be carried out.
6. Corrosion tests should be carried out on the welded joints. The effects of PWHT on the corrosion behaviour and microstructural changes of the weld joints should also be investigated.

REFERENCES

[1] "https://weldguru.com/welding-history,". Accessed on the 5th of March, 2020.

[2] " *https://www.fairlawntool.com/blog/history-of-welding*. Accessed on the 5th of March, 2020.

[3] S. Kou, *Welding Metallurgy*. 2002.

[4] Y. M. Ahmed, K. Sahari, and M. Ishak, "Australian Journal of Basic and Applied Sciences History of Elements and Welding processes (article paper) List of Abbreviations Article in," *Aust. J. Basic Appl. Sci.*, no. January 2016, 2014.

[5] J. Rigelsford, "Modern Welding Technology 5/e," *Ind. Robot An Int. J.*, 2004.

[6] E. T. Akinlabi, "characterization of friction stir welding between 5754 and 11000 copper," Nelson Mandella Metropolitan University, Port Elizabeth. South Africa, 2011.

[7] J. Norrish, "An introduction to welding processes," in *Advanced welding processes*, Woodhead Publishing Series in Welding and Other Joining Technologies, 2006, p. Pages

1-15.

[8] E. D. W.M. Thomas and C. . D. Nicolas, J.C. Needham, M.G. Murch., P. Templesmith, "US Patent Application," vol. No. 546031, 1995.

[9] P. H. Shah and V. J. Badheka, "Friction stir welding of aluminium alloys: An overview of experimental findings – Process, variables, development and applications," *Proceedings of the Institution of Mechanical Engineers, Part L: Journal of Materials: Design and Applications*, 2017.

[10] G. K. Padhy, C. S. Wu, and S. Gao, "Journal of Materials Science & Technology Friction stir based welding and processing technologies - processes , parameters , microstructures and applications : A review," vol. 34, pp. 1–38, 2018.

[11] "https://www.holroyd.com/blog/friction-stir-welding-applications." Accessed on the 4th of March, 2020.

[12] G. Wang, Y. Zhao, and Y. Hao, "Friction stir welding of high-strength aerospace aluminum Alloy and application in rocket tank manufacturing," *J. Mater. Sci. Technol.*, vol. 34, no. 1, pp. 73–91, 2017.

[13] "https://www.twi-global.com/technical-knowledge/published-papers/nz-fabricators-begin-to-use-friction-stir-welding-to-produce-aluminium-components-and-panels-august-2006." Accessed on the 4th of March, 2020.

[14] "https://www.twi-global.com/technical-knowledge/published-papers/application-of-friction-stir-welding-in-the-shipbuilding-industry-february-2000." Accessed on the 4th of March, 2020.

[15] A. Amini, P. Asadi, and P. Zolghadr, “Friction stir welding applications in industry,” in *Advances in Friction-Stir Welding and Processing*, 2014.

[16] “https://insights.globalspec.com/article/12966/applications-of-friction-stir-welding,” vol. Acessed on 5th of March, 2020.

[17] “http://www.aalco.co.uk/datasheets/Aluminium-Alloy_Introduction-to-Aluminium-and-its-alloys.” Accessed on the 10th of August, 2020.

[18] K. O. Cooke, “Structural Aluminum Alloys and Composites, Aluminium Alloys and Composites,” *IntechOpen*, vol. March 4th, 2020.

[19] R. Cobden and A. Banbury, “Aluminium: Physical Properties, Characteristics and Alloys,” *Talal*, 1994.

[20] W. L. Fink, “Aluminium and its alloys,” *Ind. Eng. Chem.*, 1936.

[21] P. S. Bulson, “Aluminium structures - a guide to their specifications and design,” *Eng. Struct.*, 1996.

[22] “Applications of aluminium alloys in civil engineering,” *Teh. Vjesn. - Tech. Gaz.*, 2017.

[23] P. Mukhopadhyay, “Alloy Designation , Processing , and Use of AA6XXX,” vol.1 2012.

[24] S. O. Adeosun, E. I. Akpan, O. I. Sekunowo, W. A. Ayoola, and S. A. Balogun, “Mechanical Characteristics of 6063 Aluminum-Steel Dust Composite,” *ISRN Mech. Eng.*, 2012.

[25] A. Medvedev *et al.*, “Enhancement of Mechanical and Electrical Properties in Al 6101 Alloy by Severe Shear Strain under Hydrostatic Pressure,” *Adv. Eng. Mater.*, 2018.

[26] “https://www.aluminum-foil.net/tag/aluminium-foil-uses/.” Accessed on the 10th of

August, 2020.

[27] “https://www.dreamstime.com/royalty-free-stock-photos-aluminium-cans-image16026618.” Accessed on the 10th of August, 2020.

[28] “https://www.triard.co.uk/category/ladders-accessories/403.” Accessed on the 10th of August, 2020.

[29] R. J. H. Wanhill, “Physical Property Significances for Aerospace Structural Materials,” 2017.

[30] “https://www.just-auto.com/analysis/the-challenge-of-vehicle-lightweighting_id154495.aspx.” Accessed on the 10th of August, 2020.

[31] “https://www.thoughtco.com/aluminum-or-aluminium-alloys-603707.” Accessed on the 10th of August, 2020.

[32] E. T. Akinlabi, A. Andrews, and S. A. Akinlabi, “Effects of processing parameters on corrosion properties of dissimilar friction stir welds of aluminium and copper,” *Trans. Nonferrous Met. Soc. China (English Ed.*, vol. 24, no. 5, pp. 1323–1330, 2014.

[33] P. L. Threadgilll, A. J. Leonard, H. R. Shercliff, and P. J. Withers, “Friction stir welding of aluminium alloys,” *Int. Mater. Rev.*, 2009.

[34] O. P. Abolusoro and E. T. Akinlabi, “Experimental Investigations of Tool Pin Geometry and Process Parameter Influence on Mechanical Property of Friction Stir Welded 6101-T6 and 7075-T651 Aluminium Alloys,” in *International Conference on Engineering for Sustainable World*, 2019, p. 1378.

[35] O.P. Abolusoro and E. T. Akinlabi “Effects of processing parameters on mechanical, material flow and wear behaviour of friction stir welded 6101-T6 and 7075-T651

aluminium alloys," *Manuf. Rev.*, vol. 7, no. 1, pp. 1–14, 2020.

[36] H. J. Liu, H. J. Zhang, and L. Yu, "Effect of welding speed on microstructures and mechanical properties of underwater friction stir welded 2219 aluminum alloy," *Mater. Des.*, vol. 32, no. 3, pp. 1548–1553, 2011.

[37] O. P. Abolusoro and E. T. Akinlabi "Review and Analysis of Mechanical Properties of Friction Stir Welds of High Strength Aluminium Alloys," *J. Phys. Conf. Ser.*, vol. 1378, no. 0 42045, pp. 1–13, 2019.

[38] K. Elangovan, V. Balasubramanian, and M. Valliappan, "Influences of tool pin profile and axial force on the formation of friction stir processing zone in AA6061 aluminium alloy," *Int. J. Adv. Manuf. Technol.*, vol. 38, no. 3–4, pp. 285–295, 2008.

[39] Y. J. Ko, K. J. Lee, and K. H. Baik, "Effect of tool rotational speed on mechanical properties and microstructure of friction stir welding joints within Ti-6Al-4V alloy sheets," *Adv. Mech. Eng.*, vol. 9, no. 8, pp. 1–7, 2017.

[40] O. P. Abolusoro and E. T. Akinlabi, "Wear and corrosion in friction stir welding of Aluminium alloys- An overview," *Int. J. Mech. Prod. Eng. Res. Dev.*, vol. 9, no. 3, pp. 967–982, 2019.

[41] P. L. Threadgill, A. J. Leonard, H. R. Shercliff, and P. J. Withers, "Friction stir welding of aluminium alloys," *Int. Mater. Rev.*, vol. 54, no. 2, pp. 49–93, 2009.

[42] X. Zhang, Y. Chen, and J. Hu, "Recent advances in the development of aerospace materials," *Progress in Aerospace Sciences*. 2018.

APPENDIX

APPENDIX A. Instron tensile testing machine

APPENDIX B: Welding machine

APPENDIX C: Welded samples

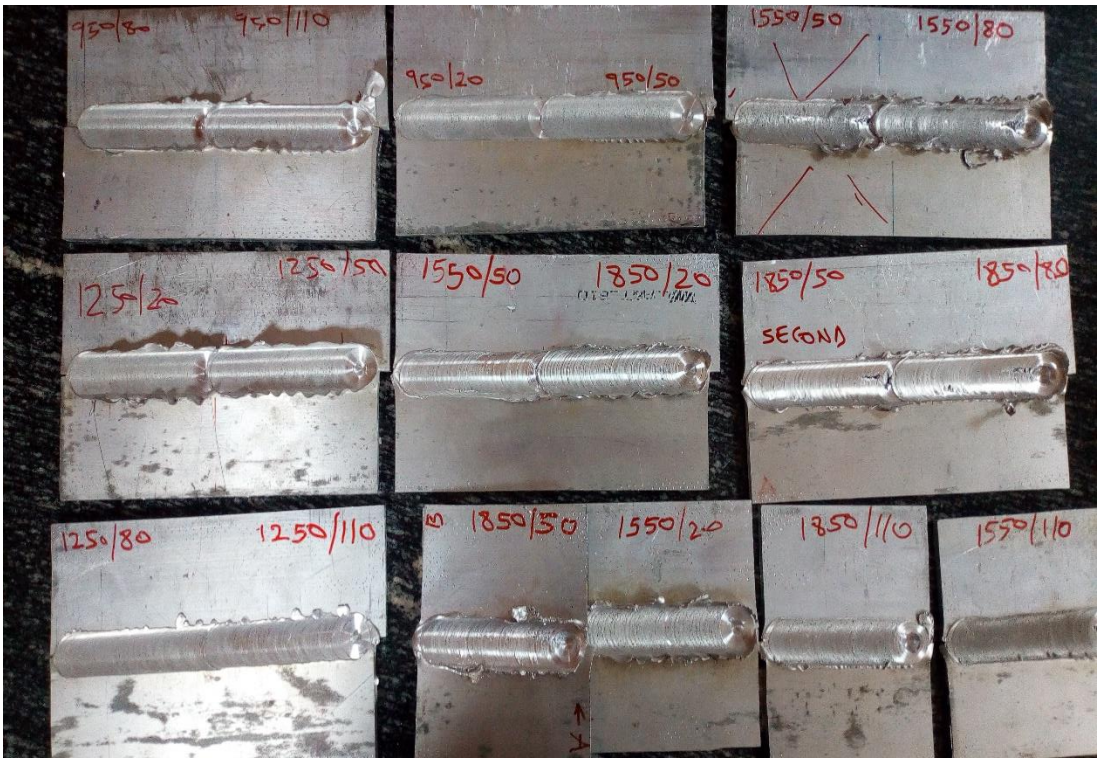

APPENDIX D: Cutting machine

APPENDIX E: Grinding and polishing machine

APPENDIX F: Vickers microhardness tester

APPENDIX G: Mounting press machine

APPENDIX H: Microscope for macrograhs observation

APPENDIX I: Scanning electron microscope